Powertrain Selection and Integration of a Single Shaft Pre and Post-Transmission Series-Parallel Plug-in Hybrid Electric Vehicle Camaro

By

Ramin Shaikhi

A thesis

presented to the University of Waterloo

in fulfillment of the

thesis requirement for the degree of

Master of Applied Science

In

Mechanical and Mechatronics Engineering

Waterloo, Ontario, Canada, 2018

Author's Declaration

I hereby declare that I am the sole author of this thesis. This is a true copy of the thesis, including any required final revisions, as accepted by my examiners.

I understand that my thesis may be made electronically available to the public.

Abstract

The ever-growing concern for the environment as well as stricter emissions has fueled the drive for the automotive industry to sway away from the conventional fossil-fueled vehicle. As the pursuit of using alternative energy sources that are cleaner and more sustainable is increasing, so is the popularity of electric vehicles. There are however, challenges associated with adopting them, such as high costs, limited driving range, long charging times, and lack of charging station infrastructure. While industries are constantly making breakthroughs to address these challenges, hybrid electric vehicles are seen as the stepping-stone to the transition from fossil-fueled vehicles to all-electric vehicles.

There is a wealth of technical literature available on topics related to the control strategies, technology development, and optimization of hybrid electric vehicles. However, it has been found that there is limited literature available regarding the process of selecting and integrating the powertrain itself. Literatures that do address the selection and integration seldom use a real-life example to demonstrate the applied theory. Therefore, the objective of this thesis is *to provide insight and guidance on theoretical and practical knowledge required for the powertrain selection and integration process of a hybrid electric vehicle, demonstrated with the use of a detailed case study on the hybridization of a Chevrolet Camaro.* This is made possible with the access to resources and tools required for a full powertrain integration provided by EcoCAR 3.

This thesis focuses on the steps taken to convert the Camaro into a series-parallel plug in hybrid electric vehicle, more specifically; it outlines the process used to determine the vehicle technical requirements through target market research, which is then translated into engineering specifications to select the vehicle architecture and powertrain components. Followed by the design and integration of the powertrain including its thermal management system. The stock V6 3.6 Liter engine has been replaced by a 2-cylinder 0.85 Liter turbo charged engine, tuned to run on E85 fuel. Two GKN electric motors capable of producing a peak power of 140 kW each has been integrated pre and post of the stock 8-speed transmission, and utilize a 16.2 kWh energy storage system integrated in the trunk of the vehicle.

To provide a deeper insight in the process of hybridizing a vehicle, the thesis highlights some the obstacles and challenges faced, and the consequent lessons learnt. Some of which are the following: simplicity is a key principle to a good design, approach a complicated problem one step at a time, always test before pursuing or implementing a solution, and last but not least, it is imperative for a driveline to be aligned as well as balanced.

Acknowledgments

I am extremely grateful for the invaluable skills that I have developed, and the unfathomable experience that I have gained through my participation with the University of Waterloo Alternative Fuels Team. My sincere gratitude to Dr. Roydon Fraser and Dr. Michael Fowler for providing this once in a lifetime opportunity. I cannot thank them enough for their unparalleled guidance, advice, and support.

My gratitude also extends to Argonne National Laboratories (ANL) and General Motors (GM) along with all the sponsors for EcoCAR 3, which has provided a unique platform for students to freely experiment with their ideas and innovation. I would also like to thank Laura Barlow, who was our GM mentor, for all of her support and valuable project management advice.

I owe many thanks to the staff at the Sedra Student Design Centre and University of Waterloo for being so accommodating and providing the facilities required. My hat goes off to the staff at the machine shop in both the E5 and E3 building, who possess a wealth of knowledge and experience.

Last but not least, it has been an absolute pleasure to work alongside the UWAFT members. Just to name a few, big thanks to Bade Akinsanya, Cole Powers, Derrick Tan, Jack Mo, Jake McGrory, Michael Wu, Patrick DiGioacchino, Paul McInnis, Radhika Kartha, Sid Kakodkar, Tim Mui, and all the past coop and ME 599 students who worked so diligently. I could not have asked for anyone better to work with, especially during those strenuous all-nighters.

Dedication

To my Mother and Father.

Thank you for the sacrifices you have made to provide me with the opportunity to be who I am and where I am today.

To my loving Wife.

Thank you for all of your support. Sorry for taking longer than promised.

To my Family and my Little Sister.

Thank you for always being there for me.

Table of Contents

List of Figures

List of Tables

List of Acronyms

ADAS	Advanced Driver-Assistance Systems
AF	Air-fuel Ratio
ANL	Argonne National Laboratory
AVTC	Advanced Vehicle Technology Competition
BCM	Battery Control Module
bmep	Brake Mean Effective Pressure
BSFC	Brake Specific Fuel Consumption
CAN	Controller Area Network
CD	Charge Depleting
CG	Center of Gravity
COP	Coefficient of Performance
CS	Charge Sustaining
CSM	Current Shunt Module
CVT	Continuous Variable Transmission
DOE	U.S. Department of Energy
EC	Energy Consumed
ECU	Electronic Control Unit
EDM	Electrical Distribution Module
EI	Emissions Index
EMI	Electromagnetic Interference
ESS	Energy Storage System
EV	Electric Vehicle
FC	Fuel Consumption
FED	Fuel Energy Density
GHG	Green House Gas

GM	General Motors
GREET	Greenhouse Gases, Regulated, Emissions, and Energy use in Transportation Model
HEV	Hybrid Electric Vehicle
HIL	Hardware in the Loop
HV	High Voltage
ICE	Internal Combustion Engine
LSD	Limited Slip Differential
LV	Low Voltage
MSD	Manual Service Disconnect
NA	Naturally Aspirated
NVH	Noise Vibration Harshness
PEU	Petroleum Energy Used
PHEV	Plug in Hybrid Electric Vehicle
PRV	Pressure Regulating Valve
PTW	Pump-to-wheel
SE	Specific Emissions
SIL	Software in the Loop
SOC	State of Charge
TC	Turbo Charged
TXV	Thermal Expansion Valve
UCE	Upstream Criteria Emissions
UF	Utility Factor
UWAFT	University of Waterloo Alternative Fuels Team
VIL	Vehicle in the Loop
VTR	Vehicle Technical Requirement
VTS	Vehicle Technical Specification
VTT	Vehicle Technical Target

WTP	Well-to-pump
WTW	Well-to-wheel

CHAPTER 1
Introduction

Ever since the industrial revolution, there has been a wide-scale extraction of fossil fuels; consumption has been continuing to increase with the increase of world population and living standards. It has come to the attention of many that fossil fuels can no longer be relied upon as an energy source as they are not sustainable and harm the environment through the extraction, refinement process, and usage. Although it is difficult to determine exactly when fossil fuels will be diminished, forecasts suggest that the reserves will be depleted by 2088; Figure 1.1 displays the estimated future energy reserves for coal, gas and oil [1].

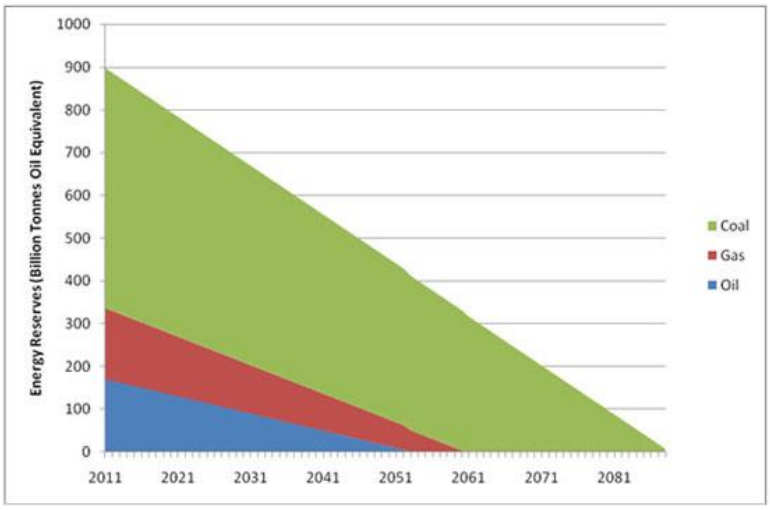

Figure 1.1: Fossil Fuel Reservoir Forecast [1]

In 2007, transportation in Canada was responsible for 27 percent of the total green house gas emissions (GHG) with road transportation accounting for 69 percent [2]. Globally, the road transport sector is responsible for 74 percent of carbon dioxide (CO_2) emissions, one of the primary GHG emissions [2]. As the total CO_2 concentration has been on a consistent rise, as shown in

Figure 1.2, it has led to excessive heat being captured on earth's surface, resulting in global warming, and leading to the instability of ecosystems.

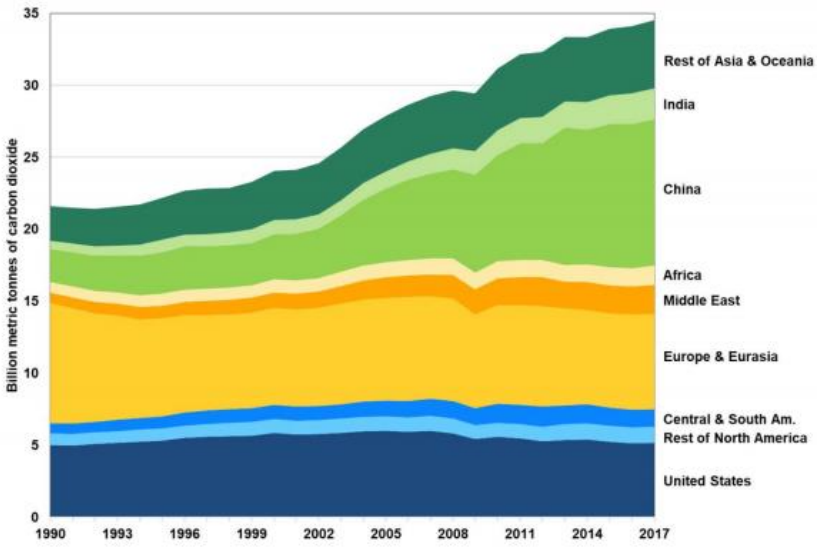

Figure 1.2: World Carbon Dioxide Emissions, 1990-2017 [3]

In addition to the production of CO_2 from tailpipe emissions, there are other emissions that can cause air pollution, affecting human and animal health. Carbon monoxide (CO), which is poisonous, forms during rich fuel mixture combustion with a lack of oxygen. Hydrocarbons, which can also be toxic, form during incomplete combustion, producing particulate matter leading to smog. Nitrogen oxides (NO_x) can also form when combustion occurs at high temperatures and pressure; it too causes health and environmental concerns, harming the ozone and also contributing to the development of smog. Thus, it is essential to move away from gasoline/diesel powered vehicles. With further urbanization, industrialization, and globalization, the number of personal automobiles has continued to grow. The number of vehicles has surpassed 1.1 billion in 2015, and the forecast state that by 2040 it would nearly double to 2 billion [4]. According to the Energy Information Administration, 25% of all energy consumption in the world is used for transportation of people and goods, with passenger transportation accounting for most of the transportation energy consumption [5]. The pie chart in Figure 1.3 shows that there is a heavy dependence on motor gasoline and diesel to fuel world transportation.

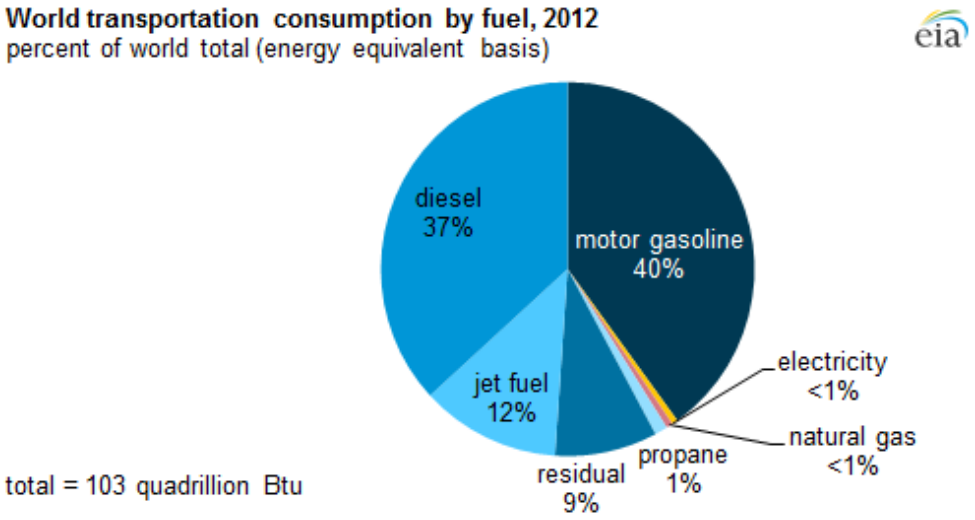

Figure 1.3: World Transportation Consumption by Fuel in 2012 [5]

Electric vehicles (EV) have proven to be a potential solution to reducing the consumption of gasoline and diesel. Well to wheel studies show that even if the electricity is generated from petroleum, the equivalent miles that can be driven with electric vehicles with one gallon of gasoline is just over three times more. This is due to electric vehicles having a higher operating efficiency than combustion powered vehicles; therefore, reducing the consumption of petroleum and making it cheaper for drivers to operate the vehicle [6]. Furthermore, electric vehicles can reduce concerns that drivers may have regarding the volatility of gasoline and/or diesel prices due to changes in the oil supply resulting from global political disputes and so on.

In light of the Paris Agreement in 2015 [7], many have increased their efforts in reducing carbon emissions. One measure is to ban fossil fuel cars on the roads, Table 1-1 outlines the countries that are aiming to do so. Current mayors of Los Angeles, Mexico City, Barcelona, Vancouver, Milan, Quito, Cape Town, and Auckland have also pledged to ban gas and diesel powered cars from "large parts" of their cities by 2030 [8]. Germany might also follow other countries in banning fossil fuel powered vehicles; they already have a target of putting 1 million electric vehicles on the road by 2020 [9].

Table 1-1: Countries Banning Fossil Fuel Powered Vehicles [7]

	Ban Announced	Ban Commences	Scope
United Kingdom	2017	2040	Gasoline and diesel
China	2017	"in the near future"	Gasoline and diesel
France	2017	2040	Gasoline and diesel
India	2017	2030	Gasoline and diesel
Ireland	2018	2030	Gasoline and diesel
Israel	2018	2030	Gasoline and diesel
Netherlands	2017	2030	All vehicles not emission free
Norway	2016	2025	Gasoline and diesel
Taiwan	2018	2040	Non-electric

Although it can be difficult to predict if electric vehicles are going to be the dominating vehicle of the future, they are slowly gaining traction. EV and plug in hybrid electric vehicles (PHEV) currently have a global market share of 1.7 percent, which has tripled since 2014 [10]. Magna International Inc. predicts EVs will grow to between 3 and 6 percent of global auto sales by 2025 [11]. Automotive manufacturers have already invested a total of at least 90 billion dollars in pursuit of developing EVs [12]. It has been estimated that there will be a total of 127 battery-electric models introduced worldwide by 2022. General Motors Co has announced plans to roll out 20 models by 2023, and Toyota Motor Corp. promised more than 10 electric models by early next decade [11]. Bloomberg New Energy Finance has forecasted that electric vehicle sales will increase significantly in the future as shown in Figure 1.4.

Currently, consumers are discouraged from electric vehicles due to the high cost, limited driving range, long charging times, and lack of charging station infrastructure. Hybrid electric vehicles however can overcome these challenges and thus seem more appealing. While industries are constantly making breakthroughs to address the EV challenges, hybrid electric vehicles for the time being can be seen as the ideal transition from all-petroleum vehicles to all-electric vehicles, while still significantly reducing fuel consumption and emissions.

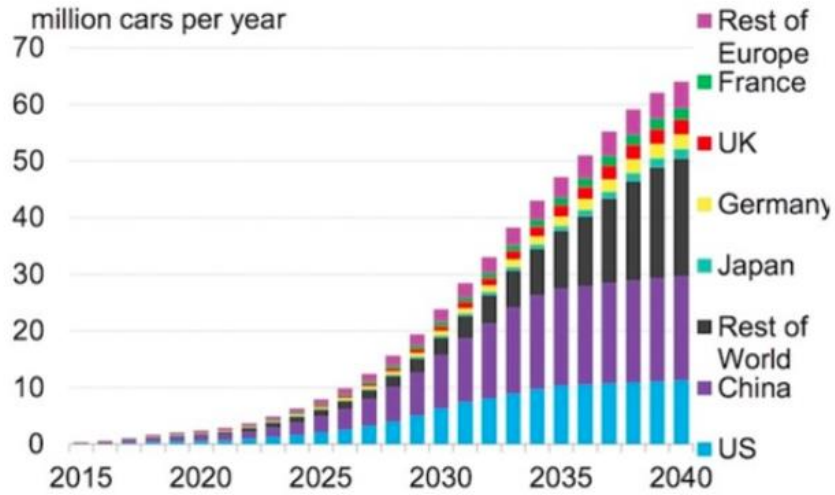

Figure 1.4: Electric Vehicles Sales Forecast [13]

1.1 Thesis Objective

As it may seem that the hybrid electric vehicles are the ideal transition to all-electric vehicles, it does come with its complexities. Electric hybrid vehicles typically consist of more critical components, as it is a combination of the internal combustion engine vehicle and electric vehicle. A deep understanding of these components are required to ensure that they are compatible with each other. For instance, it can be complicated to operate the electrical motor and combustion engine together in harmony, especially when they are mechanically coupled. Depending on the vehicle architecture, there are additional variables to consider when designing a hybrid vehicle as opposed to a vehicle that operates with a single power plant. Different "vehicle modes" come into affect and the control strategy can become challenging when trying to optimize vehicle efficiency for different vehicle driving conditions. These complexities have been experienced first hand during the conversion of the 2016 Camaro into a hybrid electric vehicle for the EcoCAR 3 competition, by the University of Waterloo Alternative Fuels Team (UWAFT).

The objective of this thesis is *to provide insight and guidance on theoretical and practical knowledge required for the powertrain selection and integration process of a hybrid electric vehicle, demonstrated with the use of a detailed case study on the hybridization of a Chevrolet Camaro.* The intent is to shed light on important factors, highlighting key concepts and fundamentals required when designing a hybrid electric vehicle. Specifically, the thesis outlines

the process used to determine the vehicle technical requirements through target market research, which is then translated into engineering specifications to select the vehicle architecture and powertrain components. Followed by the design and integration of the powertrain, including its thermal management system. Lastly, the thesis provides an intensive list of lessons learnt as a result of the experiences developed throughout the process.

This thesis also aims to encourage future students to develop more interest towards building innovative automotive architectures that further promote green technologies and environmental sustainability. One known obstacle in the adoption of electric and hybrid vehicles is due to lack of public knowledge. This thesis can help remediate this obstacle by providing information on what is "under the hood" of a hybrid electric vehicle and its capabilities.

This thesis can be used as a knowledge transfer document for future students at UWAFT and other teams. The failures and obstacles experienced including their corresponding solutions are also discussed so that they may be avoided and not repeated in the future. The author strongly believes that the best way to learn is through experience; however, the next best thing is to vicariously learn through other peoples well documented experiences.

1.2 Thesis Outline

Chapter 1. **Introduction** – Outlines the need for non-fossil fueled vehicles by discussing the affects of using fossil fuel on the environment as a primary energy source for world transportation. Multiple countries are combating the use of fossil fuels by banning fossil fueled vehicles within 15 years. Although electric vehicles have the potential to be the future dominating vehicle, hybrid electric vehicles play a big role in bridging the gap between fossil fueled cars and electric vehicles. The chapter also provides the thesis objective, which is *to provide insight and guidance on theoretical and practical knowledge required for the powertrain selection and integration process of a hybrid electric vehicle, demonstrated with the use of a detailed case study on the hybridization of a Chevrolet Camaro*.

Chapter 2. **Literature Review & Background** – The first two sections provides a brief background on UWAFT and EcoCAR 3. It then provides a brief literature review of hybrid electric vehicles; the difference between mild, micro, full hybrid and how they can be further categorized into series or parallel based on power flow of the architecture. A series hybrid is more electric heavy as it uses the electric motors for propulsion and engine to generate electricity. Parallel tends to be more engine heavy and can utilize both the engine and electric motors to provide torque to the wheels. They both have their advantages and disadvantages but series-parallel can benefit from the advantages of both while potentially being the most complicated. Chapter 2 also provides the vehicle technical requirements determined from the performed market research and selected target market. The vehicle architecture selection section serves to demonstrate the iterative process that can be undertaken in selecting an architecture and its components. It provides the decision matrix used to select the vehicle architecture.

Chapter 3. **Vehicle Technical Requirement Analysis** - Discusses how the vehicle technical requirement can be translated into power and energy requirements to help narrow down the selection of the components. For example, converting the 0-100 km/h acceleration requirement, top speed, or gradeability to the required tractive power and force requirements. Other requirements such as vehicle range can be converted to total energy requirement using the EPA drive cycles to size the battery pack appropriately. This approach can greatly reduce the complexity in selecting the appropriate powertrain components.

Chapter 4. **Powertrain Selection & Analysis** – Outlines the selected powertrain components in addition to providing a brief technology review highlighting some key information that should to be considered when making a selection. For example, which type of engines reduce emissions and fuel consumption. Why do some electric motors cost more than others, and why are some are more power dense. It also discusses the different battery chemistries available for hybrid electric vehicles, and how does its supplied voltage affect the electric motors. It also demonstrates the powertrain performance analysis required to determine if the selected

components enable the vehicle to meet the performance VTR. Lastly, it provides an overview of available vehicle modes enabled by the integrated powertrain architecture.

Chapter 5. **Powertrain Integration** - illustrates the mechanical integration of the powertrain including its design. It outlines the importance of driveline alignment and balancing by explaining the driveshaft and clutch failure experienced during vehicle testing. It also briefly covers the auxiliary components that were required for the vehicle to operate such as the fuel system, electrical integration and the placement of the components in the trunk and engine bay. Lastly, there is a discussion on how these added components have impacted the mass of the vehicle and its distribution.

Chapter 6. **Powertrain Thermal Management -** covers the fundamental theories required to design the correct thermal system for the engine as well as the electrical powertrain cooling loop. It provides the analysis required to determine the heat generation from the components to then determine the required size of the heat exchanger. It outlines the analysis required to determine the system pressure drop of three different coolant loop configuration for the electrical powertrain to size the correct water pump. Lastly, it discusses process used to design the refrigeration system and chiller system with some results to preliminary experiments to illustrate its characteristics.

Chapter 7. **Lessons Learnt & Conclusions** - Lists the lessons learnt by the author throughout the hybridization of the Camaro, either through first hand experiences or indirect experiences. The lessons learnt is provided to help avoid potential mistakes that could cost a project like this valuable time. The conclusion discusses the process used to develop the vehicle, and the challenges faced during the hybridization. It outlines the current state of the vehicle and lists its specifications to compare with the VTR. Note that the vehicle cannot be currently fully tested to compare actual test values due to the recent engine head gasket damage. So instead, simulation values are used for the missing test values.

Chapter 8. **Recommendation** - provides the recommendations on remaining tasks to finalize the vehicle. This includes recommendations regarding the engine, driveline, thermal management, vehicle testing and refinements, vehicle mass, and lastly, supplemental theses. A list of supplemental theses is provided to complement this thesis so that more detailed information can be made available for future readers on the process of hybridizing a vehicle.

CHAPTER 2
Literature Review & Background

2.1 University of Waterloo Alternative Fuels Team

University of Waterloo Alternative Fuels Team (UWAFT) has been founded by Dr. Roydon Fraser in 1996 at the University of Waterloo, and since then has been pursuing in re-engineering vehicles to reduce their emissions [14]. UWAFT has in the past converted stock vehicles to run on alternative fuels, such as propane, natural gas, ethanol, hydrogen, and more recently hybrid electric vehicles. They have participated in nine Advanced Vehicle Technology Competitions (AVTC) including EcoCAR 3 [15] [16]. The team consists of both undergraduate and graduate students, with the graduate students leading the team and supervised by faculty advisors. Over 800 undergraduate students and 23 graduate students have participated thus far. Students are challenged to solve real world engineering problems by applying theories learnt from the classroom and research, solidifying their knowledge, and contributing to the advancement of automotive technology. They are encouraged to apply the latest cutting-edge technologies while also testing out new innovative ideas.

The author shares credit with UWAFT team members and coops for the work discussed in this thesis. Over the course of the EcoCAR 3 project, the author has been heavily involved in the vehicle mechanical design, integration, and refinement. The author filled the following roles within UWAFT:

- Project Manager (June 2017 – July 2018)
- Engineering Manager (June 2016 – June 2017)
- Mechanical Team Lead (September 2014 – June 2016)
- Volunteer Team Member (April 2014 – September 2014)

2.2 EcoCAR 3

EcoCAR 3 is the 11th AVTC series, sponsored by U.S. Department of Energy (DOE) and General Motors (GM), managed by Argonne National Laboratory (ANL). The competition has tasked students from 16 North American university teams in redesigning a 2016 Chevrolet Camaro into a hybrid electric vehicle to reduce its environmental impact, while maintaining performance and consumer acceptability. The competition provides university students with a tremendous amount of resources and groundwork to develop their skills and experience in the automotive industry. The competition spans over four years, with each year having a specific vehicle development goal and competition as shown in Figure 2.1. The first year consists of designing and selecting the vehicle architecture and powertrain components. The integration begins in year-two with the goal of 50% build completion, which is followed with the refinement stage in year-three with the goal of 65% build completion. The refinements and integrations are expected to be completed within the fourth year with a 100% build completion.

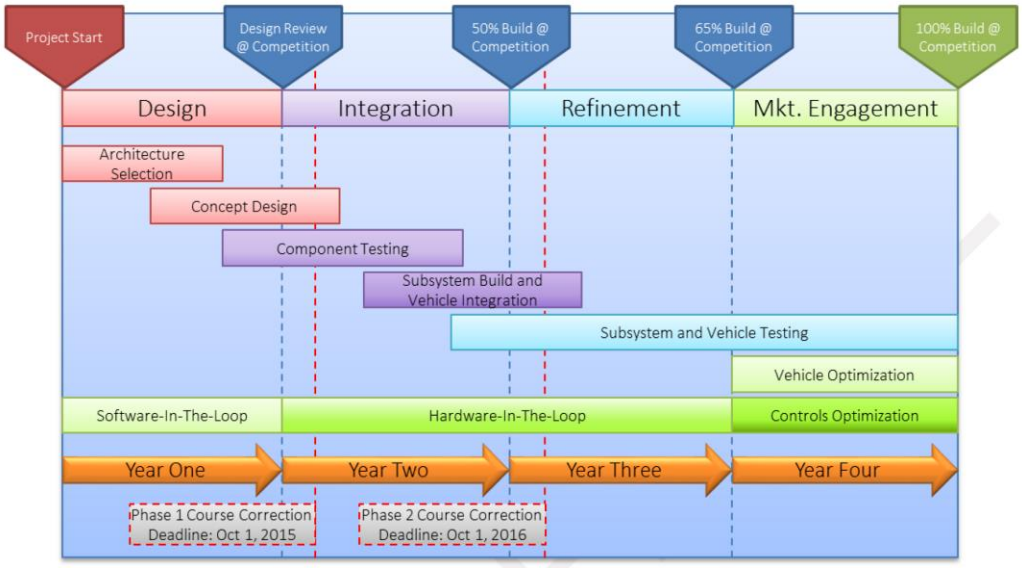

Figure 2.1: EcoCAR 3 Vehicle Development Process [17]

2.3 Hybrid Electric Vehicle Literature Review

Hybrid vehicles use two or more types of power for propulsion; hybrid electric vehicles (HEV) use a conventional internal combustion engine (ICE) in combination with an electric propulsion system such as electrical motors. The major gains in fuel economy and reduction in emissions of hybrid electric vehicles come from utilizing smaller engines, reduction of engine idling, recovering energy during regenerative breaking, and increased flexibility in operating the engine closer to its efficient point. Some hybrid electric vehicles also have the capability of running full electric for a limited range having zero tailpipe emissions for its duration.

Hybrid electric vehicles can be classified as a full hybrid, mild hybrid or micro hybrid [18]. They are categorized based on the power rating of the electric motors and operation, indicating the level of deviation from conventional ICE vehicles. The micro hybrid uses the motor solely for starting and stopping the engine or for regenerative breaking, it is typically no more than 10 kW; it does not provide the capability of propelling the vehicle on its own. A Full hybrid on the other hand can operate the vehicle using just the electric motors up to a certain power requirement and range, while the mild hybrid is in between.

A plug in hybrid electric vehicle (PHEV) differs from HEV by having the capability of also charging the energy storage system through the grid. By having this as an option, the design usually calls for a larger energy storage system to minimize engine usage for charging purposes and instead use it for range extension when required. PHEV are typically full hybrids since they are designed to provide a certain range of electric vehicle mode.

PHEVs or HEVs can be further categorized based on the architecture and power flow as being series, parallel, or series-parallel (also referred to as split-parallel), which is a combination of both [19]. A series hybrid only uses the electric motor to provide mechanical power to the wheels while the engine and generator couple, referred to as gen-set, can charge the energy storage system or provide additional electrical power to the propelling motor. A parallel hybrid on the other hand has both the engine and electric motor coupled to the wheels allowing it to blend their mechanical power for propulsion. Figure 2.2 displays an example of a series and parallel architecture.

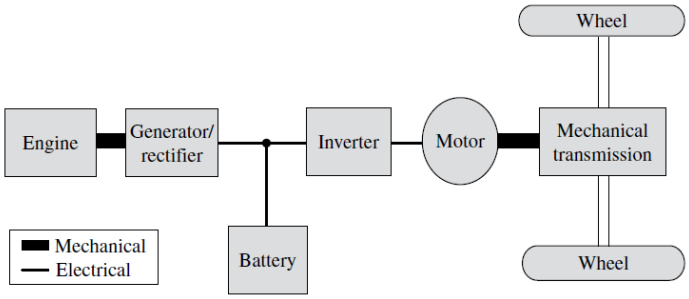

(a)

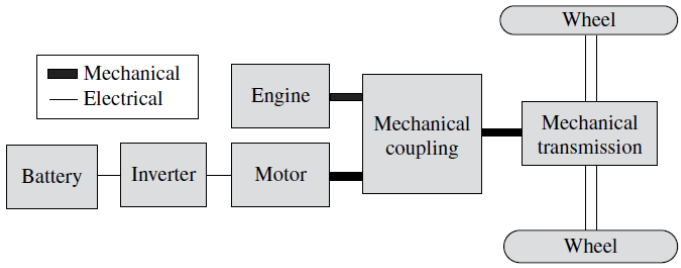

(b)

Figure 2.2: Hybrid Electric Vehicle Architecture Example – (a) Series, (b) Parallel [20]

Parallel architectures can have their drivetrain arranged as a single shaft [19]; meaning the engine, transmission, and motor are all connected together with the an inline shaft, providing the simplest arrangement. The double shaft arrangement has the engine and motor on separate shafts that provide torque to the wheels with a mechanical component coupling them, Figure 2.2 (b) is a double shaft parallel. This better allows the electric motor and engine to operate at their optimal operating speed, increasing performance and efficiency. However, this can get complicated, heavy and expensive.

Additionally, parallel hybrids can also be categorized based on the location of the electric motors within the driveline as pre-transmission parallel hybrid, post transmission, and through the road. Pre-transmission and post-transmission implies that the motor is located before the transmission or after the transmission respectively. Through the road is when the ICE powers one axle and the electric motor the other, this is the simplest design for parallel hybrids since the two power sources are not directly coupled together.

A series architecture requires at least two electric motors to function, one as a generator coupled to the engine as a gen-set, and another coupled to the wheels for propulsion. A series architecture is very similar to an electric vehicle but typically has a smaller energy storage system and uses the

gen-set for range extension purposes. The electric motor connected to the driveline needs to be sized to meet all vehicle power demands thus making it bulky, heavy, and expensive. The engine however can be relatively small, reducing fuel consumption as it is meant for range extension and supplementing electrical power under high vehicle power demand. The architecture is relatively simple since the two power sources are not mechanically coupled. Additionally, this also allows the engine to run at its most efficient operating point more often regardless of the vehicle operating speed. A series architecture can work really well for city driving with a lot of stop and go traffic.

A Parallel architecture can utilize one electric motor and does not need to rely on it to provide all the propulsion since the engine also supplements for mechanical power. However, since the engine is directly coupled to the wheels, the operating speed can no longer be independently controlled at a given vehicle speed. This reduces the capability of operating the engine close to its efficient point most of the time. On the other hand, the motor can be used to adjust the load on the engine to shift it closer to its optimal operating point. Depending on the size of the components, majority of the power could be coming form the engine, motor, or combination of both. Some vehicles utilize the electric motor for a power boost to increase performance with emissions not being so much of a priority. Although the parallel architecture benefits from not requiring more than one electric motor, reducing cost and weight, it does require a more complicated mechanical coupling resulting in a more expensive and heavier drivetrain. The engine also tends to be bigger than in series thus increasing fuel consumption and potentially emissions. The system however can be more efficient than series especially during highway driving, since series can often undergo inefficiencies through converting the engine mechanical power to electrical and then back to mechanical. Another added complexity in the parallel architecture is the controls for the torque blending between the engine and electric motor.

Electric motors can be referred to according to their location in the drivetrain as shown in Figure 2.3. A P0 motor is connected to the engine belt drive, P1 to the crankshaft of the engine, P2 is before the transmission, P3 is after the transmission, and P4 is at the axle.

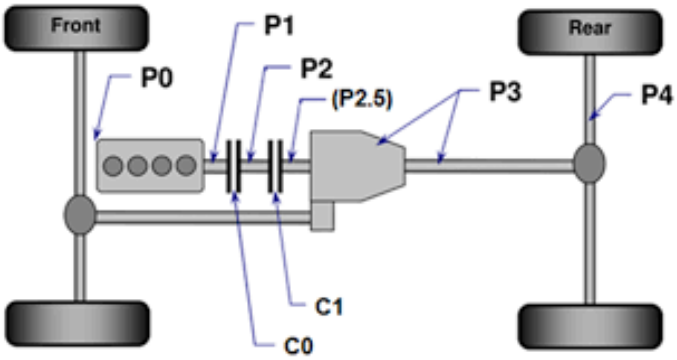

Figure 2.3: Electric Motor Positioning Terminologies [21]

These different architectures typically have multiple vehicle modes to optimize the powertrain during different vehicle operating conditions. The different modes and operating points depend on the component size, characteristics and efficiencies, the battery state of charge (SOC), as well as power and performance requirements. The general vehicle modes and their description is outlined in Table 2-1.

Table 2-1: General Hybrid Electric Vehicle Modes [20]

	Series	**Parallel**
Electric Vehicle (EV) mode	If the energy storage system has sufficient charge and the vehicle power demand can be met by the electric motor(s). Then the gen-set is not used and the vehicle is powered by the energy storage system only.	If the energy storage system has sufficient charge and the vehicle power demand can be met by electric motor(s). Then the engine is not used and the vehicle is powered by the energy storage system only.
Combined power (performance) mode	At higher power demand, the gen set is activated to aid the energy storage system in providing the required power to the electric motor(s).	At higher power demand, the engine and electric motor(s) provide mechanical power to the wheels.
Engine only mode	If the power demand of the vehicle prevents the engine from turning off, or if it may not be efficient to do so, and if the energy storage system is at a high SOC, then during highway cruising for example, the gen-set can power the electric motor(s).	If the power demand of the vehicle prevents the engine from turning off, or if it may not be efficient to do so, and if the energy storage system, is at a high SOC, then during highway cruising for example, the engine provides the mechanical power.
Power split mode	When the vehicle power demand is below the gen-set optimal power supply, and energy storage system SOC is low, then a portion of the gen-set power is used to charge the energy storage system.	When the vehicle power demand is below the optimal engine power band, and energy storage system SOC is low, then a portion of engine mechanical power is converted to electrical power by the motor(s) either through the road or through the mechanical connection.

The aim of a series-parallel architecture is to take advantage of both architectures, further optimizing the vehicle in different conditions by having the capability of switching between the

two different power flows as needed. This does however come at a cost of complexity to the mechanical system and controls strategy. The driveline requires a mechanical coupling that links the engine to the wheels when in parallel and disconnects when in series. Typically, the engine is more active in parallel vehicles while series is more electrical heavy, series-parallel could be designed to be one or the other depending on the vehicle specifications. Figure 2.4 displays an example of a double shaft series-parallel architecture.

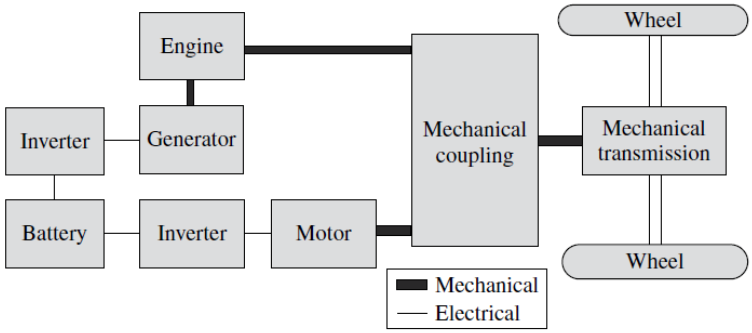

Figure 2.4: Double Shaft Series Parallel Architecture Example [20]

2.4 Market Research & Vehicle Technical Requirement

Before selecting the vehicle architecture including the required powertrain components, a vehicle technical requirement (VTR) needs to be developed to have a clear goal of the specifications required of the vehicle. In order to develop an appropriate vehicle technical requirement, a target market needs to be first determined. UWAFT chose to focus on potential target markets within Canada. The most important factors for a consumer when choosing a vehicle are reliability, cost, exterior styling, previous experience and fuel economy [22]. In pursuit to identifying the target market, information such as income, age, population density, settlement as well as performance expectations were gathered. Income is an important factor to consider as it determines the percentage of the population who would be able to purchase the vehicle.

The average household income in Canada is $76,000 CAD [23] and the average vehicle price is approximately $33,464 CAD [24]. With the average household owning 1.5 vehicles [25]. It can be estimated that on average, a Canadian household typically spends 44% of their annual income to purchase a vehicle. Using that estimate, those who have an income over $84,000 will be more likely to purchase a $37,000 V6 2016 Camaro [26]. Looking at the income distribution in Canada shown in Table 2-2, around 16% of the population in Canada would potentially purchase the Camaro at such a cost.

Table 2-2: Income Distribution in Canada [27]

Income Range (thousand $CAD)	Estimated vehicle Price Range (thousands $CAD)	Percent of individuals
up to 10	up to 4.4	13%
10-20	up to 8.8	17%
20-25	up to 11	8%
25-35	up to 15.4	13%
35-50	up to 22	16%
50-75	up to 30.8	16%
75-100	up to 44	8%
over 100	over 44	8%

The location the target market resides and commutes has a significant impact on the design of the vehicle as it determines the transportation requirements and drive cycle behaviours. Consumers living in urban cities are targeted since Canada is a highly urbanized nation, 82% of the population live in urban cities [28]. Urban cities have a high population density leading to more traffic and lower speed limits. This is mainly due to infrastructures being relatively close to each other such as shopping malls, grocery stores, place of work etc. the transportation is at a much shorter distance than rural cities. Urban cities also tend to have more charging stations available.

Age dictates the features that should be included in the vehicle as well as performance and handling requirements. Those who are generation X still appreciate the classic muscle car look and feel while the younger generation (millennials) additionally have interest in the technology as they tend to be more tech savvy. Some of the additional features they would be interested in would be connectivity with social networks, their smartphones and information provided on the infotainment system.

Upon studying the market segments, the focus has been selected to be on tech savvy enthusiasts in their late 20s and 30s with high income that live in urban areas whom are performance orientated and environmentally conscious. The target market is illustrated in the spider diagram shown in Figure 2.5, it is created using scaled qualitative (fuel economy and performance) and quantitative (age, income, rural/urban) analysis between 0 and 1. The goal is to tap into the muscle car, hybrid electric vehicle, and eco-friendly market.

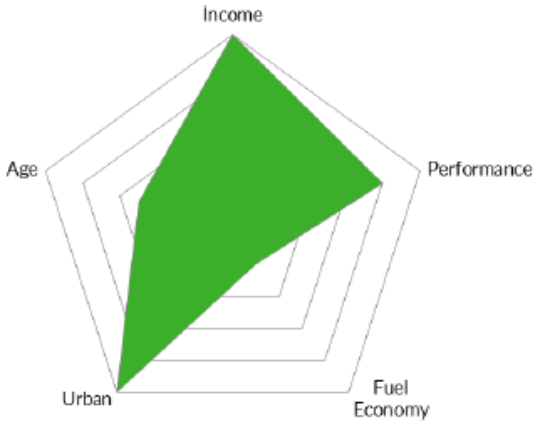

Figure 2.5: UWAFT Target Market for the Hybrid Electric Vehicle Camaro [29]

Table 2-3 lists the vehicle technical requirement established to meet target consumer needs and as a method to determine if the vehicle is market ready for the proposed vehicle market. The table outlines EcoCAR 3 competition requirements as well as UWAFT's vehicle target. The performance requirements are selected such that the vehicle would have similar performance specifications to the V6 stock Camaro in order to maintain the iconic Camaro performance. Additionally, the energy consumption requirements are selected to be competitive with other hybrid electric vehicles in the market. The utility factor (UF) is further discussed in section 3.4 Utility Factor . An EV range of 50 km has been selected, which is greater than the average daily drive length of 40.55 km specified by the Oakridge National Laboratory [30]. Although the competition does not provide a top speed requirement, it is expected that the vehicle can at least achieve the top speed requirement of the EPA drive cycles. A top speed of 240 km/h has been chosen to match the stock Camaro. Note that the established VTR is not necessarily a finalized, locked-in value. Adjustments can be allowed to reflect changes in the target market expectations however; the VTR must not be adjusted to reflect the actual specifications of the developed vehicle.

Table 2-3: Vehicle Technical Requirement [29]

	unit	EcoCAR 3 Requirement	UWAFT Target
Acceleration, 0-100 km/h	Seconds	7.9	5.8
Acceleration, 80 - 110 km/h	Seconds	9.9	3.5
Top Speed	Km/h	N/A	240
Braking, 100-0 km/h	Metre	41	35
Acceleration Torque Split (Front/Rear)	-	49% F, 51% R	0/100
Lateral Acceleration, 90m Skid Pad	-	0.8 G	0.85 G
Double Lane Change	km/h	84	86
Max Grade ability	Degrees	N/A	20
Highway Grade ability, @ 20 min	-	6% @ 100 km/h	6% @ 100 km/h
Cargo Capacity	m^3	0.07	0.08
Passenger Capacity	-	2	4
Curb Mass	kg	1938	1800
Starting Time	Seconds	15	3
Total Vehicle Range*	km	241	300
CD Mode Range*	km	N/A	50
CD Mode Total Energy Consumption*	Wh/km	N/A	268
CS Mode Fuel Consumption (gasoline equivalent)*	Lge/100km	N/A	7.8
UF-Weighted Fuel Energy Consumption*	Wh/km	N/A	736
UF-Weighted Total Energy Consumption*	Wh/km	840	758
UF-Weighted WTW Petroleum Energy Use*	Wh PE/km	750	621
UF-Weighted WTW Greenhouse Gas Emissions*	g GHG/km	250	223

* Evaluated using the EcoCAR 3 combined "4-cycle" weighting method

The vehicle range, power/energy consumption, and emissions are determined using the EcoCAR 3 "4-cycle" driving schedule, which is based on a blend of four certification cycles meant to approximate the energy use seen in the EPA 5-cycle testing [31]. The EPA drive cycles are listed in Table 2-4 including their characteristics followed by Table 2-5 outlining the weighting factor used in the EcoCAR 3 drive cycle. The vehicle velocity profile of the EPA drive cycles can be reviewed in Appendix A. The calculations used to determine the energy consumption can be reviewed in 3.6 Drive Cycle Analysis, in Chapter 3.

Table 2-4: EPA Drive Cycles [31]

Drive Cycle	Characteristics	Distance (km)	Duration (min)	Average Speed (km/h)	Top Speed (km/h)
EPA Urban Dynamometer Driving Schedule (UDDS)	City driving conditions	12.07	22.8	31.5	92.1
EPA Federal Test Procedure (FTP-75)	Identical to UDDS plus the first 505 seconds of an additional UDDS cycles	17.77	31.2	34.1	92.1
Highway Fuel Economy Driving Schedule (HWFET)	Highway driving with no stops	16.45	12.8	77.7	97
US06 Supplemental Federal Test Procedure (SFTP)	Developed to address the shortcomings with the FTP-75 test cycle in the representation of aggressive, high speed and/or high acceleration driving behaviour	12.8	10	77.9	129.2

Table 2-5: EcoCAR 3 Drive Cycle [17]

505	HWFET	US06 City	US06 Highway
29%	12%	14%	45%

2.5 Vehicle architecture selection

After establishing the vehicle technical requirement, the architecture and component selection process can start. This is a highly iterative and rigorous process as there is a multitude of powertrain component combinations available to select from. This paper does not outline all the iterative steps taken during the vehicle architecture selection however, it does demonstrate the process performed in selecting the vehicle architecture and components in this section. Chapter 3 and 4 outlines the analysis performed in selecting the architecture. Some of the potentially viable architectures are listed Table 2-6 along with their benefits and risks. Although the series architecture is considered to be the simplest to implement, it is the least popular selection. It would require the motor(s) to meet the performance VTR resulting in a big, heavy, and expensive component that would have been complicated to install due to space constraints. The vehicle would also have to rely on one propulsion component meaning that if it were to fail, the vehicle would not be able to use the engine for limp mode purposes. To avoid one bulky electric motor, the architecture could instead use two smaller ones that are more feasible to install however, this means that the vehicle would

require three electric motors increasing the cost. After further assessments of the different architecture and components, there were four proposed configurations as shown in Table 2-7

Table 2-6: Potentially Viable Architectures and Components [32]

Vehicle Type	Extended Range Battery Electric Vehicle	E85 Parallel Hybrid Electric Vehicle	B20 Split Parallel Plug-In Hybrid Electric Vehicle	E85 Split Parallel Plug-In Hybrid Electric Vehicle	E85 Series Plug-In Hybrid Electric Vehicle
Vehicle Powertrain	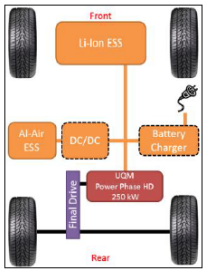	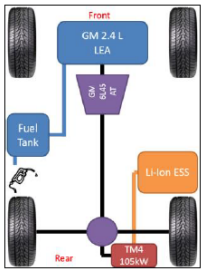	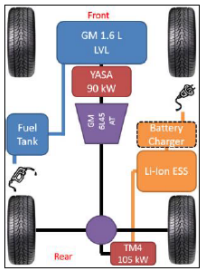	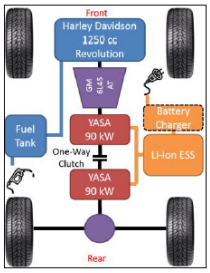	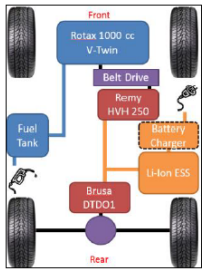
Benefits	• All electric vehicle • Utilizing the best of two battery technologies • Simplest mechanical connection to wheels	• All components can drive wheels • Minimal under-hood modifications • Small battery (weight) • TM4 motor utilized in EC2 Malibu	• Split configuration providing best of series and parallel designs • All-electric CD mode • All components can drive wheels • TM4 motor utilized in EC2 Malibu	• Smaller engine (volume, weight, cost) • Split configuration providing best of series and parallel designs • All-electric CD mode • All components can drive wheels	• Smaller engine (volume, weight, cost) • Torque vectoring built in to rear differential • Previous experience with belt drive design • Engine at optimal efficiency independent of vehicle speed • All electric drive
Risks	• Sponsorship issues with Aluminum-Air battery company • Complex electrical design including DC/DC converter • Possible prolonged charging times required between dynamic events	• LEA similar to LE9 used in EC2 Malibu • Low power CD mode • Small battery (EV range) • Engine cannot always run at optimal efficiency • Modifications to stock differential must be made	• Complex diesel emissions system • Low team knowledge of diesel engine • Complex mechanical integration of electric motor, engine and transmission • Modifications to stock differential must be made	• Complex prop shaft integration of two electric machines • Complex control of series and parallel operations • Clutch performance	• One motor acts as generator (weight, cost) • Inflated traction motor required to propel mass of non-tractive components

Table 2-7: Proposed Four Vehicle Configurations [33]

Vehicle	Architecture Configuration	Engine	Electric Motors	Energy Storage System	Inverter
1	Split-Parallel	Weber (Textron) 850cc Turbocharged	Two YASA-400 motors in P2 and P3 position	16.2 kWh A123 battery pack	PM100DXR
2	Parallel	Hyundai Theta II 2.0L	One YASA-400 in P3 position	12.6 kWh A123 battery pack	PM100DXR
3	Parallel	Hyundai Theta II 2.0L	One YASA-400 in P3 position	Enerdel PP 320-394 battery pack	PM100DXR
4	Parallel	General Motors LEA 2.4L	One YASA-400 in P3 position	12.6 kWh A123 battery pack	PM100DXR

Vehicle one has a split-parallel configuration, the small Weber engine and P2 motor are connected to the drive shaft through the GM 8L45 automatic transmission to the P3 motor and final drive. The electric motors will use an A123 6x15s3p battery with a capacity of 16.2 kWh.

Vehicle two is a parallel configuration using only one YASA-400 motor in the P3 position to supplement power form the Hyundai Theta II 2.0L turbo. In this configuration the engine is directly connected to the 8L45 automatic transmission. The P3 motor will use an A123 12.6 kWh, smaller batteries than vehicle one. In comparison to vehicle one, this larger engine will make the integration in the engine bay more challenging however, there is no complexity of sandwiching an axial flux motor in between the engine and transmission.

The difference between the second and third vehicle is the battery pack, it uses the EnerdelPP320-394 battery with a capacity of 11.2 kWh. The difference between vehicle four and two is the engine, it uses the General motors LEA 2.4L engine. Using a GM engine makes the vehicle integration simpler especially with the auxiliary components however still poses some integration challenges due to its size.

During the integration analysis, the powertrain components along with the critical auxiliary components such as electrical routing, cooling, brakes lines etc. were included in the vehicle 3D solid model to ensure that everything can fit. The integration analysis of the four vehicles and the weight analysis can be reviewed in Appendix B. The vehicle technical specifications has been developed using Autonomie and is displayed in Table 2-8 for comparison.

Table 2-8: Vehicle Technical Specifications Summary [33]

Specification	Target	Requirement	UWAFT	Veh. 1	Veh. 2	Veh. 3	Veh. 4
Acceleration, IVM-60mph [s]	5.9	7.9	5.82	6.2	6.4	6.4	6.4
Acceleration, 50-70mph (Passing) [s]	7.3	9.9	6.6	3.2	3.3	3.3	3.3
Braking, 60-0mph [ft]	128	135	121.4	121	121	121	121
Acceleration Events Torque Split (Fr/Rr)	0/100	49/51	0/100	0/100	0/100	0/100	0/100
Lateral Acceleration, 300ft. Skid Pad [G]	0.85	0.80	0.84	N/A	N/A	N/A	N/A
Double Lane Change [mph]	55	52	54.4	N/A	N/A	N/A	N/A
Highway Grade ability, @60 mph for 20 mins	6%	6%	6%	7%	27%	26%	13%
Cargo Capacity [ft^3]	2.4	2.4	2.4	2.4	2.4	2.4	2.4
Passenger Capacity	4	2	4	4	4	4	4
Curb Mass [kg greater than stock]	**	<314	275	160	180	240	200
Starting Time [s]	2	15	5	N/A	N/A	N/A	N/A
Total Vehicle Range [km]	**	226	301	304	304	293	304
CD Mode Range [km]	**	N/A	36	54.58	54.15	42.95	54.15
CD Mode Total Energy Consumption [Wh/km]	**	N/A	267.8	220.2	267.7	294.9	267.7
CS Mode Fuel Consumption [mpgge]	**	N/A	30	42	37	38	40
UF-Weighted Fuel Energy Consumption [Wh/km]	**	N/A	736.6	227.3	306.0	323.8	291.5
UF-Weighted AC Electric Energy Consumption [Wh/km]	**	N/A	23.8	116.9	91.2	99.6	91.2
UF-Weighted Total Energy Consumption [Wh/km]	700	840	758	344	397	423	383
UF-Weighted WTW Petroleum Energy Use [Wh PE/km]	420	750	621	66	87	92	83
UF-Weighted WTW Greenhouse Gas Emissions [g GHG/km]	225	250	222.6	112.6	119.3	127.7	115.7
UF-Weighted Criteria Emissions [g/km]	TBD	TBD	2.64	0.40	0.41	0.41	0.40

Given the layout of the EcoCAR 3 competition, a two stage decision matrix approach has been made to better assess the vehicle configuration. The first stage is calculating the initial vehicle score (IVS) that can be obtained during competition events as well as taking into account the best possible outcomes (BPO) determined by the team. The second stage is to adjust the score (adjusted vehicle score: AVS) based on the qualitative positive and negative risk values as well as mitigation potential. These factors cover the areas of value to the team, availability, support and knowledge of the components, and complexity and difficulty of integration. In order to better capture these factors, a positive impact factor (PIF) and negative impact factor (NIF) are determined and used in the weighting as seen in equation (2-1)

$$AVS = IVS * \frac{PIF}{NIF} \qquad (2\text{-}1)$$

The maximum points the different vehicles can achieve are outlined in Table 2-9. The decision matrix is then modified with the AVS to also reflect on the aforementioned factors as shown in Table 2-10.

Table 2-9: Quantitative Competition Scoring Vehicle Decision Matrix [33]

Criteria					Veh. 1		Veh. 2		Veh. 3		Veh. 4	
	Objective	BPO	Req.	Points	Raw Value	Score	Raw Value	Score	Raw Value	Score	Raw Value	Score
Performance	IVM-60 (s)	5.3	7.9	35	6.2	28.9	6.4	27.6	6.4	27.6	6.5	26.9
	50-70 (s)	3.2	9.9	20	3.2	20.0	3.3	19.9	3.3	19.9	3.3	19.9
	Handling (%)	50	35	30	45.7	25.7	47.8	27.8	46.3	26.3	48.2	28.2
	Autocross*	N/A	N/A	20		17.8		18.1		17.7		18.1
Energy & Emissions	Energy Consumption (Wh/km)	344.1	840	40	344.1	40.0	397.2	37.9	423.4	36.8	382.7	38.4
	WTW GHG (g GHG/km)	112.6	250	40	112.6	40.0	119.3	39.0	127.7	37.8	115.7	39.5
	PEU (Wh PE/km)	66.1	705	40	66.1	40.0	86.9	39.3	92	39.2	82.9	39.5
	Criteria Emissions (g/km)	0.4	3	30	0.4	30.0	0.41	29.9	0.41	29.9	0.4	30.0
Consumer Acceptability	Drive Quality	10	1	60	9	56.7	6	46.7	6	46.7	6	46.7
	Consumer Acceptability	10	1	40	9	37.8	8	35.6	8	35.6	4	26.7
	Cost Deduction				$ 6,057	-30.3	$ 5,510	-27.6	$ 5,090	-25.5	$ 3,514	-17.6
Score					306.6		294.2		291.9		296.3	

Table 2-10: Qualitative Vehicle Score Adjustment Decision Matrix [33]

	Objective	Weight	Raw Value	Score	Raw Value	Score	Raw Value	Score	Raw Value	Score
Positive Risk and Mitigation	Experience	15%	7	1.1	4	0.6	3	0.5	7	1.1
	Availability and Support	10%	7	0.7	5	0.5	5	0.5	9	0.9
	Facilities	15%	9	1.4	9	1.4	9	1.4	9	1.4
	Engineering Value	30%	9	2.7	7	2.1	7	2.1	2	0.6
	VTT Compliance	30%	10	3.0	5	1.5	4	1.2	6	1.8
	Positive Impact	100%		8.8		6.1		5.6		5.7
Negative Risk	UWAFT Cost	25%	10	2.5	7	1.8	7	1.8	3	0.8
	Mechanical Complexity	25%	9	2.3	5	1.3	6	1.5	5	1.3
	Controls Complexity	20%	9	1.8	7	1.4	7	1.4	5	1.0
	Packaging Complexity	15%	8	1.2	8	1.2	8	1.2	8	1.2
	Waiver Complexity	15%	5	0.8	9	1.4	6	0.9	9	1.4
	Negative Impact	100%		8.5		7.0		6.8		5.6
Factor	Impact Factor			1.0		0.9		0.8		1.0
Matrix Scoring			Veh. 1 Score		Veh. 2 Score		Veh. 3 Score		Veh. 4 Score	
	Initial Score		306.6		294.2		291.9		296.3	
	Adjusted Score		317.4 (1)		256.1 (3)		242.2 (4)		304.3 (2)	

Even though vehicle one seems to be the most complicated and has the highest negative impact, it also has the highest reward and potential to get the most points for the competition. For this reason and taking the VTR into account, the split-parallel architecture was chosen.

Figure 2.6 displays the vehicle architecture selected. Note that the Yassa motors have been replaced with the GKN motors with very similar specifications due to availability. This architecture can be described as a single shaft pre and post-transmission, series-parallel electric heavy plug-in hybrid electric vehicle.

Component Description	Performance Specifications	
Engine: Weber MPE 850cc Turbo	Peak Power	92 kW
Transmission: GM 8L45 AT	Number of Gears	8
	Type	Long. Auto
Final Drive: GM 3.73 Final Drive, eLSD	Final Drive Ratio	3.73 : 1
Motors: GKN AF 130-4	Peak Power at 292V	140 kW
	Cont. Power at 292V	64 kW
Battery: A123 6x15s3p	Capacity	16.2 kWh
	Nominal Voltage	292 V
	Peak Current	600 A
Charger: Brusa NLG513	Peak Power	3.3 kW

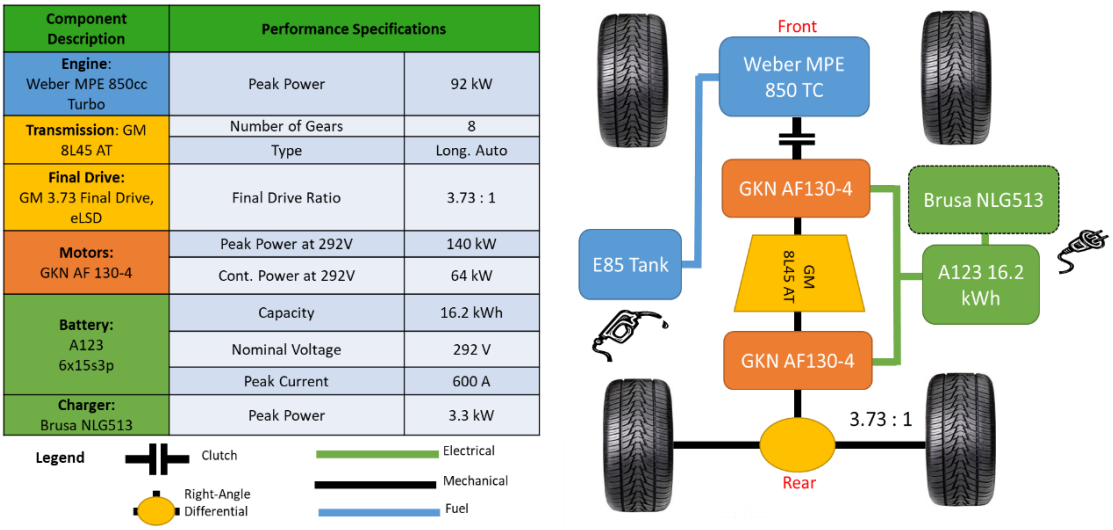

Figure 2.6: Selected Vehicle Architecture [33]

As displayed in Figure 2.7, during electric mode, the battery pack powers the P2 and P3 electric motors to propel the vehicle up to a certain vehicle torque demand, resulting in zero tailpipe emissions. The engine is not utilized in this mode and is disengaged from the driveline using a clutch. Having the electric motors positioned pre and post-transmission allows the vehicle to better utilize them at their high efficiency points. During low vehicle speeds, the transmission gear ratio allows the P2 motor to achieve a higher angular speed, bringing it closer to its more efficient operating region. At higher vehicle speeds, P3 can then operate closer to its high efficiency zone while avoiding transmission inefficiencies and energy loss from the torque converter.

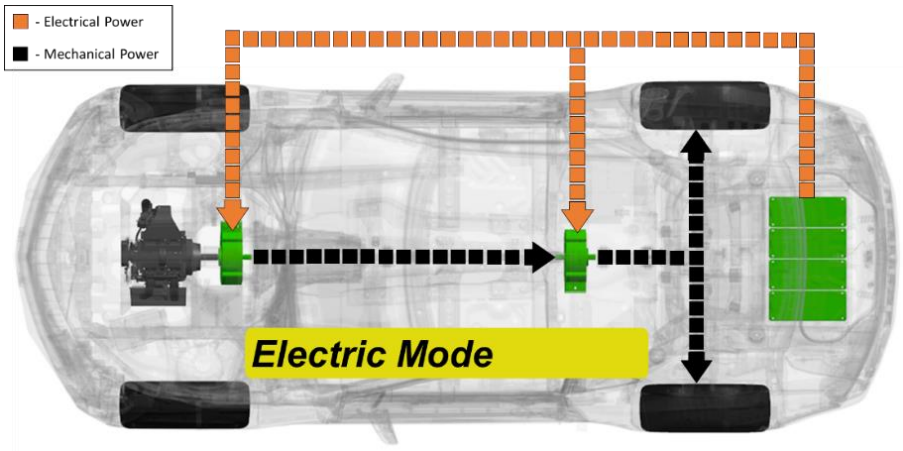

Figure 2.7: Electric Mode Power Flow

The vehicle has the capability of operating in series mode by shifting the transmission into neutral, as shown in Figure 2.8. The vehicle switches to series mode when the vehicle speed, torque

demand, and battery state of charge (SOC) is low. This mode is typically utilized when the vehicle needs to charge sustain during low vehicle speed, such as city driving.

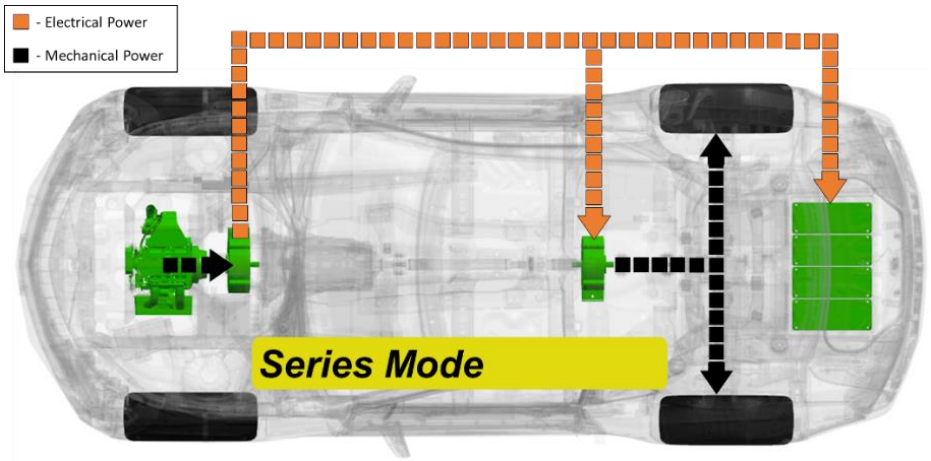

Figure 2.8: Series Mode Power Flow

When full performance is required, the clutch engages the engine, and the transmission is also engaged to allow the three propulsion components to output torque to the wheels, as shown in Figure 2.9. Parallel mode is also utilized when the vehicle needs to charge sustain while requiring a higher torque demand and/or during higher vehicle speeds such as highway driving. The vehicle operating modes are discussed in more detail in 4.6 Powertrain Operating Conditions.

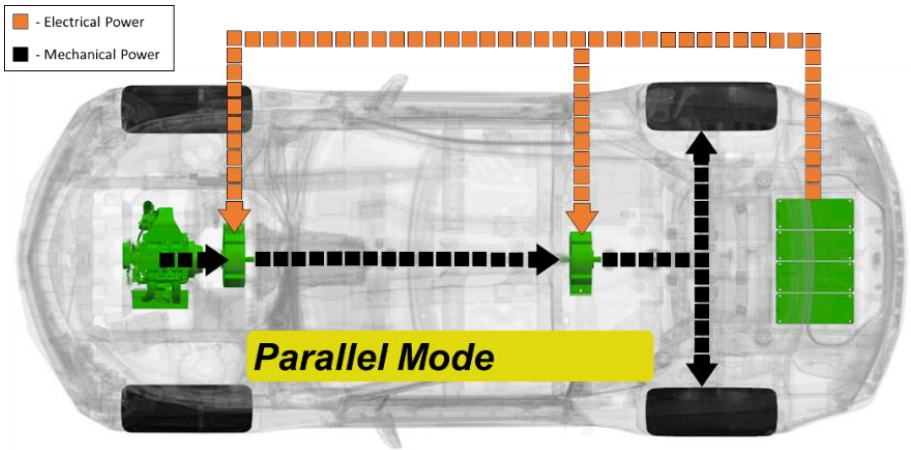

Figure 2.9: Parallel Mode Power Flow

CHAPTER 3
Vehicle Technical Requirement Analysis

The next important step after determining the vehicle technical requirements is its analysis. This section reviews the steps taken to translate the requirements into power, torque and energy requirements for the powertrain component. A proper dissection of the technical requirements is vital in making an informed decision in selecting the suitable powertrain components.

The following sections outline the fundamental calculations used to establish an estimated requirement for the powertrain components. Through modelling, the power and tractive torque requirements at the wheel of the vehicle can be solved to achieve the top speed, gradeability, performance, energy consumption and fuel requirements. Note that these following estimations do not account for the wheel slip, transient behaviours, or any inefficiencies in the driveline or powertrain components. Once the powertrain components have been selected, a more refined and complex model can then be made to better represent the vehicle.

The force that needs to propel a vehicle of mass m, is referred to as the traction force, shown in equation (3-1). This force depends on the torque output, τ, of the propulsion components, such as the engine and electric motors; it also depends on the gear ratio and final drive ratio, G, of the transmission and differential, as well as the radius of the wheels, r_{wheel}, and the efficiency of the driveline, η. The traction force will need to overcome the rolling resistance (equation (3-2)), the aerodynamic drag resistance (equation (3-3)) and the component of the vehicle's weight acting down a slope (equation (3-4)). In addition to overcoming these resistances, the traction force needs to also provide the additional force to accelerate the vehicle if the velocity is to increase, this is referred to as the linear acceleration force, shown in equation (3-5). The force required for rotational acceleration of the components with an inertial mass should to also be considered, shown in equation (3-6).

$$F_{traction} = \frac{\tau G}{r_{wheel}}\eta \quad (3\text{-}1)$$

$$F_{roll} = mgcos(\theta)C_r \quad (3\text{-}2)$$

$$F_{drag} = \frac{1}{2}\rho_{air}A_{front}C_d(v + v_o)^2 \quad (3\text{-}3)$$

$$F_{grade} = mgsin(\theta) \quad (3\text{-}4)$$

$$F_{linear\ acceleration} = ma \quad (3\text{-}5)$$

$$F_{rotational\ acceleration} = I\frac{G^2}{\eta r^2}a \quad (3\text{-}6)$$

Summing up all the forces will result in the total tractive force required to propel the vehicle, shown in equation (3-7). Note that given this is a rear wheel drive vehicle, the tractive force at each rear wheel will then be $\frac{F_{traction}}{2}$.

$$F_{traction} = F_{roll} + F_{drag} + F_{grade} + F_{linear\ acceleration} + F_{rotational\ acceleration} \quad (3\text{-}7)$$

The power the vehicle produces at a given speed and traction force can be calculated by multiplying the traction force by the vehicle speed as shown in equation (3-8)

$$P = F_{traction} \times v_{Vehicle\ Speed} \quad (3\text{-}8)$$

3.1 Top Speed

The traction force and power required to reach a top speed at a zero grade can be determined by using equation (3-7) and (3-8). It is assumed that the acceleration is zero at a given constant top speed therefore, $F_{Linear\ Acceleration} = F_{Rotational\ Acceleration} = F_{grade} = 0$. The required traction force and power at a given vehicle speed has been plotted in Figure 3.1. The required traction force increases with increasing vehicle speed, as it needs to overcome the increasing drag force. At a top speed of 240 km/h, a traction force of 2.44 kN and 163 kW is required.

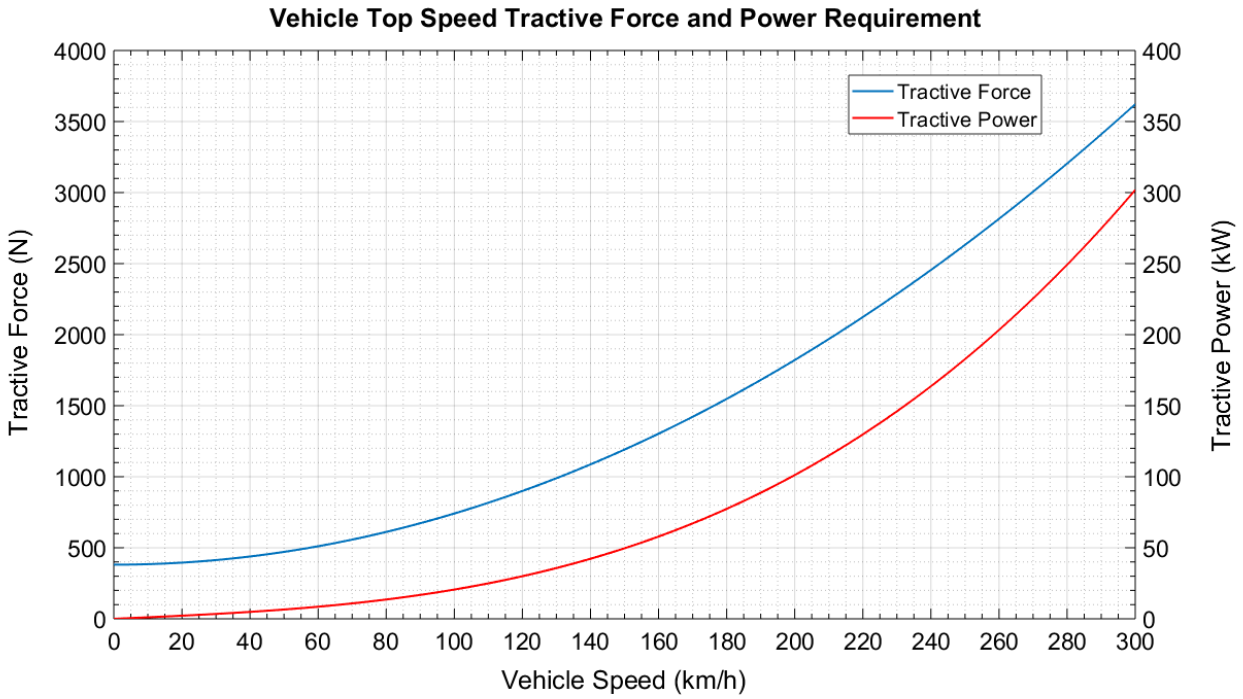

Figure 3.1: Vehicle speed load characteristic with 0 grade

3.2 Gradeability

At the maximum gradeability, it is assumed that the vehicle speed is zero, this results in $F_{drag} = F_{Linear\ Acceleration} = F_{Rotational\ Acceleration} = F_{roll} = 0$ in equation (3-7). The required tractive force at a given grade is plotted in Figure 3.2. Note that the traction force is a result of the friction force present between the tires and the ground. If the traction force surpasses the available friction force, there will be wheel slip, reducing vehicle propulsion. The static friction force can be calculated using equation (3-9), where C_s is the static coefficient of friction, which has been taken to be 0.9 for dry asphalt [34].

$$F_{static\ friction} = m_{rear\ mass} g \cos(\theta) C_s \qquad (3\text{-}9)$$

As the grade increases, so does the component of the vehicle's weight acting down the slope, this increases the traction force required to overcome it; however, it reduces the static friction force. Figure 3.2 shows that a grade greater than 26 degrees results in the required traction force surpassing the friction force, creating slip. The torque required for a maximum gradeability of 20 degrees is seen to be 6.5 kN. Additionally, using equation (3-7), the traction force required to drive

100 km/h at a grade of 6% can be calculated to be 2.4 kN. The power required is calculated to be 66.6 kW using equation (3-8).

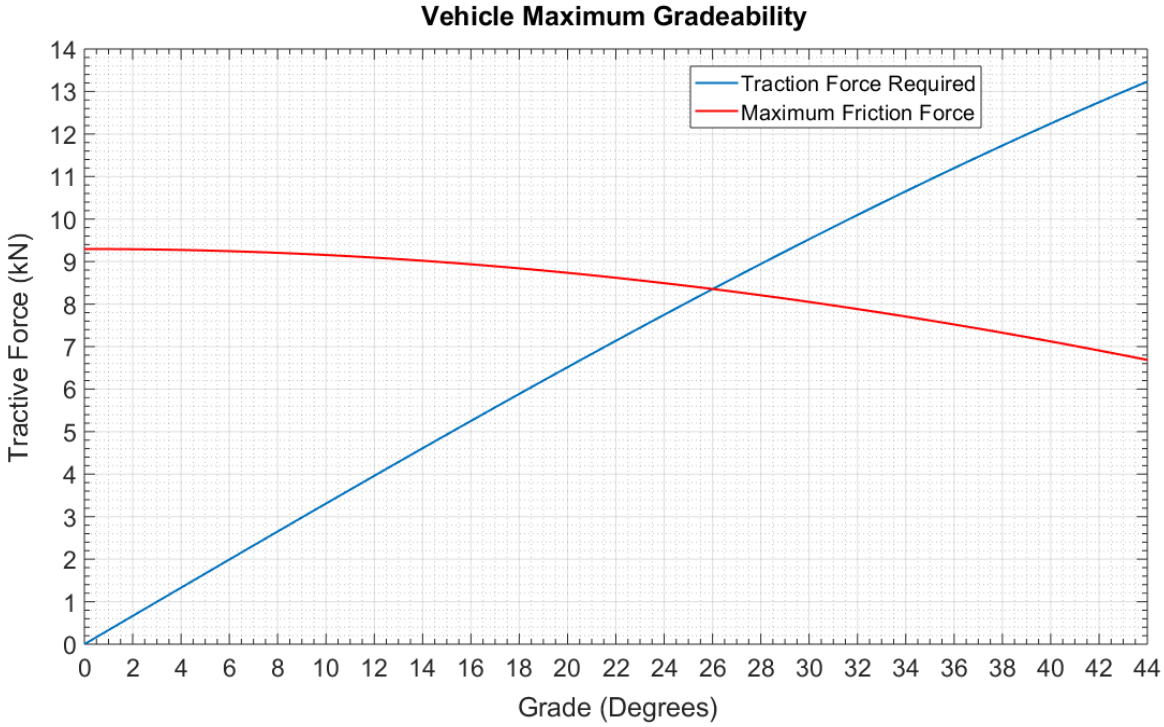

Figure 3.2: Vehicle Maximum Gradeability

3.3 Acceleration

To estimate the required power and tractive force to achieve the 0 to 100 km/h acceleration in 5.8 seconds, three different velocity profiles are considered. One with a constant traction force acceleration, a constant acceleration, and an acceleration that is considered a smooth acceleration [35]. The velocity profile for a smooth acceleration is shown in equation (3-10) [35]. The range of the exponent x is between 0.47 and 0.53, the higher value is used for faster accelerating vehicles.

$$v(t) = v_f \left(\frac{t}{t_f}\right)^x \tag{3-10}$$

The constant acceleration for 0-100 km/h in 5.8 seconds is 4.79 m/s^2, the velocity profile can be determined using equation (3-11).

$$v(t) = at \tag{3-11}$$

As for the required constant force, by rearranging and solving equation (3-7) in terms of the acceleration, which is dv/dt, the velocity profile can be determined as shown in equation (3-12).

$$v(t) = \sqrt{\frac{K_1}{K_2}}\, tanh\left(\sqrt{K_1 K_2}\, t\right) \tag{3-12}$$

Where,

$$K_1 = \frac{F_{Traction}}{m} - gC_r - mgsin(\theta)$$

$$K_2 = \frac{\rho_{air}}{2m} C_d A_{front}$$

The three velocity profiles are shown in Figure 3.3; the constant acceleration and constant traction force velocity profile have a close overlap. The power and traction force required to meet the corresponding velocity profiles can be seen in Figure 3.4. The velocity profile of the smooth acceleration calls for a significant amount of traction force in the first 0.25 seconds, which would be unfeasible. The constant acceleration profile requires the most power and traction force near the end of the acceleration. Hussain suggests that the practical approach would be to accelerate faster than the constant acceleration profile, but less than the smooth acceleration profile, and transition to constant power acceleration approximately midway through the initial acceleration [35].

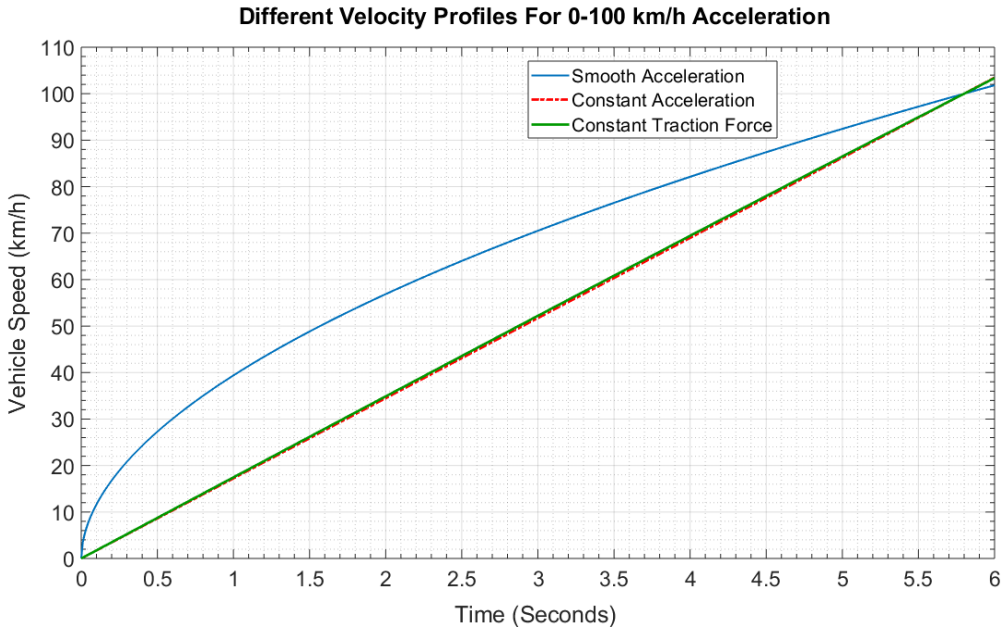

Figure 3.3: Different Velocity Profiles for 0-100 km/h Acceleration

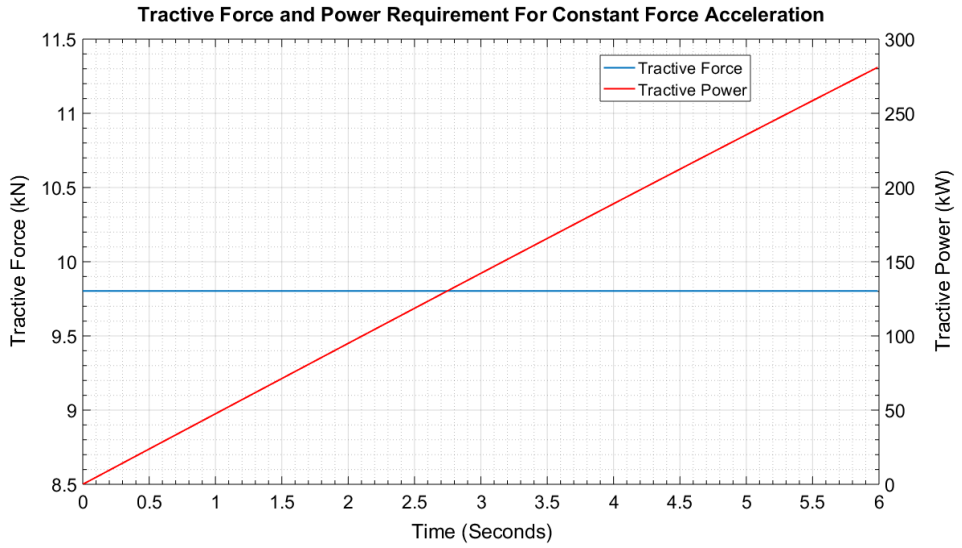

(a)

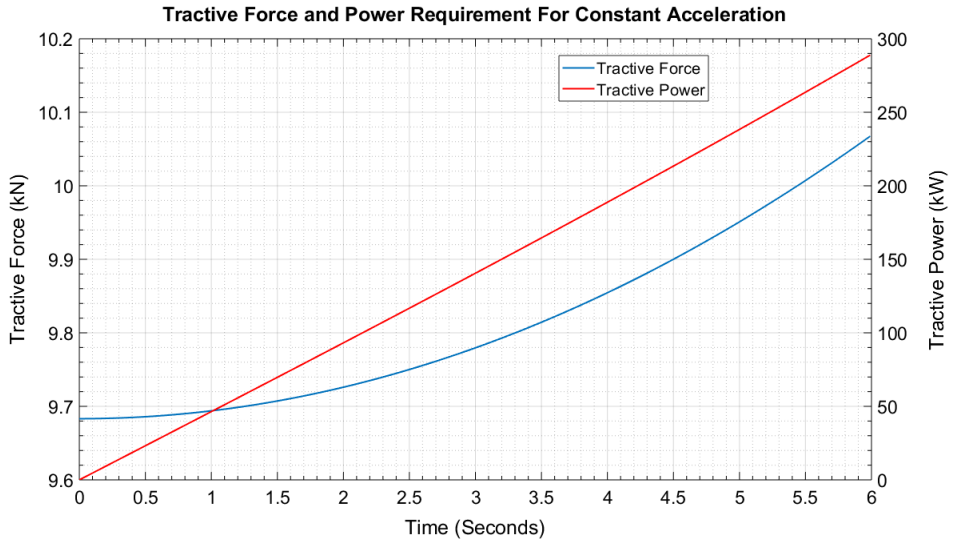

(b)

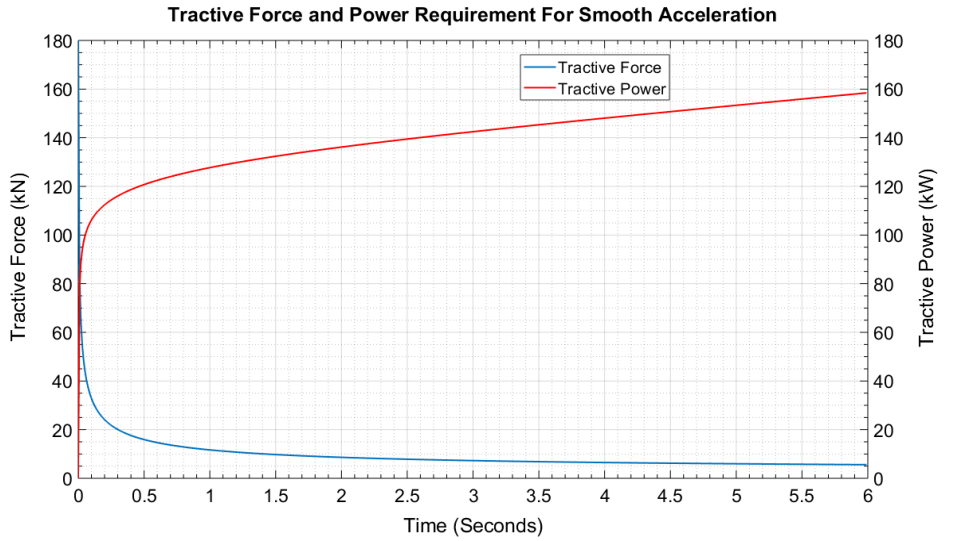

(c)

Figure 3.4: Tractive and Power Requirement for – (a) constant force acceleration, (b) constant acceleration, (c) smooth acceleration

3.4 Utility Factor

Since plug-in hybrid electric vehicles can have distinct CD and CS values for fuel and energy consumption, a utility factor (UF) is used to arrive at a final overall value. The UF essentially represents the percentage of drivers that will drive under the CD range in a given day. The SAE J2841 UF establishes a value for weighting fuel and electric energy consumption for PHEVs, based on the National Household Travel Survey data using equation (3-13).

$$UF = 1 - e^{-\left[C1*\left(\frac{x}{D_{norm}}\right)+C2*\left(\frac{x}{D_{norm}}\right)^2 \ldots + C6*\left(\frac{x}{D_{norm}}\right)^6\right]} \quad (3\text{-}13)$$

Where $D_{norm} = 399.9$, and C1 through to C6 is equal to 10.52, -7.282, -26.37, 79.08, -77.36 and 26.07 respectively. x is the CD range in miles, the UF values are valid from 0 to 400 miles. The UF curve is plotted in Figure 3.5, a 50 km range results in a utility factor of 0.53. This means that 53% of drivers can just utilize the electric mode of the vehicle during their daily commute as long as they charge the vehicle.

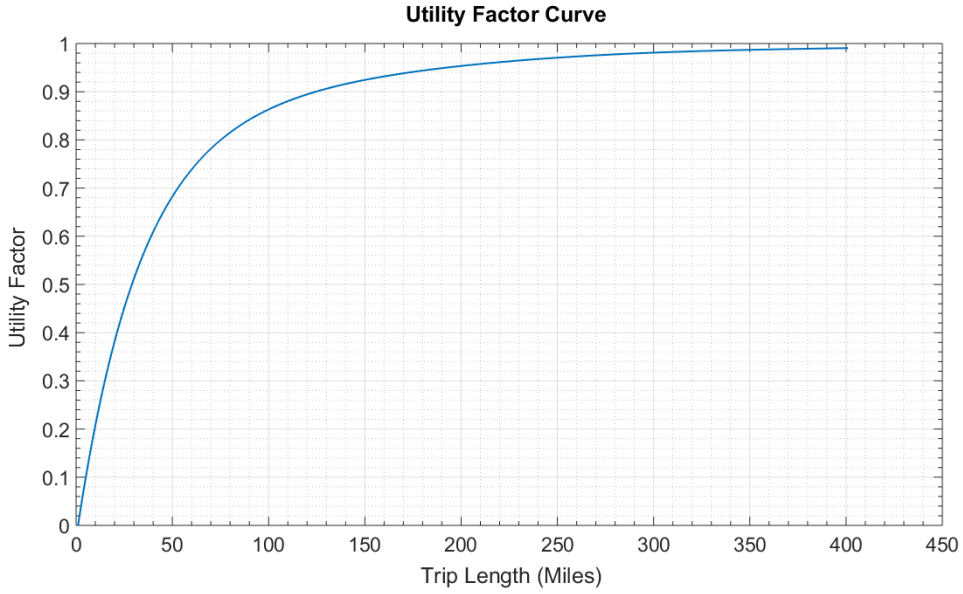

Figure 3.5: Utility Factor Curve

3.5 Energy & Fuel consumption

The following equations for determining the energy and fuel consumption has been used from the EcoCAR 3 Non Year Specific Rule Document [17]. Equation (3-14) displays how the UF value can be used to determine the UF weighted energy consumption (EC). The PHEV CD energy consumption is weighted against the UF, and the remaining percentage (1-UF) is used to weight the CS energy consumption, which will represent the remaining drivers on that same day.

$$Energy\ Consumption_{UF-weighted}\left[\frac{kWh}{km}\right] = EC_{CD}\left[\frac{kWh}{km}\right] \times UF + EC_{CS}\left[\frac{kWh}{km}\right] \times (1 - UF) \quad (3\text{-}14)$$

The energy consumption during charge depletion is the sum of the electric and fuel energy consumed as shown in equation (3-15).

$$EC_{CD} = EC_{electric,CD} + EC_{fuel,CD} \quad (3\text{-}15)$$

However, in the case of this architecture, during charge depletion, the engine is not used, since the two electric motors and energy storage system provide enough power and traction force to meet the drive cycles without requiring the engine, thus $EC_{fuel.CD} = 0$. The drive cycle will be further discussed in the next section of this chapter. To determine the CS energy consumption, the fuel consumption (FC) needs to be multiplied by its fuel-specific energy (FSE) as shown in equation (3-16).

$$Fuel\ Energy\ Consumed\ \left[\frac{kWh}{km}\right] = FC\left[\frac{kg}{km}\right] \times FSE\left[\frac{kWh}{kg}\right] \quad (3\text{-}16)$$

The Fuel consumption must be corrected to include any net DC electric energy used over the drive cycle. The correction is shown in equation (3-17), where η represents the efficiency associated with generating electric power through the gen-set, a typical value is 25%.

$$FC_{SOC-corrected}\left[\frac{kg}{km}\right] = \frac{Mass_{fuel}[kg] + \frac{EC_{electric,CS}[kWh]}{\eta} / FSE\left[\frac{kWh}{kg}\right]}{Cycle\ distance\ [km]} \quad (3\text{-}17)$$

The fuel consumption in gasoline equivalent can be determined using equation (3-18). The fuel energy density (FED) of gasoline is 8.895 kWh/L and 6.265 kWh/L for E85.

$$FC_{gasoline\ equivalent}\left[\frac{Lge}{100\ km}\right] = FC_{actualfuel}\left[\frac{L}{100\ km}\right] \times \frac{FED_{actualfuel}\left[\frac{kWh}{L}\right]}{FED_{gasoline}\left[\frac{kWh}{L}\right]} \quad (3\text{-}18)$$

3.6 Drive Cycle Analysis

As stated in the vehicle technical requirement, the electric mode of the vehicle should have a 50 km range. The drive cycles used by the Environmental Protection Agency (EPA) to determine the tailpipe emissions and fuel economy for highway and city driving are used to determine the battery capacity required to achieve a 50 km all electric range. These drive cycles were explained in Table 2-4. The drive cycles are repeated for a distance of 50 km for the assessment. By inputting the drive cycle into the vehicle model, the amount of power and traction force required to meet the velocity profile can be calculated including the energy required to meet the 50 km range. The results are shown in Table 3-1. An estimated average value of 1.2 kW power draw from the accessories on-board the vehicle has also been included in the determining the energy capacity and power requirements. Note that the negative power values represent the power required to

decelerate the vehicle during the drive cycle. This can be achieved either through the use of brakes or regenerative breaking.

Table 3-1: Power, Energy, and Force requirements for the EPA drive cycles

	UDDS	FTP-75	HWFET	US06
Min Power (kW)	-32.88	-32.88	-47.28	-75.28
Max Propulsion Power (kW)	40.65	40.65	34.05	93.14
Avg Power (kW)	2.97	3.20	8.17	8.11
Avg Propulsion Power (kW)	6.49	6.88	10.55	19.16
Avg Negative Power (kW)	-4.94	-5.15	-9.45	-17.08
Energy Consumption (Wh/km)	160	159	121	175
Total Energy Consumed (mJ)	28.71	28.66	21.84	31.52
Total Energy Loss (mJ)	-11.74	-11.50	-2.73	-13.18
Max Tractive Force (kN)	3.23	3.23	3.14	7.65

The total energy consumption of the US06 drive cycle, which is the most aggressive with the highest requirements, is used to select an energy storage system with a sufficient capacity to achieve a 50 km all electric range. The appropriate electric motor and combustion engine can also be selected by studying the vehicle power and force requirements from the drive cycle as well as the requirements determined to meet the performance specifications. Figure 3.6 provides a four-minute snapshot of the power required to meet the US06 drive cycle, calculated at a one-second interval.

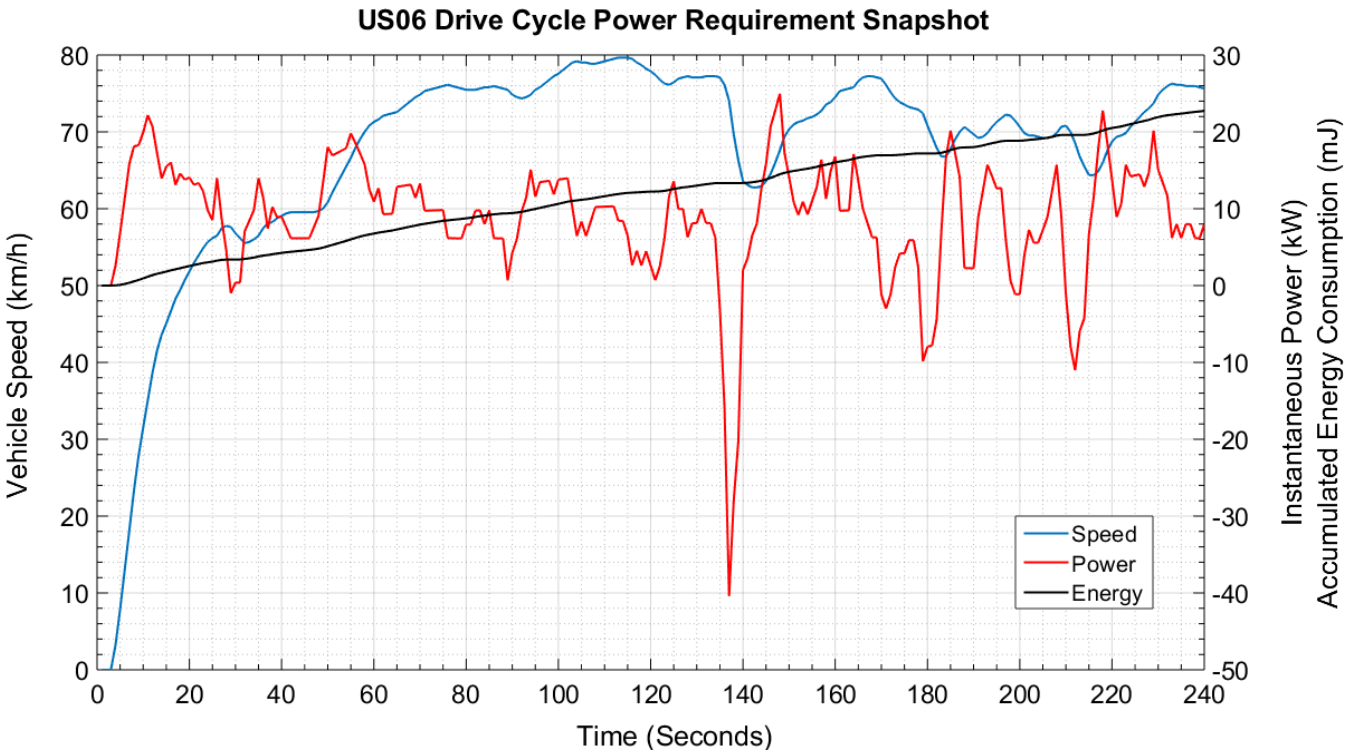

Figure 3.6: US06 Drive Cycle 4-minute Power Requirement Snapshot

The maximum required tractive power and force will be used to ensure that the powertrain component is capable of meeting the drive cycle performance demand. It is however important to understand how often these required peak powers occur, as to avoid oversizing the components. It is best to select the powertrain components so that they can operate at their optimal operating points the majority of the drive cycle, reducing vehicle energy/fuel consumption. Figure 3.7 displays the number of occurrence for a given power demand for the 50 km US06 drive cycle, each occurrence is calculated at a one-second time step.

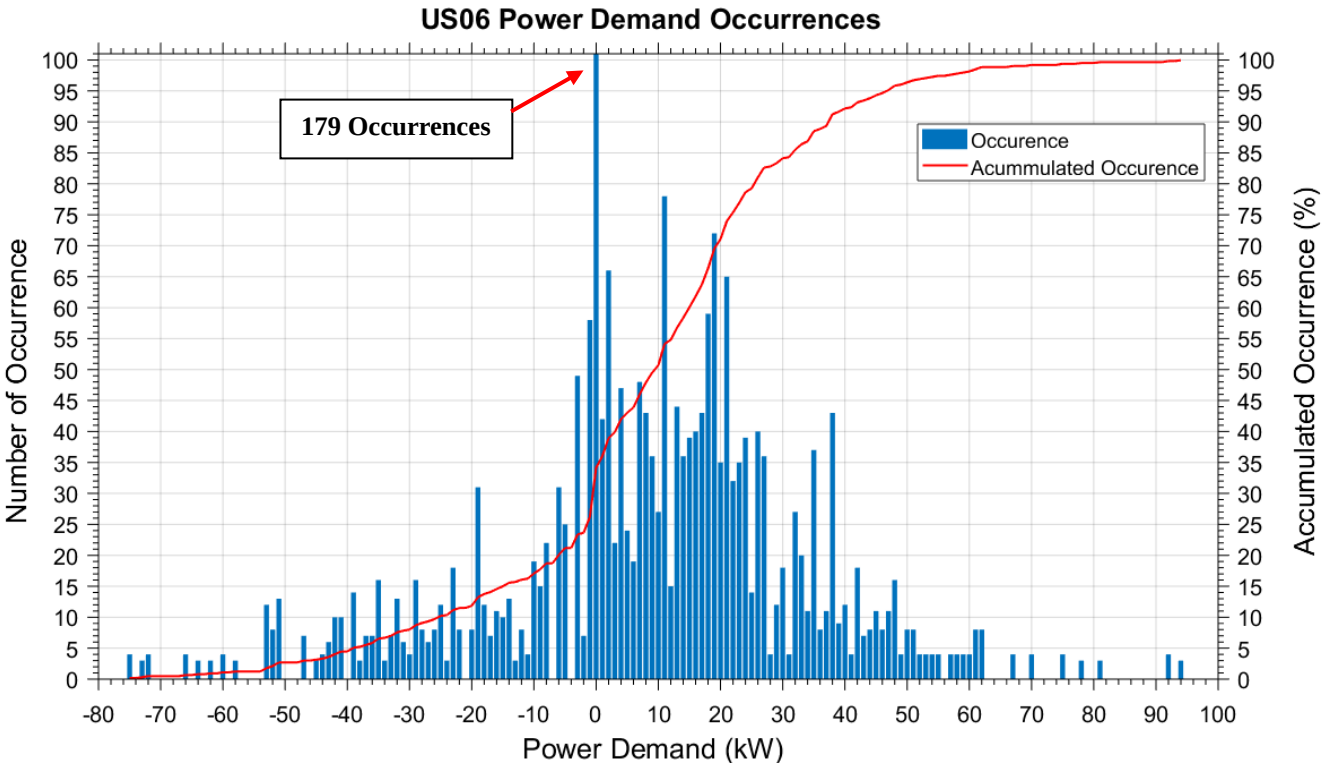

Figure 3.7: US06 Power Demand Occurrences

3.7 Well-to-Wheel

The following equations for determining the well-to-wheel emissions has also been used from the EcoCAR 3 Non Year Specific Rule Document [17]. The two primary components of the well to wheel (WTW) emissions are the upstream well-to-pump (WTP) and downstream pump-to-wheel (PTW) impacts. They can be summed to get the WTW value as shown in equation (3-19)

$$GHG_{WTW}\left[\frac{g}{km}\right] = GHG_{WTP}\left[\frac{g}{km}\right] + GHG_{PTW}\left[\frac{g}{km}\right] \quad (3\text{-}19)$$

3.7.1 Greenhouse Gas Emissions

The utility factor weighted well to pump GHG can be determined using equation (3-20)

$$GHG_{WTP}\left[\frac{g}{km}\right] = FC_{actual\ fuel,UF-weighted}\left[\frac{kWh}{km}\right] \times GHG_{WTP,actual\ fuel}\left[\frac{g}{kWh}\right] + EC_{Electric,UF-weighted}\left[\frac{kWh}{km}\right] \times GHG_{WTP,electricity}\left[\frac{g}{kWh}\right] \quad (3\text{-}20)$$

Where $GHG_{WTP,actual\ fuel}$ = -15.39 for E85 and 488.6 for electricity. The values are based on the weighting of carbon dioxide (CO_2), nitrous oxide (N_2O), and methane (CH_4) as shown in equation (3-21), which is derived from the Intergovernmental Panel on Climate Change's Fifth Assessment Report (AR5). The GHG values for each fuel is collected from the Greenhouse Gases, Regulated Emissions, and Energy use in Transportation Model (GREET) by Argonne National Laboratory [36].

$$GHG_{WTP}\left[\frac{g}{kWh}\right] = (CO_2)_{WTP} + 30(CH_4)_{WTP} + 265(N_2O)_{WTP} \quad (3\text{-}21)$$

Due to the difficulty of measuring the tailpipe emissions of CH_4 and N_2O, only CO_2 is considered for determining the PTW. The UF weighted pump to wheel GHG can be determined by using equation (3-22)

$$GHG_{PTW}\left[\frac{g}{km}\right] = \left(\frac{(CO_2)_{measured,CD}[g]}{dist_{CD}[km]}\right) \times UF + \left(\frac{(CO_2)_{measured,CS}[g]}{dist_{CS}[km]}\right) \times (1 - UF) \quad (3\text{-}22)$$

3.7.2 Petroleum Energy Use

To determine the Petroleum Energy used (PEU) in the manufacturing and use of the fuel, equation (3-23) can be used, similar to the GHG calculation process.

$$PEU_{WTW}\left[\frac{kWhPE}{kWh}\right] = FC_{actual\ fuel,UF-weighted}\left[\frac{kWh}{km}\right] \times PEU_{WTW,actual\ fuel}\left[\frac{kWh\ PE}{kWh}\right] + EC_{Electric,UF-weighted}\left[\frac{kWh}{km}\right] \times PEU_{WTP,electricity}\left[\frac{kWhPE}{kWh}\right] \quad (3\text{-}23)$$

3.7.3 Criteria Emissions

The three EPA criteria pollutants, total hydrocarbons (THC), carbon monoxide (CO), and nitrogen oxides (NO_x) are determined at the upstream and downstream. Upstream criteria emissions (UCE) are released as a result of producing the fuel used by the vehicle and it can be determined with equation (3-24). The E85 UCE factor of THC, CO, and NO_x is 0.0488, 0.0078, 0.0172 respectively and 0.0025, 0.0326, 0.0432 for Electricity. The factors are based on GREET estimates for fuel production.

$$UCE_{NO_x,CO,THC}\left[\frac{g}{km}\right] = UCE\ Factor_{\ NO_x,CO,THC}\left[\frac{g}{kWh}\right] \times EC_{actual\ fuels,UF-weighted}\left[\frac{kWh}{km}\right] \quad (3\text{-}24)$$

The downstream tailpipe emissions are determined by measuring each criteria pollutant using a portable emissions measurement system when the vehicle is operating. The tailpipe and upstream emissions for each pollutant are then summed to get the WTW total.

CHAPTER 4
Powertrain Selection & Analysis

Once the power, force, and energy requirements are determined, the available powertrain components to choose from can be narrowed down, simplifying the selection process. When looking at viable components, other factors must also be considered during the selection process, Table 4-1 lists these important key factors. They can be used in a decision matrix diagram with their weighted importance to better compare between components.

Table 4-1: key factors for component selection that lead to criteria and constraints

	Description
Safety	Safety is always the number one concern. It is important to ensure if the components have the proper certifications and if it is safe to operate in the vehicle. Any additional work required to ensure that the component can operate safely should be considered.
Mounting Points	Are the mounting points easily accessible and appropriate, especially with the orientation it will be in the vehicle? If the mounting points are badly positioned or hard to use, then the mount design can be expensive, time consuming, and possibly have a higher risk of failure.
Size	Does it fit in the available space and does it allow room for other components? If it is an awkward shape then integration can become difficult.
Weight	The weight can impact vehicle performance, handling, fuel emissions, and fuel/energy consumption. It can also increase the difficulty of integration. The heavier it is, the bulkier the mount could be, which can add complexity, cost, additional weight, and take up more space.
NVH	Noise vibration harshness (NVH) can have an impact on consumer acceptability and can potentially damage surrounding components. Dampers could be used to isolate the vibration and noise but it can be complicated and time consuming to find and determine the correct one.
Cost	Cost is naturally an important factor; a budget needs to be set to ensure that the team can afford all the required components to successfully convert the vehicle. Are there any additional benefits to the higher price tag that would justify it? How would higher cost impact the other factors discussed and does it bring the vehicle closer to meeting its VTR?
Serviceability and Maintenance	It is important to understand how often the component would require maintenance and how time consuming it could be. How easy is it to service or fix the component if something breaks? It could be detrimental to the project timeline and costly if the component needs to be sent back to the supplier, which increases lead-time and vehicle downtime.
Auxiliary Components Costs and Availability	It is crucial to understand if the component requires additional auxiliary components to operate. Some components require auxiliary parts that can be just as expensive as the component itself and/or take up a lot of space in the vehicle. Some components could even require additional parts that are hard to come by; therefore, increasing the lead-time and even cost significantly.

Spare Parts Cost and Availability	It is always important to consider having spare parts of critical components available that have a high risk of failure, especially if they have a long lead-time.
Reliability and Durability	Fully developed components tend to be more reliable if they have already been used and tested for other applications or vehicles. Newer components may be cutting edge; however, they may not yet be optimized or lack reliability as they may still have some kinks to iron out. The more durable a component is, the more abuse it can handle while learning how to use the component properly in the vehicle.
Technical Support	Depending on the complexity of the component, technical support is vital. Fully detailed documentations and CAD can help understand the component better and avoid making any mistakes that could result in damaging the component or waste time. It can also be helpful if the component supplier has experienced engineers who are available to answer technical questions.
Complexity	The more complex the component, the more time it will take to understand and the easier it can be to make a mistake. It is important to ask if the added benefits due to the complexity is justifiable. For example, sometimes the more complicated the component the cheaper it could be.
Possible operating orientation	Some components may be required to be tilted to fit in the vehicle due to their awkward shape. It is important to ensure that the component can operate in the required orientation.
Environment operating condition and harshness resistance	If the component is going to be exposed outside of the vehicle then it needs to have protection from the environment harshness such as debris, water etc. It is also important to ensure that the component can operate in environment temperatures, for example -20°C in winter or 40°C during the summer.

The following sections in this chapter outlines the powertrain components selected including a brief technology review highlighting some key features. Understanding these features will aid in making a better comparison between the components to select from. The last section outlines a basic powertrain performance analysis to determine if the powertrain components can achieve the targeted vehicle technical requirements.

4.1 Energy Storage System

The electric motors require an electrical source from an energy storage system such as batteries, ultra capacitors, or even possibly flywheels. The energy storage system can then be charged either by the ICE gen-set, from the power grid (PHEV) or from regenerative breaking. The energy storage system is one of the heaviest and costly component of electric vehicles. Three main things to keep in mind when selecting an ESS is the power capability, energy capacity, and nominal voltage; some other factors to take into account is also cost, weight and the characteristics of the ESS.

4.1.1 Energy Storage System Technology Review

There usually exists a trade off between a high energy density energy storage system (ESS) vs high power density. Higher energy would result in a longer range while higher power would result in more available power for the electric motors. For a given size and weight, a battery can typically store more energy compared to an ultra-high-capacitance capacitor (also referred to as a super capacitor), but have a lower power density. Ultra capacitors can also be drained to zero percent state of charge (SOC) and can endure a lot more charge-discharge cycles [20]. Currently, batteries are the dominant energy source due to their technological maturity and acceptable cost [19]. The comparison of power density and energy density of different ESSs is shown in Figure 4.1. For reference, gasoline has a specific energy of around 12,500 Wh/kg, which is significantly higher than batteries.

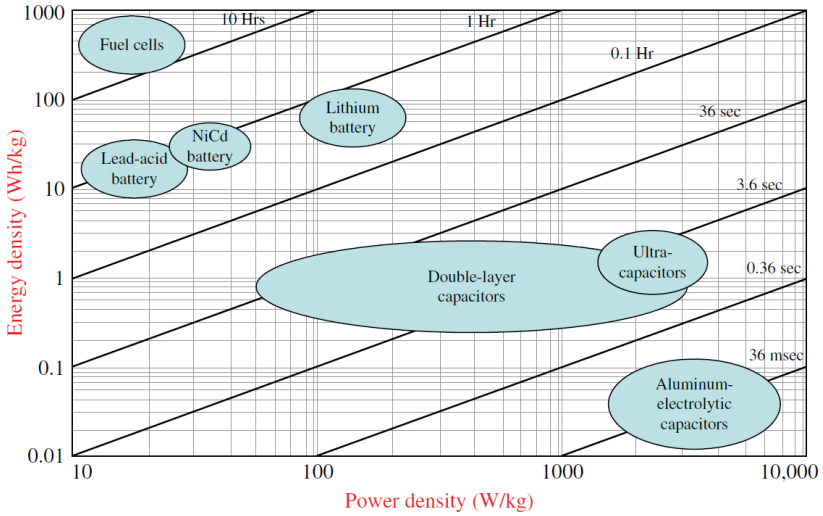

Figure 4.1: ESS Comparison of power density and energy density [20]

Often times, demanding battery peak power as opposed to the rated continuous power can reduce their lifespan. City driving usually involves frequent accelerations, requiring short burst of power, and decelerations, which can result in peak power transfer to the ESS through regenerative breaking. Combining the battery and super capacitor can allow the vehicle to take advantage of both the high energy density and power density (often called a hybrid energy system); however, the system can be complicated to integrate and control. It would also require additional power electronics making it more expensive and heavier.

The basic building blocks of a battery are the cells, once the cells are connected together they form a module. The modules are then connected together to make up the battery pack. This is depicted in Figure 4.2.

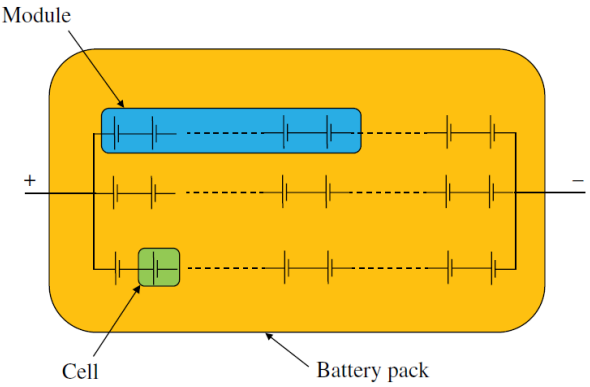

Figure 4.2: Relationship between cell, module, and battery pack [20]

The modules can be assembled in various shapes to better utilize existing space in the vehicle. Some arrangements can be seen in Figure 4.3

(a)

(b)

(c) (d)

Figure 4.3: Different Battery Arrangements - (a) 2016 Chevrolet Volt [37], (b) 2017 Chevrolet Bolt EV [38], (c) 2014 Chevrolet Spark EV [39], (d) Tesla Model S [40]

There are batteries of different chemistries available, which have their own advantages and disadvantages as listed in Table 4-2. Table 4-3 compares some of the key parameters between the different batteries.

Table 4-2: Advantages and Disadvantages of Different Battery Chemistries [19] [20] [18]

	Advantages	Disadvantages
Lead-acid battery (VRLA)	• Mature technology • Availability in a variety of sizes and design • Low cost • Fast recharge capability • High specific power • Robustness against sever temperature variation	• Low specific energy • Limited life cycle • High self-discharge rates
Nickel-metal hydride (Ni-MH)	• High specific energy, twice that of lead-acid • Fast recharge capability • Long life cycle • Wide operating temperature ranges • Environmental friendliness due to their recyclability	• High initial cost • Life cycle is sensitive to high current discharge
Nickel-Zinc (Ni-Zn)	• High specific energy • High specific power • Low cost materials • Deep cycle capability	• Short cycle life
Nickel-Cadmium (Ni-Cd)	• Long life cycle • Rapid recharge capability • Wide operating temperature range (-40°C to 85°C) • Low self-discharge rate • Availability in a variety of sizes and design	• High initial cost • Low specific energy • Cadmium can pollute the environment if not properly disposed of

Lithium-Ion (Li-Ion)	• High energy density • Good high-temperature performance • High specific power • Long life cycle • Recyclable	• High cost • High self-discharge rates • Safety concerns when overcharged or overheated

Table 4-3: Battery Parameters [18] [20]

	Cycle Life	Efficiency (%)	Specific Power (W/kg)	Specific Energy (Wh/Kg)
VRLA	500-800	50-92	180	30-40
Ni-MH	500-1000	66	250-1000	30-80
Ni-Zn	300	80	150-300	60-65
Ni-Cd	600-1200	70-90	150-300	40-60
Li-ion	500-1000	80-90	>3000	130-200

Lithium-Iron-Phosphate ($LiFePo_4$) is a type of Li-ion battery and has the advantages of being more environmentally friendly due to the recyclability of iron and phosphate. It is a relatively safe battery with a lower cost; and has a longer cycle and calendar life. The major challenges it has are estimating the SOC and balancing the cells.

Metal-air batteries have been showing a lot of promise recently as they have a higher energy density than lithium-ion batteries. The metal-air batteries use the oxygen abundantly available in the air as the cathode to "breathe", rather than storing them in liquid or solid chemicals; this makes them lighter, more energy dense, cheaper, and have a simpler structure. Phinergy has claimed that 70 percent of the weight in a conventional battery is in the cathode, mostly just to store the oxygen [41]. There are different types of metals that can be used, some of the common ones are aluminum, Zinc, Lithium, and Magnesium. Recharging these batteries could mean just simply replacing the anode when it is used up which could be done quickly and easily. Dr. Ryohei Mori at Fuji Pigment has invented a new type of aluminium-air battery and has stated that the aluminum-air battery can work just by refilling it with salty or normal water thus drastically reducing charging time [42]. Aluminum-air batteries have a theoretical specific energy level of 8,100 Wh/kg, around 40 times more than lithium-ion batteries. There are however complications with the metal anodes, the catalysts and electrolytes are hindering the development and the implementation of them.

Flywheel storage systems can store energy in a mechanical form while cruising or during regenerative breaking. The mechanical energy can then either be converter to electrical energy with a generator or transferred back to the wheels. They can achieve the potential energy storage system requirements for EV applications as they can have a high specific energy and power, high efficiency, long cycle life, quick recharging, and limited maintenance. The modern flywheel consists of a lightweight composite rotor weighing tens of kilogram but rotate in the order of ten thousands of rpm. A big concern with using the flywheel is regarding failure containment in case of an accident or failure; the stored energy can be released resulting in severe damage to other components or possibly endangering the driver. Flywheels can also have a very high amount of energy loss in a short period due to friction and their integration can also be complicated. Another issue with the flywheel is the possible gyroscopic phenomena, during cornering or travelling on a road with an incline, the generated gyroscopic forces may affect the vehicle's maneuverability.

4.1.2 Energy Storage System Selection

From Table 3-1, it can be seen that for the most aggressive drive cycle (US06), the battery needs to produce at least the maximum propulsion power of 93.14 kW so that the vehicle can operate in electric mode. Furthermore, the battery also needs to provide an energy capacity of 31.52 mJ so that it can provide the electric range of 50 km. Typically the energy capacity of an energy storage system is measured in kWh, meaning the battery can output that certain amount of constant power for an hour. So for example, a 9.7 kWh battery pack can output 9.7 kW continuously for an hour resulting in an energy capacity 35 mJ.

The efficiency of the driveline and electric motors must be considered to determine the correct energy capacity requirement. To overcome these inefficiencies and still achieve a 50 km range with a driveline efficiency of 84% [43], and average electric motor efficiency of 89%; the required energy capacity increases to 40.59 mJ. Additionally, it is also desired to operate the battery between 20% to 90% state of charge to prolong its lifecycle and health. Therefore, only 70% of the battery capacity is usable, further increasing the required energy capacity to 52.76 mJ, which is 14.66 kWh. Note that the potential energy recovery due to regenerative breaking has not been considered in determining the required energy capacity; this is to allow for a less conservative value. It is also worth keeping in mind that the bigger the battery capacity, the heavier the battery

pack will be, increasing the battery dead weight the vehicle has to carry during charge sustaining mode. Similar to determining the battery pack energy capacity, the maximum power required should be also determined by taking into account the inefficiencies of the system. Consequently, to produce a propulsion power of 93.14 kW, the battery should be capable of providing a peak power of 126 kW.

Using the determined power and energy requirements, the 16.2 kWh A123 $LiFePo_4$ battery pack system has been selected for the vehicle. The battery configuration consists of six modules connected in series, the module used is shown in Figure 4.4. Each module consists of three parallel strings, each consisting of 15 cells, totaling to 45 cells per module. The battery pack can provide a continuous discharge power of 51 kW and peak power output of 152 kW for 10 seconds at a nominal voltage of 292. Its continuous charge power rating is 18 kW, which is sufficient for the regenerative breaking as this is higher than the average negative power required to reduce the speed of the vehicle shown in Table 3-1. The peak charge of the battery for 10 seconds is rated to 94 kW, which is also sufficient for the maximum power required by the vehicle to decelerate for any of the drive cycles.

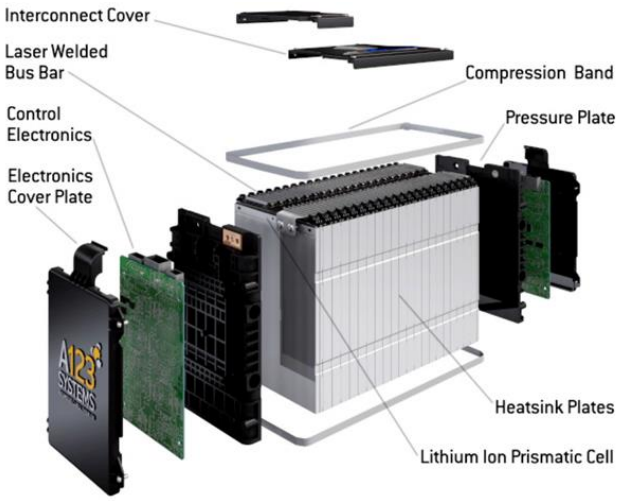

Figure 4.4: A123 Battery Module [44]

Taking into account the inefficiencies, this means that the battery pack can provide 114 kW of peak tractive power and 39.4 kW of continuous tractive power. Looking back on the power requirement occurrences of the US06 drive cycle in Table 3-1, it can be seen that the continuous tractive power can meet 90% of the occurrence and the other 10% can be met with the peak power. Therefore, the battery can provide the necessary power for the vehicle to meet the drive cycles in

all electric. Additionally, the battery capacity of 16.2 kWh surpasses the 14.66 kWh requirement to achieve a 50km electric range. As for the required battery nominal voltage, the requirement depends on the electric motor since it influences its base speed. This is further discussed in the 4.2 Electric Motors section and shown in the 4.5 Powertrain Performance Analysis section.

4.2 Electric Motors

Upon selecting an electric motor, the type, performance, physical size, weight, as well as cost must be considered. These specifications will dictate where the motors should be placed, how many is required and if a gear ratio is required. Since the selected vehicle architecture is a series-parallel, there is a need for at least two electric motors. One that can be used as a generator during charge sustaining while the other can propel the vehicle under low torque demands. The two electric motors must be capable of providing enough torque for the vehicle to meet the US06 drive cycle as to ensure that it can operate in an all electric mode for the 50 km range. Furthermore, the combination of the electric motors and engine must allow the vehicle to meet the vehicle technical performance requirements.

4.2.1 Electric Motor Technology Review

A typical rule of thumb is that unless a high performance cooling system is implemented, most motors of similar size usually have similar torque capabilities. This is due to the material property limitations of the specific magnetic and electric loading. The torque of the motor with a rotor of diameter D and length L can be determined by using equation (4-1). The copper wire used for the windings can only carry a limited amount of current before it is damaged, limiting the specific electric loading. And the flux density in the iron is also capable of reaching a saturation point therefore limiting the specific magnetic loading [45].

$$T = \frac{\pi}{2}\bar{B}\bar{A}D^2L \qquad (4\text{-}1)$$

Where,

$\bar{B}$ = Specific magnetic loading

$\bar{A}$ = Specific electric loading

It can be seen that for given values of specific magnet and electric loadings, the torque for any motor is proportional to the rotor volume, which is proportional to D^2L. The power output can be determined using equation (4-2)

$$P = T\omega = \frac{\pi}{2}\bar{B}\bar{A}D^2L\omega \qquad (4\text{-}2)$$

To reduce cost, size, and weight, manufacturers tend to reduce the rotor volume while increasing the operating rotor speed to compensate for the power loss. This however means that a gearbox will be required due to the drop of torque in the motor. The higher speed can result in a higher acoustic noise and be more unforgiving to any misalignment and shaft imbalances. And the gear box required can also add weight to the vehicle and introduce inefficiencies in the driveline.

The most common shaped electric motors in the market are either cylindrical, illustrated in Figure 4.5(a) or "pancake" shaped, shown in Figure 4.5(b). The most practical shape depends on the required position of the electric motor and the available space. Pancake shaped motors can have splined shafts on both ends allowing them to be positioned inline with the driveshaft. They can be positioned after the engine, post-transmission, post-differential or even in the wheel (Figure 4.5(c)) depending on the vehicle architecture. Manufacturers such as GKN and Bosch have developed their own gear box system specifically for their electric motors to allow for a compact system replacing the differential all together, shown in Figure 4.5 (d) and (e).

(a)

(b)

(c)

(d) (e)

Figure 4.5: Common Shaped Electric Motors - (a) TM4 Motive [46], (b) Phi Power [47], (c) Protean in-wheel [48], (d) GKN eDrive [49], (e) Bosch eAxle [50]

The electric motors can be broken down to alternating current (AC) and direct current (DC) motors. DC motors were widely used for EV vehicles in the past however with the advancement of power electronics, AC motors are taking over, with Synchronous motors taking the lead. IDTechEx surveyed 123 manufacturers and has discovered that 83% of the motor types sold are synchronous motors and 11% are Asynchronous [51]. Typically, AC motors have a higher efficiency, higher power density, more effective regenerative braking, higher robustness, reliability and less need of maintenance [52]. B.C. Groen has developed a detailed breakdown of electric motors as shown in Figure 4.6; he has also shown a very useful motor comparison chart in his appendix for a more detailed comparison. Some might break motors down even further based on the arrangement, manufacture and usage of the components within the motor.

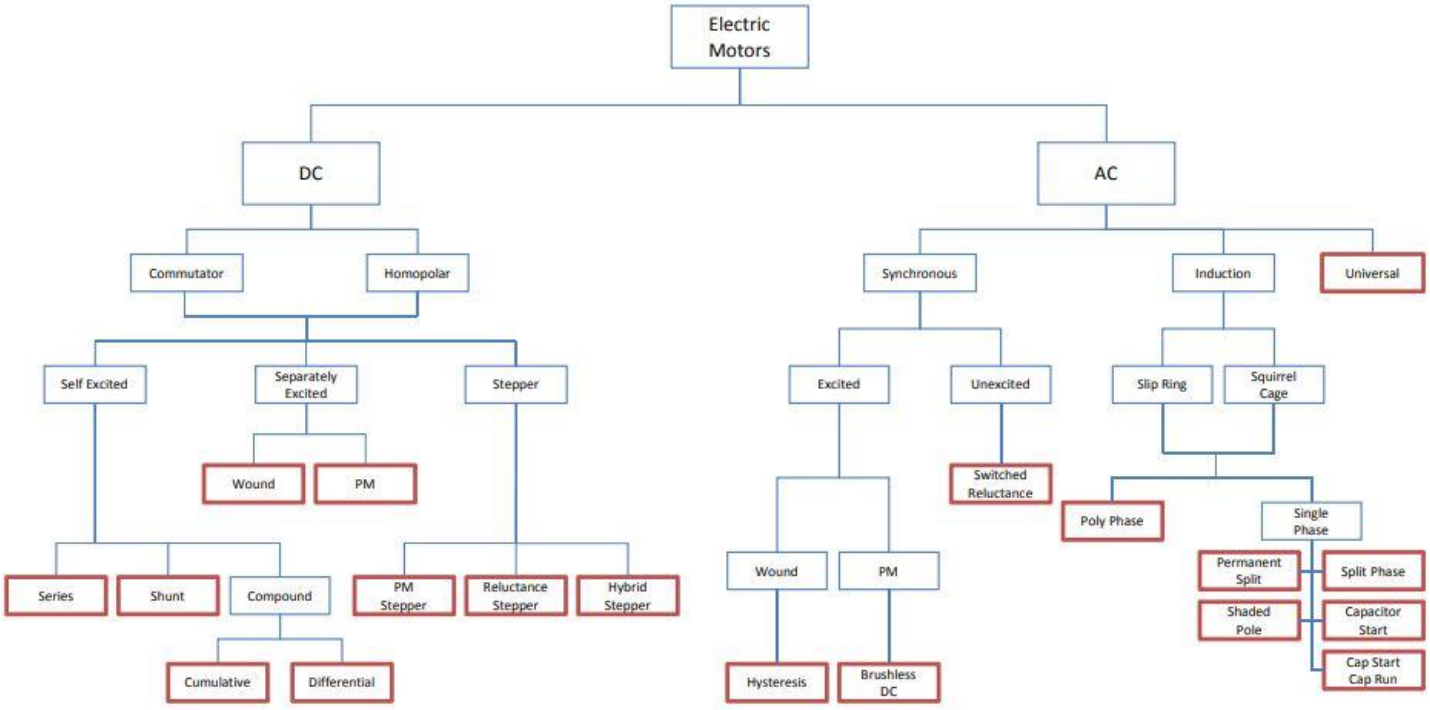

Figure 4.6: Electric Motor breakdown [53]

The most common DC motors available for hybrid vehicles are series wound, shunt wound and separately excited DC motors [19]. Series motors have the field winding and armature in series, it can develop a large amount of starting torque but cannot hold constant speed under different loads. Series motors should never run without load as the speed can reach high enough to damage itself. Shunt motors however, have their field winding connected in parallel to the armature. This allows for a better speed regulation than series but its starting torque is lower than series. Compound motors have the field and armature connected in both series and parallel to take advantage of both arrangements. Separately excited DC motors use a separate supply for the field and armature windings. This means that the torque can be varied by varying flux without changing armature current if the stator is using windings. Permanent magnet DC motors use magnets to supply the field flux but they are limited to the amount of load they can drive. The speed-torque characteristic of permanent magnet motor is similar to shunt motors, it has a relatively higher efficiency and higher power density [54]. Brushless permanent magnet DC motors can overcome some of the downfalls of brushed DC motors however the permanent magnets and controller increases the price. They can run at higher rpms and have lower maintenance costs, less acoustic noise as well

as higher efficiency and can provide a higher torque for the motor size [55]. Their speed-torque characteristics are shown in Figure 4.7.

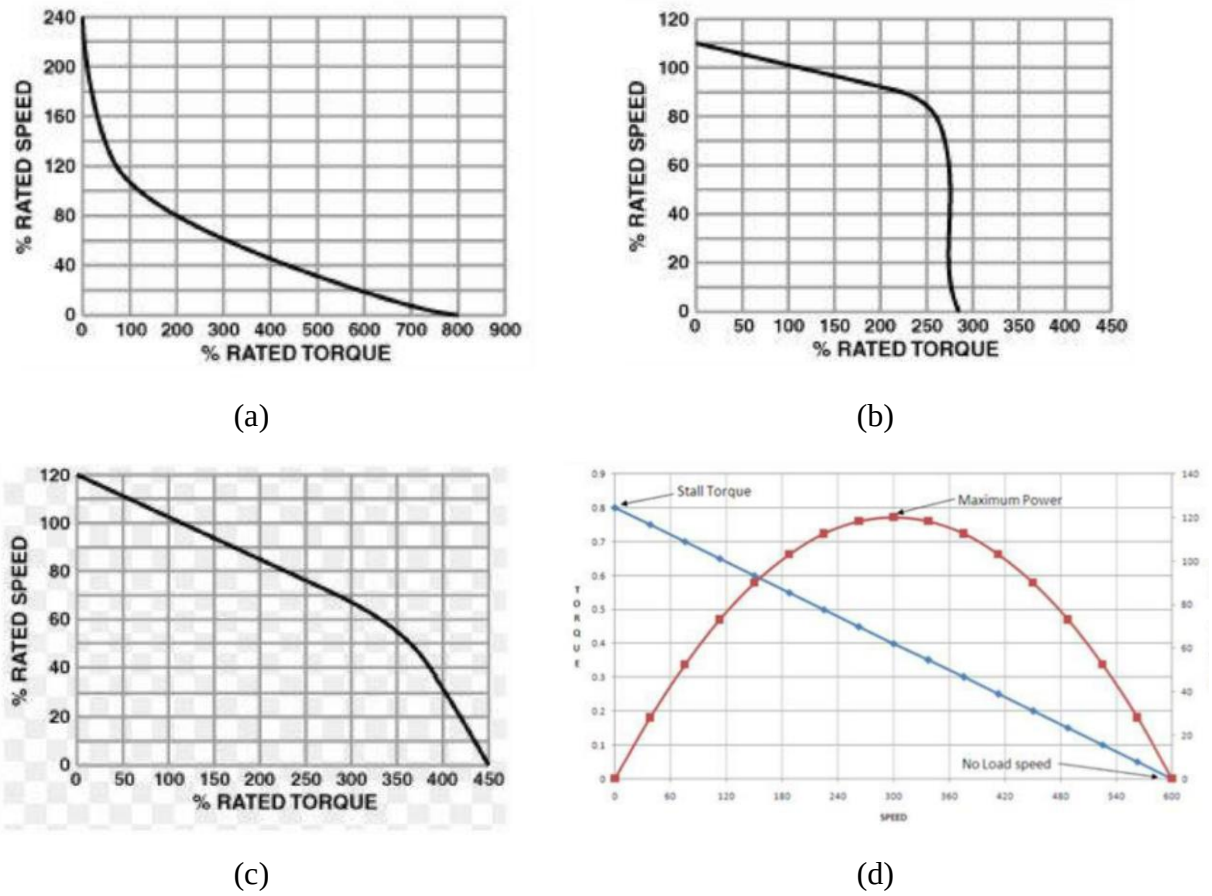

Figure 4.7: DC Speed-Torque Characteristics - (a) Series motor (b) Shunt motor (c) Comulative Compound Motor (d) Brushless DC motor [55]

In AC motors, the stator generates a rotating magnetic field which as a result creates a torque in the rotor. AC motors can be further separated into synchronous and asynchronous (induction) motors, the stator windings are practically the same and operate in the same manner, it is the rotor that varies. The Synchronous motor uses a rotor that is either a D.C. excited winding or permanent magnets, they allow the rotor to synchronise with the rotation of the magnetic field thus having no slip. This allows the rotor to continue spinning at the same speed as the field rotation (synchronous speed) regardless of the load as long as it does not exceed the pull-out torque, which would force the rotor out of synchronism. Permanent magnet motors are more efficient as they do not need the D.C. power to excite the rotor however the field can no longer be controlled. The key benefit of permanent magnet motors is the high power density and efficiency but the permanent magnets

make them expensive. According to the U.S. Department of Energy [56], 50% to 75% of the motor costs are magnetic material costs.

AC induction motors work on the principle of electromagnetic induction in which the stator generates a changing magnetic field inducing an emf across the rotor thus resulting in the rotation. Induction motors are cheaper than permanent magnet motors however they are not as power dense and efficient as permanent magnet motors. Typically, induction motors can be found in larger vehicles such as SUV and buses.

Switched reluctance motors have been seen to have a good potential for hybrid and electric vehicles as they have a simple construction, have low manufacturing costs, and have very good torque-speed characteristics. Switched reluctance motors are not feasible as of yet as they have a high acoustic noise and produce torque rippling [54].

The number of poles influences the speed of AC motors while not so much for DC motors. The Synchronous speed rpm of an AC motor can be determined using equation (4-3). With f being the varying frequency (Hz) of the power supply from the inverter and p being the number of poles the motor has.

$$N_s = \frac{120f}{p} \tag{4-3}$$

If the stator resistance, leakage inductance, and magnetic loss can be ignored, the stator voltage can be calculated using equation (4-4) [20]. Where k_s is the machine constant and the φ is the total flux.

$$V_s = k_s 2\pi f \varphi \tag{4-4}$$

For an electric motor with defined number of poles, equation (4-3) shows that the frequency needs to be increased in order to increase the motor speed. If the torque output (constant total flux) is to be kept constant while increasing the speed, equation (4-4) shows that the stator voltage will also increase. When the stator voltage reaches the maximum allowed voltage or if the power supply can no longer supply a higher voltage, the flux must be reduced/weakened to allow for higher frequency/speed. This would reduce the torque but maintain a constant power output, known as the constant power region or field weakening region. The point at which the motor enters its constant power region is referred to as the base speed. Therefore, the nominal voltage of the energy

storage system can influence the base speed of the electric motor. A typical torque-speed characteristic of an AC motor is illustrated in Figure 4.8.

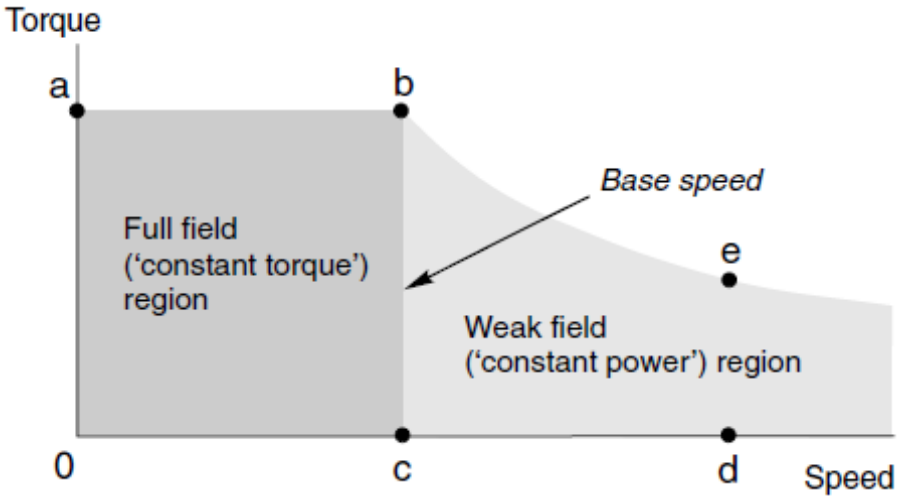

Figure 4.8: Torque-Speed Characteristics of an AC Motor [45]

In addition to the nominal power and torque output found in the specifications of the electric motor, the peak power and torque values that the motor can achieve for a limited amount of time is also usually provided, similar to an energy storage system. The duration and magnitude of this peak load is due to the thermal limitations of the electric motor. It is also critical to review the electric motors efficiency map to ensure that it will operate mostly near its high efficiency point in the vehicle. Figure 4.9 displays a typical electric motor efficiency contour plot.

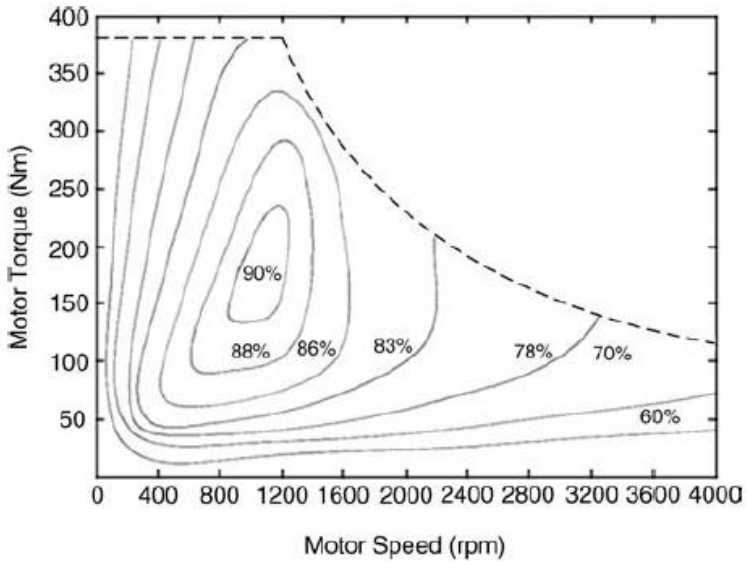

Figure 4.9: Typical Electric Motor Efficiency Map [19]

4.2.2 Electric Motor Selection

Based on the vehicle power requirements, selected vehicle architecture, and compactness required, the GKN pancake shaped motors were selected, shown in Figure 4.10. One is positioned as the P2 motor and the other as P3, their location and integration can be reviewed in Chapter 5 Powertrain IntegrationChapter 5. They are a three-phase, AC permanent magnet motor with axial flux technology. Although they are expensive, the high torque and power density in a compact and light-weight system justifies this extra cost. The compactness of the through shaft motor makes the driveline integration relatively simple with minimal vehicle body/chassis modifications required.

Figure 4.10: GKN AF-130 Electric Motor [57]

Each motor can provide a nominal output power of 64 kW and nominal torque of 145 Nm. The peak output power is 140 kW and peak torque is 350 Nm for 20 seconds. The motors can operate up to a maximum speed of 8000 rpm which is within the range of a typical combustion engine. The power output of the two electric motors is sufficient in meeting the vehicle performance requirements as shown in section 4.5 Powertrain Performance Analysis. The power output of the motor is also sufficient for the purpose of using the P2 as a gen-set with the internal combustion engine during charge sustaining, since it meets the A123 charging power rating.

These motors are available in different number of stator windings, which range from three to six windings. These different windings do not affect the power and torque specification of the motors but does affect the motor constants, which influences the base speed. The lower the winding, the higher the base speed the electric motor can have at the same voltage supply. Initially, the four winding motors were selected for both motors but the P2 motor had to be replaced with a readily

available three winding motor. This was due to the spline damage discussed in 5.3.1 P2 Motor to Torque Converter Interface. This was the only GKN motor that was available at the time of failure for a replacement. The higher base speed of the three winding motor allows for a higher torque and power output however the limitations of the battery power, and restrictions due to the friction force at the wheels, prevents the vehicle from benefiting from this. Therefore, the lower winding does not make a difference in the vehicle performance as explained in 4.5 Powertrain Performance Analysis.

4.3 Internal Combustion Engine

Internal combustion engines are the primary mode of power generation for vehicles today, powering over 600 million passenger cars [58]. They are well-established components that have undergone countless refinements and advancements over the past 150 years leading to various shapes, sizes, and configurations available. Just to mention the few variations, engines can be designed to use different fuel, have different shapes, different number of ignition chambers, and have different methods of injecting fuel and igniting them. The wide variety of different engines available can be overwhelming but is critical to understand how it effects their characteristics, such as their suitable operating conditions, their efficiency map, torque and power map, including their emissions. Another important consideration is the noise vibration harshness (NVH) of the engines, as they can be loud and produce a lot of vibrations, which can impact consumer acceptability.

It is also important to ensure that the engine is compatible with the electric motor it is being coupled to as a gen-set. For example, the engine and electric motor must not have conflicting operating speed requirements. It would be ideal to select an engine that can operate at its optimal operating speed when coupled to the electric motor. The internal combustion engine must also be capable of producing enough power to maintain vehicle charge sustaining mode and meet the performance requirements.

4.3.1 Internal Combustion Engine Technology Review

When comparing engines, the brake mean effective pressure (bmep) is an important parameter to use to simplify the power and torque comparison as it is independent of engine size and speed. The bmep can be obtained using equation (4-5), where w_b is brake work and V_d is the displacement volume. The term brake implies that the power is at the output shaft of the engine, after the mechanical friction and parasitic loads from other components.

$$bmep = \frac{w_b}{V_d} \tag{4-5}$$

The break power and torque can then be determined using equation (4-6) and (4-7) respectively. With N being engine speed and n being the number of revolutions per cycle. The equations indicate that for a given bmep, the brake power and torque will be higher with a higher displacement volume.

$$P_b = \frac{(bmep)V_d}{n} N \tag{4-6}$$

$$\tau = \frac{(bmep)V_d}{2n\pi} \tag{4-7}$$

The brake specific fuel consumption (bsfc) is another important parameter to use when comparing the efficiency of different engines. It measures how effectively the engine converts the stored chemical energy in the fuel to mechanical energy. The bsfc can be determined by using equation (4-8), with $\dot{m}_f$ representing the fuel mass flow rate. The lower the bsfc, the more efficient the engine is, the higher the fuel economy.

$$bsfc = \frac{\dot{m}_f}{P_b} \tag{4-8}$$

The bsfc is typically measured in g/kWh and is represented using as a contour plot, function of engine speed and torque or bmep. A typical example of the contour plot for an engine can be seen in Figure 4.11; the x-axis represents the engine speed in revolutions per minute and y-axis as the mean effective pressure in bar, which is another way to define the engine torque. The lowest bsfc usually tends to be at the mid range rpm and at a high load. In order to minimize vehicle fuel consumption, the engine should be sized such that it mostly operates in that low bsfc region.

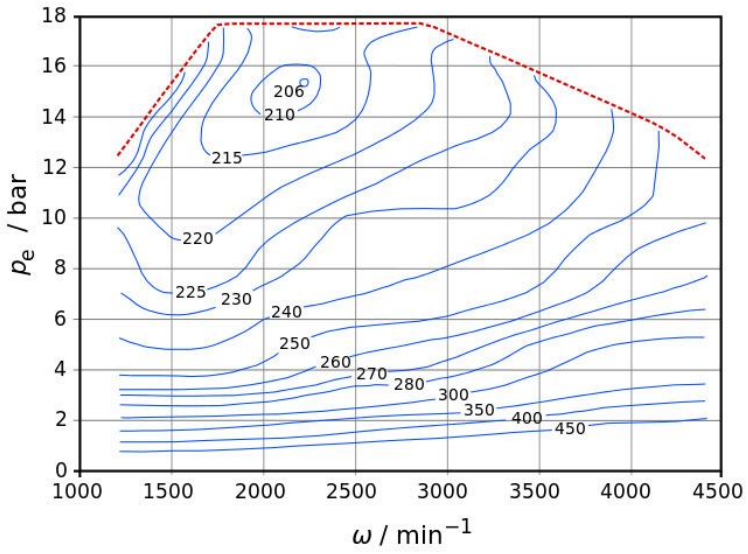

Figure 4.11: Engine Brake Specific Fuel Consumption Example [59]

The emissions are measured using the specific emissions (SE) method or emissions index (EI). SE measures the mass flow rate of the emissions in gm/hr per brake power while EI measures the emissions mass flow rate per fuel flow. There are four main engine exhaust emissions that need to be controlled, carbon monoxide, hydrocarbons, nitrogen oxides, and solid particulates.

The combustion process in the engine requires a sufficient amount of an air to fuel ratio (AF), it can be determined by dividing the mass of air by the mass of fuel. To allow for complete combustion, the engine should operate at the stoichiometric AF, the correct air-fuel ratio required for complete combustion. Being above the stoichiometric AF (referred to as running lean) would result in better fuel economy but higher nitrogen oxide emissions since the engine will run hotter. The engine can produce more power if the AF is less than stoichiometric (referred to as running rich) but the carbon monoxide and hydrocarbon emissions will increase as a result of incomplete combustion.

As mentioned, the internal combustion engine has a wide variety of different configurations available, Table 4-4 outlines some engine classifications to review [60]. Note that this is not an exhaustive list of classifications, however, it does provide some of the fundamental classifications that are important to understand and keep in mind when comparing different engines.

Table 4-4: Engine Classification [60]

Classifications		Description
Ignition	Spark Ignition (SI)	Combustion is initiated with the use of a spark plug
	Compression Ignition (CI)	Air-fuel mixture self-ignites due to high temperature caused by the high compression
Engine Cycle	Four-Stroke Cycle	Four piston movements over two engine revolutions for each cycle
	Two-Stroke Cycle	Two piston movement over one revolution for each cycle
Motion	Reciprocating	The reciprocating motion of one or more pistons in their cylinder rotate the output crankshaft with the use of mechanical linkages
	Rotary	Cylinders are in a radial configuration, the crankcase and attached cylinders rotate around the crankshaft.
Air intake	Naturally Aspirated (NA)	Air intake at atmospheric pressure
	Turbo Charged (TC)	Engine exhaust gas is used by the turbine-compressor to increase intake air pressure
	Super Charged	A compressor that is driven off the engine crankshaft is used to increase intake air pressure
Cylinder arrangement of reciprocating engines	Single Cylinder	One cylinder and piston connected to the crankshaft
	In-Line	Cylinders are positioned in a straight line, one after another
	V engine	Even number of cylinders are at an angle from each other along a single crankshaft. The angle between them can range from 15° to 120°
	Opposed Cylinder Engine (Flat engines)	Even number of Cylinders opposite of each other on a single crankshaft, essentially a V engine that is 180°
	W engine	The cylinder banks resemble a w, same way the V engine resembles a V. Three banks of cylinders sharing a common crankshaft
	Opposed Piston Engine	Two pistons in each cylinder with combustion chamber in the middle, in between. A single combustion causes two power strokes at the same time with each piston delivering power to a separate or single crankshaft
	Radial Engine	Odd number of pistons positioned in a circular plane around the central crankshaft. Not commonly used for automotive
Valve Location	Overhead valve	Valve is in the head (I Head engine)
	Flat head	Valve in the block (L head engine)
Fuel Input	Carbureted	Works on Bernoulli's Principle, the static pressure developed form the air flow determines the amount of fuel drawn into the airstream
	Port Fuel Injection	One or more injectors at each cylinder intake
	Throttle Body Fuel Injection	Injectors upstream in intake manifold

4.3.1.1 Fuel Type and Ignition

The fuel the engine uses has a significant impact on the engine torque-speed characteristics, power density, cost, emissions, and fuel economy. Gasoline fuel is used in spark ignition engines and diesel is used in compression engines; diesel engines tend to be heavier, have a higher NVH and achieve lesser speeds but produce higher torques than gasoline engines. Diesel can achieve a higher

efficiency and fuel economy than gasoline due to it operating at a higher compression ratio, although it does come at a cost. Since diesel operates at a higher temperature due to the higher compression ratio, it can produce more soot, declining air quality as well as more nitrogen oxides (NOx). Particulate filters in the exhaust can significantly reduce the particulate matter but they require good operating conditions and regular maintenance.

Ethanol has been used as fuel for the internal combustion engines for many years now. The ethanol fuel is usually 85% ethanol blended with 15% gasoline, referred to as E85. The interest in using E85 is due to it being a renewable fuel that can be derived from plant material. The entire fuel life cycle GHG emissions of E85 is lower than that of gasoline, Argonne National Laboratory found that the GHG of ethanol is on average of 34% lower than gasoline. That does depend on the source of energy used during ethanol production. E85's tailpipe emissions produces less nitrogen oxide than gasoline, similar amounts of carbon dioxide but a higher amount of carbon monoxide [61]. It is worth noting that there has been studies that state the energy consumed and footprint required to produce ethanol could cause more environmental damages than using gasoline, so there exists a bit of a controversy. It is also found that using cellulosic ethanol can further reduce the GHG emissions by up to 108% [62]. Ethanol is less energy-dense, 30 percent less powerful than a pure gasoline, leading to a higher consumption of the fuel, lowering fuel economy. However, due to E85 having a higher octane rating of around 113 compared to gasoline that could range up to 93, E85 has a higher resistance to pre-detonation [63]. This means that the charged air can be compressed further increasing the power output and potentially efficiency. Lastly, proper precautions need to be taken when using E85, ethanol can damage the engine due to fuel water contamination and corrosion in the fuel system.

4.3.1.2 Four-stroke vs. Two-stroke

There is a popular belief that the four-stroke engines consume less fuel than 2-stroke engines since they consume fuel per every two-engine revolutions. 2-stroke engines can waste fuel when some of the fresh charge of air and fuel mixture exits with the exhaust. The 2-stroke engines are also seen as producing more emissions since the lubrication oil is mixed with the fuel and then gets ejected with the exhaust. On the other hand, two stroke engines can produce more power, they are simpler, have less components and thus are lighter but have a higher NVH. Often times, there is an unfair comparison between these type of engines since usually a cheap 2-stroke engine from a

chainsaw or bike is being compared to an extensively researched and high quality, expensive automotive 4-stroke engine. Enrico et al. made a comparison between a 2-stroke loop scavenged SI engine and 4-stroke engines for a 30 kW range extender. They discovered that the fuel efficiency of the 2-stroke was slightly better while being 15 kg lighter [64]. They also reported that direct injection allows the 2-stroke engine to address many of the typical issues related to fuel consumption and emissions. With the modern goal of reducing engine size to reduce fuel consumption while increasing power density, two stroke engines could have a come back and should not be ruled out during engine selection. Ecomotors has managed to develop a two-stroke, opposed-piston, opposed-cylinder turbodiesel engine that is 30 percent lighter and can have a 15-50 percent increase in energy efficiency [65]. Renault's 'POWERFUL' (POWERtrain for Future Light-duty vehicles) project is looking into developing a 2-stroke 2-cylinder 730cc super-charged and turbo-charged engine that could produce between 35kW-50kW with 112-145Nm of torque from 1,500rpm [66].

4.3.1.3 Air Intake

Engines can either be naturally aspirated, super charged or turbo charged. Turbochargers, like superchargers, compress and force air into the engine's intake manifold. This would allow a smaller displacement, allowing the engine to produce the same power with a reduction of fuel consumption and emissions by 2 to 6 % than a naturally aspirated engine with a larger displacement [67].

4-cylinder turbo charged engines in the capacity range of 2-2.5 liter engines are growing in popularity in the pursuit to reduce emissions and fuel consumption while still maintaining performance. Both Ford and Chevrolet have used a 2-Liter 4 cylinder turbo charged engine in their entry level muscle cars, so are Cadillac, BMW and Porsche. Volvo, Mazda, Nissan, Mercedes and many more also offer similar sized, turbo engines. These engines on average are 15-20 percent more fuel efficient versus naturally aspirated six cylinder engine with similar power, they are also lighter and smaller. These engines can be found in compact cars, luxury sports sedans, SUV's and commercial vans [68].

One must take caution that a turbo charged smaller engine does not always have better fuel consumption and emissions. This is because the engine control unit can sometimes inject more

fuel than required to cool down the cylinders in order to prevent detonation due to the high compression to avoid damaging the engine. This usually occurs during hard accelerations creating a really high pressure [69]. In conclusion, the emissions and fuel consumption of the engine can be low as long as the driver is not aggressive. Hybrid vehicles can reduce the load on the engine supplementing the power with the electric motor or it can run it at a set operating point if in series, ensuring low emission and fuel consumption.

4.3.1.4 Cylinder Arrangement and Motion

Some of the major deciding factors regarding selecting the engine configuration depends on available space, engine capacity/power required and cost. Figure 4.12 illustrates the different cylinder arrangements; inline engines are less wide, compact, and simple but are longer than V-engines and have a higher centre of gravity. Flat engines are small in height and thus help with reducing the center of gravity of the vehicle. It is important to keep in mind that the different engine configurations also have an impact on the noise and vibration harshness. Typically, the inline engines are the worst for vibrations while the V-engines are better followed by the flat engine being the best. For two cylinders engines, in line engines are the cheapest to make however have the worst vibrations. Flat engines are very smooth engines since their primary and secondary forces are well balanced. They are however, complicated, expensive, and maintenance can be challenging. Other configurations like W engines are typically used in high-performance or heavy-duty vehicles, and radial engines are more suitable for aviation.

The rotary engine (Wankel engine), directly converts the pressure into rotating motion instead of using reciprocating pistons and a crankshaft. This makes the engine smoother, compact and high power-to-weight ratio while being able to reach higher speeds. It is approximated to be one third of the size of a piston engine of equivalent power. The major downfall however is the high emissions and low fuel economy. The non-uniform temperature within the chamber makes it challenging to have a good seal. The oil injected in the combustion chamber to maintain the seal is not good for emissions. It also tends to push some unburnt fuel out of the exhaust.

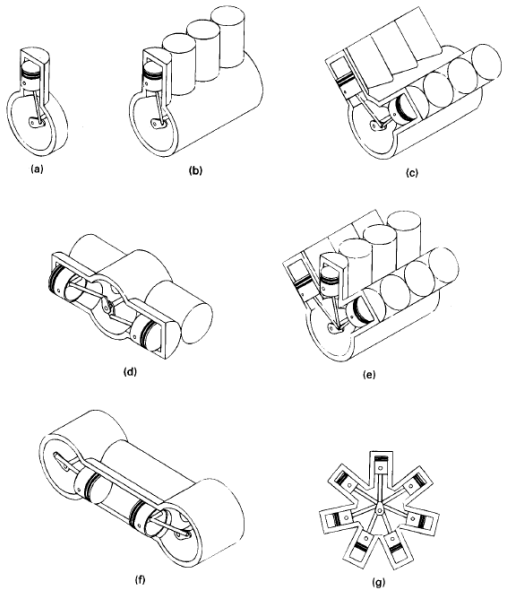

Figure 4.12: Cylinder Arrangements - (a) Single, (b) In-line, (c) V, (d) Opposed (flat), (e) W, (f) Opposed Piston, (g) Radial [60]

4.3.2 Internal Combustion Engine Selection

The engine is to be used for two different purposes for the selected vehicle architecture. The first purpose is to produce sufficient power for charge sustaining mode with the gen-set, either during city driving or highway driving. The second purpose is for the engine to provide the required power in conjunction with the other two electric motors to meet the vehicle performance requirements. Additionally, the engine should be sized such that is meets the charge sustaining mode fuel consumption, UF-weighted fuel energy consumption, UF-weighted total energy consumption, including the UF-weighted WTW Petroleum energy use and GHG emissions requirements listed in the vehicle technical requirements in Table 2-3.

During the selection process, a downsized turbocharged engine had the most appeal since within the scope of hybrid vehicles, turbocharged engines have shown to decrease fuel consumption up to 27% [70]. As a result, the Textron inline two-cylinder, 846cc turbo charged, four-stroke multi purpose engine has been selected as shown in Figure 4.13. This engine has been converted to run from gasoline to E85 and is controlled using an aftermarket motec engine control unit; Patrick Ellsworth covers this fuel conversion process [71]. The engine has been converted to E85 to reduce the greenhouse gas emissions and criteria emissions of the vehicle.

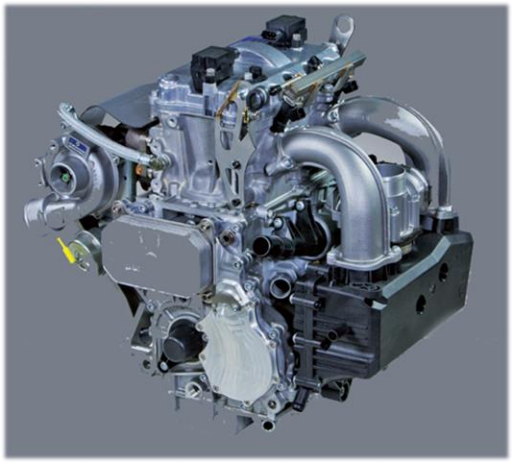

Figure 4.13: Textron Internal Combustion Engine [72]

The engine is capable of producing a max power of 88 kW and torque of 120 Nm; the performance curve is provided in Figure 4.14. The maximum engine speed is 8,000 rpm, which lines up with the operating speed of the GKN electric motors selected.

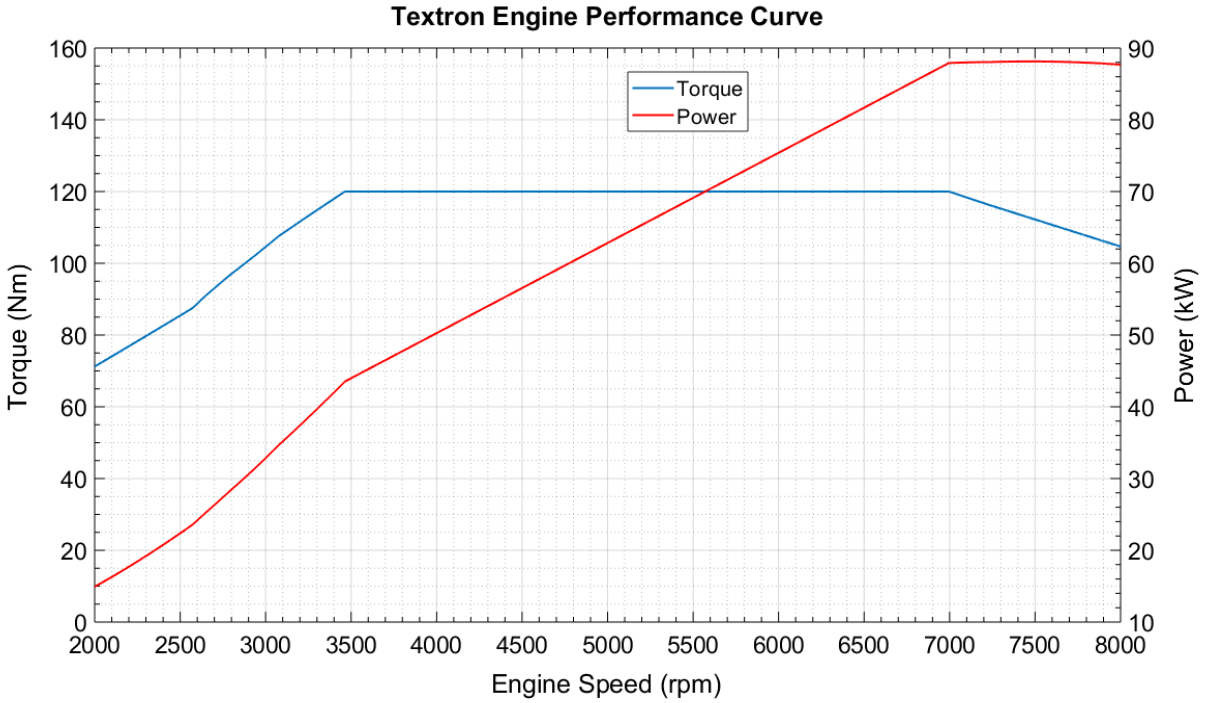

Figure 4.14: MPE-850 Performance Curve

In series mode, taking the electric motor efficiency to be 89%, the engine can provide up to 20 kW of power, which would allow the P2 gen-set to produce power up to 18 kW, this being the maximum continuous charging power for the A123 battery pack. The remaining electrical power generated by P2 through the engine can be provided directly to the P3 motor for propulsion or if

the transmission is engaged, then the additional mechanical power from the engine can go directly to the wheels for propulsion. If required, the A123 battery can also accept the peak power from the engine for 10 seconds to charge, since its peak charging power is 94 kW. The operation of this engine will depend on vehicle speed, vehicle power demand, battery state of charge, and energy/fuel consumption efficiency. Section 4.5 Powertrain Performance Analysis shows that the engine in conjunction with the electric motors allows the vehicle to meet the performance requirements.

4.4 Driveline

The vehicle driveline is required to transfer power from the power plant components, i.e., engine and motor to the wheels for propulsion. The driveline components consist of a gearbox (or transmission), propeller shaft (also referred to as driveshaft), differential, and half shafts (also referred to as axle shaft), including clutches for engaging and disengaging power transmission.

As previously discussed, one of the biggest advantages of an electric motor over a combustion engine is its wider maximum torque band. It can reach its peak torque almost instantly and maintain it up to a relatively high rpm. Typically, to avoid having an unfeasibly big, heavy and expensive electric motor, they are designed to run up to a high rpm but with a lower torque output, thus requiring a gearbox to increase the torque. Depending on the electric motor, it usually only requires a one speed gear ratio. The base speed of the electric motor should also be considered, higher gear ratio will result in the motor reaching its base speed at a lower vehicle speed, consequently reducing performance at high speed as well as limiting top speed. Using a transmission will allow more flexibility in adjusting the motor speed to operate it in its most efficient rpm range. However, the added complexity, weight, and cost as well as the inefficiencies of the transmission itself may not be worth it.

4.4.1 Technology Review

Given that the selected architecture of the vehicle is a series-parallel, a transmission is required for the engine to provide sufficient torque to the wheels at various vehicle speeds, similar to an internal combustion vehicle. The primary types of transmissions are manual, automatic, and continuously variable transmission (CVT). The manual transmission would require the driver to change the gears however, this can be complicated and confusing for the driver, as the drive mode of the vehicle changes based on the vehicle operating condition.

A CVT typically consists of a drive belt that runs within a grooved pulley system with hydraulic actuators providing an unlimited number of gear ratios seamlessly. This means that it can maintain the rpm of the engine in the most efficient rpm region or highest torque region during operation. The CVT can provide an increase in fuel economy, reduced emissions, and improved vehicle performance while also being lightweight and more compact. The CVT does have its own technical challenges like slipping due to lack of minimum traction between the pulleys for example, but they have been successfully integrated in vehicles. Currently, more than 10 percent of vehicles use CVTs [73]. One major obstacle in the acceptance of CVT is due to consumer acceptability; consumers have been dissatisfied with the noise and the sensation experienced during acceleration with a CVT. Since the CVT maintains the engine at a constant rpm during a hard acceleration and does not provide that "bump" that is typically experienced during a transmission shift, it can give a sluggish feel when accelerating, reducing the thrill.

General classification of CVTs are mechanical, which are available as friction or ratcheting systems, and non-mechanical, which can be sub-divided between hydraulic and electrical systems. Currently, the most commonly used CVT systems are variable-diameter pulley or pulley-based CVTs, toroidal or roller-based CVTs and hydrostatic CVTs [19]. Electrical CVT (e-CVT) is used as a power-splitting device to combine the engine and the electric motor/generator power through a planetary gear set. Planetary gear sets can have a combination of two input shafts and one output or vice versa. The Toyota Prius, Honda Civic, Ford Escape and many more hybrid electric vehicles utilize the e-CVT, it has been globally accepted as a standard transmission for hybrid vehicle systems [18]. Another interesting electrical CVT is the magnetic CVT. They achieve the torque transmission and gear ratios using magnetic materials, thus removing the need for mechanical

contact through the teeth and as a result have lower energy losses, less noise, and require no lubrication; however, they are still in development and are expensive.

Generally, a parallel or series-parallel plug in hybrid electric vehicle requires a means to disconnect the engine from the drive train to allow the vehicle to operate in full electric mode. A series-parallel architecture also requires a way to decouple its engine gen-set from the driveline to operate in series. Components such as the friction clutch, or a one way clutch such as the cam clutch, trapped roller clutch or overrunning clutch can be used to prevent power transmission as needed.

The friction clutch allows the transfer of torque through friction, it operates by providing a clamping force on the friction disk from the diaphragm spring. To disengage the clutch, the diaphragm spring must be depressed by an actuator to release the friction disk. A Friction clutch can also operate electrically, referred to as an electromagnetic friction clutch, it uses the electromagnetic force to engage the disk. This removes the need for any mechanical linkages providing a faster and smoother operation without slip, reducing wear. Its disadvantage is high cost and the electromagnetic actuator can dissipate a lot of heat. causing it to overheat over prolonged use.

A trapped roller clutch works differently to the friction clutch, instead of mechanically disengaging the driveline, it allows for transfer of torque in only one direction. Illustrated in Figure 4.15, when the outer race of the trapped roller clutch rotates in the counter clockwise direction, the springs push the balls out, jamming them in between the ramp of the inner race and outer race causing the inner race to also rotate. When the outer race rotates in the clockwise direction, the ball will be pushed against the spring and will have enough clearance for the outer race to rate without rotating the inner race.

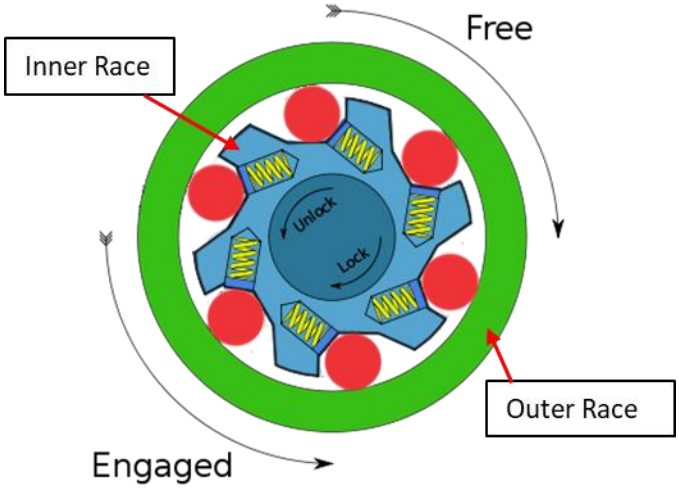

Figure 4.15: Trapped Roller Clutch [74]

The trapped roller clutch's inner race can be connected to the electric motor and the outer race to the combustion engine while positioned in between the two components. During EV mode, the inner race can free spin with the electric motor without spinning the outer race, thus not transferring torque to the engine. If the engine is to operate, it will spin the outer race as well as the inner race transferring torque through the driveline, the electric motor can also operate when required to supplement torque to the driveline. The cam clutch, overrunning clutch (also referred to as a freewheel), and sprag clutch all operate in a similar fashion with the sprag clutch being able to withstand the most amount of torque. The 2017 Toyota Prius Prime uses a one way clutch to allow it to run in EV mode without running the engine [75]. These one way clutches provide a smoother and faster operation than a friction disk clutch since they no longer need to be actuated. They are however expensive and more sensitive to harsh environments and misalignment. They also prevent the capability of quick starting the engine using the P2 motor.

4.4.2 Driveline Selection

Given the limited human resources, budget, and timeline, the stock eight-speed automatic transmission has been kept in the vehicle in the same location. A new transmission would add complications to the conversion of the vehicle; new mounting structures would be required, adding cost. Another benefit to using the stock GM transmission is the resources and information provided by GM making it easier to control the transmission to function with the rest of the components. Automatic transmissions are very complicated, therefore using a non-GM transmission without

any support would have been difficult to implement with the vehicle controls. Designing a custom planetary gear-set would have also been costly and would have required extra human resources. The severity of the risks attributed to designing a custom planetary gear-set is high given that its failure would be detrimental to the operation of the vehicle. The stock GM transmission has shown that it has the appropriate gear ratio to allow the vehicle to achieve the performance requirement, as shown in 4.5 Powertrain Performance Analysis. Figure 4.22 is used to show the total post-transmission torque output of the engine and P2 motor as a result of the different gear ratios at a given vehicle speed, which is used to determine the vehicle performance. Another role the transmission also provides is the capability of disconnecting the engine P2 gent-set from the drivetrain by going into neutral, allowing for series operation.

The architecture still requires a mechanical component that would allow the P2 motor to disconnect from the engine to operate in electric vehicle mode. A hydraulic actuated friction disc has been selected for this application. The one-way clutch is too expensive and has higher risk of failure. Additionally, no off-the-shelf one-way clutch could be found for this application. The stock, 2.77 final drive ratio differential and half shafts has been replaced with a 3.73 final drive GM differential and its half shafts. The new differential and half shafts are compatible with the chassis of the Camaro, requiring no modifications for the integration. The final drive ratio has been increased to allow the P3 motor to output more torque to the wheels, allowing it to meet the drive cycle when the vehicle is in series mode. Lastly, the shaft connecting the engine to the P2 motor, the coupler that connects the P2 to the torque converter of the transmission, the driveshaft connecting the transmission to P3, and the driveshaft connecting P3 to the differential are all made in-house; with the exception of the driveshaft connecting the transmission to the P3 motor, which was outsourced for fabrication. The design and integration of these components can be further reviewed in Chapter 5 Powertrain Integration.

4.5 Powertrain Performance Analysis

Once the combination of the powertrain components are determined, a basic vehicle dynamics model can be developed and used to compare to the vehicle technical requirements analysis, outlined in Chapter 3. The model utilizes the equations outlined in Chapter 3 along with the component parameters to develop the results. This will aid in determining if the powertrain

components are correctly selected. This will then be followed by a more detailed and refined vehicle model that includes plant and controller models, once more specifications are known and/or attained from tests/experiments. This section serves as an example to represent how a basic model can be developed to ensure that the vehicle can meet the performance values of the vehicle technical requirement.

Figure 4.16 displays the peak tractive force and power the two electric motors can provide to the wheels at a given vehicle speed. An average driveline efficiency of 84% has been used to represent the total inefficiency of the transmission, propeller shaft, universal joints, differential and driveshaft [43]. The inefficiency of these components depend on the speed, and in the case of the transmission and differential, the fluid temperature. Notice that the peak power of P2 and P3 do not reach the rated 140 kW. This is because the base speed at which the motors enter their constant power region is lowered due to the limited voltage available from the energy storage system. For this reason, the peak power of P2 is seen to be 92 kW, and 66 kW for P3, totaling to 158 kW. P2 is the motor that has been replaced by a three winding configuration while the P3 motor has the four winding configuration. This means that the base speed of the P2 motor is higher for the limited voltage available, hence the higher peak power. It can also be seen in Figure 4.16 that the P2 motor approaches its constant power region at a lower vehicle speed. This is due to the gear ratio of the transmission.

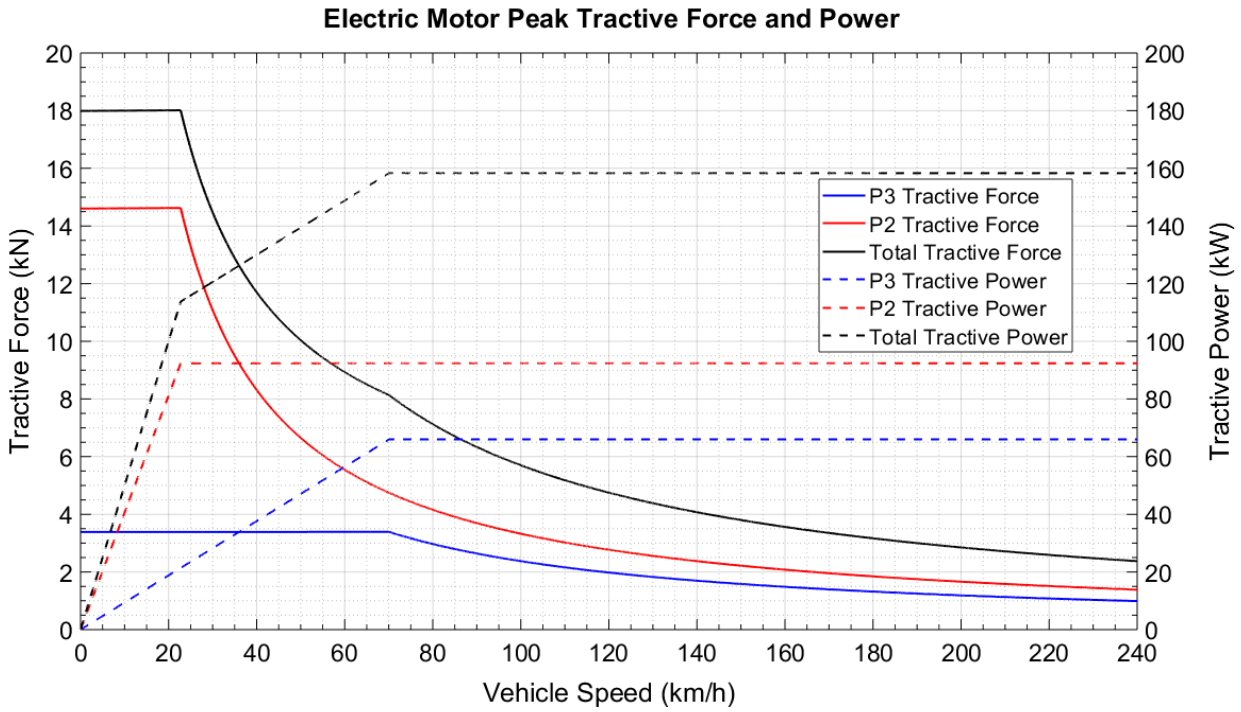

Figure 4.16: Electric motor peak tractive force and power

Although Figure 4.16 is taking into account the voltage limitation of the battery to determine the peak available power from the electric motors. Another limiting factor that should also be considered is the available power from the energy storage system. The A123 batteries selected are capable of providing a peak power output of 152 kW for 10 seconds. With the average motor efficiency taken to be 89%, the two electric motors are limited to produce a total maximum power output of 135 kW. Furthermore, taking into account the average driveline efficiency of 84%, the maximum power at the wheels of the vehicle is reduced to 114 kW. To maximize vehicle performance, the control strategy prioritizes the available battery power to the P2 motor as it has the transmission torque gain advantage. The remaining available battery is then provided to P3. Figure 4.17 displays the available peak power from the electric motors when the battery power limit is included.

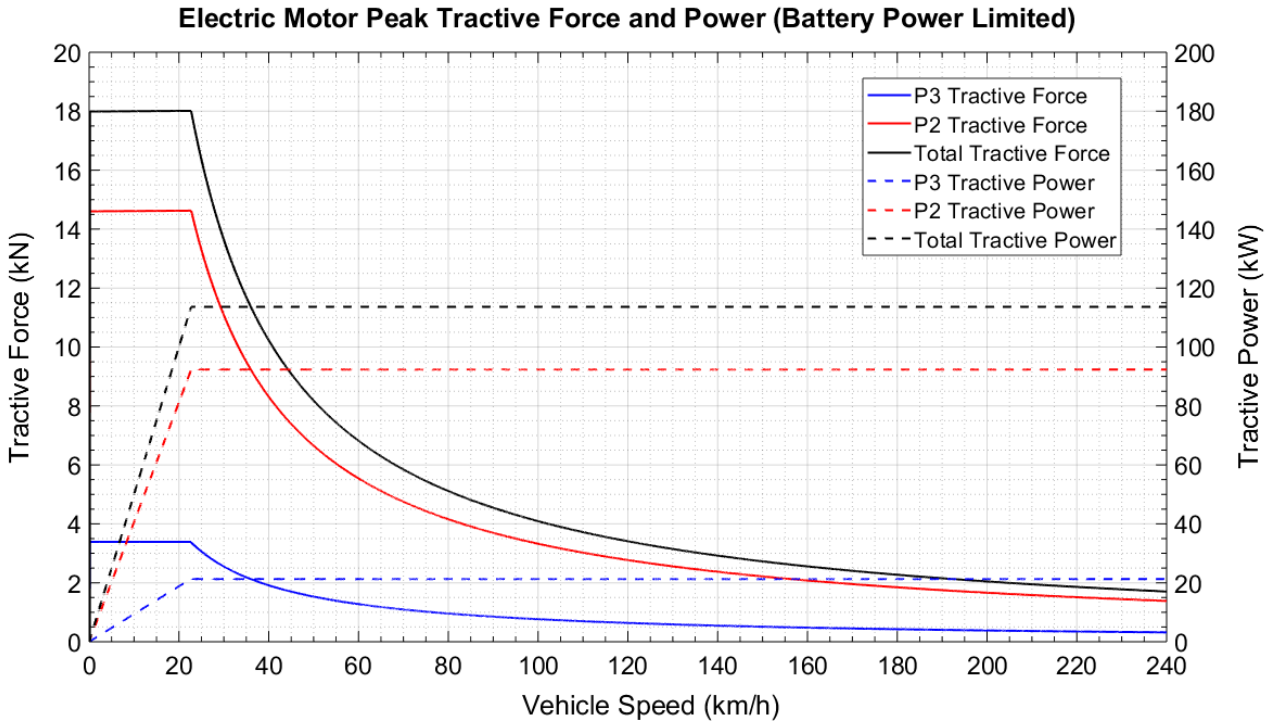

Figure 4.17: Electric Motor Peak Tractive Force and Power (Battery Power Limited)

As discussed in section 3.2 Gradeability, the traction force is a result of the friction force on the wheels. If the traction force surpasses the available friction force, there will be wheel slip, reducing vehicle propulsion. Using equation (3-9), it is found that the maximum traction force before wheel slip is 9.3 kN, assuming a static coefficient of friction of 0.9 and at zero grade. This results in a maximum acceleration of 4.6 m/s^2 (0.47G). However, the load transfer to the rear of the wheels as a result of the acceleration force must also be considered as this increases the normal force, increasing the maximum traction force before wheel slip. Assuming a rigid suspension and considering the location of the center of gravity determined in section 5.9 Vehicle Mass Analysis, the load transfer can be calculated using equation (4-9). This equation has been developed by summing the forces on the vehicle in the vertical direction and taking the total moment about the point under the center of gravity. Where A is the longitudinal distance from the front tire to the center of gravity, B is the distance from rear tire to center of gravity, and C is the vertical distance from the contact point between the tire and ground to the center of gravity.

$$N = \frac{mg(A)+ma(C)}{A+B} \qquad (4\text{-}9)$$

The maximum normal force present on the rear wheel during acceleration is calculated to be 12.2 kN, this results in a maximum traction force of 11 kN that produces an acceleration of 5.64 m/s^2 (0.58G). Note that this is only an estimated value, as the tire load sensitivity nor the additional load on the rear wheel due to downforce present from drag force, is not being considered. These factors can be taken into account when a more detailed model is being developed.

Figure 4.18 displays the total available peak tractive force and power of the powertrain from the two electric motors and combustion engine. Notice that the tractive force available from the powertrain exceeds the maximum friction force up to a vehicle speed of 61 km/h, where the transmission shifts to second gear; therefore, the output torque of the components must be limited. Although this may suggest that the gear ratio in the first gear of the transmission is too high, resulting in excess maximum torque, it does allow the components to operate at a more efficient point when not operating at peak conditions.

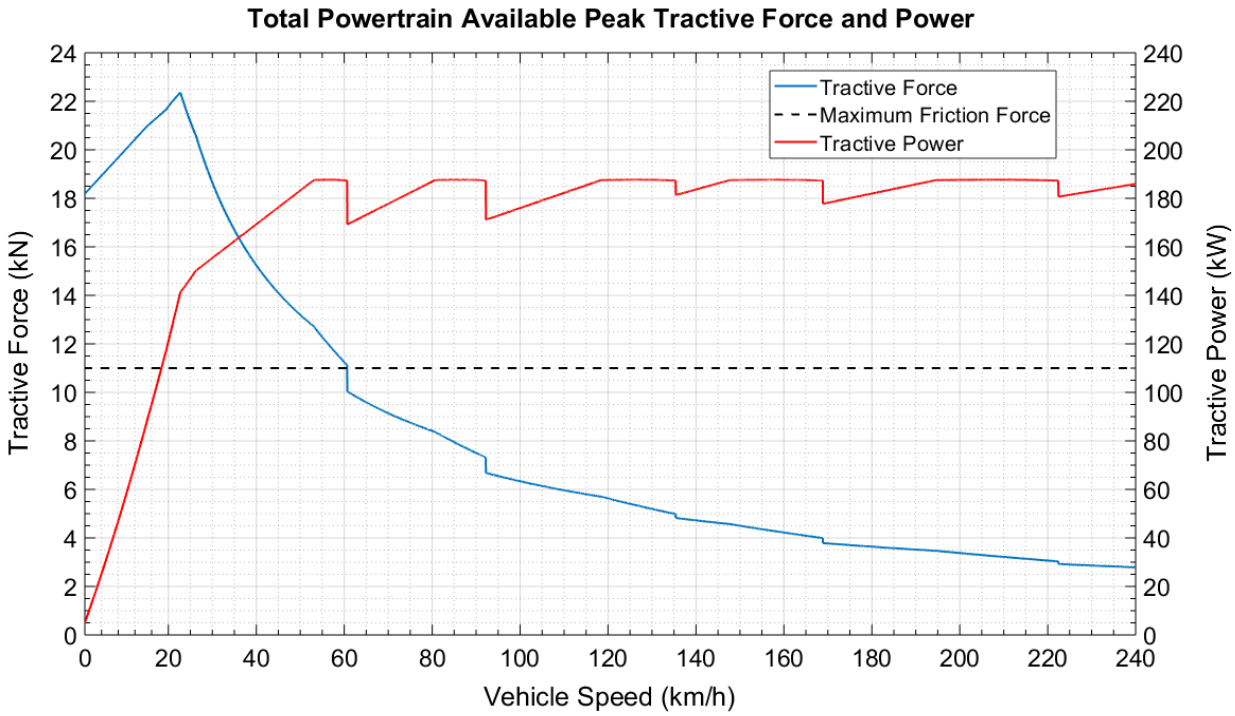

Figure 4.18: Total Powertrain Available Peak Tractive Force and Power

A numerical analysis can be performed to determine the velocity profile of the vehicle during acceleration by re-arranging equation (3-7) to equation (4-10).

$$v_{n+1} = \left(\frac{F_{traction} - mgcos(\theta)C_r - mgsin(\theta) - \frac{1}{2}\rho_{air}A_{front}C_d(v_n)^2}{m}\right)dt + v_n \qquad (4\text{-}10)$$

The velocity profile for the vehicle's acceleration from 0-100 km/h is shown in Figure 4.19. Including the battery voltage and power limitations as well as the maximum friction force; the vehicle can accelerate from 0 to 100 km/h in 5.95 seconds, 0.15 seconds longer than the vehicle technical requirement. In electric mode, the vehicle can reach 100 km/h in 8.27 seconds. From Figure 4.19 it can also be seen that it takes the vehicle 2.65 seconds to accelerate from 80 km/h to 110 km/h, which is below the targeted vehicle technical requirement of 3.5 seconds. In electric mode, it would take 4.52 seconds to accelerate from 80 km/h to 110 km/h. If the vehicle could maintain the estimated maximum acceleration of 5.64 m/s^2, its time to accelerate from 0 to 100 km/h would have been reduced to 4.92 seconds. Note that this is not taking into account the brief power loss from the engine and P2 electric motor during transmission gear shifts.

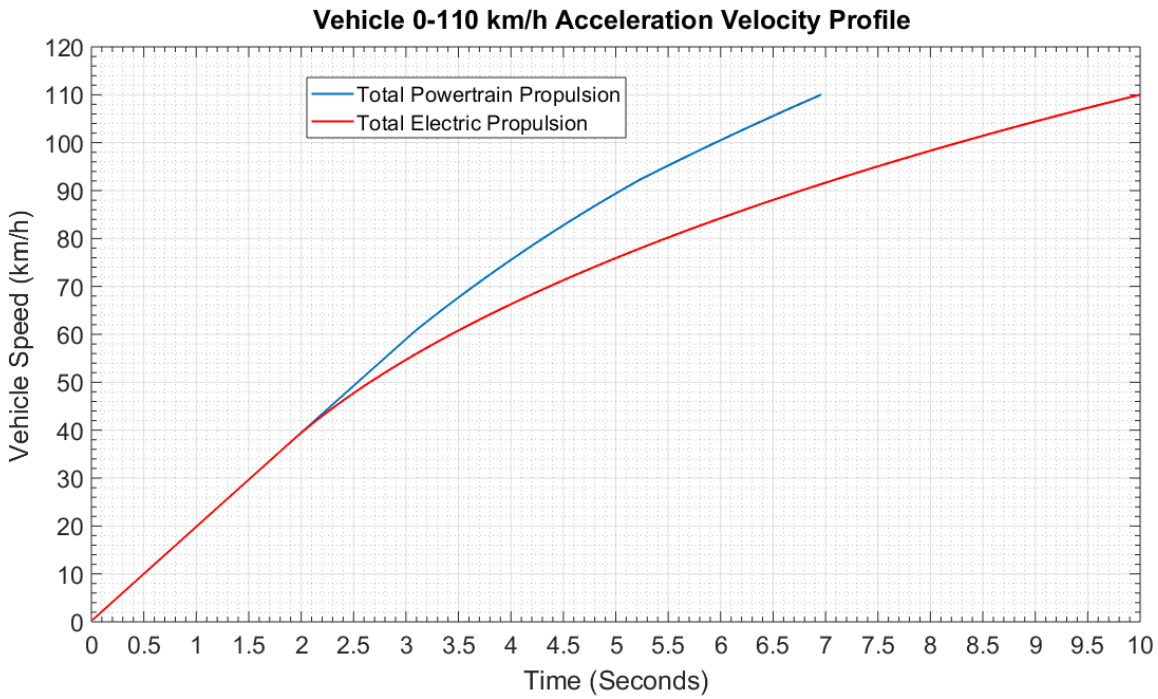

Figure 4.19: Vehicle 0-110 km/h Acceleration Velocity Profile

As previously mentioned, the P2 and P3 motors integrated were initially selected to be 4-winding motors; however, in light of the P2 failure during vehicle testing, it was subsequently replaced with a 3-winding motor due to its availability. For comparison purposes, the electric motor peak tractive force and power with a 4-winding P2 motor is shown in Figure 4.20; this is not accounting

for the battery power limitation. The 4-winding motor produces a lower peak power output of 62 kW whereas the 3-winding can produce 92 kW since it can operate at a higher constant power region at the same rated battery voltage as shown in Figure 4.16.

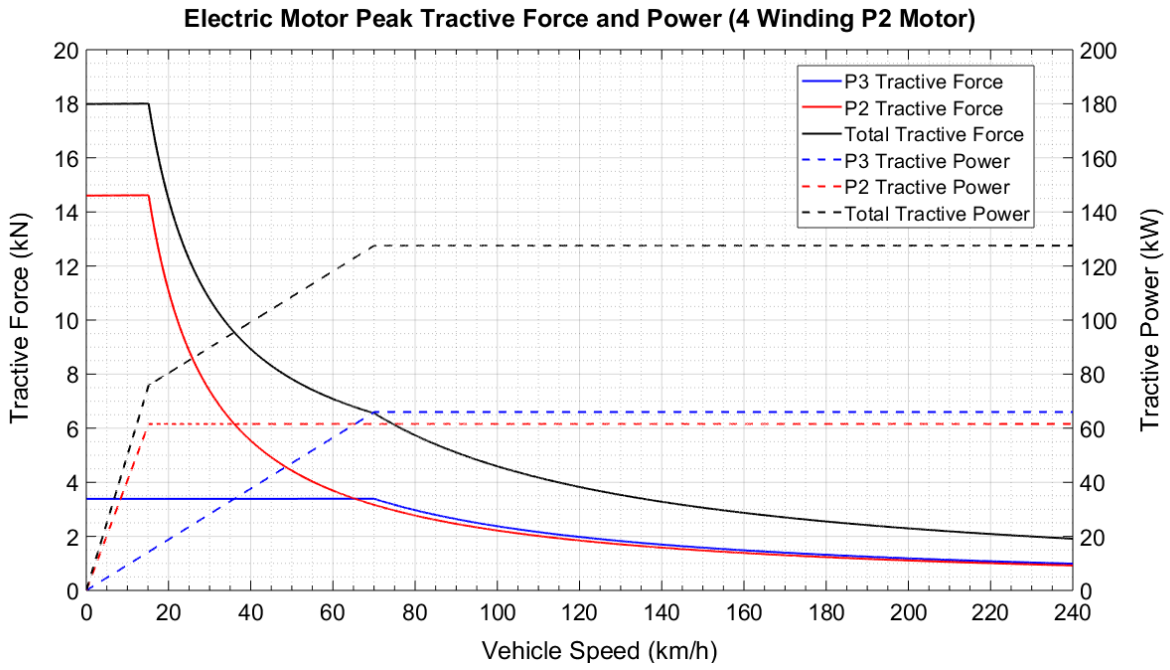

Figure 4.20: Electric Motor Peak Tractive Force and Power (4 Winding P2 Motor)

Although the 3-winding P2 motor can produce additional power and maintain its peak torque output at a higher rpm, the battery power limitation and maximum friction force restriction, renders it ineffective. Looking at Figure 4.21, the total electric peak traction force with the 3-winding motor is higher, up until the vehicle speed of 55 km/h, at which the 4-winding motor also reaches the maximum battery power, limiting the motors to the same total traction force output. Considering the estimated maximum friction force, the brief difference between the traction force output of the electric motors before merging, results in a 0-100 km/h acceleration time difference of 0.13 seconds; when being propelled by the two electric motors. The 4-winding takes 8.4 seconds while 3-winding reduces it to 8.27 seconds. With the additional power from the engine, the total powertrain peak traction force falls below the maximum friction force after 61 km/h. At this point, both the 3-winding and 4-winding motors would be battery power limited making no difference to the total powertrain traction force, thus not influencing the acceleration time from 0-100. Therefore, the additional power and traction force developed from the 3-winding motor is not usable in this case.

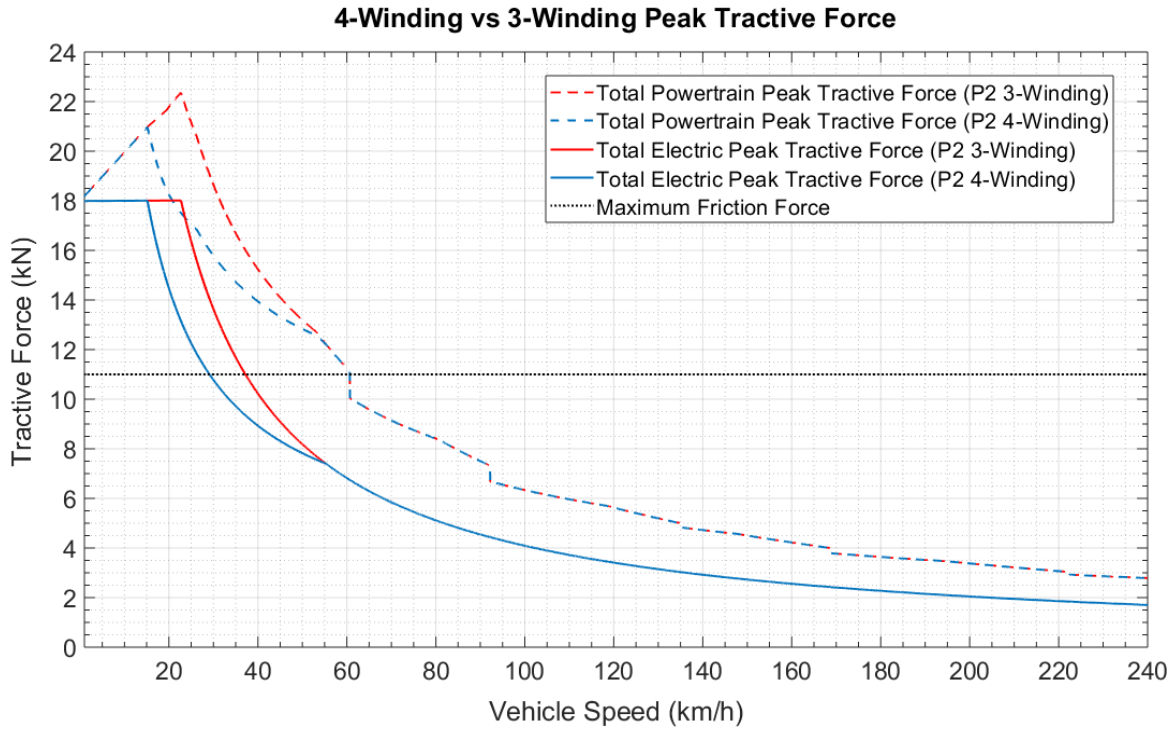

Figure 4.21: 4-Winding vs 3-Winding Peak Tractive Force

Figure 4.22 displays the post-transmission peak torque and traction force output available from the combustion engine and P2 motor at a given vehicle speed and transmission gear ratio. The engine and P2 motor are rated at a maximum 8000 rpm; the numbers on the plotted line indicate the pre-transmission rpm, which is also the engine and P2 rpm. It can be seen that to achieve a maximum torque output, the transmission should shift when the components reach their maximum speed. Therefore, the transmission should shift into 2nd gear at the vehicle speed of 61 km/h and 3rd gear at 92 km/h to achieve maximum performance for the 0-100 km/h acceleration.

Post-Transmission Peak Torque and Tractive Force Output

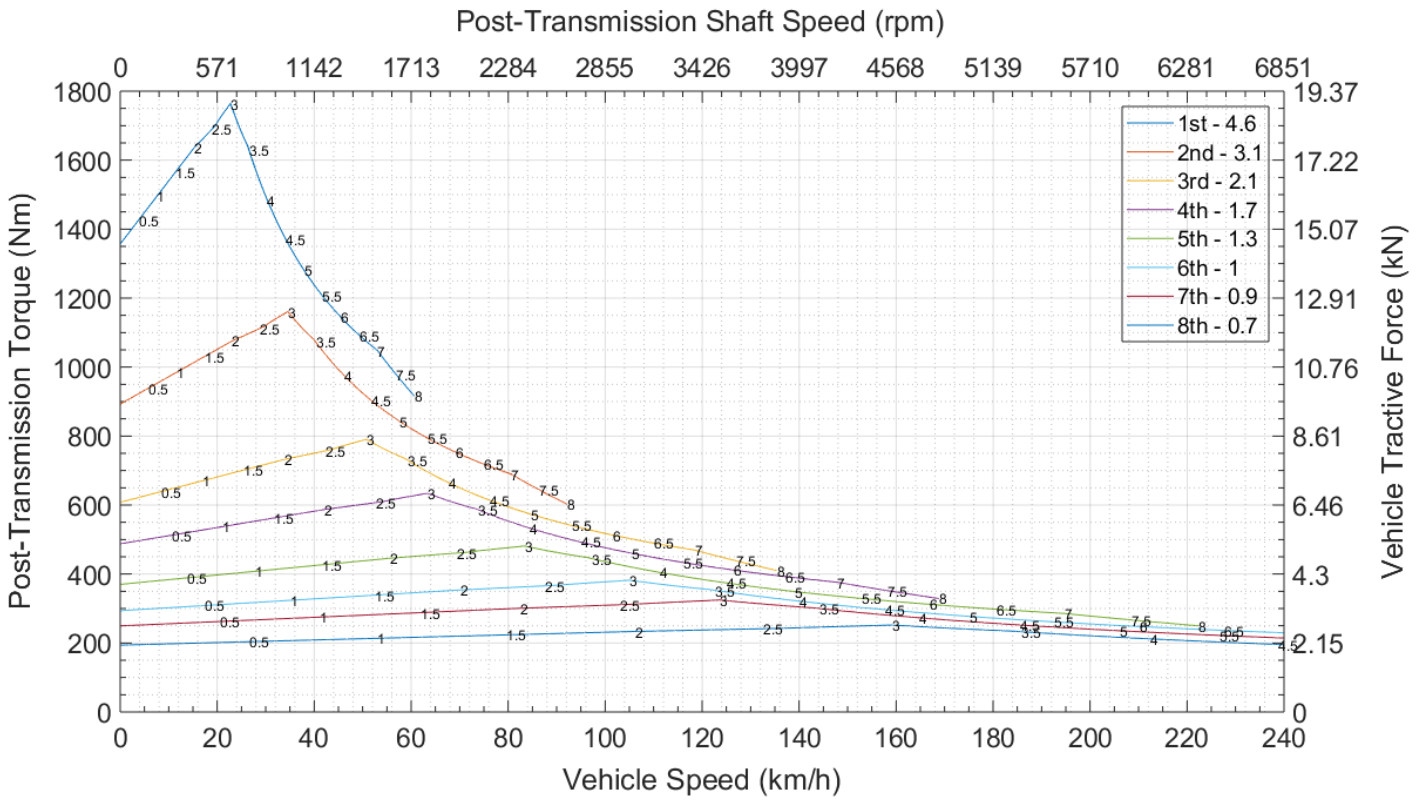

**the numbers on the lines indicate the pre-transmission rpm*

Figure 4.22: Post-Transmission Peak Torque and Tractive Force Output

Note that when the electric motor is in its constant power region, the different gear ratios do not impact the torque output, as illustrated in Figure 4.23. It merely changes the operating speed of the electric motor. The main reason the electric motor would require a multiple speed gear box would be to ensure that it can operate within its rpm range at all vehicle speed.

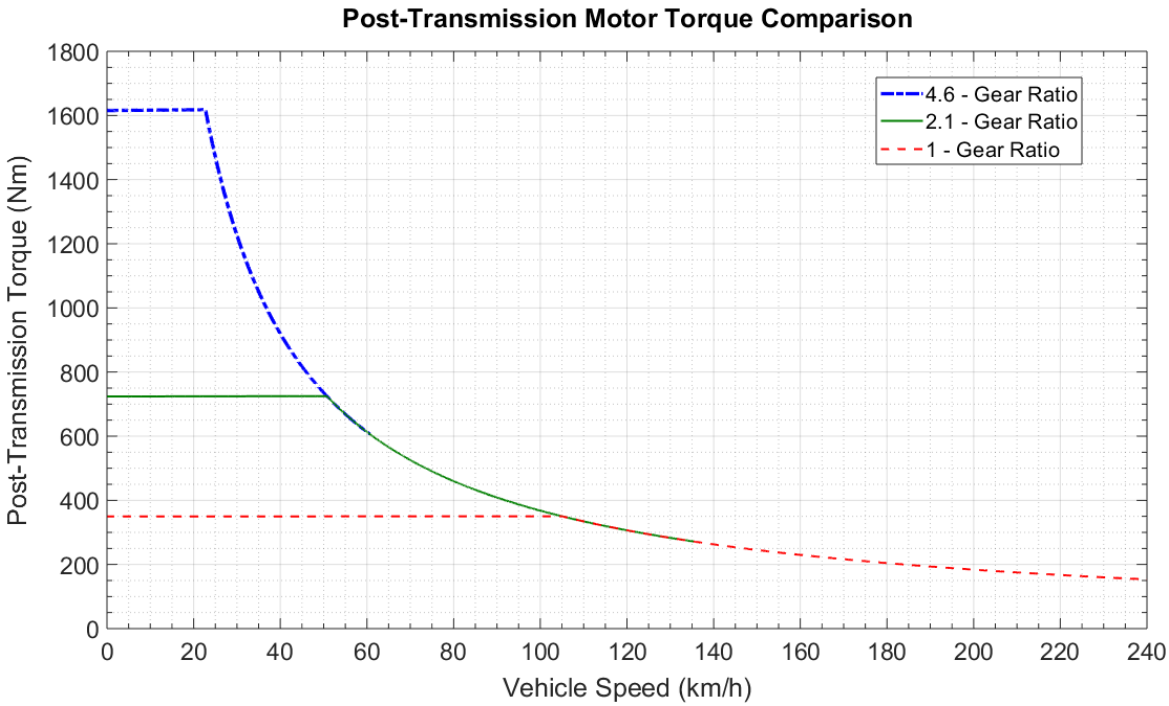

Figure 4.23: Post-Transmission Motor Torque Comparison

4.6 Powertrain Operating Conditions

The selected series-parallel architecture and components allows the vehicle to have six different vehicle modes, outlined in Table 4-5 with the state of the clutch, transmission, engine, P2, and P3 during the modes. A rule based control strategy is implemented that takes the vehicle speed, torque demand, state of charge, and overall efficiency as inputs to determine the most optimal vehicle mode during vehicle operating conditions. Figure 4.24 is displayed to illustrate the six different vehicle modes further. For more information on the vehicle control strategy refer to the paper provided by Radhika Kartha [76].

Table 4-5: Hybrid Electric Vehicle Camaro Operating Modes

	Clutch State	Transmi-ssion state	Engine State	P2 State	P3 State	Operating Conditions
Charge Depleting P3 Only Mode	Engaged	Neutral	Off	Off	On	When the SOC is high and the torque demand can be met by P3
Charge Depleting Full Electric Mode	Disengaged	In Gear	Off	On	On	When SOC is high and torque demand can be met by P2 and P3
Charge Depleting Performance parallel Mode	Engaged	In Gear	On	On	On	When the engine, P2, and P3 must provide the propulsion power to meet the torque demand
Charge Sustaining Series Mode	Engaged	Neutral	On	On	On	When SOC is low and torque demand can be met by P3. Simultaneously, the P2 engine gen-set provides the required electrical power
Charge Sustaining Parallel Mode	Engaged	In Gear	On	On	On	When SOC is low and torque demand cannot be met by P3 only. The engine provides supplemental power to the wheels to meet the torque demand while the extra power is being converted into electrical power by P2
Charge Sustaining Engine only Mode	Engaged	In Gear	On	Off	Off	When it is more efficient to operate the engine for propulsion under low torque demand while the ESS SOC is low, as oppose to CS series or CS parallel.

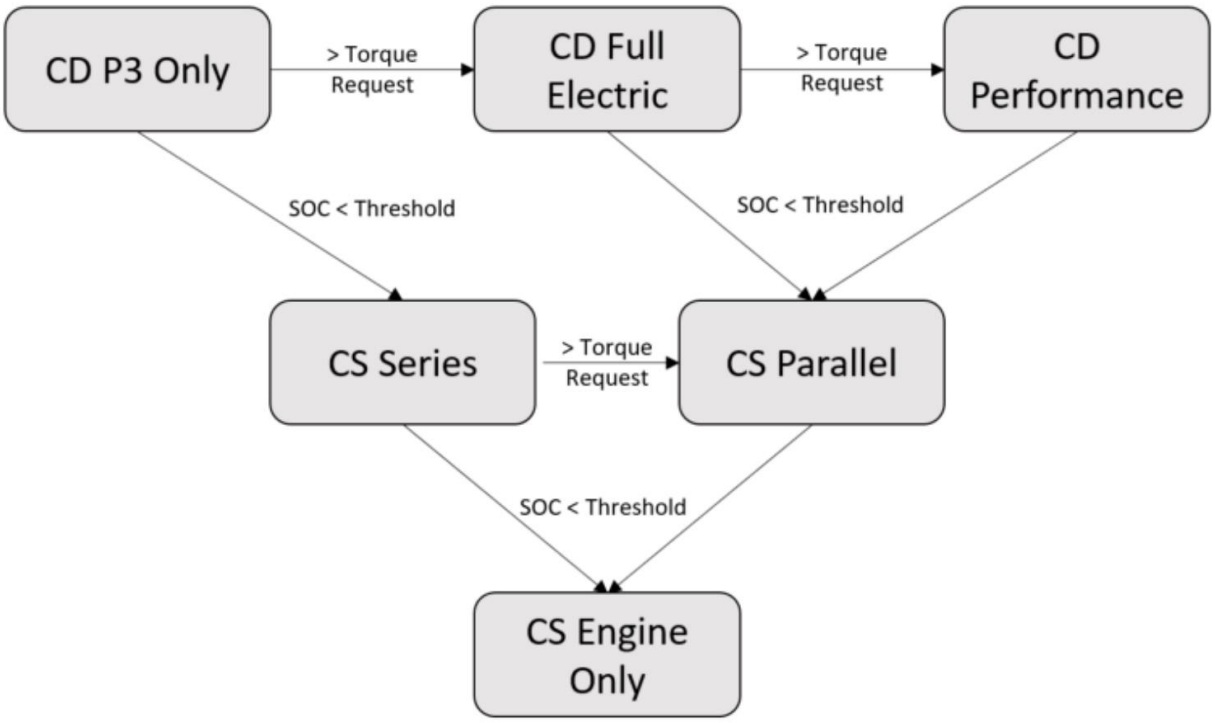

Figure 4.24: Hybrid Electric Vehicle Camaro Operating Modes Illustration [77]

CHAPTER 5
Powertrain Integration

This chapter outlines the integration of the powertrain including the challenges and component failures experienced. The chapter aims to provide a unique opportunity in understanding the integration process of the powertrain for a series-parallel architecture. It serves to help in avoiding failures in a future project simliar to this by illustrating the critical failures experienced. The sections include the integration of the internal combustion engine, P2 motor, clutch system and the custom made bellhousing in between the transmission and engine. It also includes the integration of the P3 motor, driveline and the energy storage system. Lastly, it briefly covers the auxilliary components that are also installed in the vehicle followed by a vehicle mass analysis.

Upon designing the mounts for the components and determining their location in the vehicle, priority has been given to minimizing the weight, size, cost, and complexity of the mounts without risking their structural integrity. Additionally the mounts have been designed with assembly and serviciability in mind, the aim is to make it a simple, quick, and a safe installation. The energy storage system and pre-transmission assembly proved to be the most challenging to design and integrate due to the their compactness and limited available space. One of the most common root cause of the failures was due to the misalignment and imbalance of the driveline. It resulted in the failure of the support bearing of the propeller shaft, the P2 motor spline shear, and the shatter of the friction disk.

5.1 Powertrain Overview

Figure 5.1 calls out the mechanical and high voltage (HV) components of the powertrain, and displays their relative position to the vehicle. Figure 5.2 displays the 3D rendered image of the powertrain assembly including the custom made bellhousing.

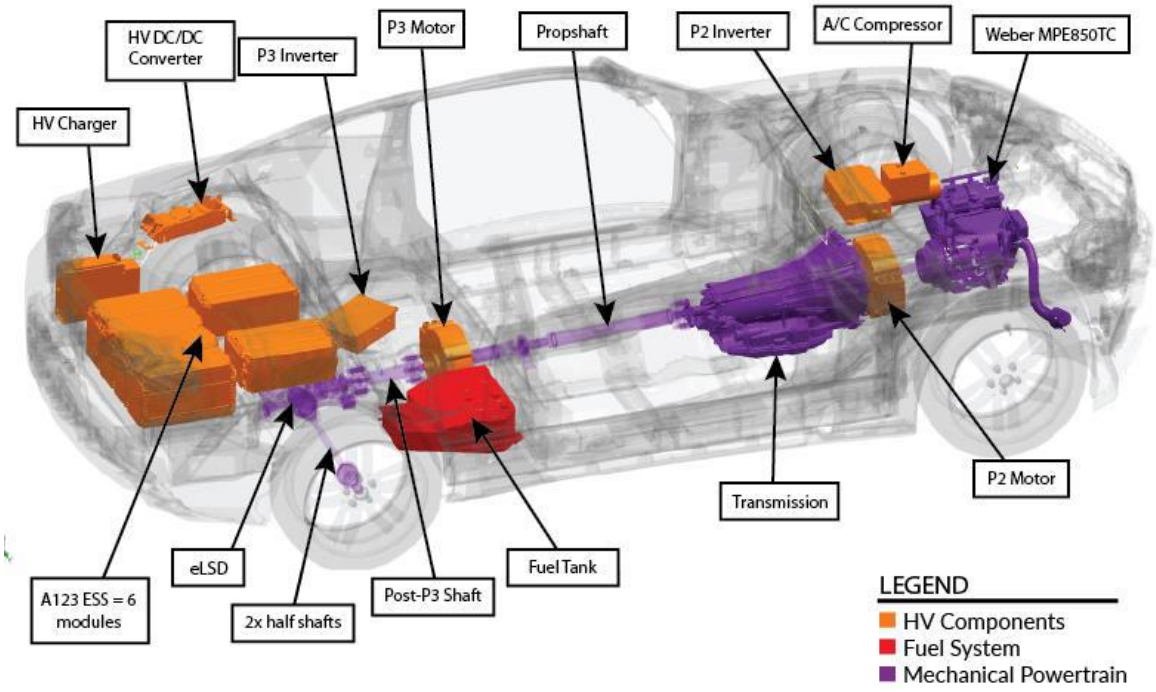

Figure 5.1: Vehicle Integrated Powertrain Callout

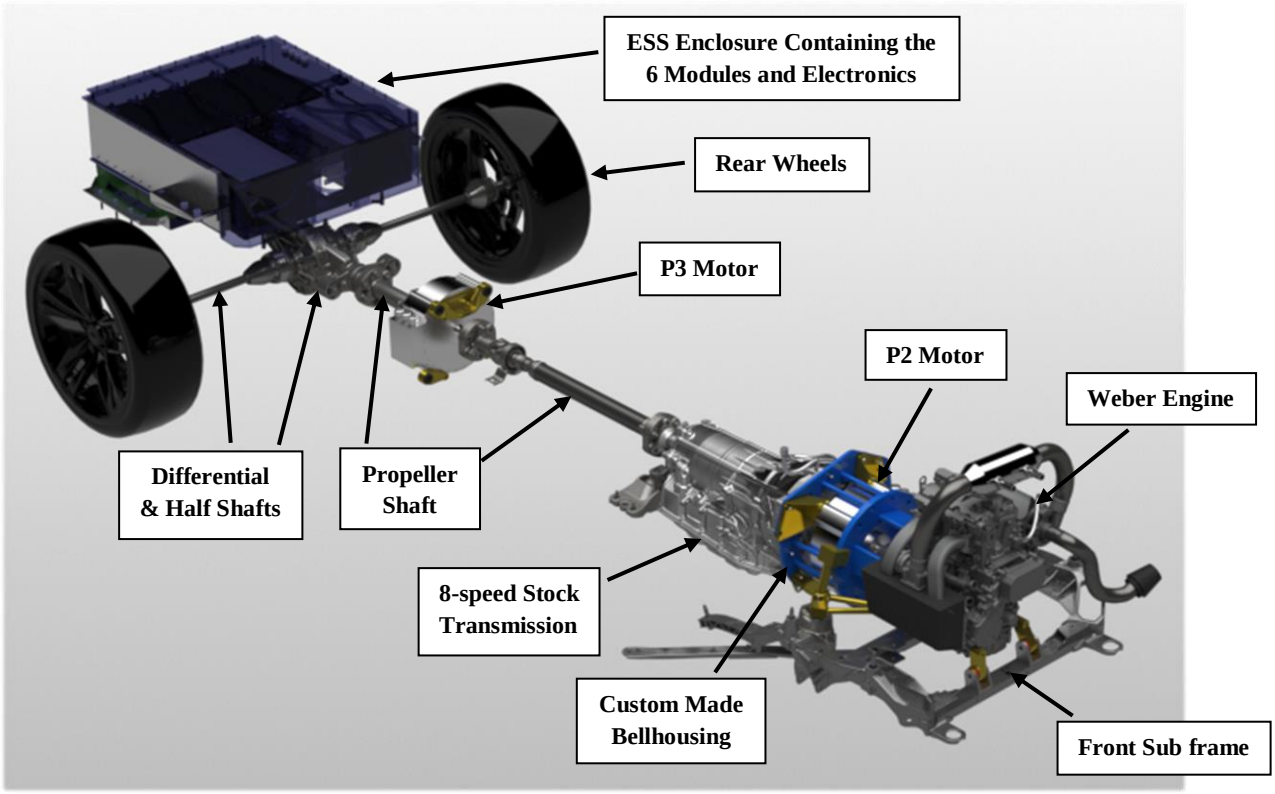

Figure 5.2: 3D Rendered Image of Powertrain Assembly

The supporting structures of the vehicle chassis and subframe are used to mount the powertrain as shown in Figure 5.3. The internal combustion engine is mounted on the un-modified subframe and the rest utilize the chassis while ensuring that they do not affect its structural integrity. Dampers are incorporated into all the mounting points to prevent powertrain vibrations from transferring to the vehicle cabin in order to maintain consumer acceptability. The dampers also allow for some flexibility at the mounting points protecting it from experiencing a high stress during transient vehicle power demands.

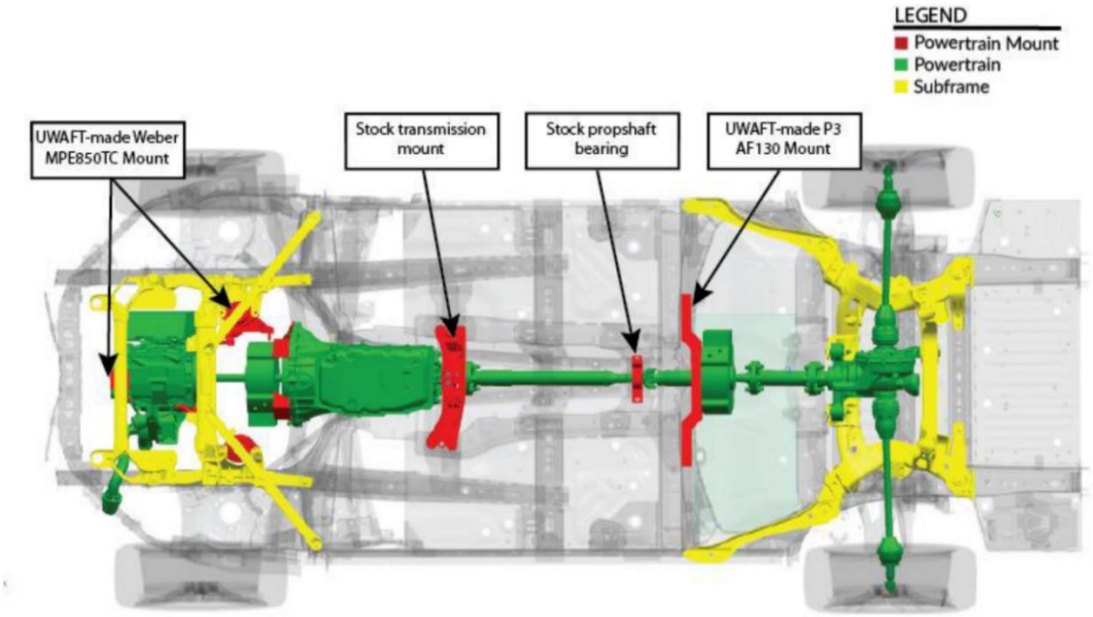

(a)

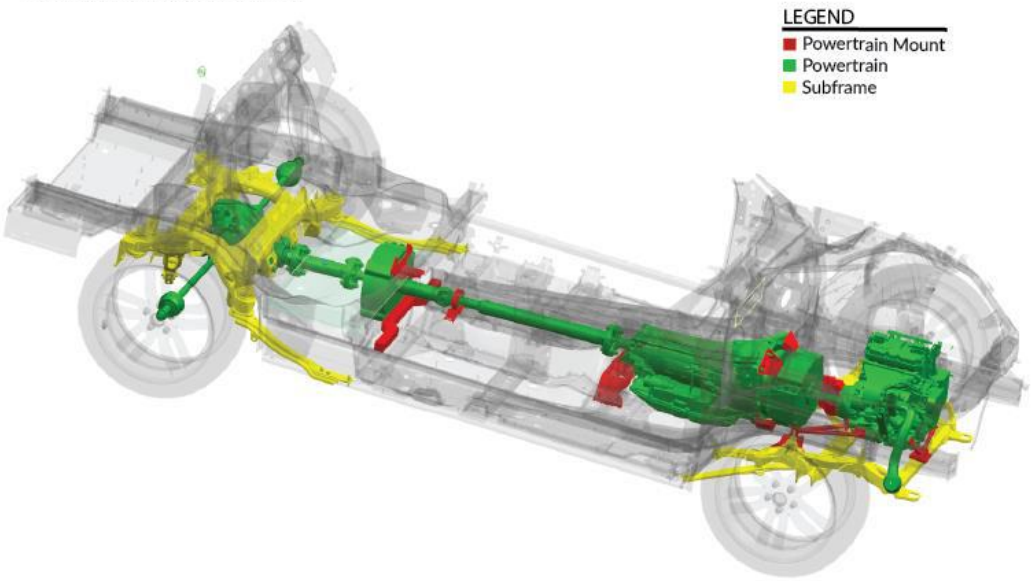

(b)

Figure 5.3: Overview of Powertrain Mounts – (a) bottom view, (b) trimetric view

5.2 Internal Combustion Engine

The engine is mounted to the front subframe using four mounting points, two towards the front of the vehicle and one on each side. Figure 5.4 provides CAD 3D images of the mounting points on the subframe and Figure 5.5 illustrates the mounting points in the vehicle by displaying both the CAD 3D image and pictures taken. The base of the two stock engine mounts including their dampers located on the sides of the engine have been repurposed. The mounts on the front are welded to the subframe and the side of the engine facing the P2 motor is additionally supported by the custom bellhousing extended from the transmission. Note that the front mounts shown in Figure 5.4 is a previous design iteration.

Upon operating the engine in the vehicle, it was discovered that the high vibration traveled to the body of the car making it noticeable and uncomfortable for the driver. It was later realized that this was due to reusing the stock engine dampers, which were too stiff, since they were designed to be used with a much heavier engine with different vibration characteristics.

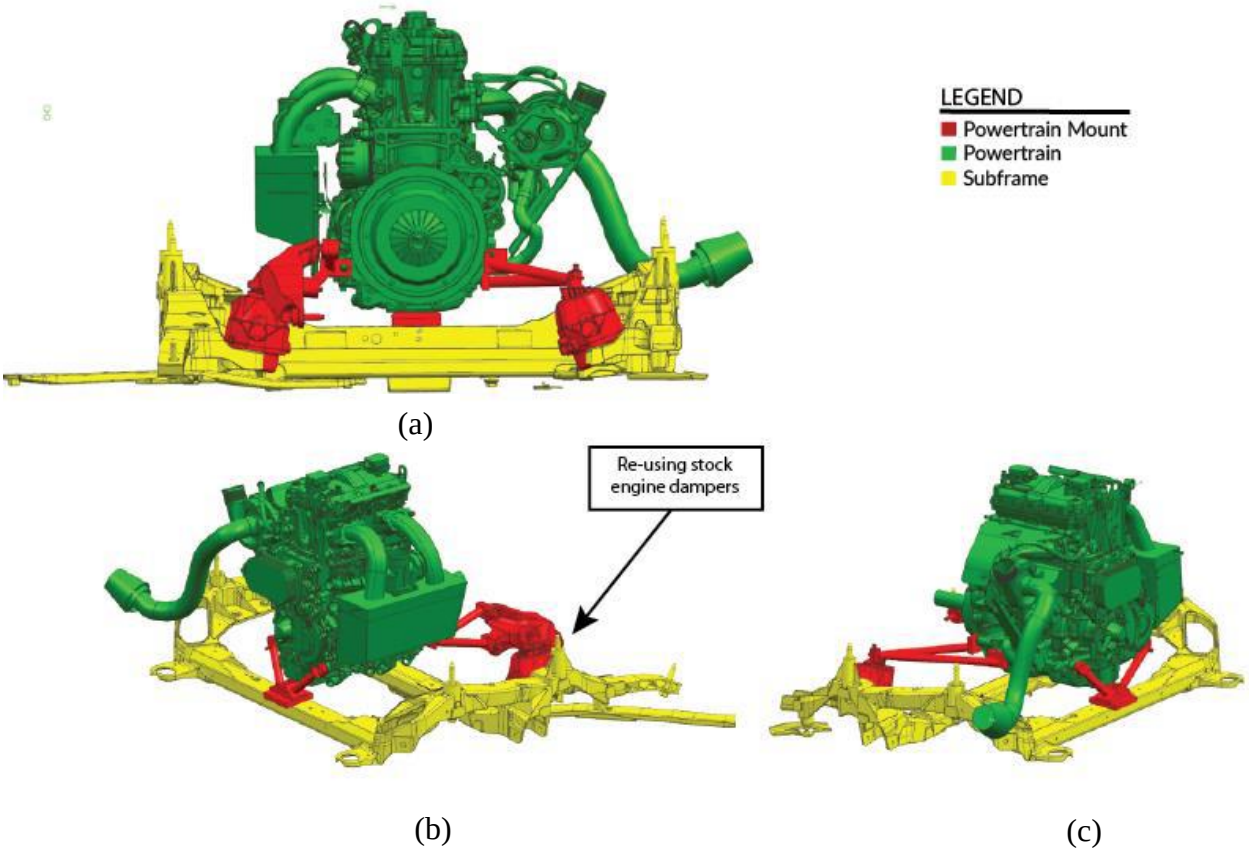

Figure 5.4: Engine Powertrain Mount – (a) rear view, (b) (c) isometric view

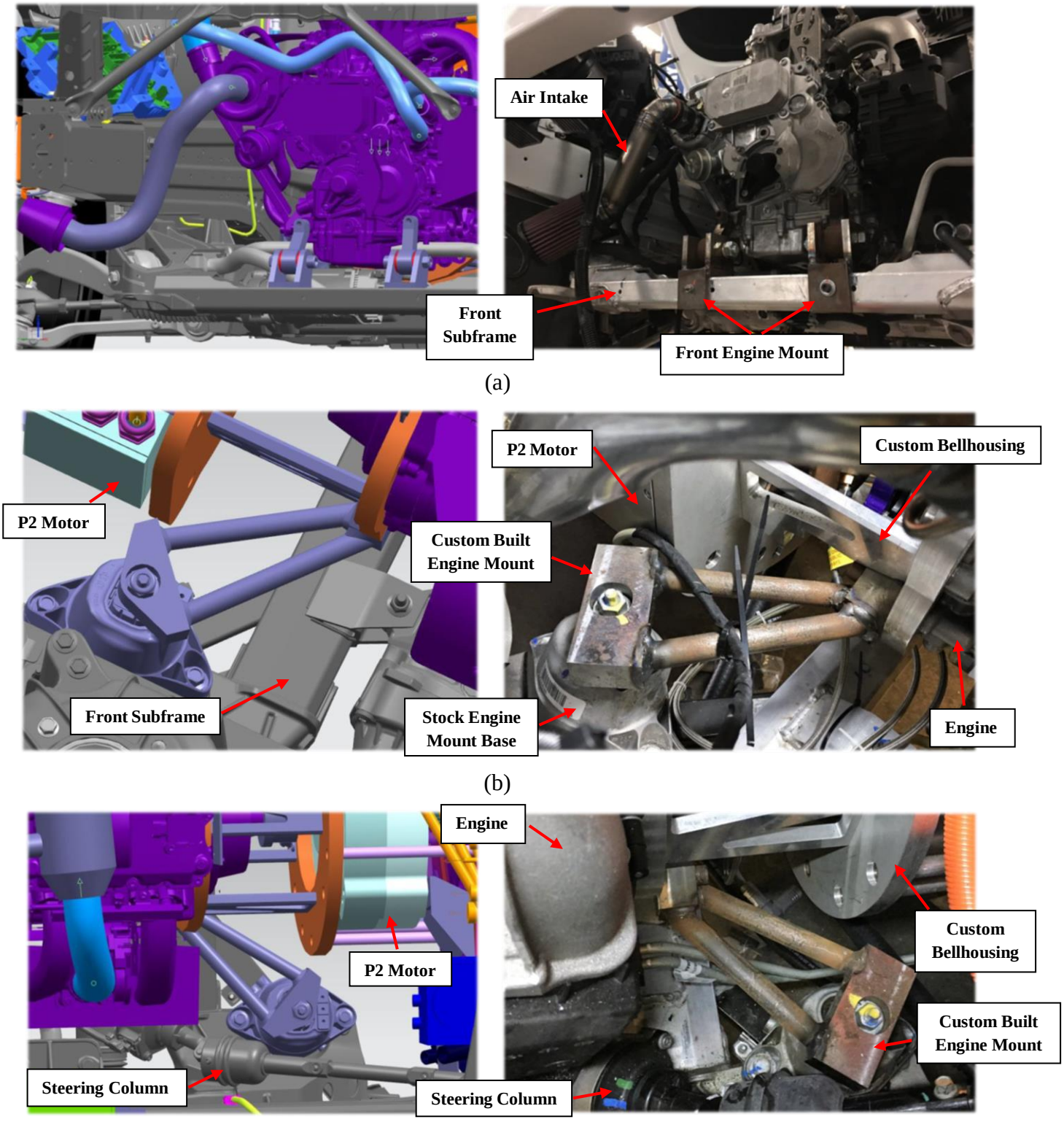

Figure 5.5: Engine Mounting Positions in Vehicle - (a) front view, (b) passenger side view, (c) driver side view

5.3 P2 Motor and Custom Bellhousing

The bellhousing of the stock transmission, highlighted in Figure 5.6 (b), is designed to house the toque converter and bolt directly to its stock engine, therefore leaving no room for integrating an electric motor in between. By replacing the V6 stock engine with the smaller Weber engine and positioning it closer to the front of the vehicle, the necessary space for the P2 motor and clutch is made as shown in Figure 5.6. There was no need to reposition the transmission closer to the rear of the vehicle for the additional space, this helps simplify the powertrain integration as the stock transmission mount can be reused. An additional benefit to positioning the engine closer to the front of the vehicle and not shifting the transmission back is to counter the ESS mass in the rear for a more 50/50 weight distribution. The weight distribution of the vehicle is further discussed in section 5.9 Vehicle Mass Analysis.

The custom bellhousing, illustrated in blue in Figure 5.6 (b), is designed as a structural component that extends from the face of the transmission bellhousing to the engine; while containing and supporting the weight of the P2 motor and clutch. It ensures that the pre-transmission assembly is properly aligned and a one rigid piece, preventing any cantilevered stress experienced by the shaft that connects P2 to the clutch as well as the torque converter coupler. It is also shields the surrounding components from the rotating mass in case of a failure. Note that the pre-transmission assembly and mounts are designed with ease of serviceability as a high priority. This is to simplify and minimize the procedure time of removing the powertrain from the vehicle for troubleshooting and testing. Removing the pre-transmission powertrain requires unfastening the stock transmission mount and front subframe, as well as disconnecting the propeller shaft, steering column, cooling lines, including low voltage and high voltage cables. Once the powertrain is unfastened and disconnected from the vehicle, it can rest on a platform positioned underneath it, after which the vehicle can be raised using a vehicle lift to allow for the removal of the powertrain. Essentially, the design allows the powertrain to be dropped from the vehicle as one piece when required; the drop can be completed within six hours with two people. The image in Figure 5.6 (a) shows the one piece pre-transmission powertrain resting on a platform after it has been disconnected from the vehicle.

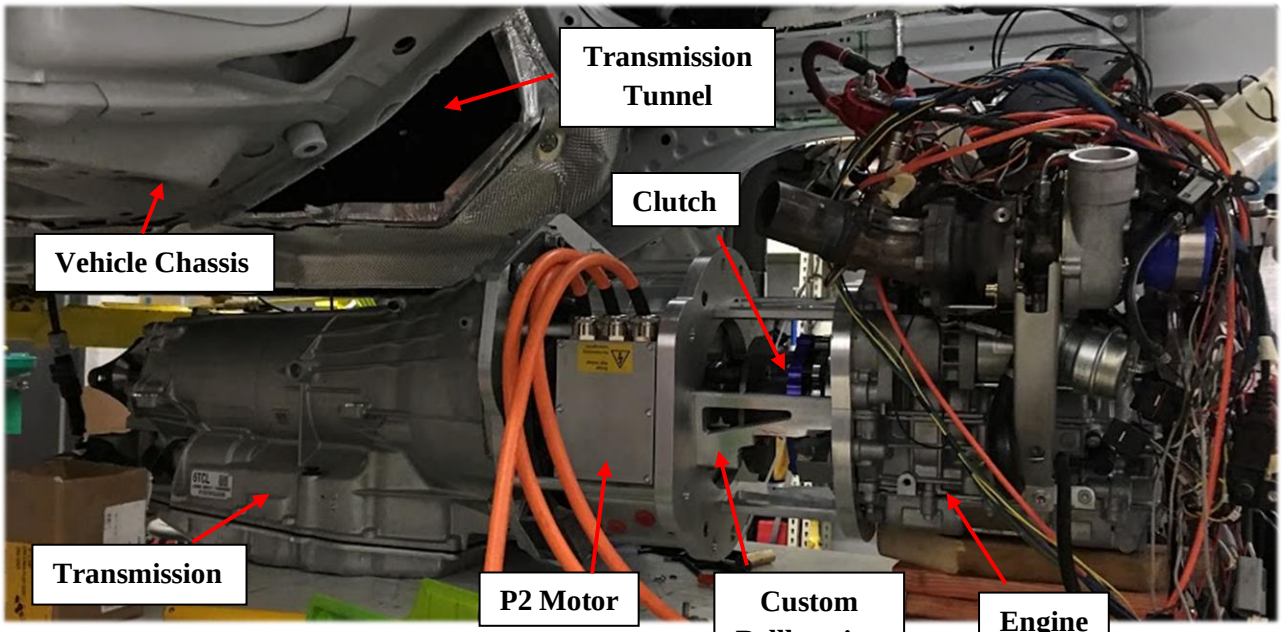

(a)

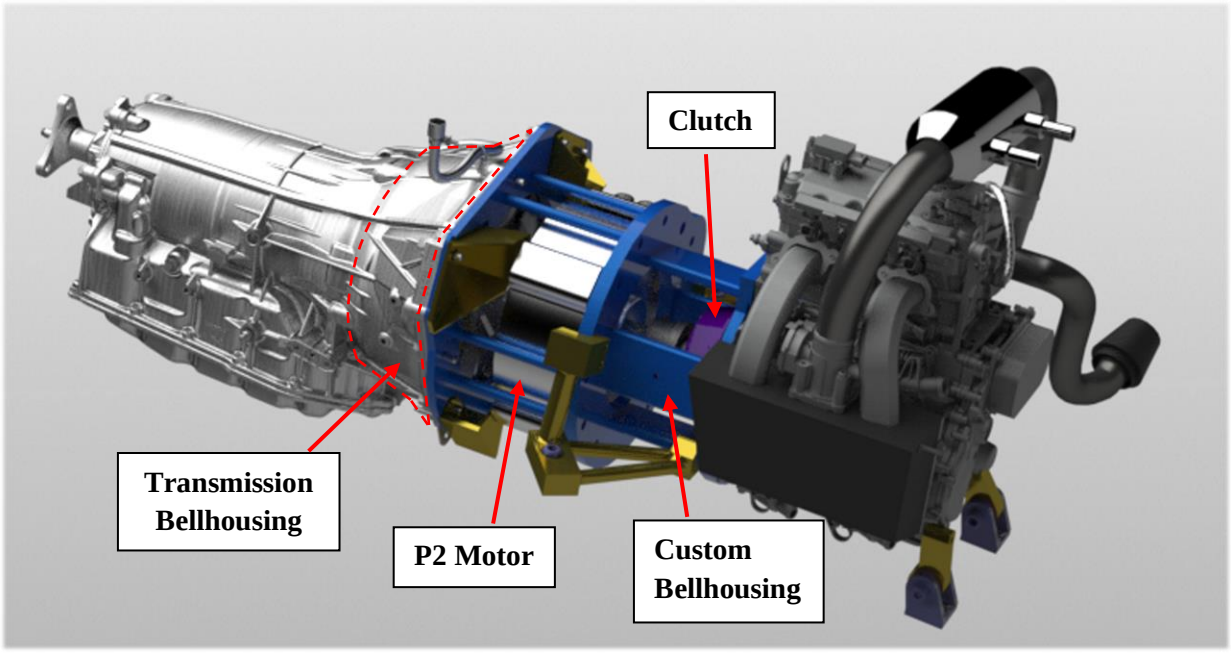

(b)

Figure 5.6: Transmission, Engine, P2 motor, and Bellhousing Assembly - (a) assembly prior to installation, (b) CAD assembly

The custom bellhousing design was narrowed down to six different designs as shown in Figure 5.7. After performing a decision matrix analysis considering size, weight, complexity, installation, reliability, design 4 was selected (highlighted in red). With the addition of using flanges to connect P2 to the transmission so that the thickness of the bellhousing transmission faceplate can be

reduced in order to decrease the weight. Design 4 has been found to be one of the cheapest and lightest designs, which also has one of the simpler assemblies; the gaps in between the connections also allows for access and inspection points which can be useful for troubleshooting. The assembly consists of three faceplates, one for the face of the transmission bellhousing, another for the face of the P2 motor, and the third for the face of the engine. They are connected using connecting rods, connecting flanges, and connecting beams. The assembly procedure of the bellhousing is illustrated in Figure 5.8.

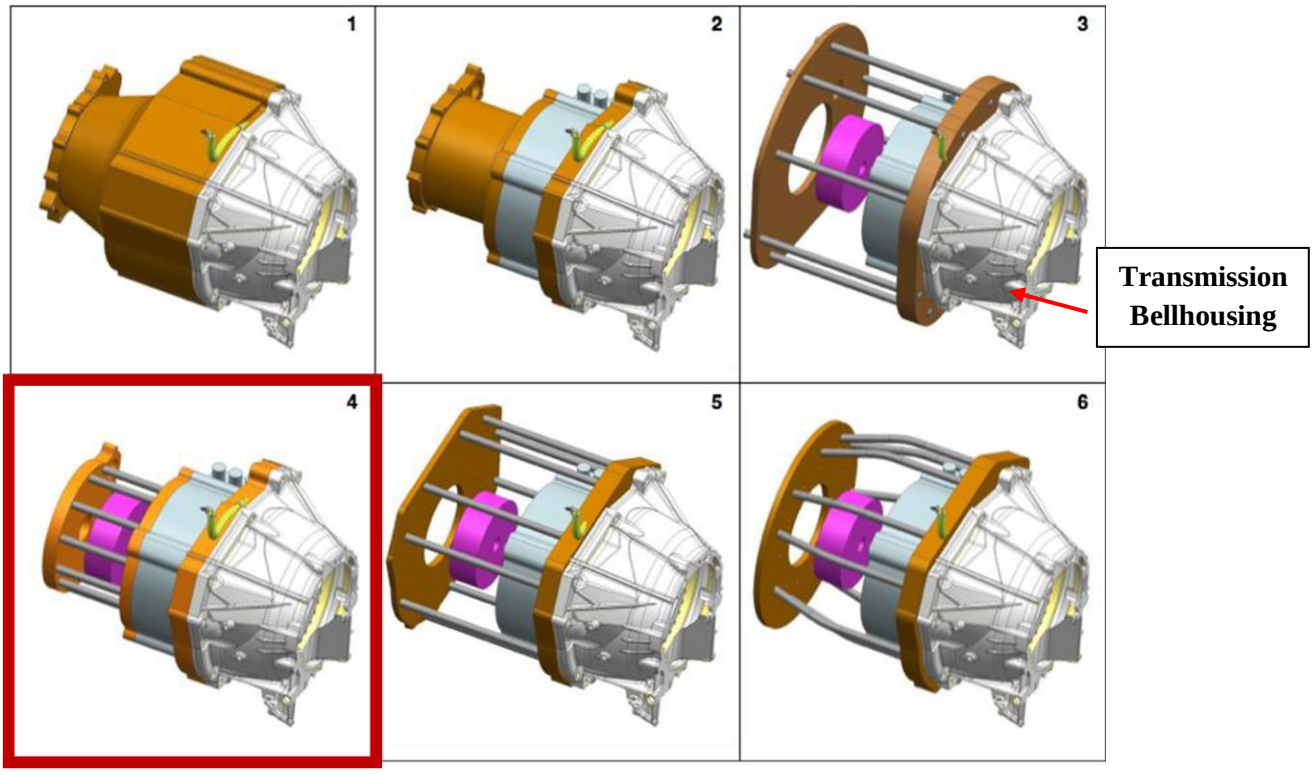

Figure 5.7: Selected Custom Bellhousing Design

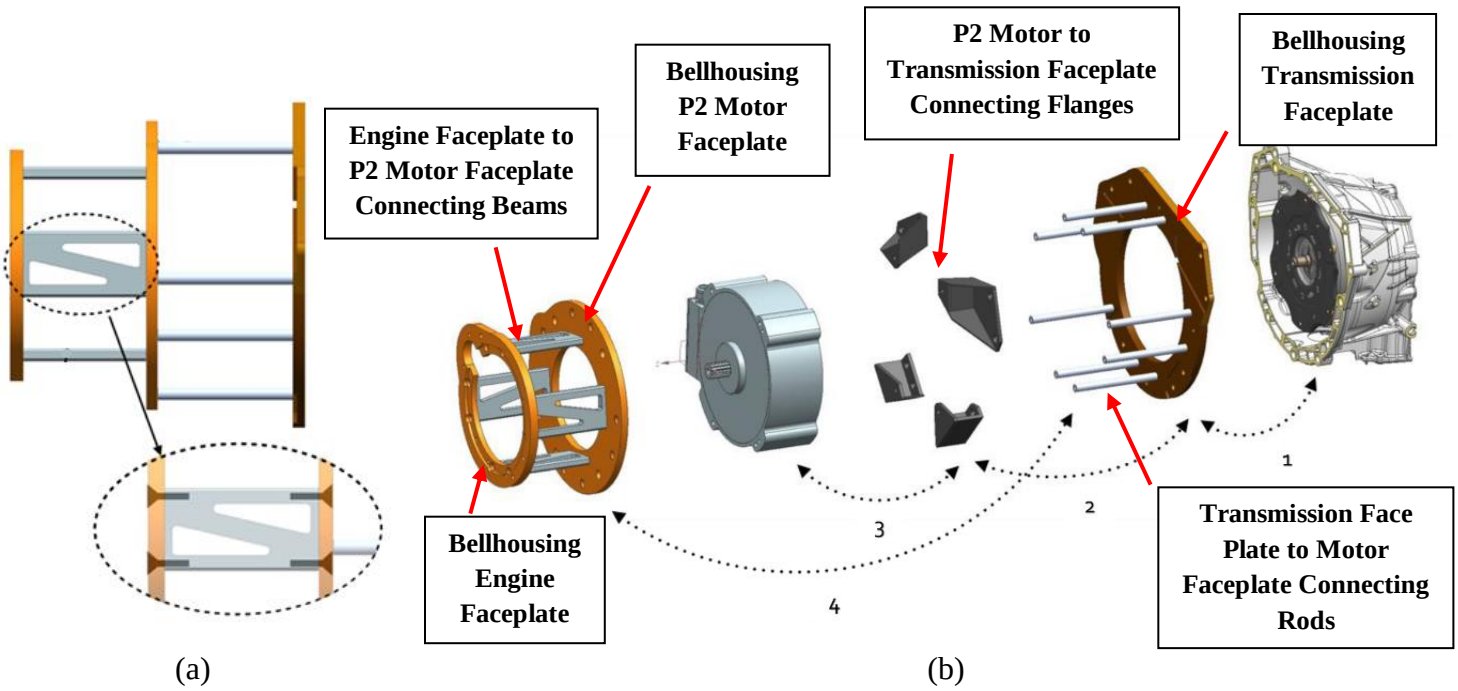

Figure 5.8: Actual Custom Bellhousing Assembly – (a) side view of custom bellhousing, (b) custom bellhousing assembly

5.3.1 P2 Motor to Torque Converter Interface

A coupler is required to transfer torque through the transmission from the engine and P2 by coupling the P2 splined shaft to the torque converter in the transmission bellhousing. A torque converter coupler has been machined (shown in Figure 5.9) to match the bolt pattern on the torque converter that was intended to directly couple to the stock engine flywheel. The coupler also has a female spline machined in to mate with the male spline of P2's shaft.

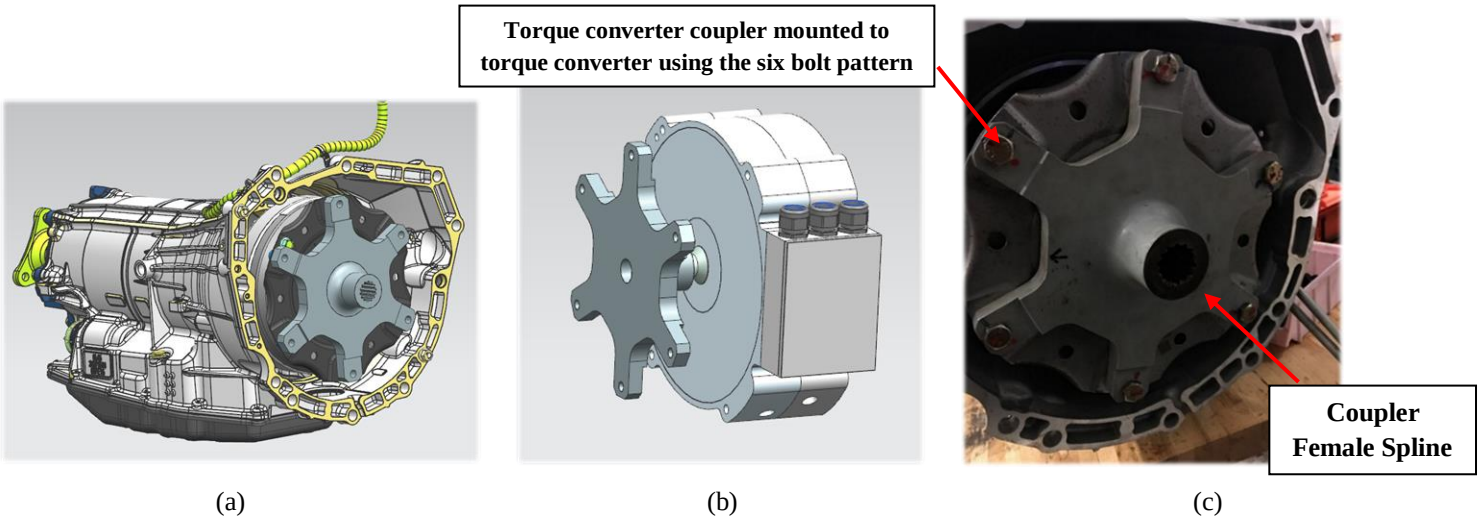

(a) (b) (c)

Figure 5.9: Torque Converter Coupler – (a) mounted on the transmission torque converter in CAD, (b) mated onto the splined shaft of the P2 motor in CAD, (c) bolted unto the transmission torque converter

Given that the torque converter mates with the splined input shaft of the transmission, and that the torque converter coupler also mates with the P2 splined shaft; the torque converter and coupler piece has a degree of freedom to slide back and forth in the axial direction along the splined shafts of the transmission and P2. This degree of freedom is not present when the torque converter is directly bolted to the stock engine flywheel as it used to be, since the flywheel is directly connected to the crankshaft. To remove this degree of freedom, a spacer was implemented to remove any room for the torque converter and coupler piece from shifting once installed. The spacer was threaded into the end of the splined shaft of the motor to extend it further, as shown in Figure 5.10 (a). The cross sectional sketch in Figure 5.10 (b) illustrates how the spacer bumps up against the dowel of the torque converter, removing that extra space.

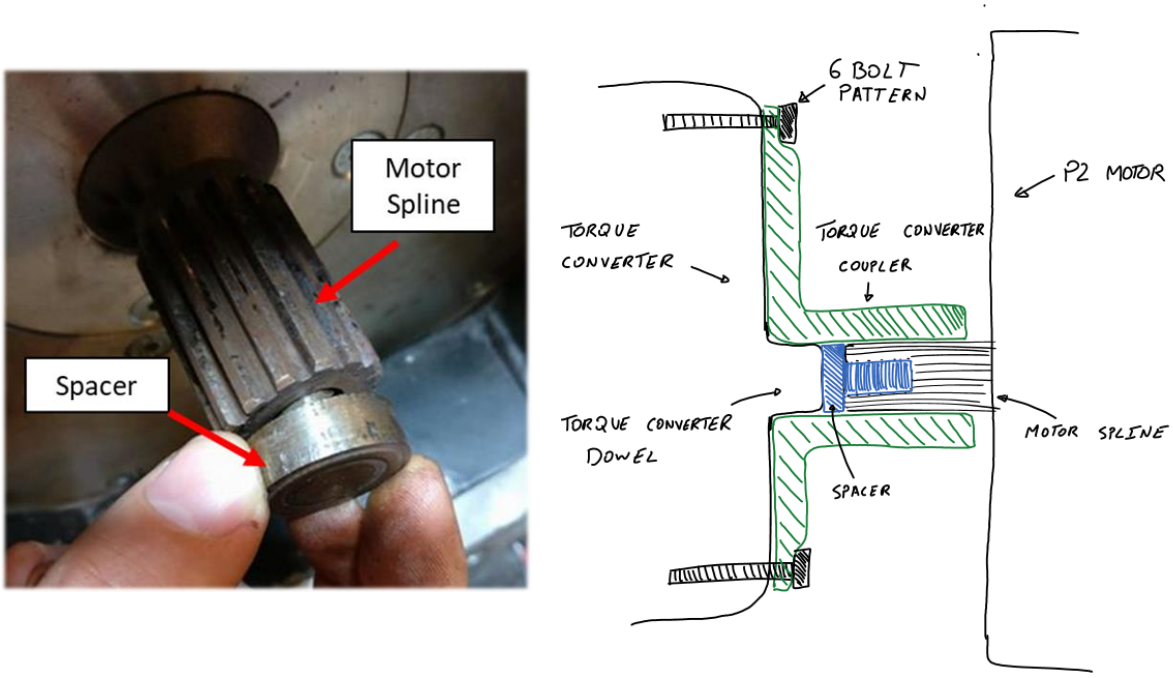

(a) (b)

Figure 5.10: Torque Converter Spacer – (a) spacer, (b) cross section sketch

During vehicle testing, 500 km after the integration of the spacer, the pre-transmission started jamming, stalling the engine and preventing the P2 motor from rotating at a low torque output. While disassembling the powertrain to investigate the problem, it was discovered that the spacer was sheared and that the torque converter was stuck inside the transmission. Upon putting a significant force to pry out the torque converter, it ripped off the transmission housing, exposing the transmission oil pump chain. The transmission oil pump sprocket was found to be fused to the torque converter preventing it from rotating or coming out, the damage is shown in Figure 5.11. The failure investigation resulted in the spacer being the root cause. The spacer limited the required clearance in between the torque converter and the housing of the transmission. When the torque converter operates, it can slightly expand due to the centrifugal forces experienced from the fluid, which is often termed as ballooning. The scrape marks on the torque converter and transmission housing indicates that there was an interference between them.

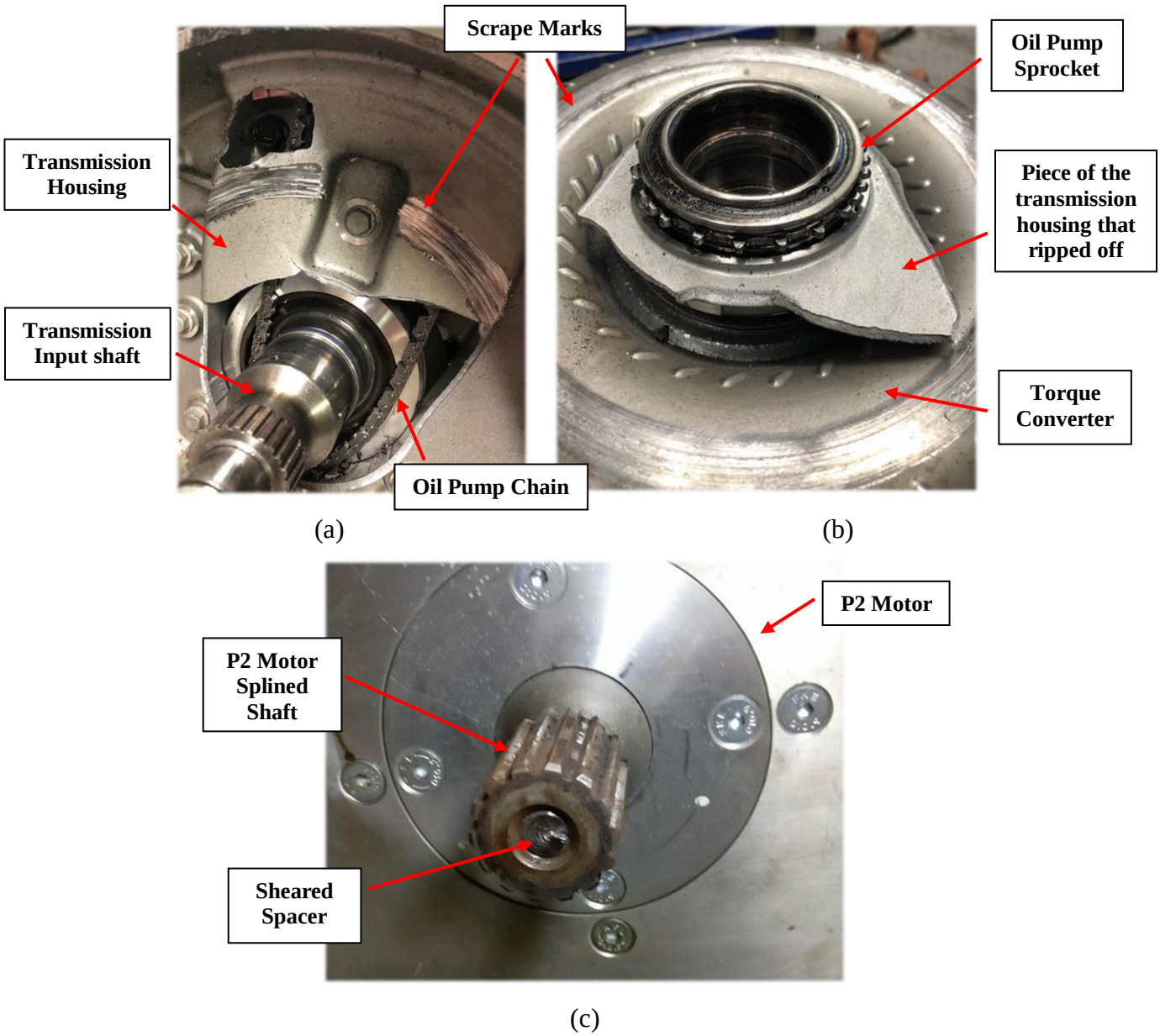

Figure 5.11: Transmission Damage – (a) transmission face, (b) torque converter, (c) sheared spacer

To prevent this failure from occurring again with the spare transmission, the spacer was made 0.2 inches shorter to accommodate for the expansion of the torque converter. However this time, upon vehicle testing, the spline of the P2 motor that mates with the torque converter coupler sheared off, as shown in Figure 5.12. It was concluded that the torque converter had some play since it was not up against the transmission anymore, therefore, swiveling (or wobbling) about the spline, putting a lot of stress on the motor spline. A red powder was also discovered on the surface of the spline, indicating that microscopic welds formed during operation from abrasion due to the play.

Additionally, having the motor spline support the weight of the torque converter could also have had a part in the failure, as it too produces stress.

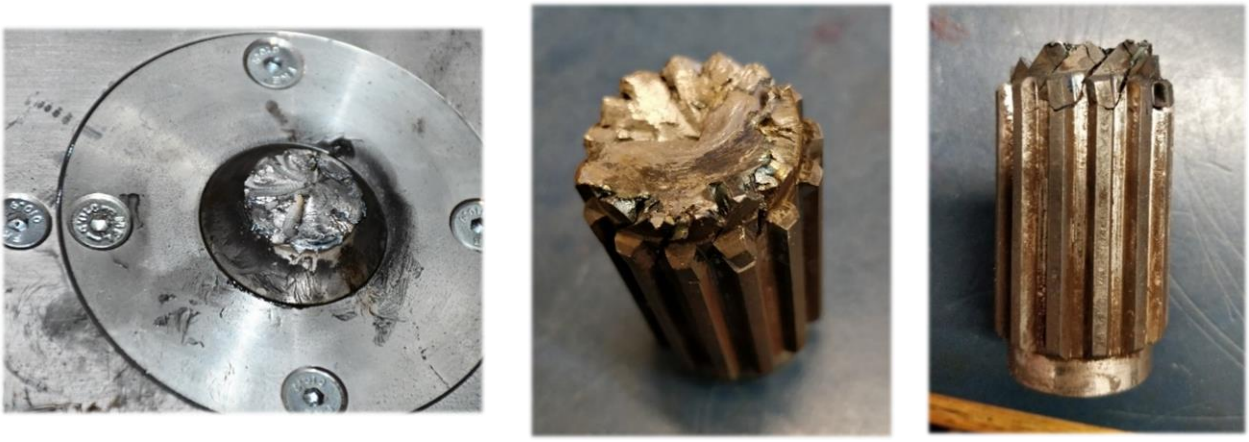

Figure 5.12: Sheared P2 Spline

Thus, a design is required to keep the torque converter in place and only allow for rotational motion while also providing sufficient clearance between the torque converter and the transmission face. The design has to also support the torque converter, removing the weight from the motor shaft. The new design that accomplishes this, consists of an additional face plate, referred to as the torque converter coupler support plate that can be integrated in the bellhousing, in between the motor and torque converter, shown in Figure 5.13 (a). The press fitted radial ball bearing in the middle of the support plate supports the coupler and allows it to rotate freely. Additionally, a step has been machined on the side of the torque converter coupler facing the torque converter so that a bolt can fasten it to the motor spline, locking it in place, preventing it from shifting back and forth as illustrated in the sketch in Figure 5.13 (d).

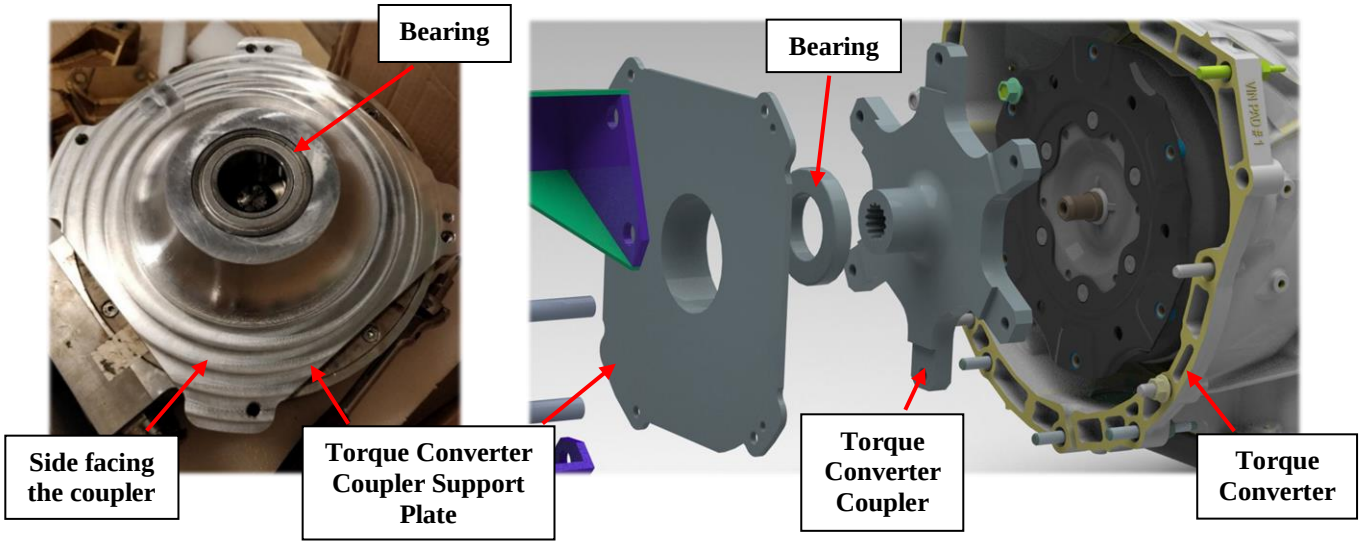

(a) (b)

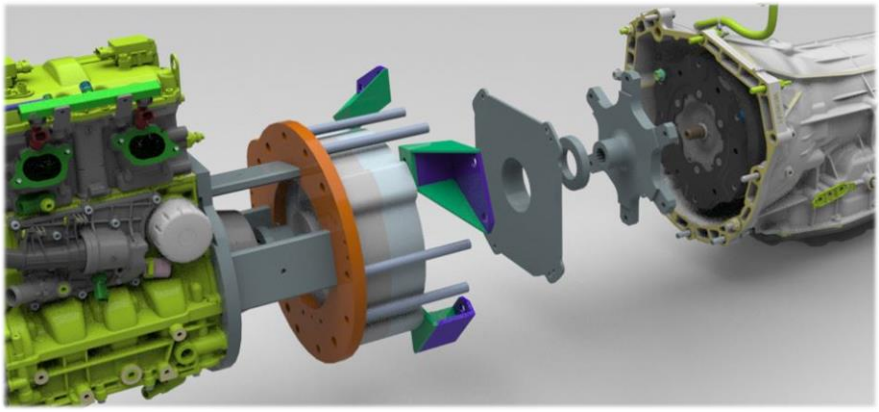

(c)

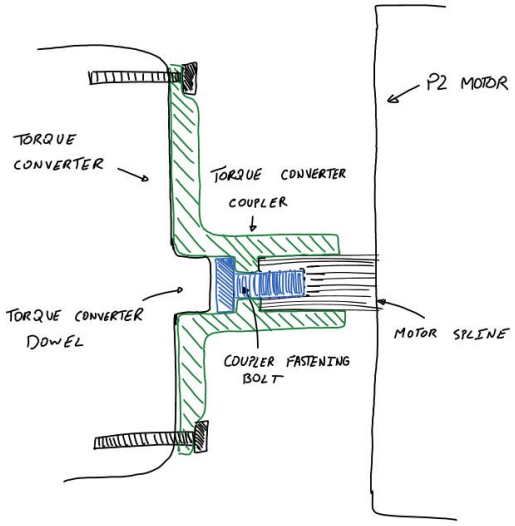

(d)

Figure 5.13: Torque Converter Coupler Support - (a) support plate, (b) exploded view, (c) exploded view zoomed out, (d) torque converter cross section sketch

5.4 Clutch System

During vehicle full electric mode, the engine does not run and so there is a requirement to disconnect it from the drivetrain when in this mode. A clutch is used to disengage the non-operating engine from the P2 motor as to prevent it from dry spinning. This will remove unnecessary resistance losses and prevent engine damage. The clutch is mounted to the existing five bolt pattern on the flywheel, connected to the crankshaft of the engine as seen in Figure 5.14.

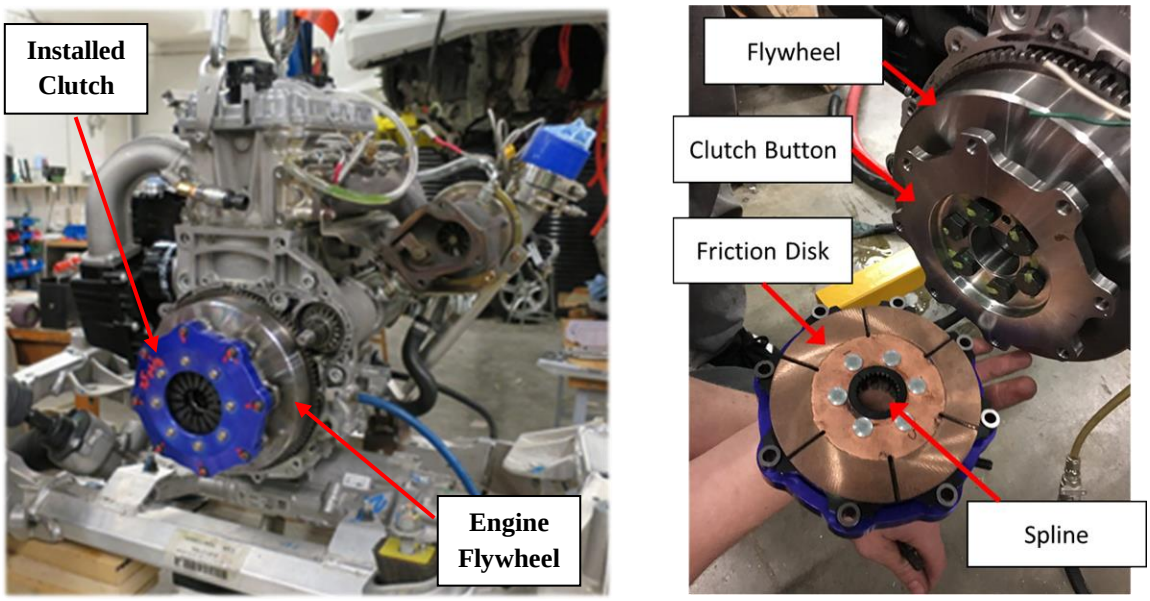

Figure 5.14: Friction Clutch – (left) installed clutch, (right) disassembled clutch

The shaft fabricated to connect the P2 motor to the clutch is shown in Figure 5.15 (b). The shaft has a male spline on one end to mate with the female spline of the friction disk and a female spline on the other end to mate with male spline of the P2 motor. The clutch is always engaged in the default state, meaning that the diaphragm springs of the clutch presses the friction disk up against the clutch button. When the flywheel spins, the friction disk also spins transferring torque by friction and in turn spins the shaft connected to P2. To disengage the clutch, meaning that the friction disc is released to free spin, a release bearing (also referred to as slave cylinder) is required to press up against the diaphragm springs, the release bearing can be seen in the assembly in Figure 5.15 (a) & (c). The release bearing requires a hydraulic system including a master cylinder to actuate it. Typically, when a clutch is used for a manual transmission, the external force pressing on to the master cylinder is from the foot of the driver on the clutch pedal. In the application of this vehicle, it is not feasible to require the driver to provide the external force, it needs to be

automated. Therefore, a linear electrical actuator shown in Figure 5.15 (d) has been put in place to provide the external force to press on the master cylinder, pressurizing the line.

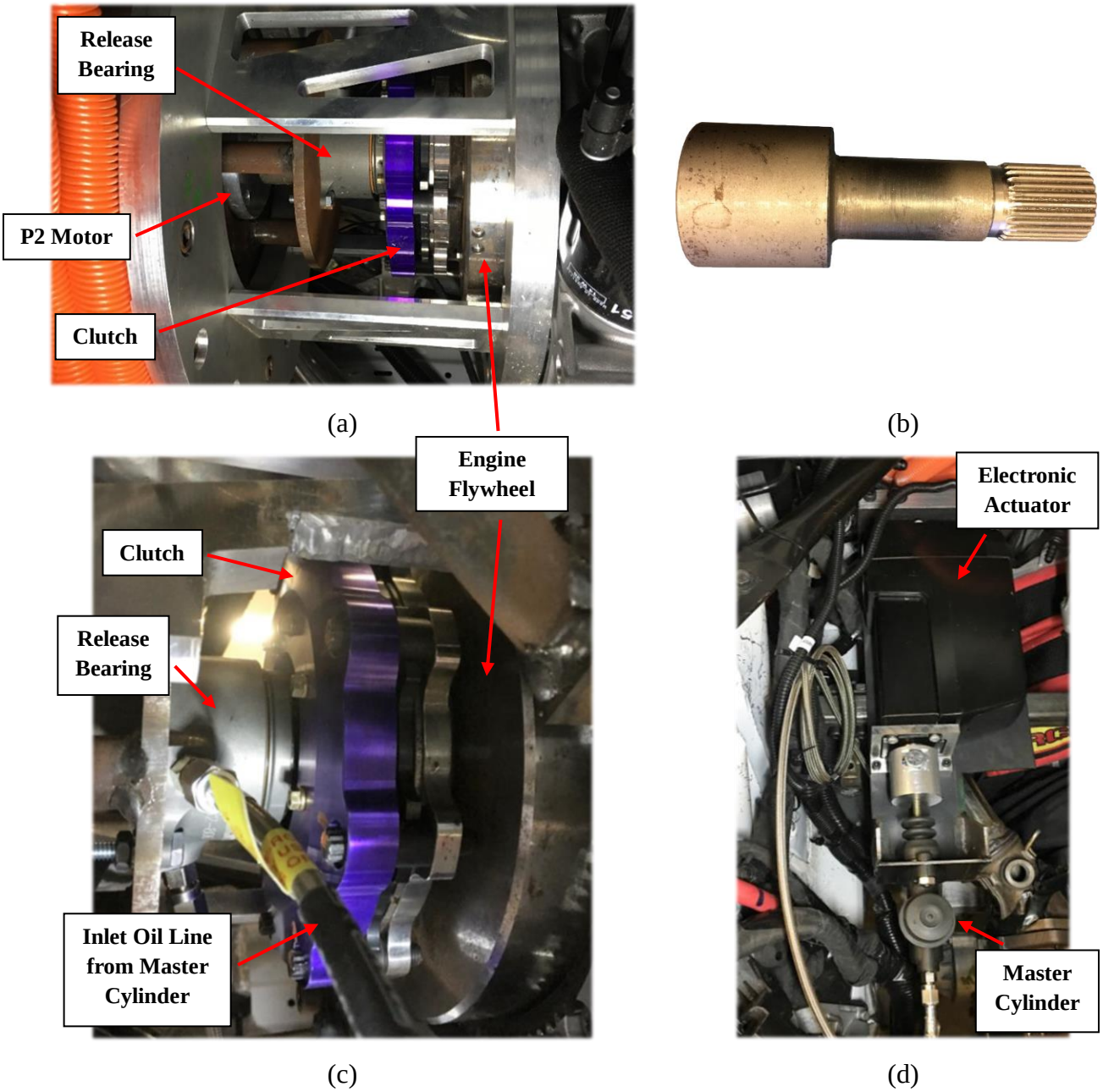

Figure 5.15: Clutch Integration – (a) clutch integration in bellhousing, (b) P2 motor to clutch shaft, (c) clutch integration close up, (d) electrical actuator and master cylinder

The clutch supplier specified that the diaphragm spring requires 500 Newton of force to be depressed by a distance of 9.5mm. To select the correct hydraulic system size for this application and the required output force from the actuator, Pascal's law can be used as shown in equation (5-1).

$$F_{Actuator} = \frac{F_{clutch}}{A_{Release\ Bearing\ Piston}} \times A_{Master\ Cylinder\ Bore} \quad (5\text{-}1)$$

The release bearing of a piston area of 784mm^2 is chosen with a master cylinder having a 22.2 mm bore diameter. This results in the force required from the actuator to be around 200N. Meaning that the hydraulic system would give a mechanical advantage of 2.5. The current actuator selected is capable of providing 2,600N which is certainly over specified as there is no need to require any more than the calculated 200N. However, this component is selected due to its high actuation speed of 32mm/s, allowing the vehicle to quickly engage and disengage the clutch. Other reasons as to why this component is selected is of its high weather resistance (IP67) and that it is an automotive grade equipment that communicates through CAN making it more reliable to control with the hybrid supervisory controller.

During vehicle testing, the clutch friction disk shattered while it was engaged, the damage can be seen in Figure 5.16 (a). After the investigation, it was concluded that the failure occurred due to misalignment. To mitigate this issue, dowels have been placed in the bellhousing face plates to ensure alignment between the engine and P2. Furthermore, a dowel has been also inserted into the shaft as shown in Figure 5.16 (b), the dowel is meant to fit into the pilot hole in the crankshaft of the engine as shown in Figure 5.16 (c).

(a)

(b)

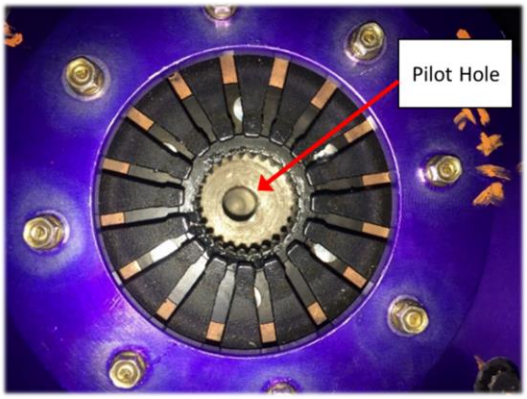

(c)

Figure 5.16: Clutch Failure and Solution - (a) shattered friction disc, (b) shaft with dowel, (c) pilot hole in crankshaft

5.5 P3 Motor

The P3 motor is mounted to a frame, depicted in red in Figure 5.17, which utilizes the mounting points of the stock fuel tank just after the transmission tunnel.

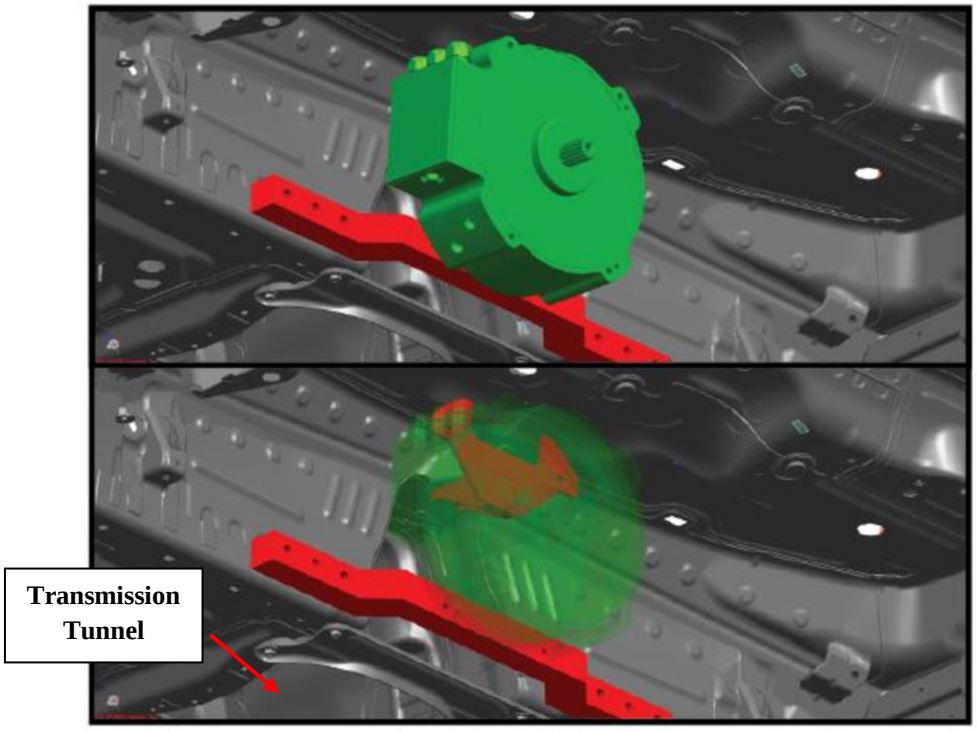

Figure 5.17: P3 Motor Mounting

In order to correctly align the P3 motor to the differential during installation, a custom three-part dowel alignment tool is created, shown in Figure 5.18.

(a)

(b)

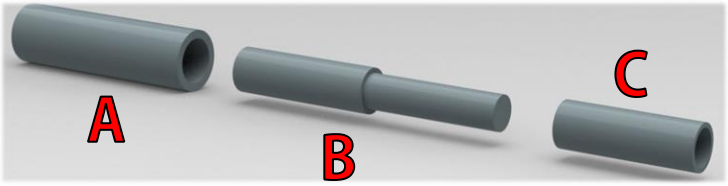

(c)

Figure 5.18: P3 Alignment Tool - (a) Expanded, (b) Compacted, (c) Exploded View

The tool is used before tightening the P3 mounts and before installing the driveshaft. The back up P2 shaft that connects P2 to the clutch is first slipped on the spline of the P3 motor as a dummy shaft, shown in Figure 5.19 (b). The tool is compacted and held up in between the dummy shaft and the eLSD, then is expanded so that part A firmly slides unto the eLSD dowel. Part C is then extended to reach the end of the dowel on the dummy shaft as seen in Figure 5.19 (a). At this point, the motor is slowly shifted and once it lines up with part C of the tool, it extends to slide on the dummy shaft as shown in Figure 5.19 (b). A dial gauge is also used to ensure that the dummy shaft and tool run true indicating alignment shown in Figure 5.19 (c). Once aligned, the motor mount is then tightened while the tool is holding it in place, the tool is then contracted and removed and so is the dummy shaft and the driveshaft is then installed as seen in Figure 5.20.

(a)

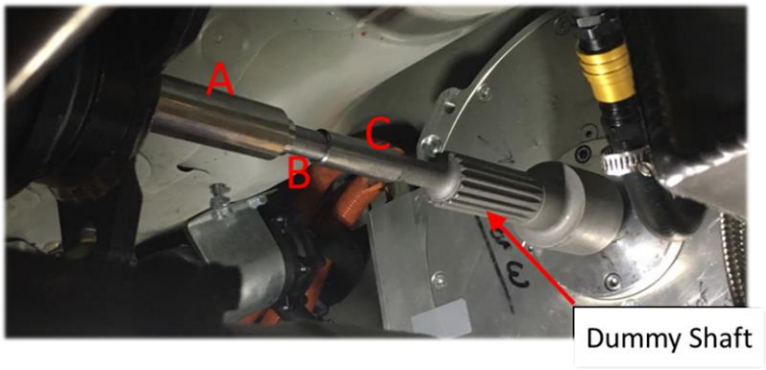

(b)

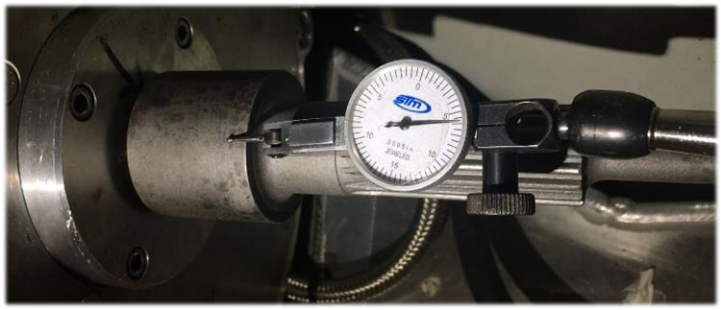

(c)

Figure 5.19: P3 Alignment Tool Procedure - (a) before aligning the motor, (b) after aligning the motor, (c) using a dial gauge

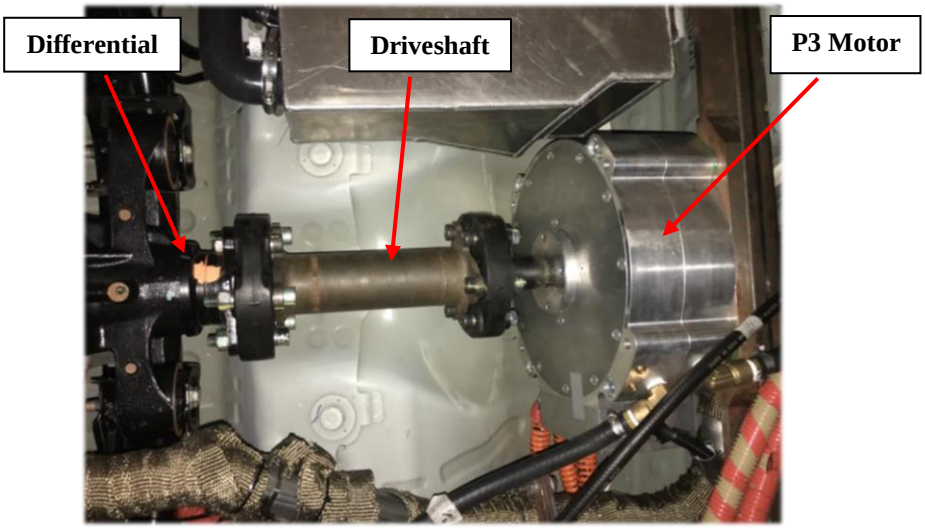

Figure 5.20: Bottom View P3 Driveshaft Installation

5.6 Driveline

The vehicle uses two new propeller shafts (also referred to as driveshaft), one that connects the transmission to the P3 and another that connects P3 to the eLSD. The half shafts are stock and did not require any modifications

5.6.1 Pre-P3 Driveshaft

The stock driveshaft shown in Figure 5.21 (a) is meant to connect the transmission's output shaft directly to the limited slip differential, it has a support bearing that mounts in the transmission tunnel and a universal joint right after. The stock driveshaft cannot be used as is since the P3 motor comes in between the transmission and differential so it was modified to make it compatible. The driveshaft was cut right after the universal joint and a fitting was welded instead so that it can connect with the P3 motor as seen in Figure 5.21 (b). Figure 5.21 (c) displays how the modified driveshaft connects the transmission to the P3 motor.

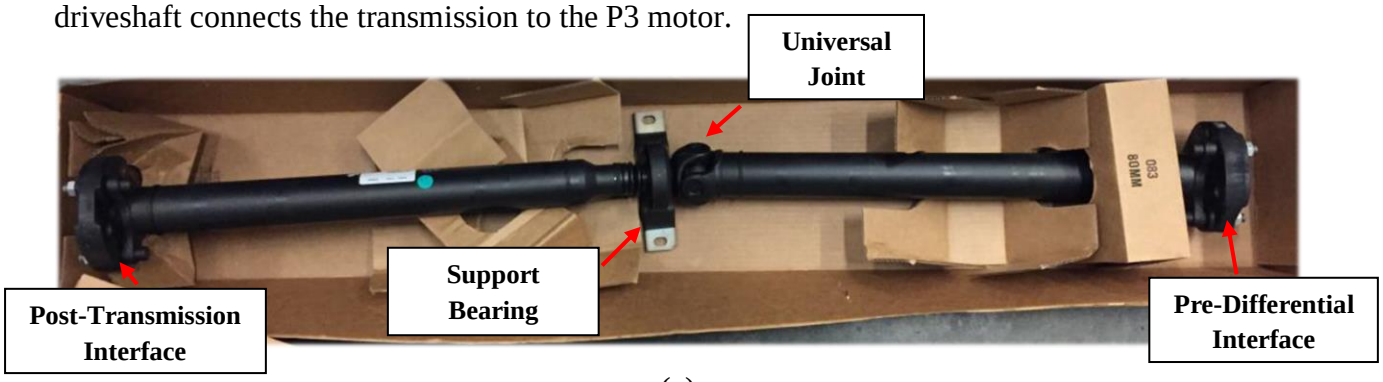

(a)

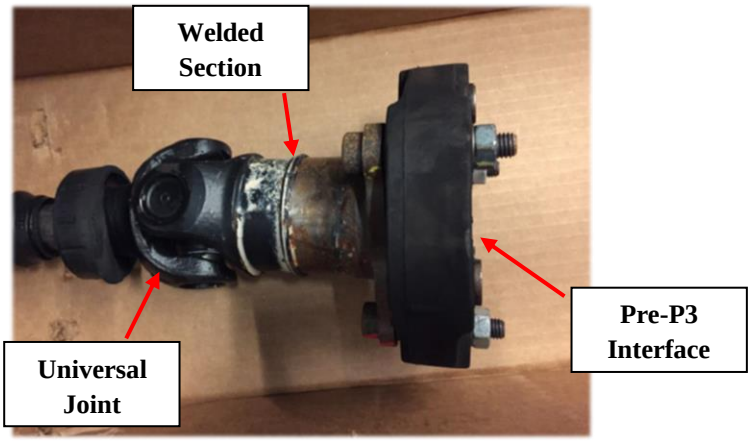

(b)

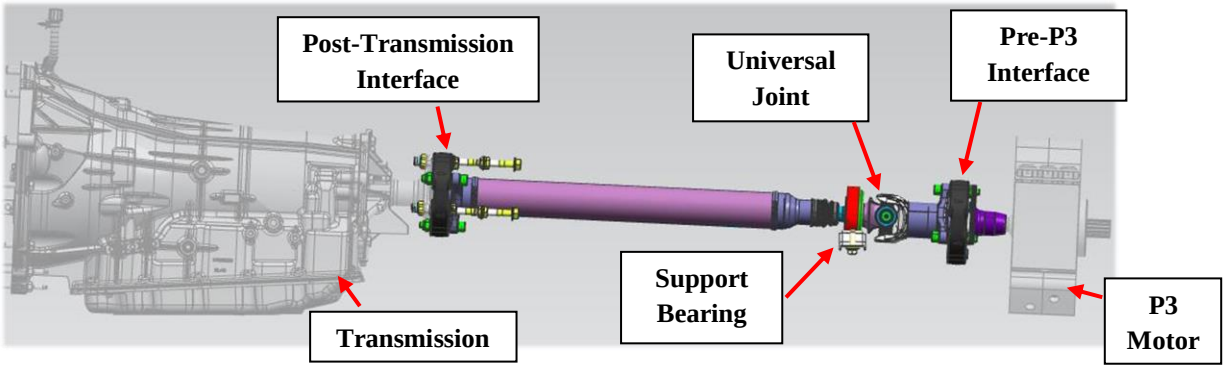

(c)

Figure 5.21: Stock Driveshaft Modification – stock driveshaft (a), welded fitting (b), modified driveshaft integration (c)

During vehicle testing, a noticeable vibration was present when the vehicle approached a speed of 20 km/h or higher. Visual inspection did not aid in determining the issue so the vehicle was driven to better pinpoint the source of the vibration during the investigation. As the test was ongoing, the vibration lead to the fracture of the support bearing housing as shown in Figure 5.22. It was then clear that the vibration stemmed from the driveshaft leading to the failure of the support bearing indicating that the driveshaft was imbalanced. The imbalance was due to the modifications made to the driveshaft.

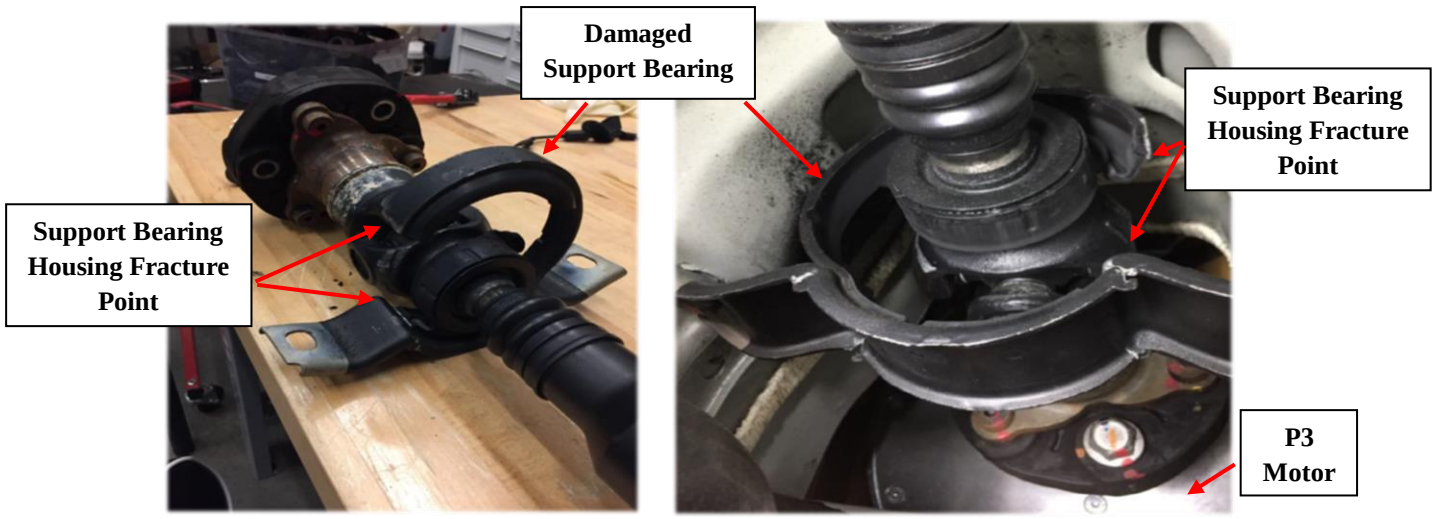

Figure 5.22: Driveshaft Failure Support Bearing Failure

A new balanced driveshaft, shown in Figure 5.23 (a), has been made out of aluminum as the replacement piece. The shaft has a boot joint plunger, and two universal joints on both ends making it more forgiving to misalignments. The interfaces on both ends of the shaft have a locating hole, shown in Figure 5.23 (b), for the insertion of the locating dowels on both the P3 and transmission,

shown in Figure 5.23 (d) & (e), allowing for the alignment of the shaft. A locating dowel has been fabricated to thread into the P3 spline as shown in Figure 5.23 (c) & (e). The installed new driveshaft can be seen in Figure 5.24.

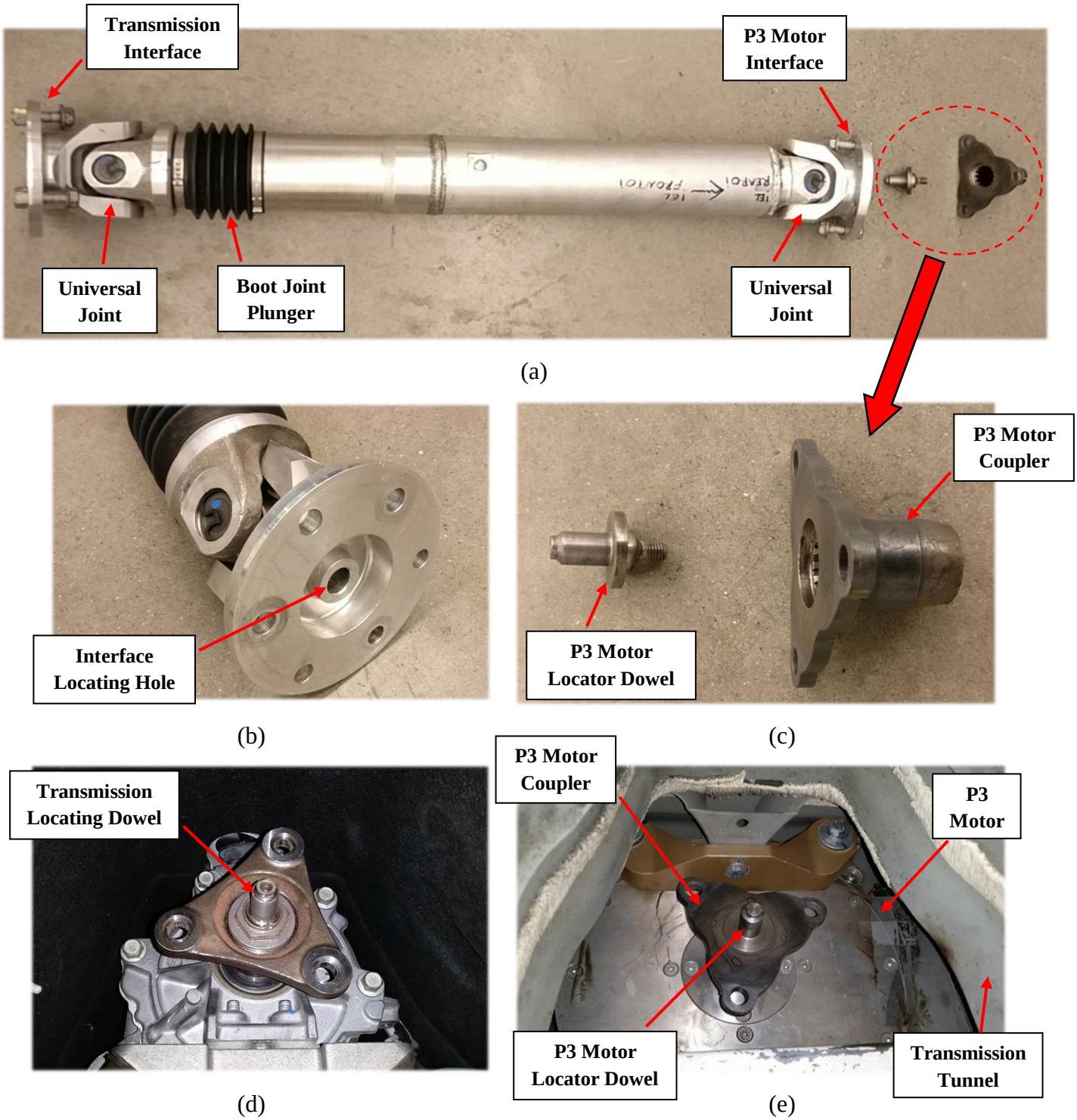

Figure 5.23: New Driveshaft Design – (a) driveshaft, (b) driveshaft locating hole, (c) P3 motor locator dowel and coupler, (d) transmission locating dowel, (e) installed P3 motor locator dowel and coupler

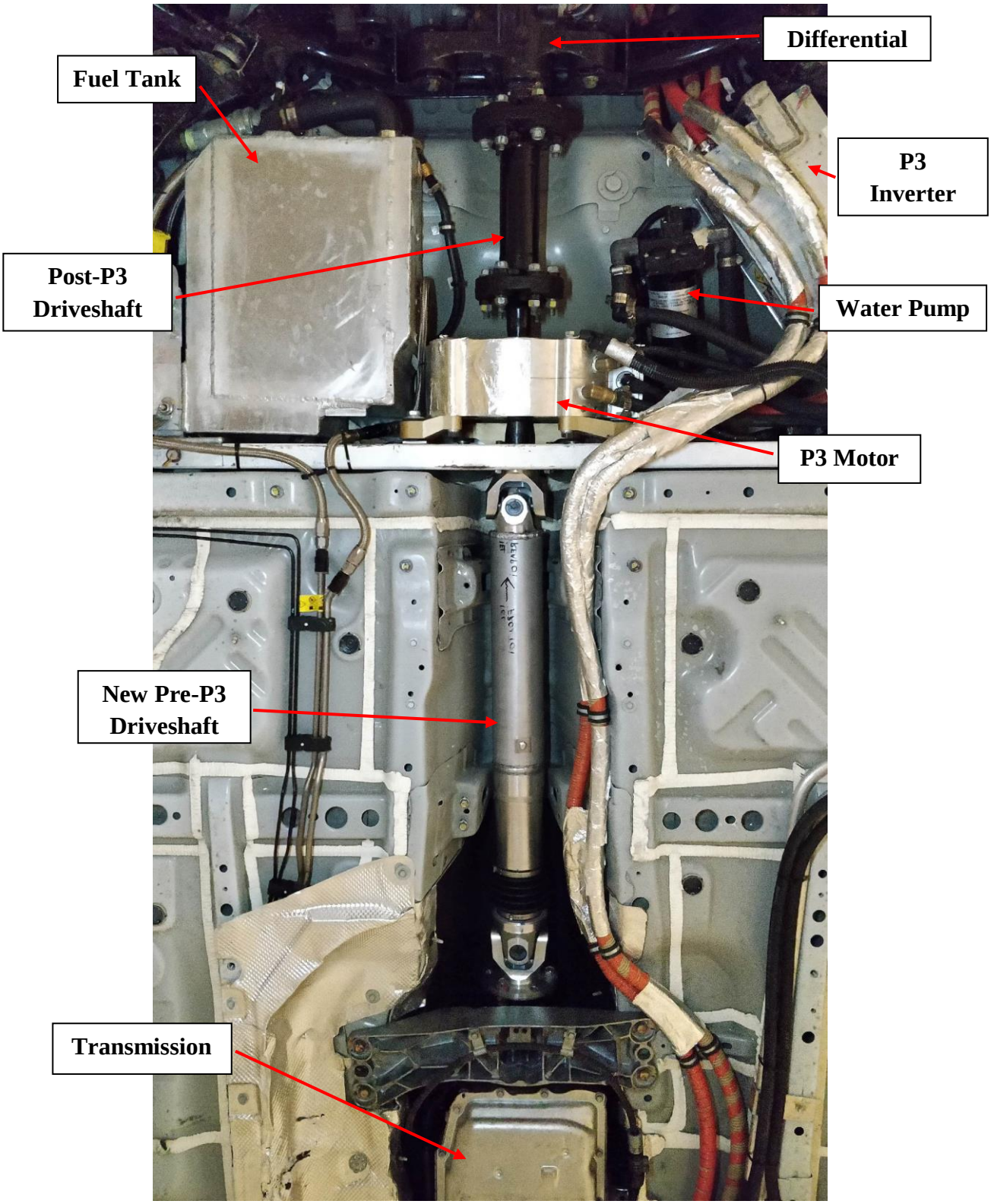

Figure 5.24: Bottom view of installed new pre-p3 driveshaft

5.6.2 Post-P3 Driveshaft

The propeller shaft seen in Figure 5.25 is connected between the P3 motor and electric limited slip differential (eLSD). The design includes two rubber couplings (flex discs) that allow some torque transient dampening and resistance to axial loading damage. On either end of the shaft are the coupling welded on to mate with the P3 motor spline and eLSD. The design specification summary shown in Table 5-1 is used to design the shaft.

Figure 5.25: Isometric and Side View of Post-P3 Shaft [33]

Figure 5.26: Coupling welded to both ends of shaft (left), female spline for P3 motor (center), rubber coupling (right) [33]

Table 5-1: Design Specification Summary [33]

	Design Requirement	Actual
Torque Transmission	1200 Nm	3400 Nm
Rotational Speed	8000 RPM	88000 RPM
Interface with Camaro Sub-Systems	DIN 5480 Spline/Differential Bolt Pattern	DIN 5480 Spline/Differential Bolt Pattern
No Plastic Deformation	All Stresses Below Yield Strength	All Stresses Below Yield Strength
Durability - Fully Reversed WOT cycles	15,000	17,000
Mass	10 kg	4.93 kg
Cost Prototyping	$900	$1,200

5.7 Energy Storage System

The energy storage system (ESS) is located in the trunk of the vehicle as seen in Figure 5.27 (a). The ESS consists of six modules with two positioned horizontally on the top frame and four vertical on the bottom frame as shown in Figure 5.27 (b). Figure 5.27 (c) calls out the other auxiliary components included in the system. These auxiliary components consist of the manual service disconnect (MSD) which is a high voltage fuse, the current shunt module (CSM) which measures high voltage and current. There is also the electrical distribution module (EDM) which contains a pre-charge resistor and contactors to allow the ESS to become live when commanded. Additionally, the battery control module (BCM) which is a non high voltage component, is responsible for triggering data measurements from the cells and interfaces with the vehicle through the hybrid supervisory controller, MicroAutoBox [78]. A significant amount of effort has been invested in simplifying the assembly procedure of the battery pack as they are fragile, heavy (26 kg each) and dangerous, so it is imperative to be able to handle it with care. The high voltage tools tend to be bulky and the use of high voltage rubber gloves make it even more difficult to have access to tight points. The priority was to design the assembly to be as simple and safe as possible while also minimizing the amount of space it would take in the trunk to maintain consumer acceptability. The goal was to also maintain enough cargo space to fit two large overnight luggage.

It was also important to consider the routing of the high voltage wires as they are thick and have very little flexibility.

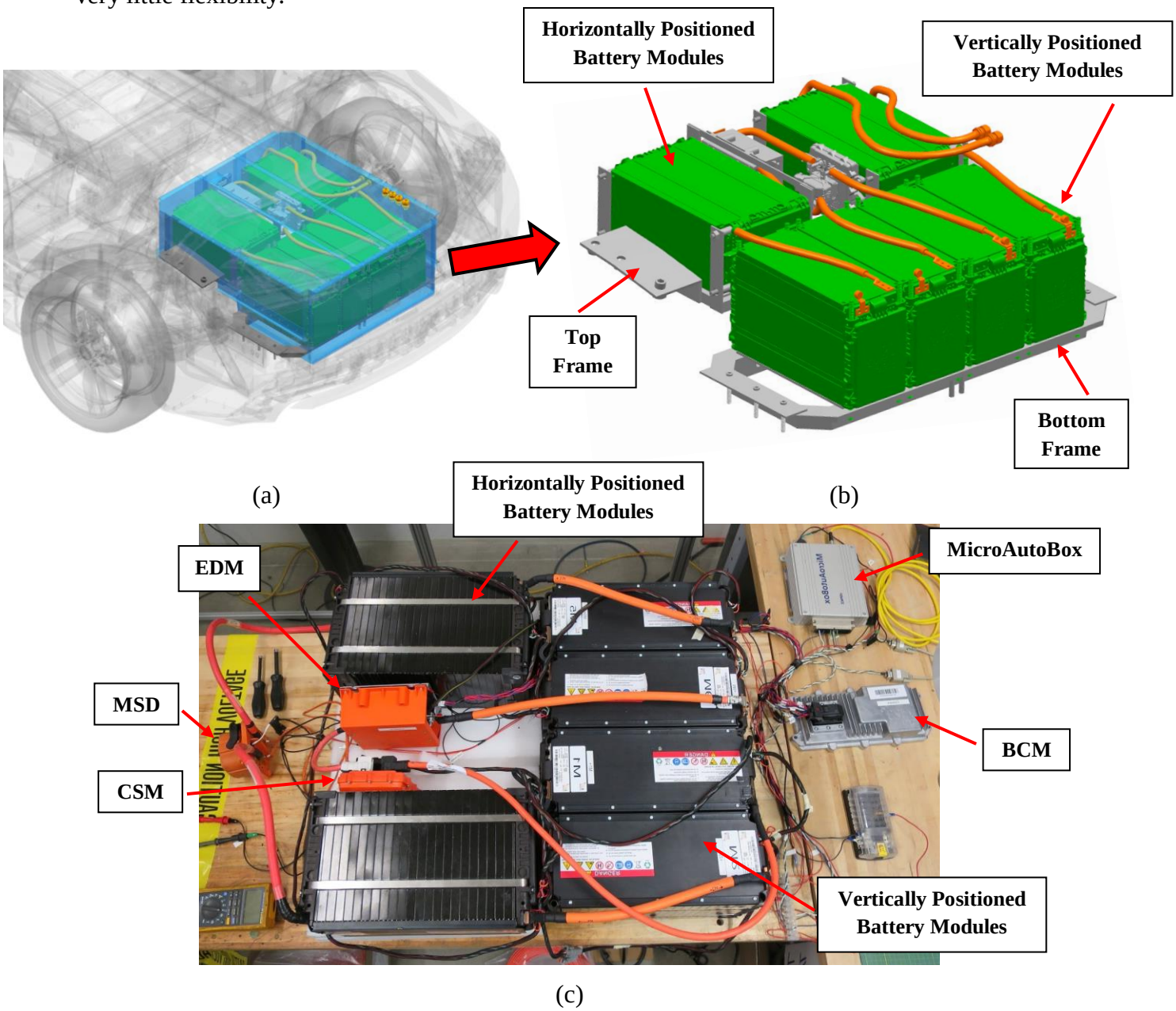

Figure 5.27: Energy Storage System Assembly – (a) ESS location, (b) ESS assembly CAD, (c) ESS arrangement and components

As mentioned, the two modules are positioned horizontally on the top frame with room for the EDM and CSM in between them. The top mount is designed to be in two parts so that they can fit through the trunk entrance and then fasten together. Weld nuts are welded on to the structural side of the trunk to support the frame as seen in Figure 5.28 (a). Once the frame was in place, the modules and the high voltage components were installed and fastened to the frame as shown in

Figure 5.28 (b). The wiring and the wall of the enclosures are then installed afterwards, prior to installing the other four modules as shown in Figure 5.28 (c).

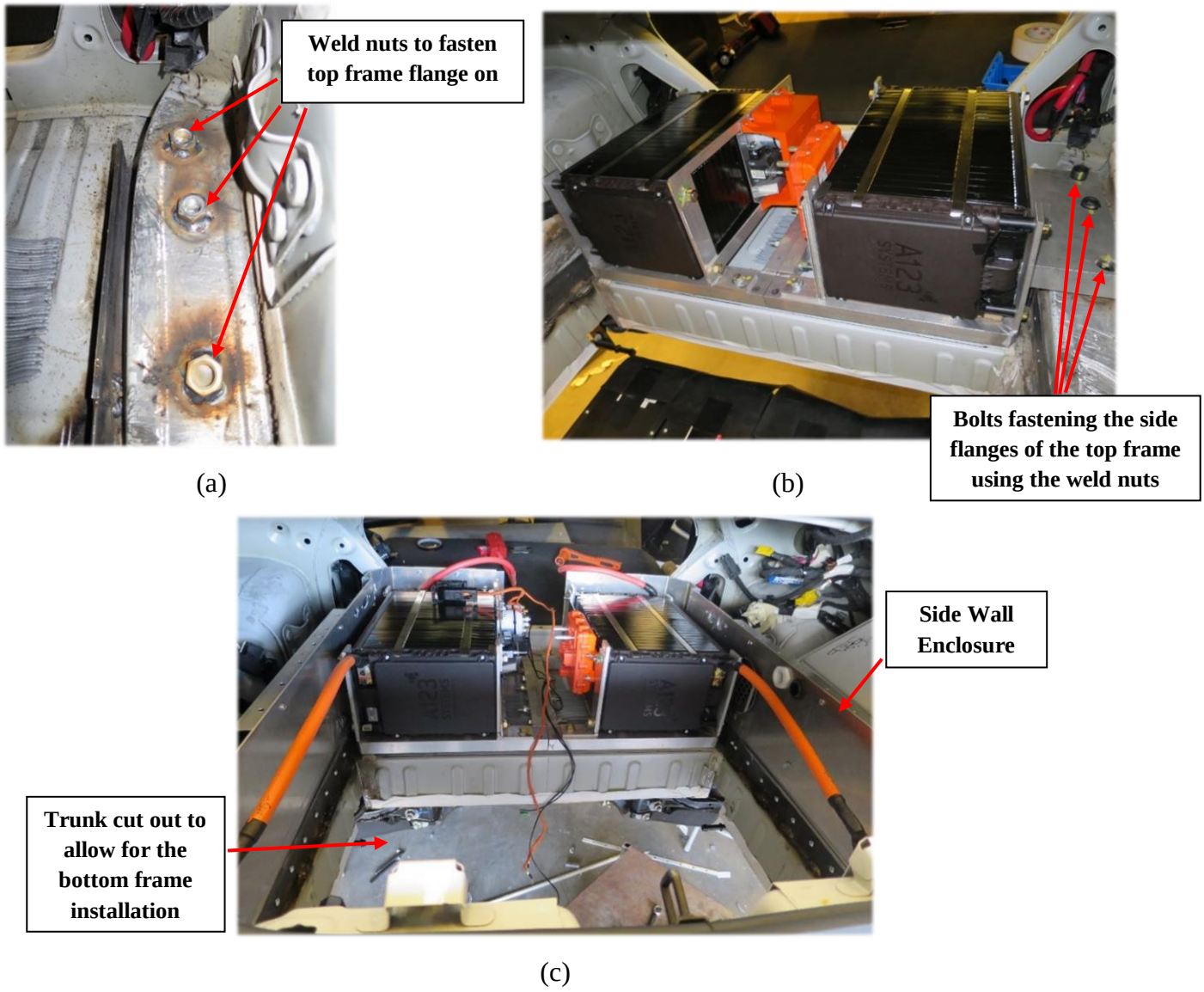

Figure 5.28: Top Frame Integration – (a) weld nuts, (b) integration, (c) wire and side enclosure integration

The floor of the trunk where it contained the air compressor and tools for removing the wheel of the vehicle was cut off to allow for the four modules to enter through, this cut out can be seen in Figure 5.28 (c). Steel bars with threaded rods were welded under the vehicle on both structural sides of the vehicle as mounting points for the bottom frame as shown in Figure 5.29 (a). The four modules were positioned on a table with their wiring connected under the vehicle which was suspended by a vehicle hoist. The hoist was then lowered until the lower frame could be fastened to the mounting points as seen in Figure 5.29.

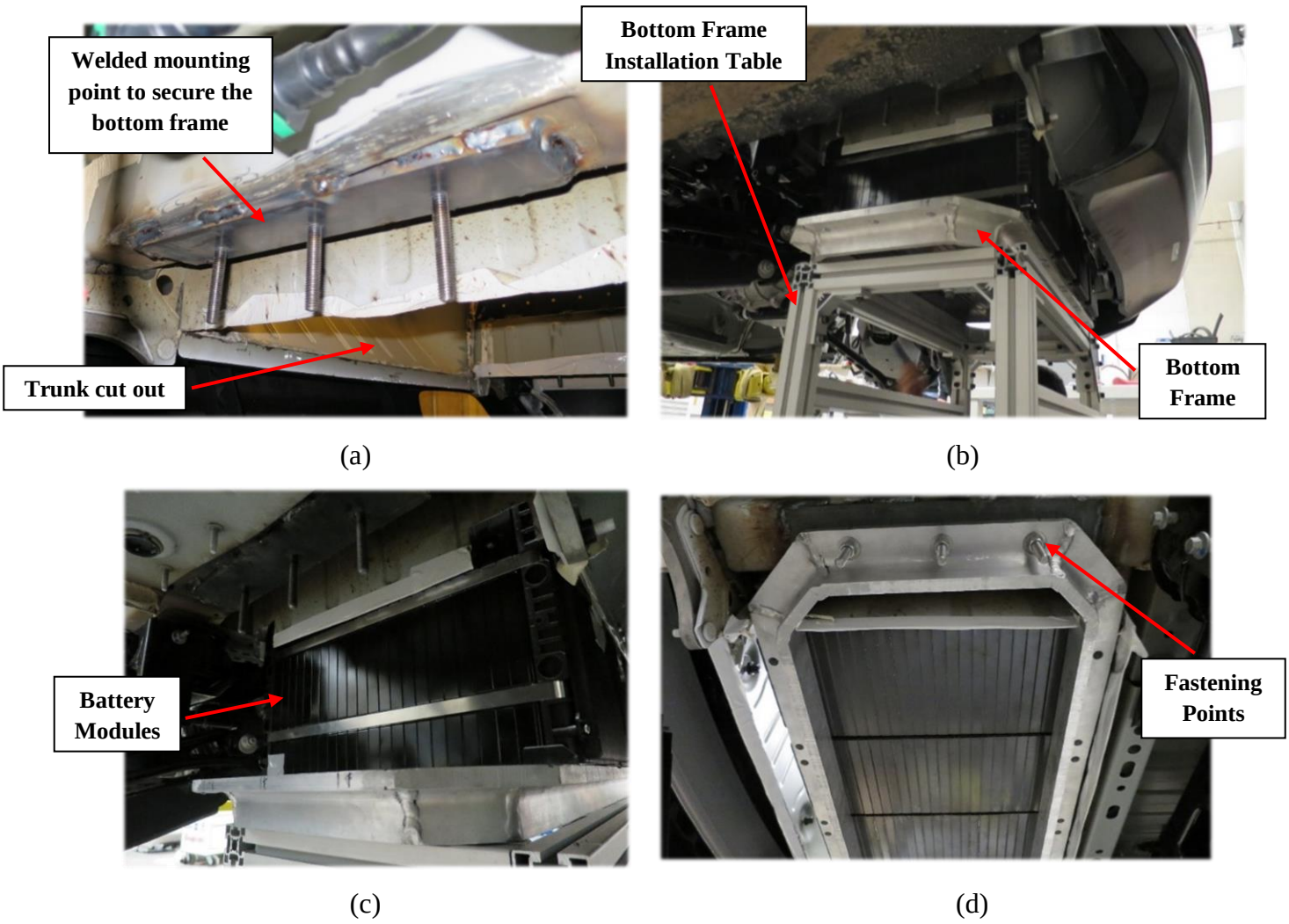

Figure 5.29: Lower Frame Integration – (a) lower frame mounting point, (b) & (c) lower frame integration, (d) mounted lower frame

The high voltage and low voltage are then all connected once everything is in place as shown in Figure 5.30. This assembly method allowed for a relatively simple integration. The two horizontal modules were easy to access for installation in the vehicle and the four modules were easily fastened and wired outside of the vehicle before the installation through the bottom. Given how tightly packed the modules were to maximize trunk space, it was not feasible to position all the modules one by one through the trunk opening or from the back seat with proper leverage while being able to properly fasten them and connect them with tools.

Figure 5.30: ESS Wiring

Finally, the top and bottom enclosure are then installed as shown in Figure 5.31. In order to prevent the disassembly of the enclosure while the battery is live, the assembly has been designed such that the MSD has to be disconnected first before anything else can come off. The middle strip of the top enclosure is clamped in place with the MSD, the middle strip clamps down on the side top enclosure and they clamp down the side walls. The top enclosure also clamps on to the bottom enclosure as seen in Figure 5.31 (c). Thus as a safety feature, the first thing that needs to come off to take off any part of the enclosure is the MSD.

(a)

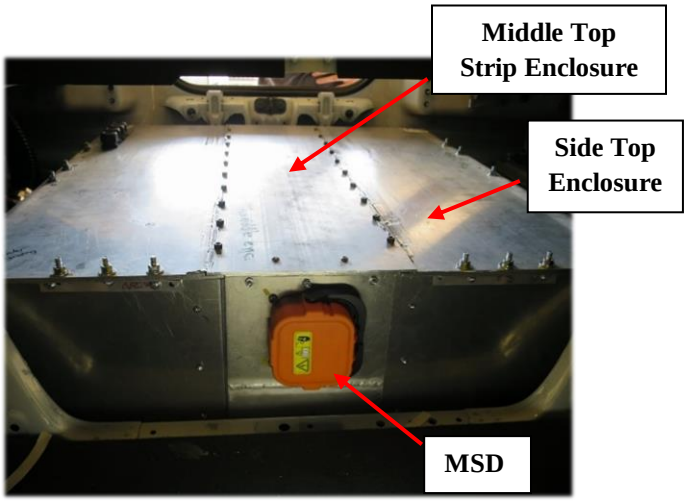

(b)

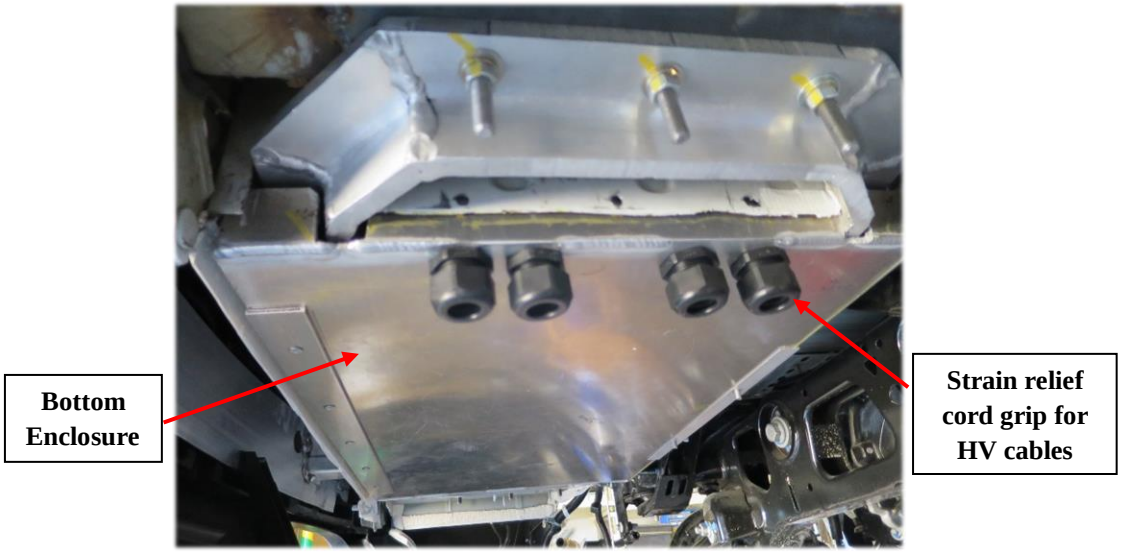

(c)

Figure 5.31: ESS Enclosure - (a) view from trunk, (b) view from back passenger seat, (c) view from bottom

5.8 Auxiliary components

This section outlines the additional non-powertrain components that are required for the vehicle to successfully operate as a hybrid electric vehicle. Table 5-2 outlines the different components with a brief description of their use and where they are located in the vehicle. The engine bay and trunk sections display their location.

Table 5-2: Auxiliary Components

	Location	Description
DC/DC Converter	Trunk	Drops the HV battery voltage to 12v to power accessories as well as charging the 12v battery. Takes place of the engine alternator that typically runs off the timing belt.
Electric Compressor	Engine Bay	This is required to operate the refrigeration system. Takes place of the mechanical A/C compressor that typically runs off the timing belt of an engine.
Inverters	Next to P2 and P3	This is required for each AC electric motor so that it can convert the DC current from the HV battery to AC current as well as control the motor.
HV battery charger	Trunk	This is required for all plug in hybrid electric vehicles. It allows the battery pack to be charged using the grid.
Vacuum Pump	Engine Bay	This is required for the hydraulic brake system. It pulls air from the chamber reducing the amount of force required to press on the brake pedal. Typically there is a vacuum line from the gasoline engine that does this however the engine does not run at all times so a vacuum pump is required instead.

High Voltage Junction Boxes	Trunk and Engine Bay	This is a distribution box that effectively distributes the HV power from the battery pack to other HV components. The bus bars inside are connected to fuses to protect the components.
Electronic Control Units	Trunk and Engine Bay	Typically every component in the vehicle that needs to be controlled has its own control unit, LV or HV.
Fuel System	Routes from fuel tank to the engine in the engine bay	Consists of the fuel tank, fuel lines, fuel regulator, evaporation lines and the carbon canister. Similar to an internal combustion vehicle
Coolant System	Routes from the engine bay to the powertrain components	Consists of the radiator, reservoir, pump, and coolant lines. Similar to an internal combustion vehicle
Exhaust	Routes from the engine and to the back of the vehicle	This had to be redesigned and rerouted through the vehicle. It is critical to keep the exhaust in mind when space claiming vehicle components to allow room for routing

5.8.1 Engine Bay

Replacing the 3.6L V6 stock engine with the smaller Textron engine has freed up a lot more room in the engine bay for the additional components, which are labeled in Figure 5.32. The 12v battery was originally located in the trunk of the vehicle but has been moved to the engine bay to make room in the trunk for the energy storage system. The stock components kept in the engine bay are the 12V fuse box, the controllers and some of the necessary electrical harness, the brake system, and the engine radiator.

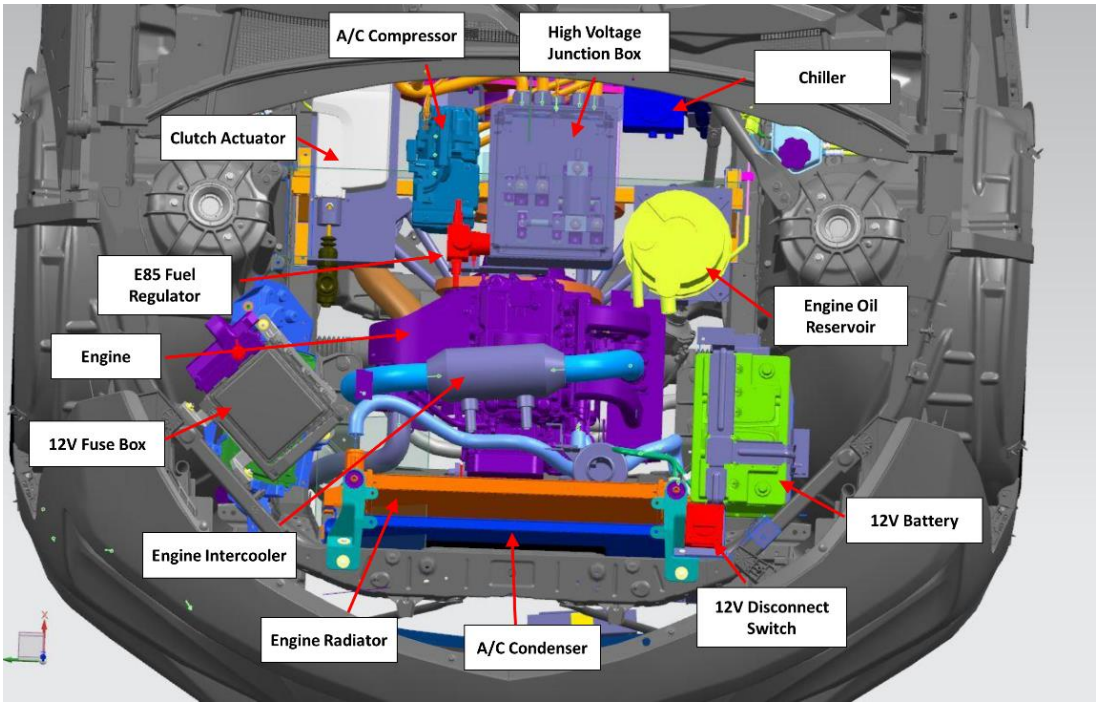

(a)

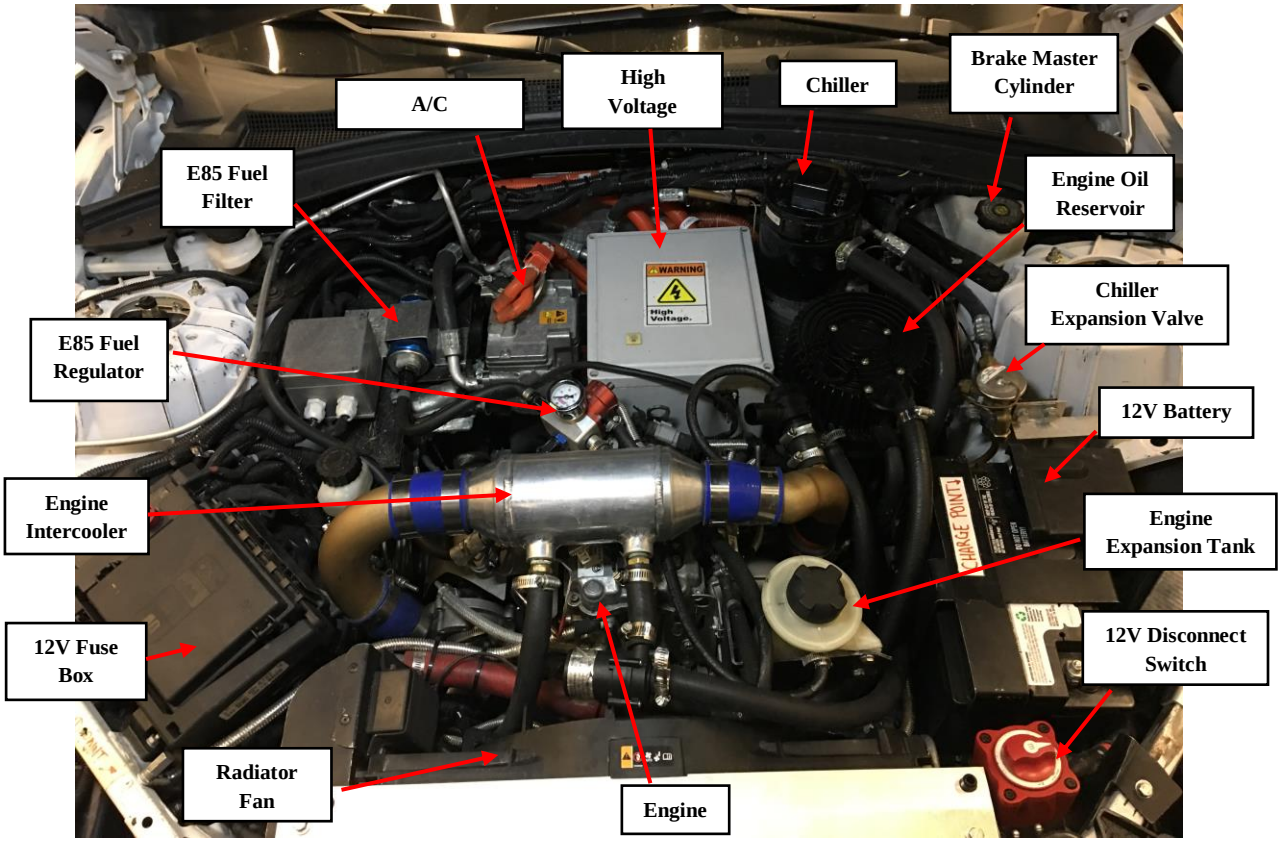

(b)

Figure 5.32: Engine Bay Components – (a) CAD component callout, (b) image component callout

5.8.2 Trunk

In addition to the ESS located in the trunk, the HV junction box, DCDC, and charger have been integrated on the sides, above the wheel well, shown in Figure 5.33. Some of the LV components such as the supervisory controller (MicroAutoBox) and stock electronic control units (ECU) have been also integrated on the ceiling and sides of the trunk.

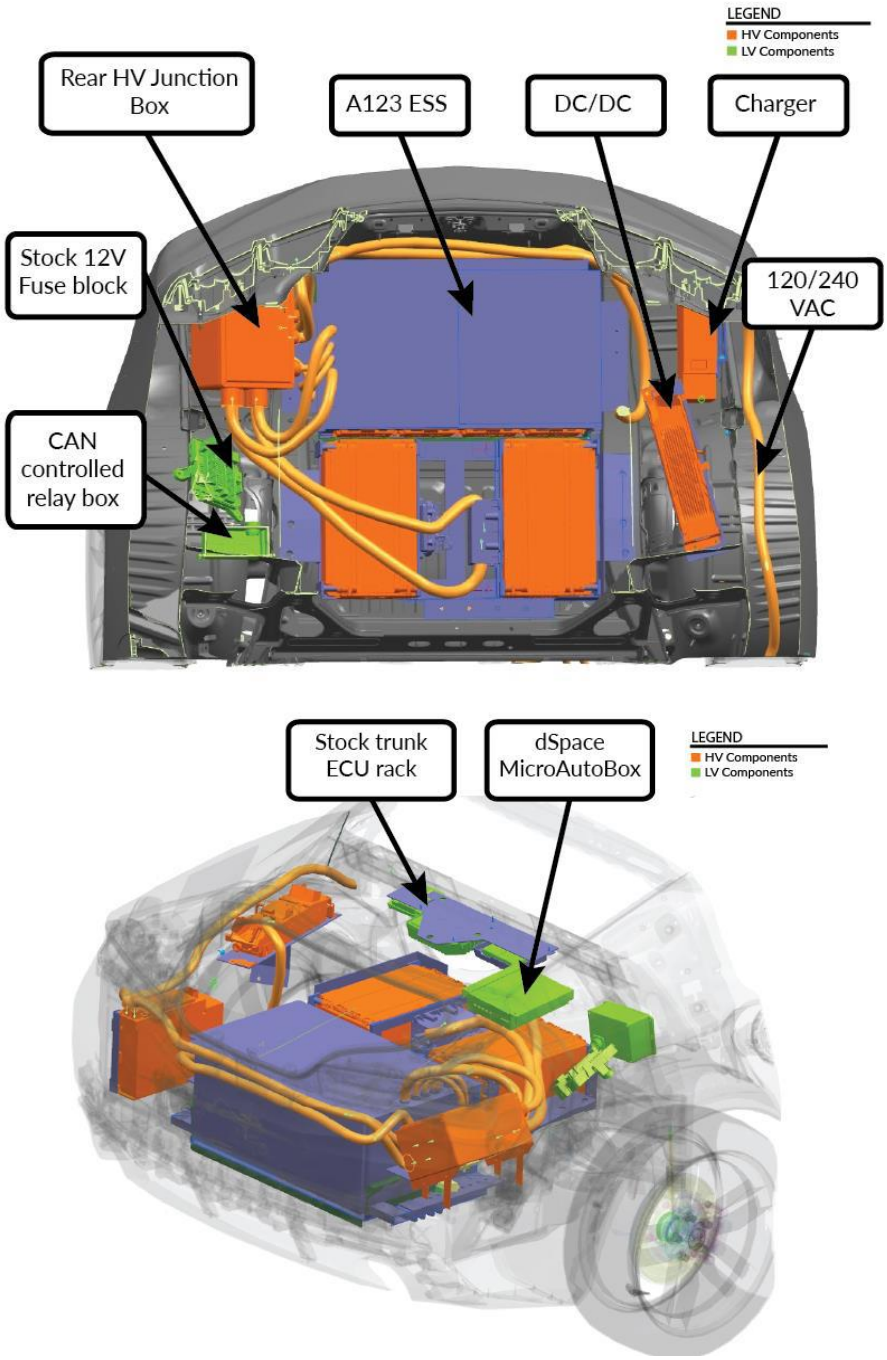

Figure 5.33: Trunk Auxiliary Component Call Out

5.8.3 Fuel System

The Textron fuel system documentation is used as reference to determine the inputs and outputs required for the fuel tank and the components required for the system. Figure 5.34 outlines the fuel system layout required from the installation manual

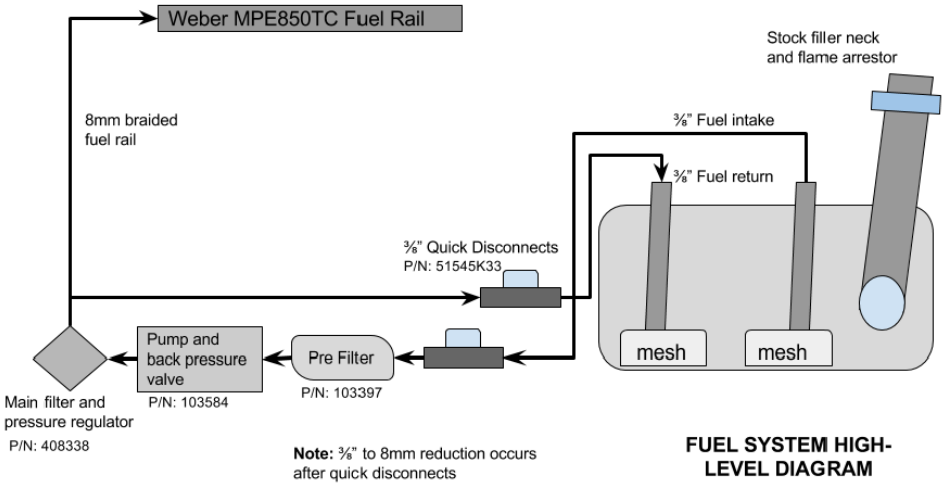

Figure 5.34: Textron Fuel System Layout [79]

Additional to the fuel system requirement, the Camaro stock evaporative emissions control system is connected to the fuel tank using a rollover valve to provide a safe exit for expansion of gases into the carbon canister. Figure 5.35 illustrates the design of the fuel tank and its inputs and outputs. The fuel tank has been sized to have a capacity of 20L to provide the additional 250 km range to meet the total vehicle range requirement of 300km

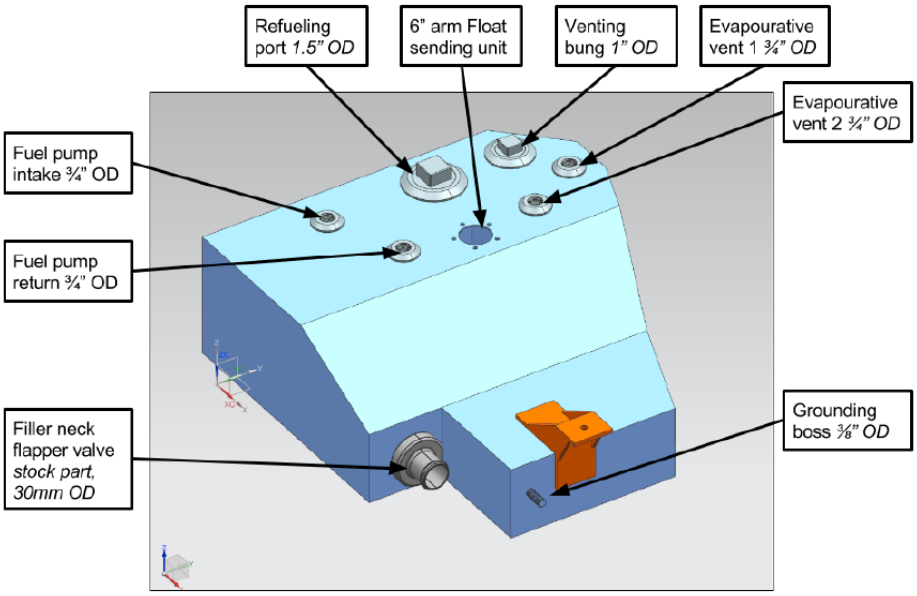

Figure 5.35: Fuel Tank I/O

5.8.4 Electrical Integration

Planning out the routing of the HV and LV electrical wires is key to avoiding mistakes that can cost a significant amount of time. The HV lines used are 2/0 cables with a 15mm diameter that are not very flexible and have a limited bend radius. It is important to include the HV cables in the CAD to ensure that the planned routing is feasible and that it is adhering to the bend radius limitations as shown in Figure 5.36. Due to the inflexibility of the HV cable, the components have been orientated and positioned to allow for the best routing possible.

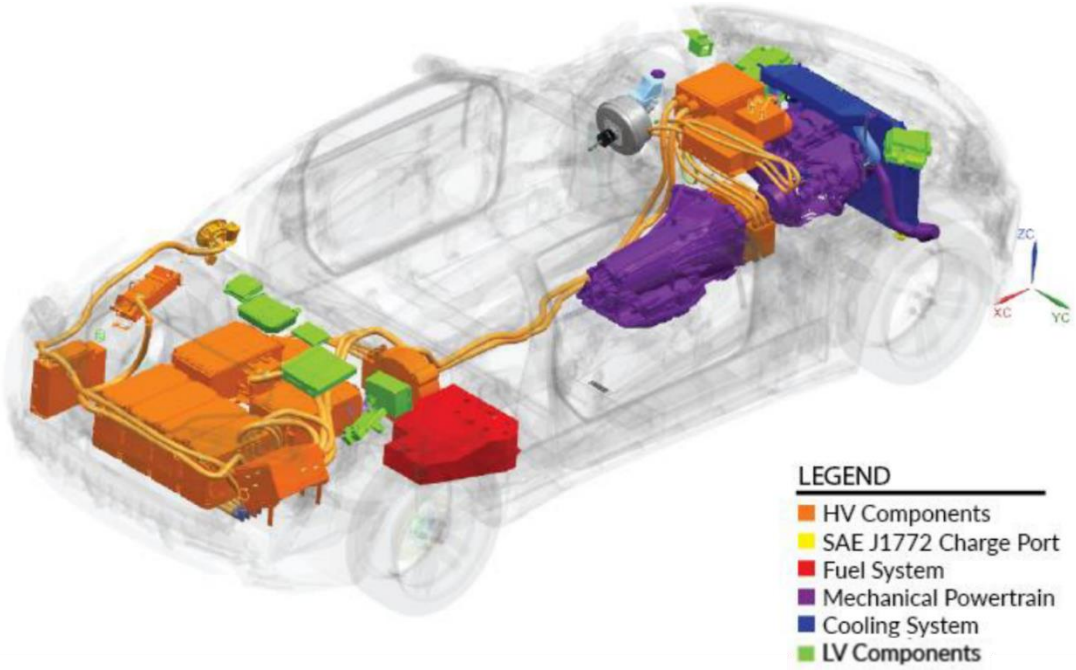

Figure 5.36: HV routing

The HV lines have been routed while also ensuring that they are not near any sharp or pinching points, they are also routed away from the coolant lines, exhaust and any rotating objects. The HV lines are routed outside of the vehicle as it is dangerous to route them through the cabin. The HV lines are selected to be orange so that it is clear to anyone that they are HV lines and they should be careful when handling them or working around them. In order to protect the cables from any sharp debreis, they have been routed in hard conduit as shown in Figure 5.37

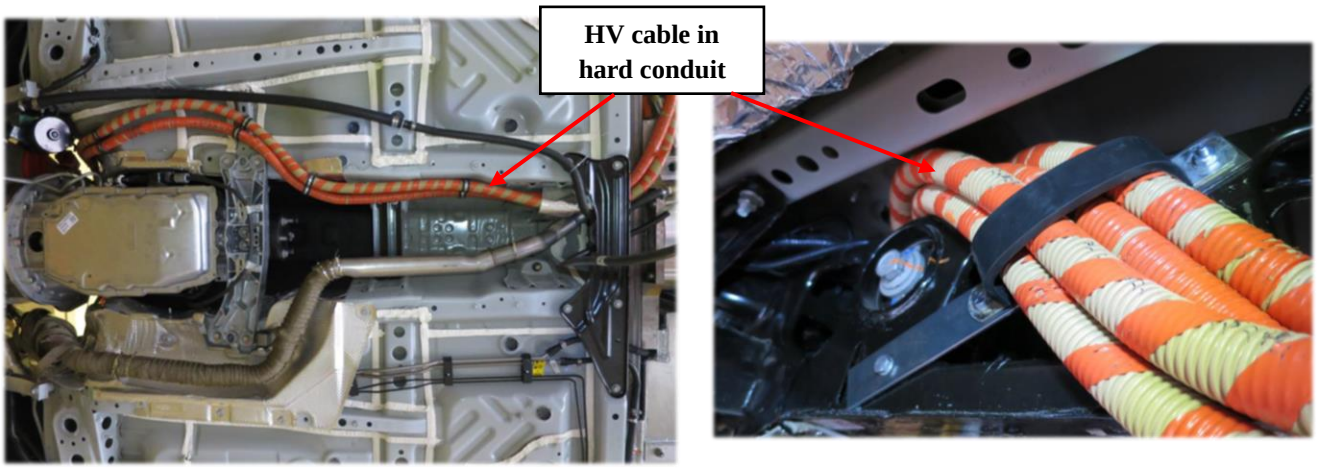

Figure 5.37: HV Conduit Routed Underneath the Vehicle

Including the LV wire in the CAD can be a very time consuming process due to there being a lot more LV wires than HV. Since the LV wires are a lot smaller and more flexible than the HV wires, the return on using the CAD is not seen to be worth the time it takes, and so instead a different approach has been taken. The coordinates of the connecting points of the LV system have been determined on the CAD as shown in Figure 5.38 and used to build a 3D peg board seen in Figure 5.39, this is not including the stock harness that is already in the vehicle or modified. The required wire lengths were determined and the harness was built on the 3D peg board to then route in the vehicle.

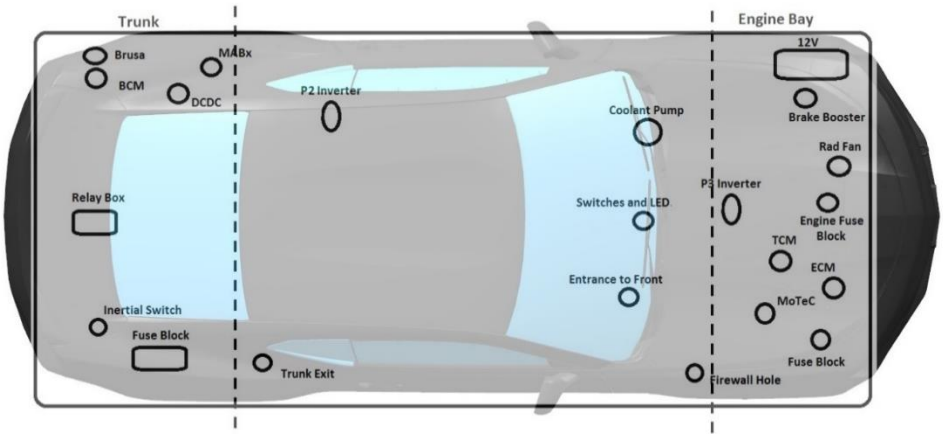

Figure 5.38: LV Locations of Interest

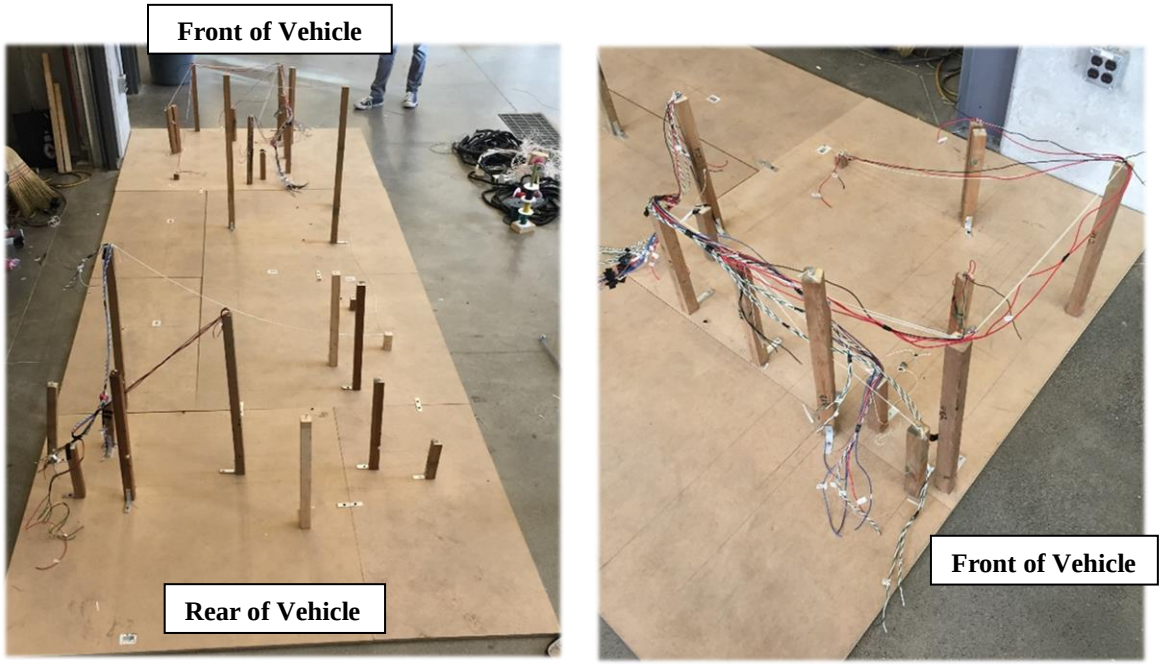

Figure 5.39: LV 3D Peg Board

Apart from ensuring that the low voltage harness is not routed near any physical hazards, it is important to consider the electromagnetic compatibility of the regions. Areas of the vehicle that an electromagnetic interference (EMI) can exist are identified in Figure 5.40. The engine ignition system in the engine bay produces significant quantities of high-intensity EMI, which could interfere with the signals of the CAN bus lines. Regions around the motor and inverters which switch between high current signals at high frequencies can also create an interference. The LV wires that could not have avoided the EMI zones have been wrapped with EMI shielding as shown in Figure 5.41.

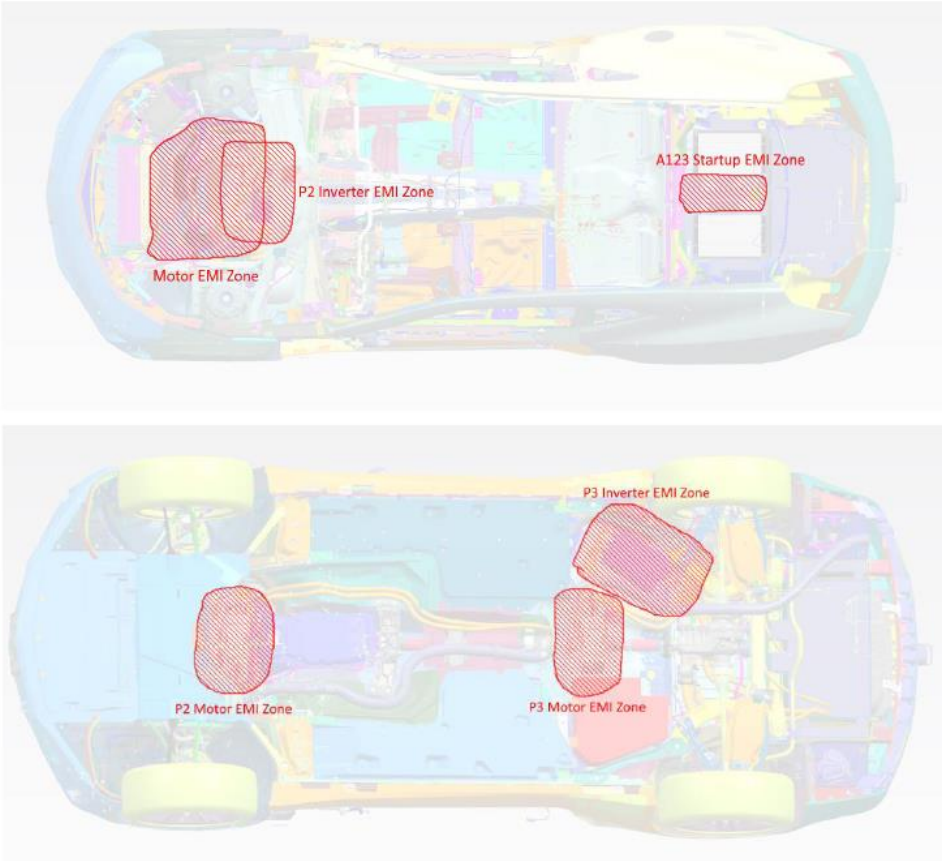

Figure 5.40: Vehicle EMI Zones [33]

Figure 5.41: LV EMI Shielding

In addition to all the physical safety precautions taken to protect the electrical lines, the HV distribution/junction box and LV fuse block is also used to protect the components from any unintended current spikes. There are two HV junction boxes, one located in the trunk and another in the engine bay, they contain bus bars and fuses for the lugs to attach to as seen in Figure 5.42 (a). There are a total of three LV fuse blocks in the vehicle, an additional fuse block has been integrated in the engine bay with the stock fuse block and the other in the trunk as shown in Figure 5.42 (b)

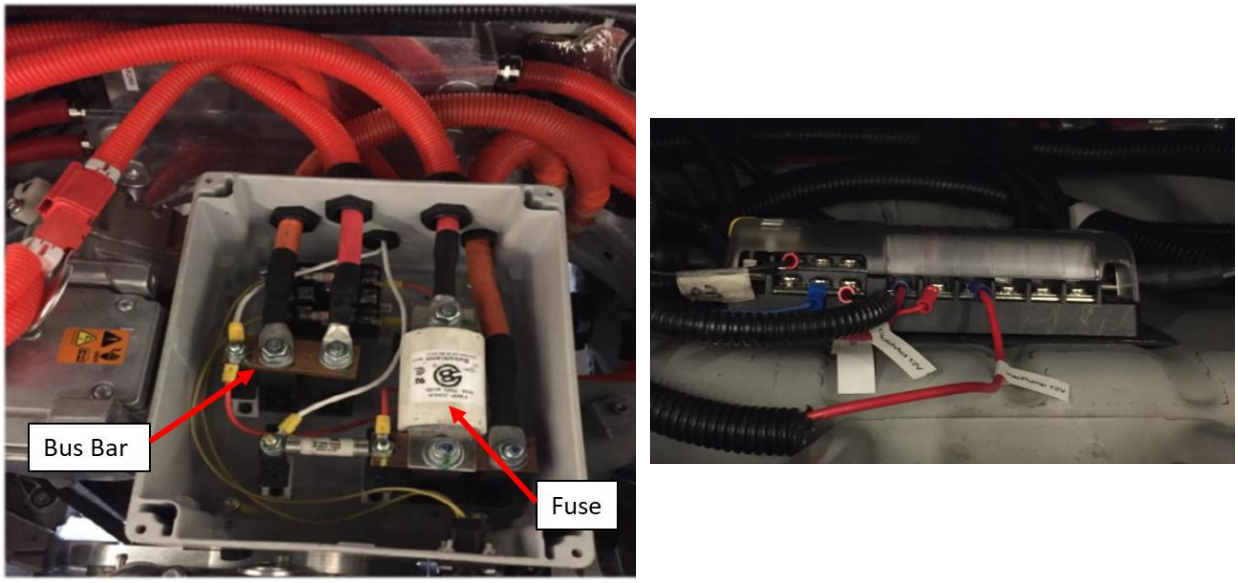

(a) (b)

Figure 5.42: LV and HV Fusing – (a) HV Junction box in engine bay, (b) LV fuse block in trunk

5.8.5 Controls Integration

The newly integrated powertrain components and their auxiliary components including the stock components have their own dedicated electronic control units (ECU) for their operation. However, there is a need for a controller to oversee and command the individual ECUs so that the vehicle operates accordingly. A controller for this purpose is referred to as the master controller or hybrid supervisory controller (HSC). The HSC contains the vehicle control strategy code and logic that takes in the input of the driver demands, component feedback, and vehicle status to output the appropriate command signals to safely operate the vehicle as required. The HSC manages the vehicle mode operation and transition, it provides the required powertrain torque distribution (or blending) and energy management strategy. The HSC control strategy is responsible for optimizing the powertrain efficiency, performance, driveability and minimizing the fuel/energy consumption. The component utilized for the hybrid supervisory controller is the dSPACE MicroAutoBox. Figure 5.43 provides a high level schematic of the HSC's connection to the other ECUs that are either stock or developed for the vehicle. For more information on the vehicle controls development, refer to the paper provided by Radhika Kartha [76].

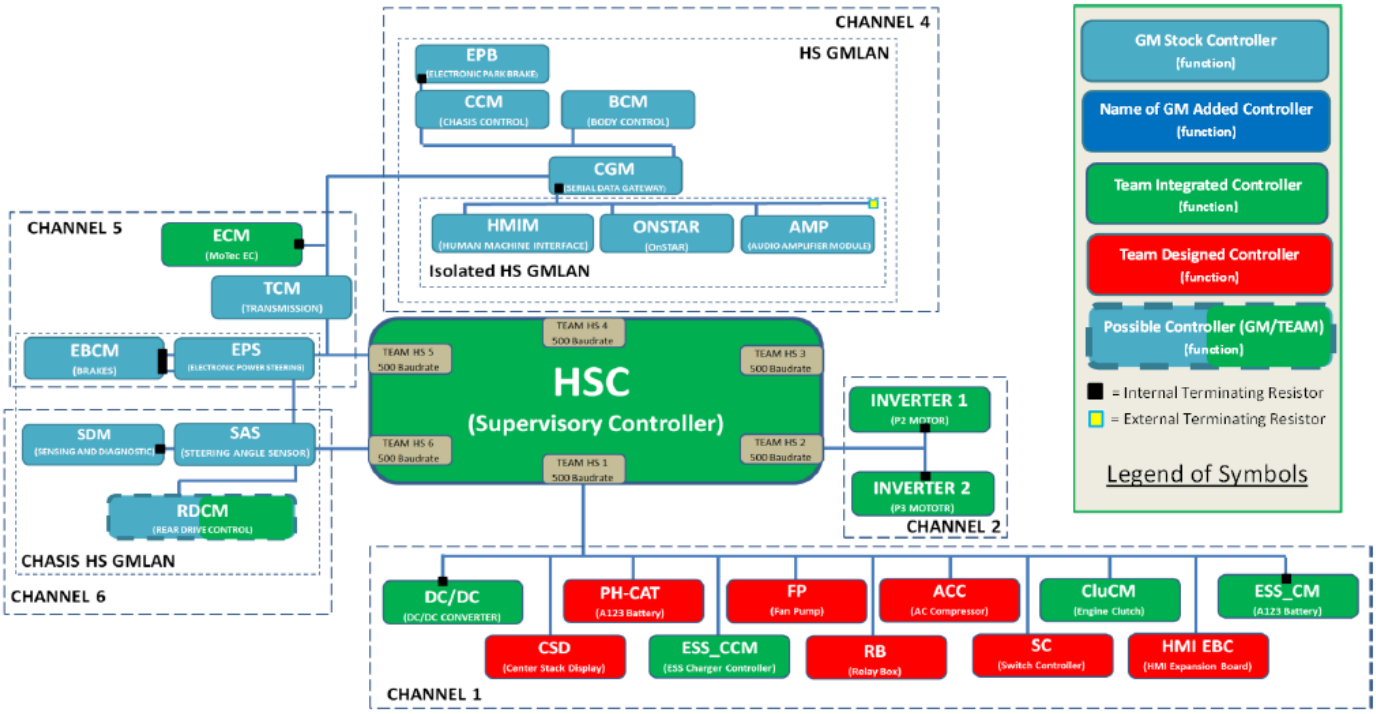

ECU Name	ECU Function	ECU Name	ECU Function
ACC	Denso AC Compressor	FP	Fan Pump Controller
BCM	Body Control Module	HMI EBC	HMI Expansion Board Controller
CGM	Serial Data Gateway Module	ESS_CM	Energy Storage System Control Module
CCM	Chassis Control Module	HMIM	Human Machine Interface Module
CluCM	Engine Clutch Control Module	INVERTER1	Inverter for P2 Motor
CSD	Center Stack Display Controller	INVERTER2	Inverter for P3 Motor
DC/DC	Denso DC/DC Converter	PH-CAT	Pre-Heated Catalytic Converter
EBCM	Electronic Brake Control Module	RB	Relay Box Controller
ECM	MoTEC Engine Control Module	RDCM	Rear Drive Control Module
EPB	Electronic Park Brake	SAS	Steering Angle Sensor
EPS	Electronic Power Steering	SC	Switch Controller
ESS_CCM	ESS Charger Control Module	SDM	Steering and Diagnostic Module
ESS_CM	Energy Storage System Control Module	TCM	Transmission Control Module

Figure 5.43: High Level HSC Schematic [33]

5.9 Vehicle Mass Analysis

The change in vehicle mass and its distribution is important to consider as it has an impact on the performance and handling of the vehicle including fuel/energy consumption. Table 5-3 displays the change in mass of the front and rear of the vehicle after the vehicle conversion. Note that the new mass of 1,872 kg surpasses the 1,800 kg VTR.

Table 5-3: Summary of Vehicle Curb Mass Changes

	Stock Mass	Added Mass	New Mass	Front/Rear Ratio	
Total (kg)	1565	307	1872	**Stock**	**New**
Front Mass (kg)	820	37	857	52%	46%
Rear Mass (kg)	745	270	1015	48%	54%

The vehicle has gained an additional 307 kg, and the weight distribution has also been shifted from 52/48 front heavy to 46/54 rear heavy. The added rear mass is mainly due to the ESS, its enclosure, and mounts located in the trunk, which sums to a total of 222 kg. The gained mass results in the vehicle having to output a higher traction force and power to achieve the required acceleration. The change of the mass distribution will also affect the vehicle handling, a rear heavy vehicle is susceptible to over steering or fish tailing. To accommodate for the new mass distribution, the spring and dampers of the suspensions system are replaced with stiffer ones in order to correct the ride height and adjust the vehicle handling. The new location of the center of gravity (CG) of the vehicle as a result of the mass distribution is shown in Figure 5.44.

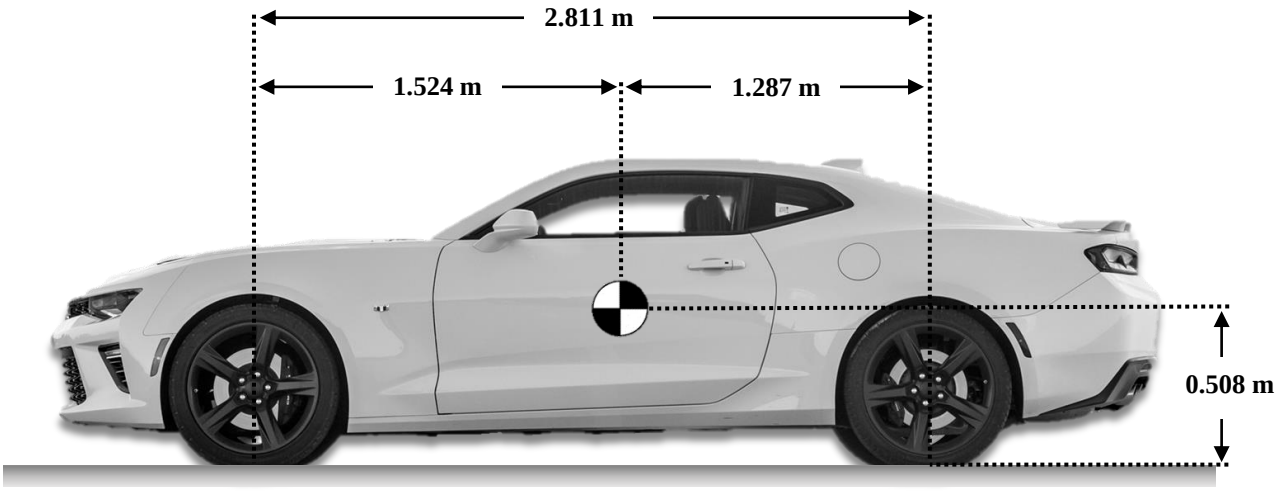

Figure 5.44: Vehicle's Shifted Center of Gravity

Although the shift of CG to the rear of the vehicle may impede the vehicle handling, it can improve the 0-100 km/h acceleration performance for a rear wheel drive vehicle. This is due to the load transfer to the rear wheels as a result of the acceleration force discussed in section 4.5 Powertrain Performance Analysis. As the distance from the front wheels to the CG increases, depicted as A in equation (4-9), the normal force on the rear wheel will increase leading to a higher traction grip.

The detailed mass analysis outlining the mass changes is provided in Table 5-4. The ESS enclosure is made out of relatively thick aluminum plates, and the mounts have been over designed, it is estimated that if the enclosure is replaced by carbon fiber and if the mounts are optimized then the mass could be reduced by 17 kg. Replacing the trunk decklid with carbon fiber could also save an additional 8 kg. Most of the other mounts including the auxiliary and powertrain mounts have also been overdesigned, optimizing them could save another 15 kg at least.

Table 5-4: Detailed Vehicle Mass Analysis

	Vehicle Mass Change (kg)
ADAS Equipment	7
Auxiliary Mounts	42
Clutch System	10
Coolant	5
Coolant Lines	3
Coolant Pumps	4
Coolant Reservoir	2
DC/DC Converter	3
Electric Compressor	7
Electric Motors x2	61
Electric Motors Mount	10
eLSD	45
Engine Mount & Custom Bellhousing	16
ESS Charger	6
ESS Enclosure	19
ESS Frame	38
ESS Modules and electronics	165
Fuel	18
Fuel Tank	5
High Voltage Harness	15
High Voltage Junction Boxes x2	9
Inverters x2	18
Low Voltage Harness and ECU	12
Microautobox	1.5
Miscellaneous Electrical Components	8
New Engine	59
New Exhaust	21
P3 to Differential Shaft	5
Transmission to P2 Shaft	10
Vacuum Pump	4
Stock Differential	-36
Stock Driveshaft	-13
Stock Engine and Accessories	-157
Stock Exhaust	-51
Stock Fuel	-49
Stock Fuel Tank	-14
Total	307

CHAPTER 6
Powertrain Thermal Management

Sizing and integrating the thermal system correctly is as critical as the powertrain components themselves. Without the proper thermal system in place, the vehicle will be limited in its performance as to avoid overheating, or the individual components can completely shut down during operation as a safety precaution. Worse yet, if a safety precaution is not in place, the components may be damaged, costing a significant amount of money and time to replace or fix. Historically at UWAFT, the thermal management has consumed a lot of time and resources since its correct component and configuration would have been determined through trial and error. Performing the correct analysis to size the heat exchangers and determining the pressure drop of the system to correctly size the water pump as discussed in this chapter will remove the need for a trial and error approach, saving time.

The first section discusses the components that require a thermal management system to avoid overheating; this includes the internal combustion system, the engine intercooler, and the electric powertrain, which encompasses the two electric motors and inverters. For this prototype vehicle's expected operation and scope, it has been determined that a thermal management system for the energy storage system is not critical as it does not generate a significant amount of heat that could cause it to overheat. This is further discussed in the battery thermal management section. Lastly, since the transmission oil cooling system has not been modified, an analysis on the system was not required and therefore not included.

The second section of this chapter explains the implemented vehicle thermal system layout, including the component cooling requirements determined from the worse case heat generation analysis and manufacturer recommendations. The electric powertrain and intercooler share the same cooling loop to simplify the overall thermal management system and to reduce costs. The

loop also utilizes a refrigerant chiller system which runs in parallel to the stock refrigerant line for the in-cabin evaporator. Since the engines recommended coolant temperature is much higher than the other components, it has its own thermal loop which utilizes the stock V6 engine radiator.

The third section focuses on the thermal management design of the electrical powertrain and the intercooler. It highlights the analysis carried out to size the radiator and intercooler. It discusses the configuration and arrangement of the thermal loop i.e. series vs parallel routing and provides the analysis required to size the coolant pump. The section also covers the current refrigeration system design and the future work required.

6.1 Heat Generating Components

6.1.1 Internal Combustion Engine

The combustion engine, being a heat engine, operates by converting the thermal energy to useful work. Engine efficiency is measured in thermal efficiency and can be determined as the ratio of useful work done to the heat input. However, most of the input heat energy is dissipated as waste heat that can be absorbed by the engine which can lead to component damage i.e. warping, melting. Currently, with the advancement of engines today, the maximum thermal efficiency can come close to 40 percent [80]. In order to prevent the engine from overheating, there is a need for a cooling system, a typical thermal system of a combustion engine is illustrated in Figure 6.1. The engine cooling system, much like most engines, consists of an internal water pump connected to the crankshaft to provide flow for coolant through the water channels located within the engine. The radiator and the fan are used to reject the heat out of the coolant while the expansion tank is meant to reduce the pressure in the system at high temperatures. The cooling system of an engine is also used to heat the cabin as required by the user. Hybrid electric vehicles that do not utilize the engine at all times, like this vehicle, can use an electrical heater to heat up the coolant to provide heat to the cabin.

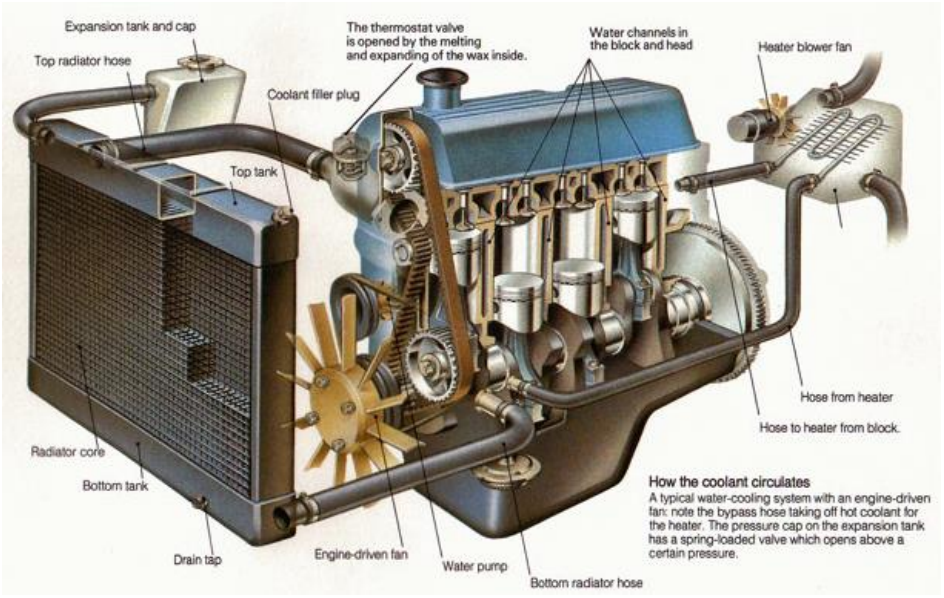

Figure 6.1: Engine Thermal System Example [81]

The amount of energy/power available for use in an engine can be determined by using equation (6-1), where $\dot{m}_f$ is the fuel mass flow rate and Q_{HV} is the heating value of the fuel used.

$$\dot{W} = \dot{m}_f Q_{HV} \tag{6-1}$$

The power generated is distributed into the output power at the crankshaft, the energy lost at the exhaust flow, the energy lost to the surroundings by heat transfer, and the power to run engine accessories; this is represented in equation (6-2) [60]. In the case of this Textron engine, the only accessory it is running is the internal water pump. The heat loss to the surroundings includes the heat transfer to the oil, coolant and ambient. Energy lost at the exhaust also accounts for the chemical energy of the unburnt fuel. Figure 6.2 displays the energy flow diagram of the total fuel energy input.

$$Power\ generated = \dot{W}_{shaft} + \dot{Q}_{exhaust} + \dot{Q}_{loss} + \dot{W}_{acc} \tag{6-2}$$

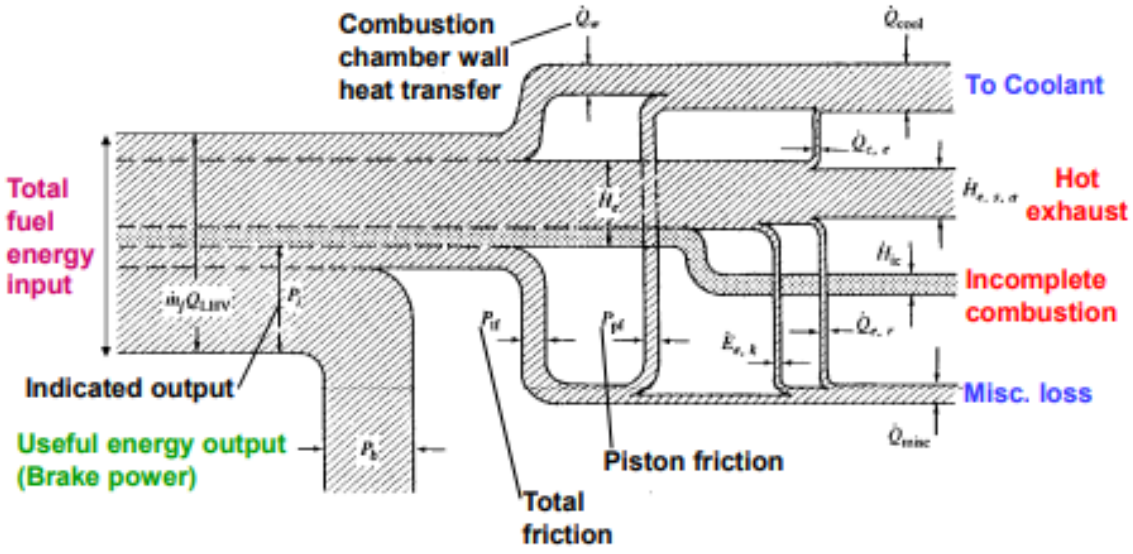

Figure 6.2: Energy Flow Diagram for an IC Engine [82]

Although the amount of heat the coolant is required to draw from the engine varies depending on engine load, thermal efficiency, and combustion efficiency, in general it is approximated to be 1/3 of the input energy [83]. Equation (6-3) can be used to develop a ballpark value of how much heat needs to transfer to the coolant, with η_t being the thermal efficiency.

$$\dot{Q}_{out\ coolant} = \frac{1}{3} \times \frac{\dot{W}_{shaft}}{\eta_t} \qquad (6\text{-}3)$$

The preliminary tune for using E85 with the Textron engine has shown that the efficiency is around 20 percent with peak being 22 percent [84]. Therefore, at a peak power output of 92 kW from the Textron engine, using equation (6-3), there should be a heat rejection of 153 kW to the coolant and out of the radiator to prevent the engine temperature from raising further.

Due to the limited available resources and project timeline, the stock V6 engine radiator of the Camaro has been kept to be used for the Textron engine. The stock radiator is designed in two partitions for compactness, the one section is to reject heat from the coolant of the V6 engine and the other is for cooling the transmission oil. Replacing the stock radiator would require having to select and purchase a separate radiator for the transmission oil, increasing costs and human resources needed. Given that the V6 engine is rated at 250 kW [85], it is expected that the stock radiator would be more than sufficient to reject the required heat from Textron engine as its power output is around 1/3rd of that.

6.1.2 Electric Powertrain

The electric powertrain components that require cooling are the two electric motors and the two corresponding inverters. Determining the heat generation of the electric powertrain is simpler than the combustion engine. The inefficiency of the components are taken to be the waste heat generated at the given torque and speed. For an overestimated value as a safety factor, it is assumed that there is no heat loss from the components due to convection or conduction to the ambient air and that the waste heat can only transfer through the coolant. The electric motors and inverts are designed to have an input and output port for coolant to flow through allowing it to draw heat from the components similar to the combustion engine. Equation (6-4) and (6-5) are used to determine the heat generation of the electric motor and inverter respectively at the given operating speeds.

$$\dot{Q}_{out\ Coolant,motor} = \frac{\tau\omega}{\eta_{motor}} \times (1 - \eta_{motor}) \tag{6-4}$$

$$\dot{Q}_{out\ Coolant,inverter} = \frac{\tau\omega/\eta_{motor}}{\eta_{inverter}} \times (1 - \eta_{inverter}) \tag{6-5}$$

Based on the electric motor and inverter efficiency maps, it has been found that the most heat is generated during maximum performance demand. Recall that in section 4.5 Powertrain Performance Analysis, the maximum power the two electric motors can generate is limited to the maximum available power from the energy storage system. This is taken into account to determine the maximum possible heat generation. Using equation (6-4) and (6-5) the heat generation vs motor speed is calculated for both the P2 and P3 motor and inverter pair, which is displayed in Figure 6.3 and Figure 6.4 respectively. The maximum heat generation of P2 and Inverter set is found to be 14.6 kW at 3,000 rpm and 6.4 kW at 6,700 rpm for the P3 set, totalling to 21 kW.

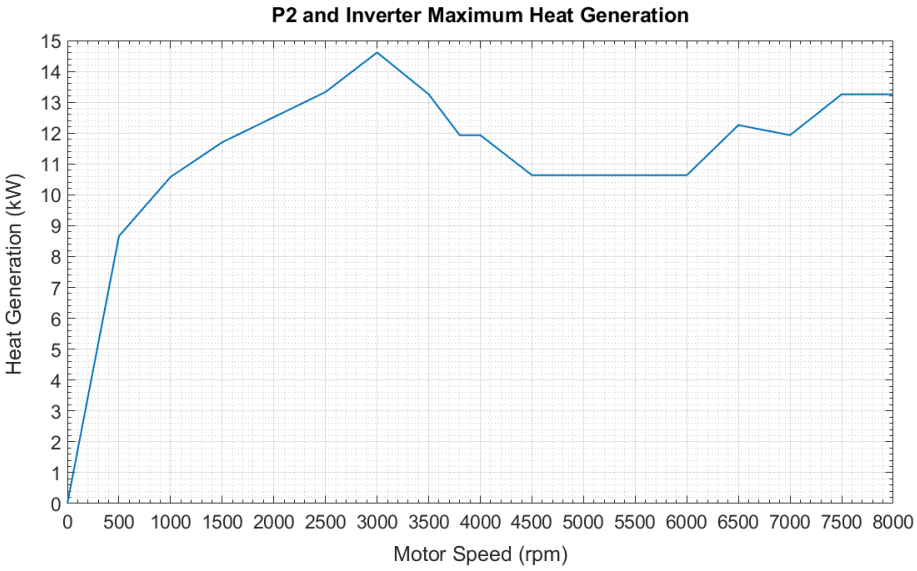

Figure 6.3: P2 and Inverter Maximum Heat Generation

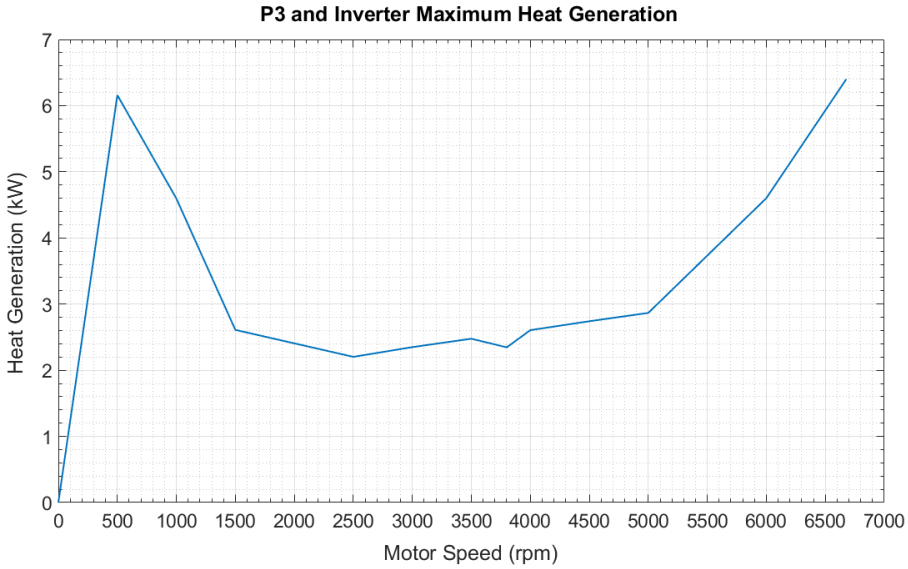

Figure 6.4: P3 and Inverter Maximum Heat Generation

The maximum heat generation of 21 kW in addition to the maximum heat generation of the intercooler (discussed in the next section) will be used to design the thermal system. It is worth noting that by sizing the thermal system to dissipate the maximum worse case heat generation, it will be overdesigned and oversized. This is because the vehicle will not be always operating with a maximum power demand as the drive cycle analysis section suggests. This is however a good parameter to use for the first thermal system design iteration. Sufficient data can be gathered and analysed during vehicle testing to better characterize the thermal system including the thermal capacity of the coolant and components to establish a more representative thermal model. The next

thermal system design iterations can then further downsize and optimize the system, which will reduce the pump power draw required.

6.1.3 Intercooler

A turbo charged engine typically requires an intercooler to cool the compressed charged air exiting the turbo, before entering the engine. If the charged air is allowed to get too hot, it may lead to a pre-ignition detonation resulting in engine knocking. Engine knocking can overheat the engine and produce high pressure pulses which can cause damage. Furthermore, the cooler the air is, the more dense it is, allowing more oxygen in the chamber, increasing power output. The engine parameters required to determine the air flow rate and temperature increase are listed in

Table 6-1.

Table 6-1: Engine Parameters

	Variable	Value
Compression ratio	r_e	9:1
Gas constant	R	287.05 J/kg K
Stroke length	S	0.068 m
Bore diameter	B	0.089 m
Clearance volume	V_c	$5.29x10^{-5}$ m^3
Displacement volume per cylinder	V_d	$4.23x10^{-4}$ m^3
Turbo charger isentropic efficiency	η_s	70%
Number of cylinders	-	2

To determine the charged air temperature after compression, the isentropic process of ideal gas equation (6-6) is used. Where k is the specific heat ratio (c_p/c_v), and P_1, T_1 is the atmospheric pressure and temperature entering the turbo charger respectively. P_2, T_2 is the charged pressure and temperature exiting the turbo charger respectively.

$$T_2 = T_1 \left(\frac{P_2}{P_1}\right)^{\frac{(k-1)}{k}} \tag{6-6}$$

The isentropic efficiency (η_s) of the turbo charger is then used to determine the actual outlet temperature as shown in equation (6-7).

$$T_{2,actual} = T_1 + \frac{T_2 - T_1}{\eta_s} \quad (6\text{-}7)$$

Using the engine compression ratio value and the displacement volume, the volume at the bottom dead center can be calculated as shown in equation (6-8) and (6-9). Then, the mass of air present in a cylinder chamber can be calculated using equation (6-10). Once the chamber air mass is determined, the air mass flow rate can be determined using equation (6-11).

$$r_e = \frac{V_d + V_c}{V_c} \quad (6\text{-}8)$$

$$V_{BDC} = V_d + V_c \quad (6\text{-}9)$$

$$m_a = \frac{P_2 V_{BDC}}{R T_2} \quad (6\text{-}10)$$

$$\dot{m}_a = m_a \times (2\ cylinders) \times rpm \times \left(\frac{1\ minute}{60\ seconds}\right) \times \left(\frac{1\ cycle}{2\ rev}\right) \quad (6\text{-}11)$$

Figure 6.5 displays the maximum air manifold pressure vs engine rpm at wide-open throttle, based on the preliminary tune developed from dynamometer testing.

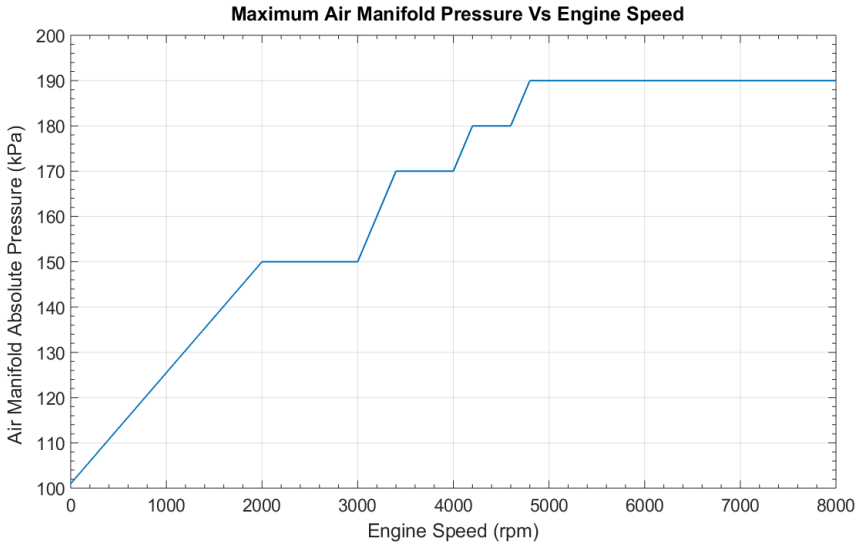

Figure 6.5: Maximum Air Manifold Absolute Pressure Vs Engine Speed

Using equations (6-7) and (6-11), the charged temperature and air mass flow gas vs engine speed is plotted in Figure 6.6. The ambient air temperature has been assumed to be at a worse case scenario of 45°C. It can be seen that the charged air temperature can reach up to 135°C once passed an rpm of 4,700.

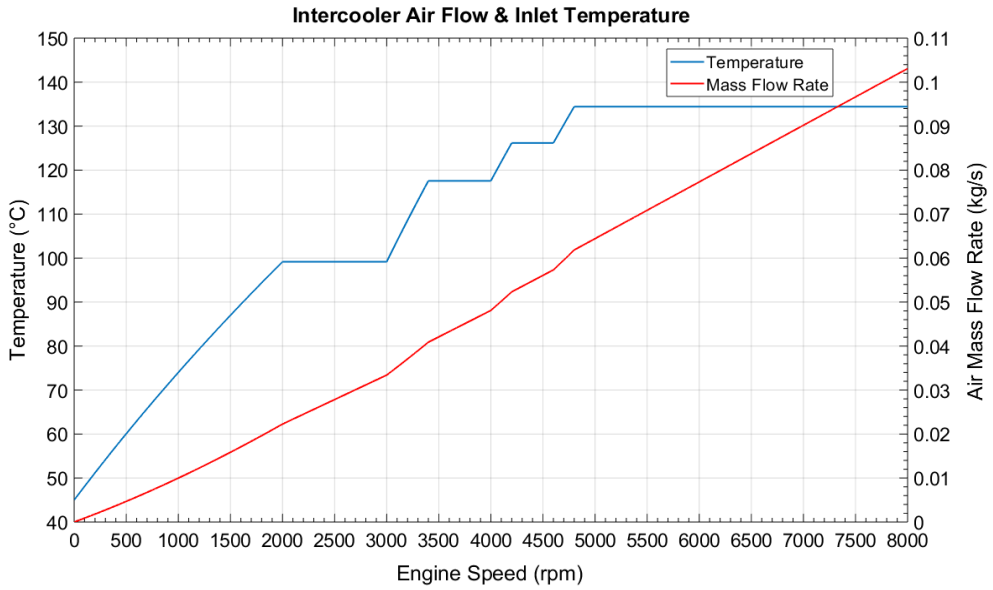

Figure 6.6: Intercooler Air Flow and Temperature

Based on the dynamometer test results, it has been determined that the charged air manifold temperature should not exceed 90°C to prevent the engine from overheating or pre-igniting. Seeing that the charged air temperature can pass 90°C when the engine speed passes 1,600 rpm with ambient temperature being 45°C, an intercooler is required.

Using the heat transfer equation (6-12), the heat transfer required to drop the charged air temperature to below 90 degrees celcius can be determined. With $T_{h,i}$ being the charged air entering the intercooler and $T_{h,o}$ being the air temperature exiting the intercooler. Figure 6.7 displays the heat transfer required to reduce the air outlet to a given temperature $T_{h,o}$ at a given engine speed, whith $T_{h,i}$ selected to be 45°C. Picking the charged air to be 90°C ($T_{h,o}$) with an assumed ambient temperature of 45°C ($T_{h,i}$), the heat transfer required from the intercooler is around 4.6 kW. Summing the maximum heat generation of the intercooler and electric powertrain results in a total heat generation of 25.6 kW.

$$q = \dot{m}_h c_{p,h}\left(T_{h,i} - T_{h,o}\right) \qquad (6\text{-}12)$$

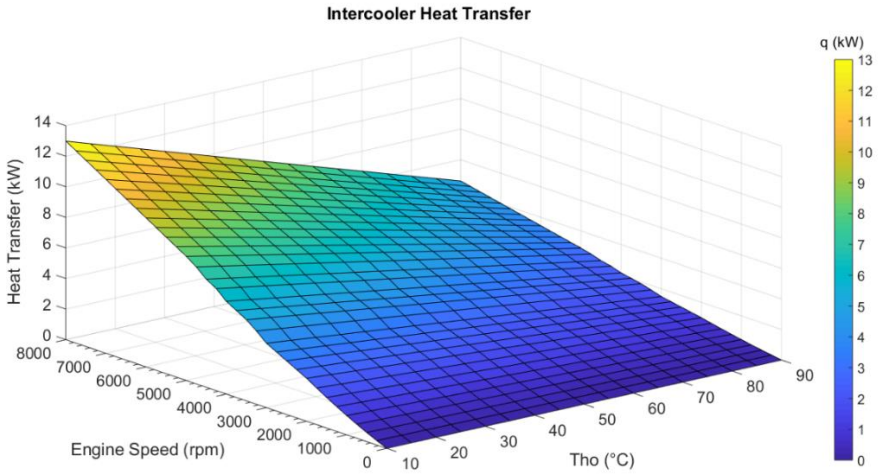

(a)

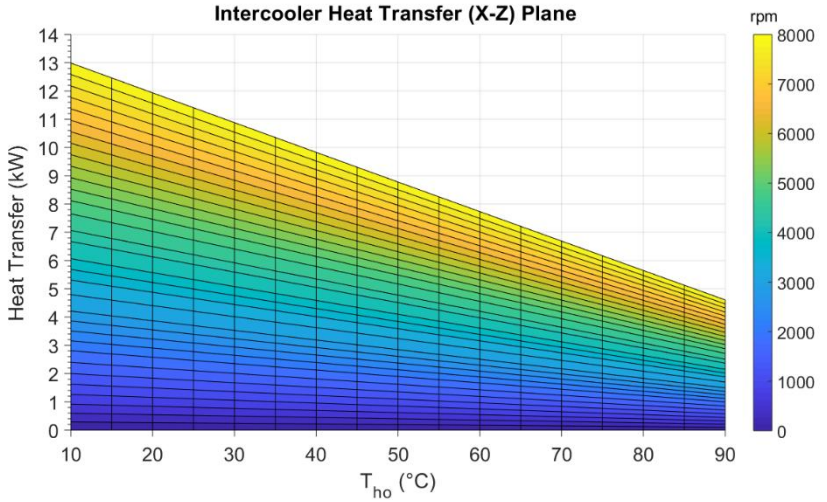

(b)

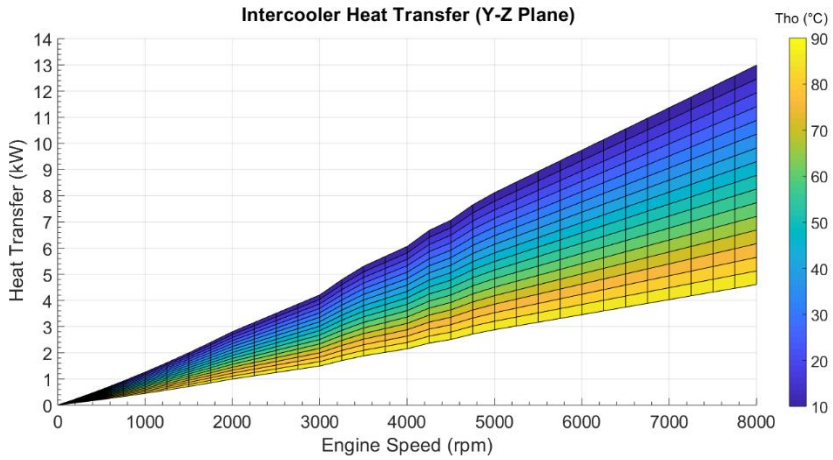

(c)

Figure 6.7: Intercooler Heat Transfer - (a) 3D plane, (b) X-Z plane, (c) Y-Z plane

6.2 Thermal System Layout and Requirements

The diagram in Figure 6.8 displays the four separate cooling loops present in the vehicle. The GM transmission oil loop has not been modified and uses the dual partitioned stock radiator (3), while the other partition is used for the engine coolant loop. The electrical powertrain (electrical motor and inverters), and engine liquid to air intercooler share the same cooling loop. The electrical motor and inverter pair are separated in parallel and the heat is rejected through the additional radiator (1) as well as the chiller (6). The chiller is also utilized as the reservoir for the coolant pump (8). The stock refrigeration system for the cabin air conditioning has been modified to accommodate for the chiller. This modification consists of an additional refrigeration line that has been implemented in parallel to the stock system with its own thermal expansion valve (4) located before the chiller. The stock mechanical compressors has also been replaced with an electrical compressor (7). The remaining unmodified stock thermal system components are: in-cabin evaporator (9), fans (11),(5), condenser (2), and cabin expansion valve (10).

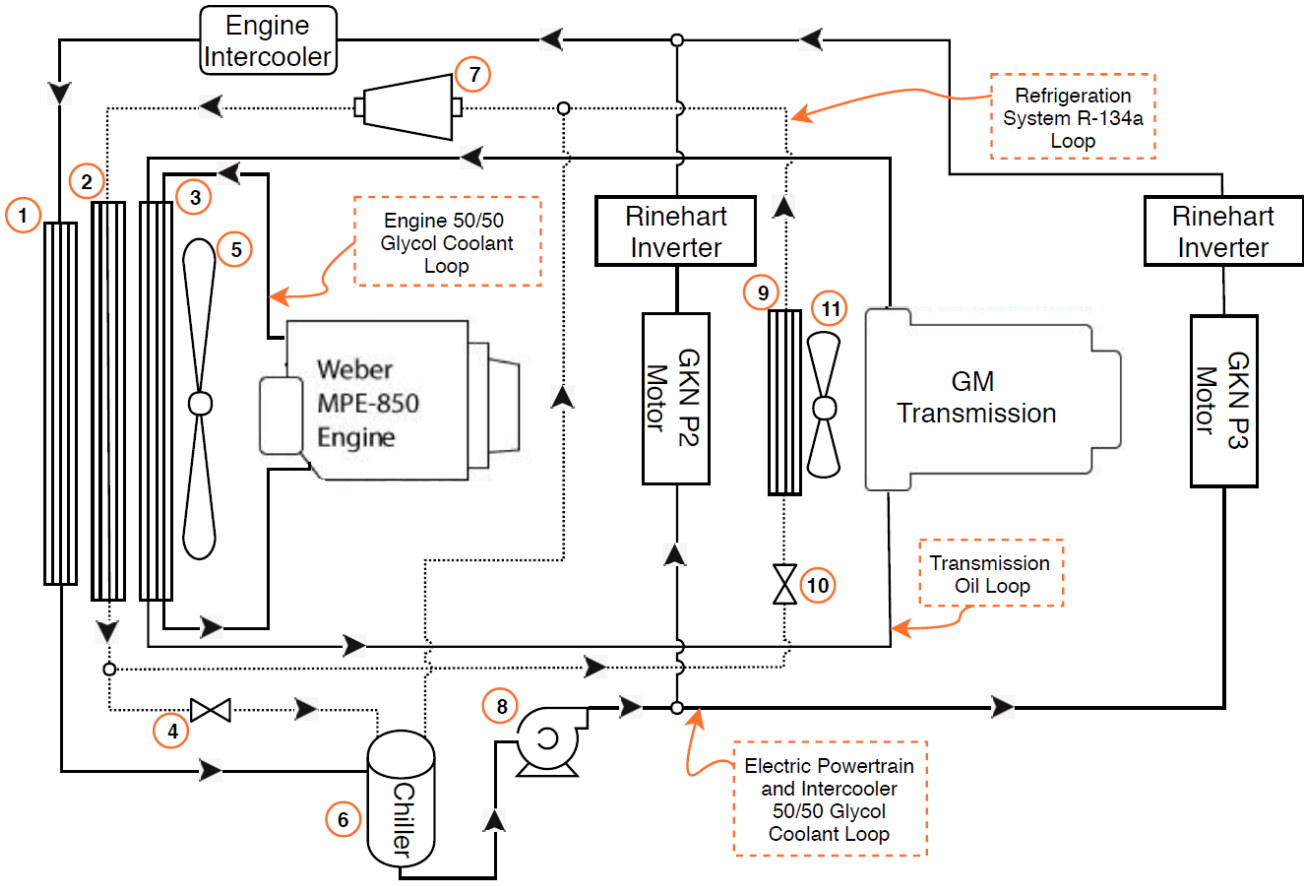

1: Electric powertrain and intercooler radiator
2: Refrigeration system condenser
3: Engine coolant and transmission oil stock radiator
4: Chiller thermal expansion valve
5: Radiator fan
6: Chiller
7: Refrigeration system compressor
8: Electric powertrain and intercooler coolant pump
9: In cabin evaporator for air conditioning
10: In cabin evaporator thermal expansion valve
11: In cabin evaporator fan

Figure 6.8: Vehicle Cooling System Diagram

Upon designing the thermal system, the maximum heat generation, flow rate, and temperature has been taken into consideration as listed in Table 6-2. The maximum coolant temperature has been determined from the specifications, for the intercooler however, it has been determined in section 6.3.2 Intercooler Sizing. The recommended coolant flow rate has also been gathered from the specifications and the maximum heat generation values have been developed in section 6.1 Heat Generating Components.

Table 6-2: Thermal System Requirements

	Maximum Heat Generation (kW)	Recommended Coolant Flow Rate (liter/minute)	Maximum Coolant Temperature (°C)
Weber Engine	153	>65	110
Electrical Motor	Total = 21	8	55
Inverter		8-12	80
Intercooler	4.6	>14	84

The powertrain electronics and intercooler thermal system is designed to utilize one loop to reduce weight, minimize points of failure, and reduce costs. Having an additional line would require an addition water pump, radiator, reservoir and increase the total coolant lines required. Furthermore, there is already a limited space available at the front of the vehicle to place another radiator to benefit from the maximum available air mass flow rate. The heat generating components are positioned in order of increasing maximum allowable coolant temperature to the flow of the coolant. The electric motor is positioned first, followed by the inverter and then the intercooler being last. The chiller has been positioned at the highest point of the system since it is also a reservoir and the pump has been positioned at the lowest point of the system. This is to ensure that the reservoir always supplies coolant to the pump to avoid cavitation. The compressor on the other hand has been located at the highest point of the system to avoid refrigerant liquid from pooling in the component, which could be damaging.

A liquid to air intercooler has been selected over the air to air type intercooler to take advantage of its benefits. A liquid to air intercooler is a more complicated system and requires more components, such as a radiator and a coolant pump. However, having it in the same cooling loop as the electric powertrain reduces the need for these additional components. Having coolant as the fluid for the heat transfer is a lot more effective than air due to its higher heat capacity. Additionally, the liquid to air intercooler can be positioned as close to the engine as possible reducing turbo lag as the positioning is not dictated by the available air flow rate.

The radiator is designed to allow for a coolant flow rate of up 70 L/minute however the coolant loop is limited to provide the recommended flow rate of 8 L/minute for the electric motor as well as the resulting system pressure drop. This is further discussed in the 6.3.3 System Pressure Drop & Pump Selection. The radiator and condenser heat exchangers in front of the vehicle are positioned in order of coolest to the hottest, illustrated in Figure 6.9. This is to limit the heat

exchanger at the front from transferring heat into the next heat exchanger. The radiators are positioned such that there is a minimum of 10mm gap in between them to reduce airflow obstruction and heat transfer between them.

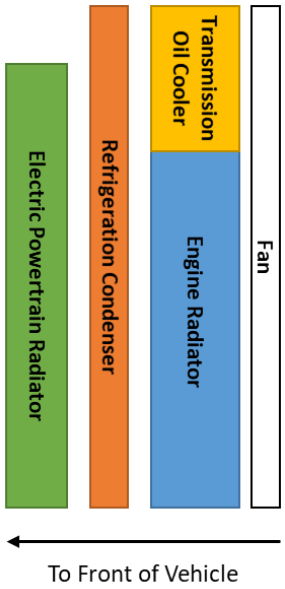

Figure 6.9: Radiator Positioning

6.3 Electrical Powertrain & Intercooler Thermal System Design

6.3.1 Radiator Sizing

There are many variables that need to be taken into consideration when sizing a radiator such as the air and coolant mass flow rate as well as their temperature. The following equations are used to determine the parameters required for the radiator to reject the expected heat energy. The equations used are from the Principles of Heat and Mass Transfer text book [86] unless specified otherwise.

The heat transfer rate of the radiator is calculated by the effectiveness(ε)-NTU method. The effectiveness ratio is given by equation (6-13).

$$\varepsilon = \frac{q}{q_{max}} \qquad (6\text{-}13)$$

q is the heat transfer rate to the ambient and q_{max} is the maximum heat transfer the radiator can achieve calculated using equation (6-14). Where $T_{h,i}$ is the hot coolant temperature entering the radiator and $T_{c,i}$ is the cold air temperature entering the radiator.

$$q_{max} = C_{min}(T_{h,i} - T_{c,i}) \quad (6\text{-}14)$$

The equation (6-13) and (6-14) can be combined and re-arranged to equation (6-15).

$$q = \varepsilon C_{min}(T_{h,i} - T_{c,i}) \quad (6\text{-}15)$$

The heat capacity C can be determined by multiplying the specific heat capacity of the fluid to its mass flow rate as shown in equation (6-16).

$$C = \dot{m}c_p \quad (6\text{-}16)$$

The minimum heat capacity of the two fluids is then chosen as shown in equation (6-17) with the subscript c referring to the cold (air) side and subscript h referring to the hot (coolant) side. Typically in this case, C_{min} is the coolant since the air mass flow rate is usually significantly higher.

$$C_{min} = min[(\dot{m}c_p)_h, (\dot{m}c_p)_c] \quad (6\text{-}17)$$

The mass flow rate of the coolant can be determined by comparing the system pressure drop to the selected pump's pressure curve, this will be further discussed in 6.3.3 System Pressure Drop and Pump Selection section. The coolant mass flow rate can also be determined by simply using an inline flow meter similar to the Sotera digital meter [87]. Determining the mass air flow rate that goes through the radiator is more complicated as it varies with vehicle speed and fan speed. The mass air flow through the radiator can be determined using equations (6-18), (6-19), and (6-20) [88].

$$\dot{m}_{air} = \sqrt{\frac{k_l}{k_r}\dot{m}_{ram}^2 + \frac{k_f}{k_r}\dot{m}_{fan}^2} \quad (6\text{-}18)$$

$$\dot{m}_{fan} = \frac{4\pi^2 \rho_{air} r_m^3 \phi_m N_f n}{60}\left(\frac{1-v^2}{1+v^2}\right) \quad (6\text{-}19)$$

$$\dot{m}_{ram} = v_{ram} A_r \rho_{air} \quad (6\text{-}20)$$

Where,

$k_I =$ *Pressure coefficient at the air inlet*

$k_r =$ *Pressure coefficient at the radiator*

$k_f =$ *Pressure coefficients at the fan*

$\dot{m}_{ram} =$ *Ram air mass flow rate*

$\dot{m}_{fan} =$ *Fan air mass flow rate*

$v_{ram} =$ *Ram air velocity*

$r_m =$ *Fan mean radius* $\left[\sqrt{\frac{1}{2}\left(r_{fan\ tip}^2 + r_{hub\ radius}^2\right)}\right]$

$N_f =$ *Fan speed*

$\rho_{air} =$ *Density of air*

$n =$ *Number of fans*

$v =$ *Fan Hub ratio (fan hub radius/ fan tip radius)*

$\phi_m =$ *Fan flow rate coefficient*

$A_r =$ *Radiator area*

For a cross flow, single pass, unmixed fluid heat exchanger, the effectiveness (ε) can be determined by equation (6-21).

$$\varepsilon = 1 - exp[(\frac{1}{C_r})(NTU)^{0.22}\{exp[-C_r(NTU)^{0.78}] - 1\}] \quad (6\text{-}21)$$

Where the heat capacity ratio, C_r and NTU can be determined by using equation (6-22) and (6-23) respectively.

$$C_r = \frac{C_{min}}{C_{max}} \quad (6\text{-}22)$$

$$NTU = \frac{UA}{C_{min}} \quad (6\text{-}23)$$

The overall heat transfer coefficient UA is a specification of the radiator. This specification however has been difficult to attain from suppliers or manufacturers thus equation (6-24) can be used to determine the UA value.

$$\frac{1}{UA} = \frac{1}{h_{coolant}A_{coolant}} + \frac{1}{h_{air}A_{air}} \quad (6\text{-}24)$$

The area of the coolant and air side of the radiator can be calculated using equation (6-25) and (6-26) respectively [89]. Note that the thermal conductivity of tube is considered to be high due to the small thickness of the tube. Additionally, it is assumed that there are no fouling in the tubes either.

$$A_{coolant} = Number\ Of\ Tubes \times (2 \times Tube\ Height \times Radiator\ \ Length + 2 \times Tube\ Width \times Radiator\ Length) \quad (6\text{-}25)$$

$$A_{air} = \left(Number\ of\ Rows\ of\ Fins \times \frac{Radiator\ Length}{Fin\ Distance}\right) \times 2 \times Fin\ Distance \times Fin\ Height + 2 \times Fin\ Height \times Fin\ Width \quad (6\text{-}26)$$

The coolant heat transfer coefficient for turbulent flow in a pipe can be determined by calculating the Nusselt number using the correlation in equation (6-27), where k is thermal conductivity of the coolant, Re is Reynolds number, Pr is prandtl number, and D_h is the hydraulic diameter used to equate any flow geometry to that of a round pipe as shown in equation (6-28). With A_c being the cross sectional area and P being the wetted perimeter.

$$Nu_{coolant} = \frac{h_{coolant} D_h}{k} = 0.023 Re^{0.8} Pr^{\frac{1}{3}} \quad (6\text{-}27)$$

$$D_h = \frac{4A_c}{P} \quad (6\text{-}28)$$

The heat transfer coefficient for air can be determined using equation (6-29) similar to the coolant heat transfer coefficient.

$$h_{air} = \frac{Nu_{air} k_{air}}{Tube\ Width} \quad (6\text{-}29)$$

To determine the Nusselt number of the air side, a j-factor correlation is used [90] as shown in equation (6-30) and (6-31).

$$j = \frac{Nu_{air}}{RePr^{\frac{1}{3}}} \quad (6\text{-}30)$$

$$j = Re^{-0.487} \left(\frac{L_\alpha}{90}\right)^{0.257} \left(\frac{F_p}{L_p}\right)^{-0.13} \left(\frac{H}{L_p}\right)^{-0.29} \left(\frac{F_d}{L_P}\right)^{-0.235} \left(\frac{L_l}{L_p}\right)^{0.68} \left(\frac{T_p}{L_p}\right)^{-0.279} \left(\frac{\delta f}{L_p}\right)^{-0.05} \quad (6\text{-}31)$$

Where L_α is the louver angle in degrees, F_p is the fin pitch, L_p is the louver pitch, H is the fin height, F_d is the flow depth, L_l is the louver length, T_p is the temperature in Kelvin, δf is the fin thickness

To summarize, there are a few factors that can influence the rate at which the radiator can reject heat. These factors consists of the radiator overall heat transfer coefficient (UA), the effectiveness, the ambient temperature, and the mass flow rate of the air and coolant. As shown in equation (6-15), as the effectiveness approaches closer to one, the heat exchanger heat transfer rate approaches to its maximum. Based on equation (6-21), the effectiveness depends on the NTU and Cr. Figure 6.10 provides a surface plot illustrating the affect Cr and NTU has on the effectiveness.

Figure 6.10 (a) illustrates that to increase the effectiveness value, the NTU value must increase and heat capacity ratio should be lowered. Figure 6.10 (b) and (c) show that the NTU has a significant impact on the effectiveness as it increases before it starts to plateau in comparison to the Cr.

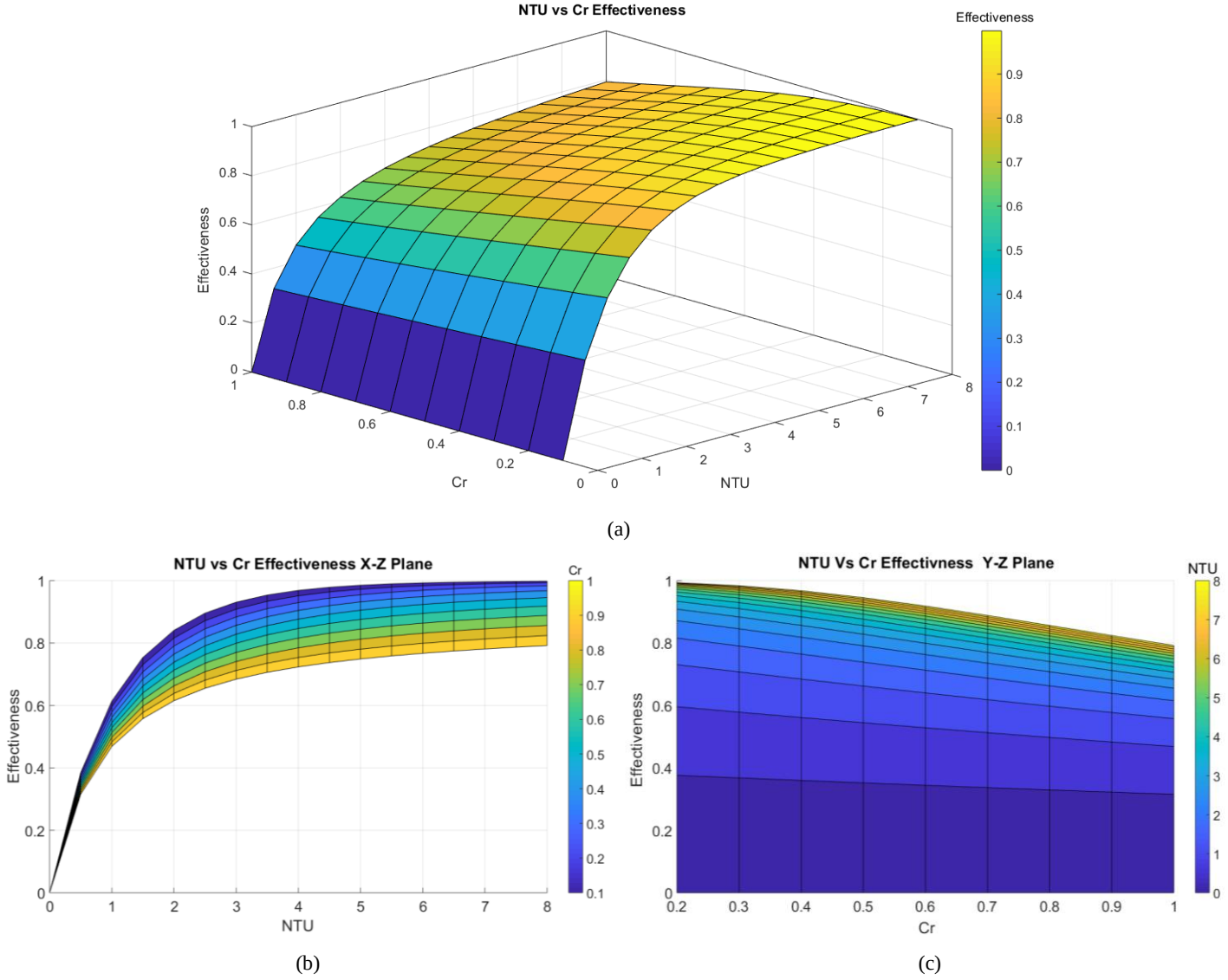

Figure 6.10: NTU vs Cr Effectiveness - (a) 3D layout, (b) X-Z plane, (c) Y-Z plane

Based on equation (6-22), Cr decreases with the increase of Cmax which can be increased by increasing the air flow rate through the radiator. Additionally, NTU can be increased by increasing the UA value of the radiator as seen in equation (6-23). The ambient temperature will directly influence the heat rejection rate shown in equation (6-15). The hotter the day, the higher $T_{c,i}$ will be resulting in a lower temperature difference, decreasing heat transfer. Increasing the mass flow

rate of the coolant will increase C_{min} which will also increase the heat transfer rate, however, as the C_{min} increases, Cr will decrease reducing ε unless C_{max} is also increased.

Figure 6.11 displays the required radiator effectiveness vs ambient temperature to transfer the maximum heat generation of 25.6 kW. The radiator outlet coolant temperature (Tho) has been selected to be 50°C, 5°C below the maximum allowable coolant temperature for the electrical motor (Table 6-2). The inlet coolant temperature (Thi) has then been calculated to be 76.9°C.

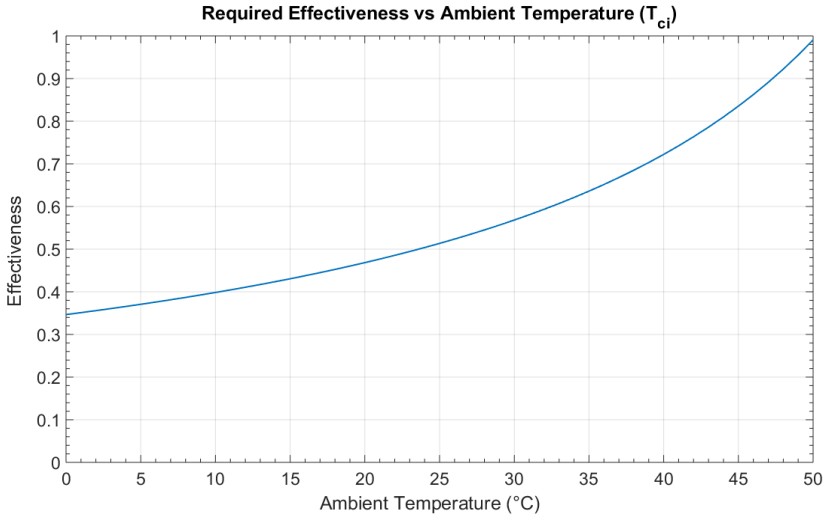

Figure 6.11: Required Effectiveness Vs Ambient Temperature

Figure 6.12 displays the air mass flow rate requirement vs ambient temperature at a given overall heat transfer coefficient (UA) to achieve a heat transfer rate of 25.6 kW. From Figure 6.12 (b), it can be seen that a UA value higher than approximately 1,250 W/K is required to reject the required heat at an ambient temperature of above 40°C. This is due to it not being able to achieve the effectiveness required as shown in Figure 6.11 and Figure 6.10, if the UA value is too low. Figure 6.12 (c) also shows that the higher the UA value, the less air mass flow is required to achieve the required heat transfer; once again, due to the effect is has on the effectiveness.

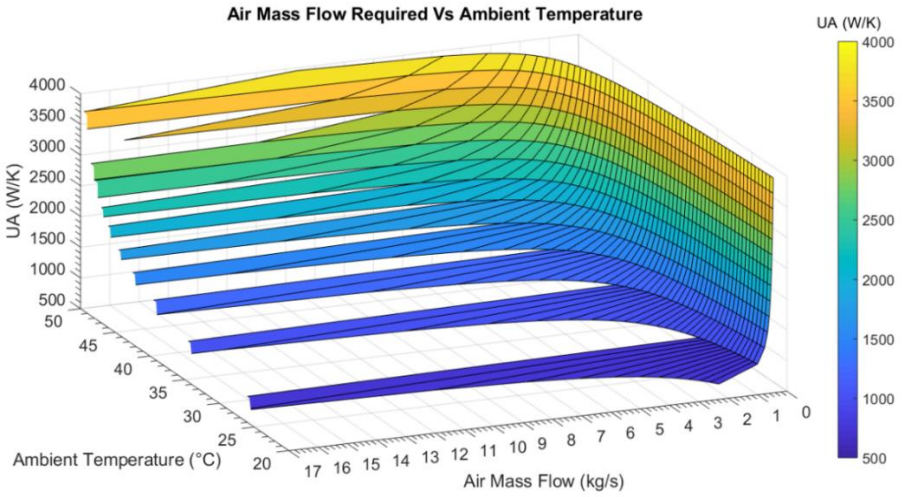

(a)

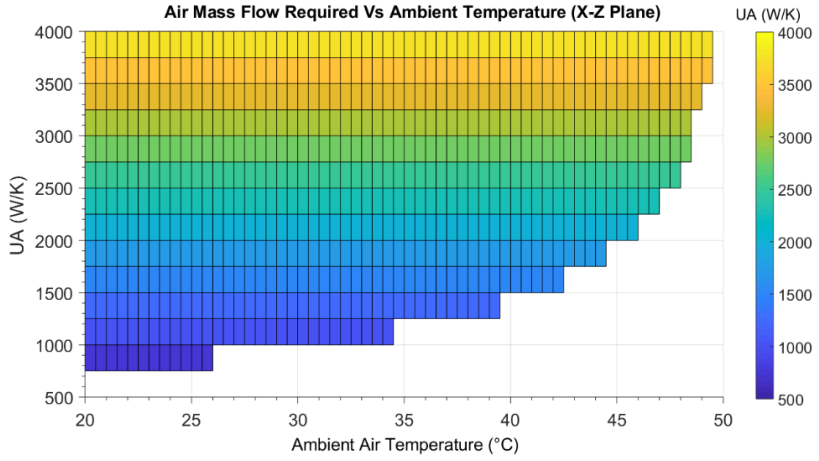

(b)

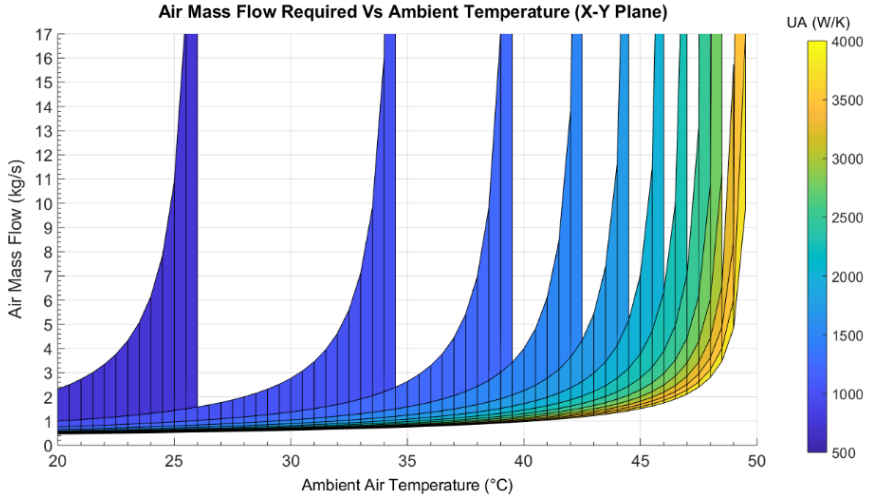

(c)

Figure 6.12: Required Air Mass Flow vs Ambient Temperature – (a) 3D plane, (b) X-Z plane, (c) X-Y plane

The radiator selected for the vehicle is estimated to have a UA value of 2,500 W/K. Figure 6.13 displays the heat transfer the radiator can achieve vs the air mass flow at the ambient temperature of 45°C. Notice that the effectiveness starts at one and declines until 1 kg/s of air flow, which it then picks up again as the mass flow rate increases. This is because below an air mass flow rate of 1 kg/s, Cmin is the air flow which then becomes Cmax after approximately 1kg/s. It can be seen that to have the radiator reject the maximum heat generation, the mass flow rate should be over 2.5 kg/s across the radiator, which results in an effectiveness of 0.83. As illustrated in Figure 6.11, that is the effectiveness required to transfer the maximum heat at an ambient of 45°C. It is estimated that the fan can achieve an air mass flow rate of 1.5 kg/s, this means that at standstill the radiator can reject a heat transfer rate of 23.4 kW, which is just shy of the 25.6 kW max heat generation. This is not considered to be a concern since it is being calculated at the worse case ambient temperature at a worse case heat generation which occurs at a high vehicle speed resulting in an air mass flow rate greater then 2.5 kg/s. Therefore, a radiator with a UA value of 2,500 W/K is adequate for the thermal system.

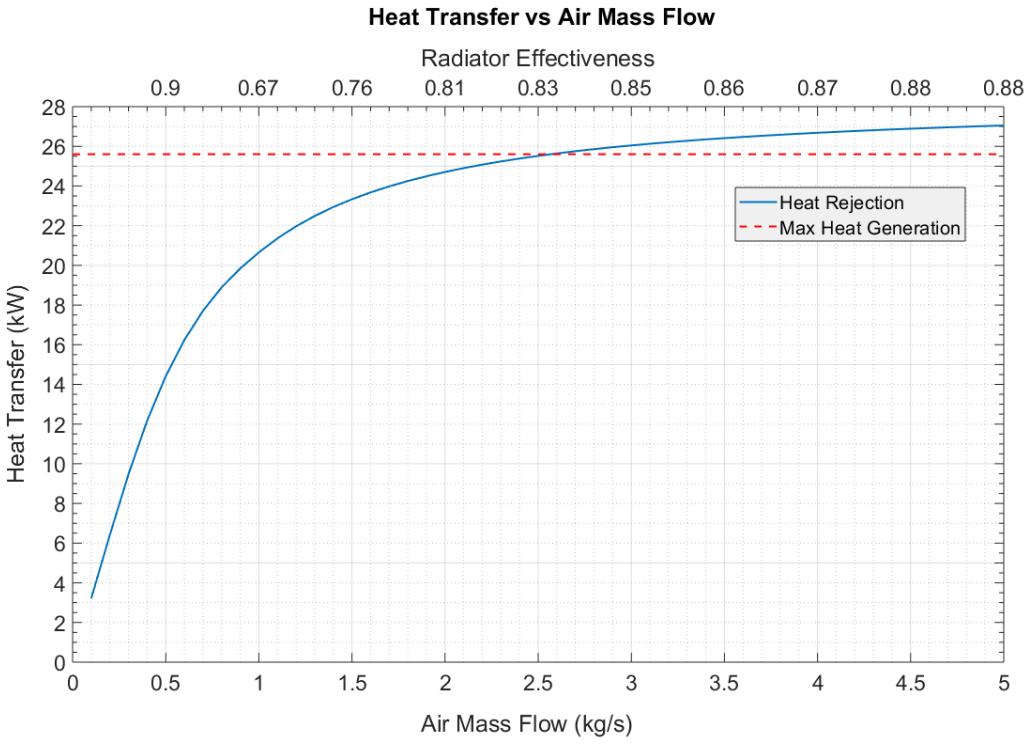

Figure 6.13: Heat Transfer vs Air Mass Flow Rate

6.3.2 Intercooler Sizing

Liquid to air intercoolers are typically in a barrel shape form as shown in Figure 6.14. They are usually a shell and tube, counter-flow heat exchanger with one shell pass and n number of tube passes.

Figure 6.14: Barrel Style Liquid to Air Intercooler [91]

Similar to the radiator selection, the effectiveness(ε)-NTU method can be used to determine the intercooler size required. The effectiveness for this kind of heat exchanger is given in equation (6-32).

$$\varepsilon = 2\left\{1 + C_r + \sqrt{1 + C_r^2} \times \frac{1+exp\left[-(NTU)(1+C_r^2)^{1/2}\right]}{1-exp\left[-(NTU)(1+C_r^2)^{1/2}\right]}\right\}^{-1} \quad (6\text{-}32)$$

Figure 6.15 can be used to determine the intercooler coolant inlet temperature (T_{ci}) required to transfer heat for a given UA value to a required charged air temperature (T_{ho}). The coolant mass flow rate has been taken to be 16 L/min and ambient air to be at 45°C.

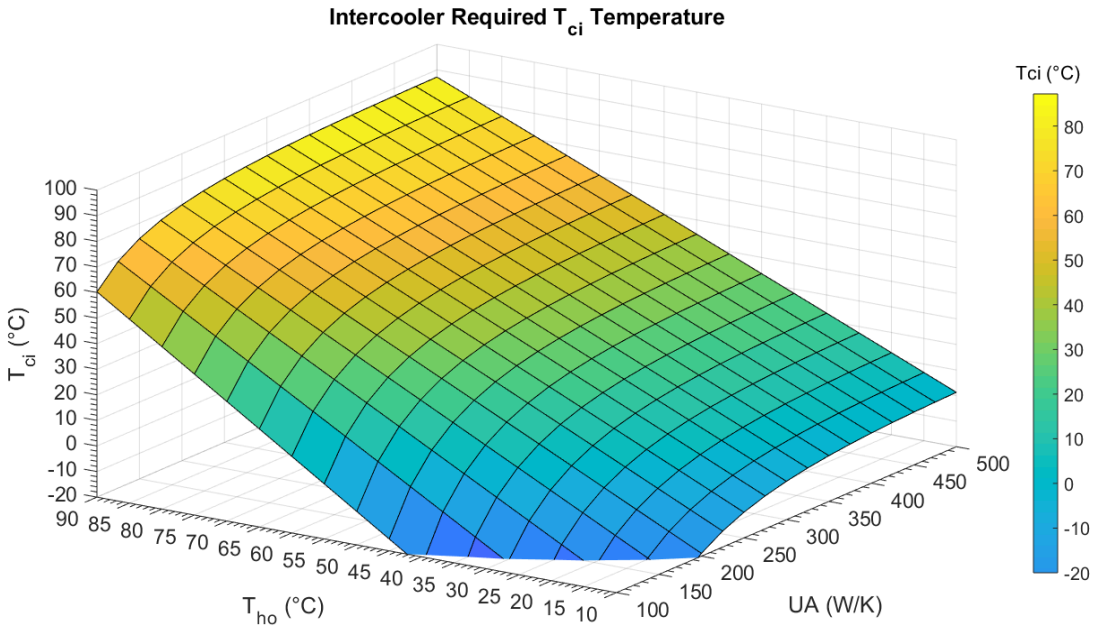

(a)

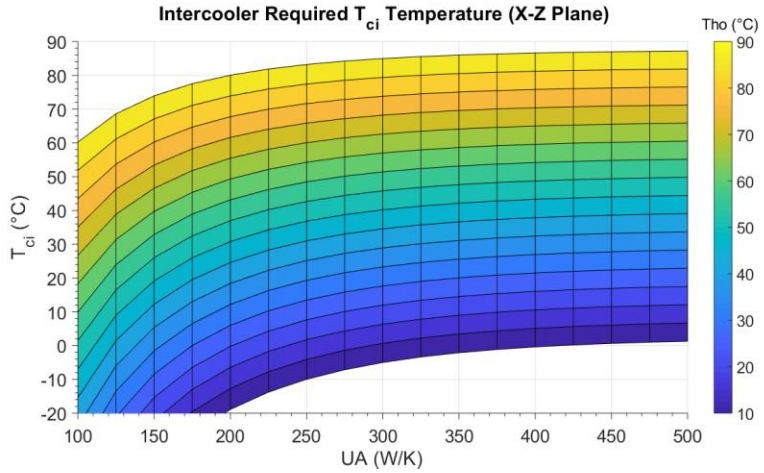

(b)

Figure 6.15: Intercooler Required T_{ci} Temperature – (a) 3D plane, (b) X-Z plane

As mentioned in section 6.2 Thermal System Layout and Requirements6.2, the maximum allowable coolant temperature for the electrical motors is 55°C. Considering this as the worse case scenario, the maximum coolant temperature exiting the radiator should be 55°C. Using the heat transfer equation (6-12) and the maximum heat generation of the electric powertrain, the maximum coolant temperature entering the intercooler (T_{ci}) can be calculated to be around 77°C. This means that designing for the worse case scenario, the intercooler should be sized to drop the charged air temperature below to 90°C with an inlet coolant temperature of 77°C. Looking back at Figure

6.15, or using the NTU relation in equation (6-33) and (6-34), the UA value required to bring the charged air temperature to 85°C should be 243 W/K.

$$NTU = -(1 + C_r^2)^{-1/2} ln\left(\frac{E-1}{E+1}\right) \quad (6\text{-}33)$$

$$E = \frac{2/\varepsilon - (1+C_r^2)}{(1+C_r^2)^{1/2}} \quad (6\text{-}34)$$

The intercooler selected is estimated to have a UA value of 280 W/K, this means that the maximum inlet coolant temperature can be up to 84 °C to be able to drop the charged air temperature to 90 °C. Figure 6.16 displays the intercooler heat transfer performance at varying engine rpm in comparison to the heat transfer required to drop the charged air temperature to 90 °C. Once again, the coolant inlet temperature and ambient air is selected to be 77°C and 45°C respectively.

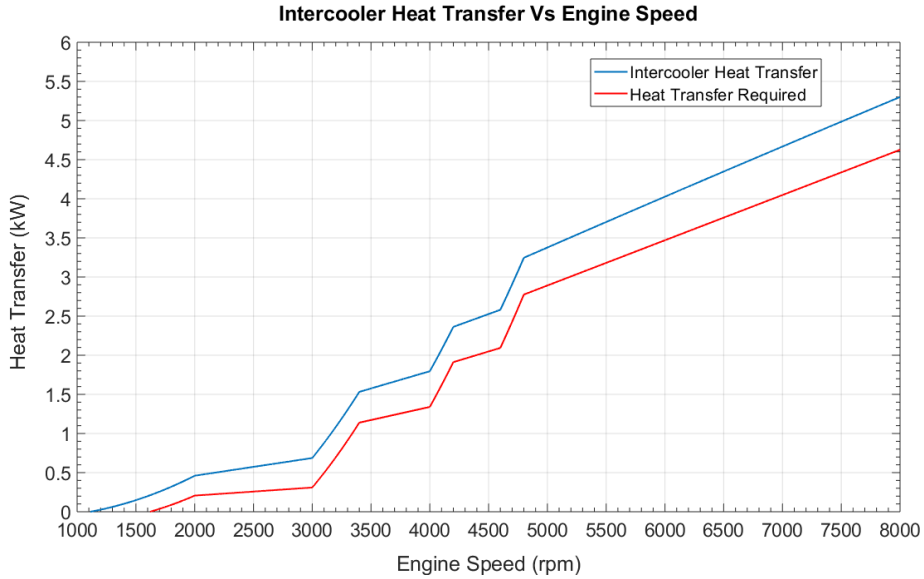

Figure 6.16: Intercooler Heat Transfer Vs Engine Speed

6.3.3 System Pressure Drop & Pump Selection

To correctly size a water pump that can provide the required coolant flow rate, the total pressure drop of the thermal system must be considered. In addition to the components themselves having a resistance to flow, other factors such as the fittings, elbows, bends, hose diameter and the configuration of the system also contributes to the total pressure drop and head loss. The incompressible steady flow energy equation (6-35) can be used to determine the head loss and

pressure drop. Note that the following equations in this section are from Frank M White [92] unless otherwise specified.

$$\left(\frac{P}{\rho g}+\frac{\alpha}{2g}V^2+z\right)_{in}+h_{pump}=\left(\frac{P}{\rho g}+\frac{\alpha}{2g}V^2+z\right)_{out}+h_{loss} \quad (6\text{-}35)$$

The head loss is the sum of the major and minor losses, the head loss in the hose can be found by using Darcy's equation (6-36). Calculating the Reynolds number of the fluid in the system indicates that the flow is turbulent therefore the friction factor is determined using the Moody chart [93].

$$h_f = f\left(\frac{L}{d}\right)\left(\frac{V^2}{2g}\right) \quad (6\text{-}36)$$

The minor head losses developed from the fittings and bends can be calculated using equation (6-37), the resistance coefficient K of the fittings is usually provided by the manufacturer.

$$h_m = \left(\frac{V^2}{2g}\right)K \quad (6\text{-}37)$$

90° bends in the pipes will also develop minor losses, their resistance coefficient can be calculated using equation (6-38).

$$K \approx 0.388\left[0.95+4.42\left(\frac{R}{d}\right)^{-1.96}\right]\left(\frac{R}{d}\right)^{0.84} Re_d^{-0.17} \quad (6\text{-}38)$$

The resistance coefficient of reduction and expansion fittings can also be determined using equation (6-39) and (6-40) respectively [94].

$$K = (0.6+0.48f_1)\left(\frac{D}{d}\right)^2\left[\left(\frac{D}{d}\right)^2-1\right] \quad (6\text{-}39)$$

$$K = (1+0.8f_1)\left[1-\left(\frac{d}{D}\right)^2\right]^2 \quad (6\text{-}40)$$

As mentioned, the configuration and arrangement (i.e. series or parallel) of the thermal system has an impact on the total pressure drop. The fluid flow in a multiple pipe system can be classified into series or parallel similar to electrical circuits. While in electrical circuits, there is a balance between the voltage, current, and resistance given by Ohms law; in a fluid circuit, there is a balance between the pressure drop, flowrate and flow resistance [95]. Equation (6-36) can be rewritten as equation (6-41) to show the relation between the head loss h, flow rate q, and flow resistance R* which is proportional to friction factor f.

$$h = R^* q^2 \tag{6-41}$$

$$\text{where, } R^* = \frac{f(8L)}{\pi^2 g d^5}$$

When the pipes are connected in series, the flow rate will be constant due to the conservation of mass principle for steady incompressible flow. This means that the total head loss can be the sum of the individual head losses connected in series as shown in equation (6-42)

$$h_{total} = R_1^* q^2 + R_2^* q^2 + \cdots R_n^* q^2 = R_{eq}^* q^2 \tag{6-42}$$

With a parallel connection, the total flow rate will be the sum of the flow rates in the individual pipes and the pressure drop (or head loss) in each pipe must be the same. Equation (6-43), (6-44), and (6-45) are the governing equations for a parallel system.

$$h_{total} = h_1 = R_1^* q_1^2 = R_2^* q_2^2 = \cdots R_n^* q_n^2 \tag{6-43}$$

$$\sqrt{\frac{h}{R_{eq}^*}} = \sqrt{\frac{h}{R_1^*}} + \sqrt{\frac{h}{R_2^*}} + \cdots \sqrt{\frac{h}{R_n^*}} \tag{6-44}$$

$$\therefore \frac{1}{\sqrt{R_{eq}^*}} = \frac{1}{\sqrt{R_1^*}} + \frac{1}{\sqrt{R_2^*}} + \cdots \frac{1}{\sqrt{R_n^*}} \tag{6-45}$$

As previously mentioned, the goal is to have the intercooler and electrical powertrain components share one loop to reduce weight, minimize points of failure and reduce cost. Three separate configurations have been investigated for the system; (i) series connection, (ii) motor and inverter pair on their own parallel lines, and (iii) motors and inverters on their own lines resulting in a total of four parallel lines. The calculated total pressure drop in the system vs the flow rate for the three different configuration is shown in Figure 6.17. The pressure drop in the series configuration is the highest, parallel lines can reduce the pressure drop but will require a higher flow rate from the pump to adequately flow through the parallel lines. Therefore, a balance between flow rate and pressure drop must be maintained.

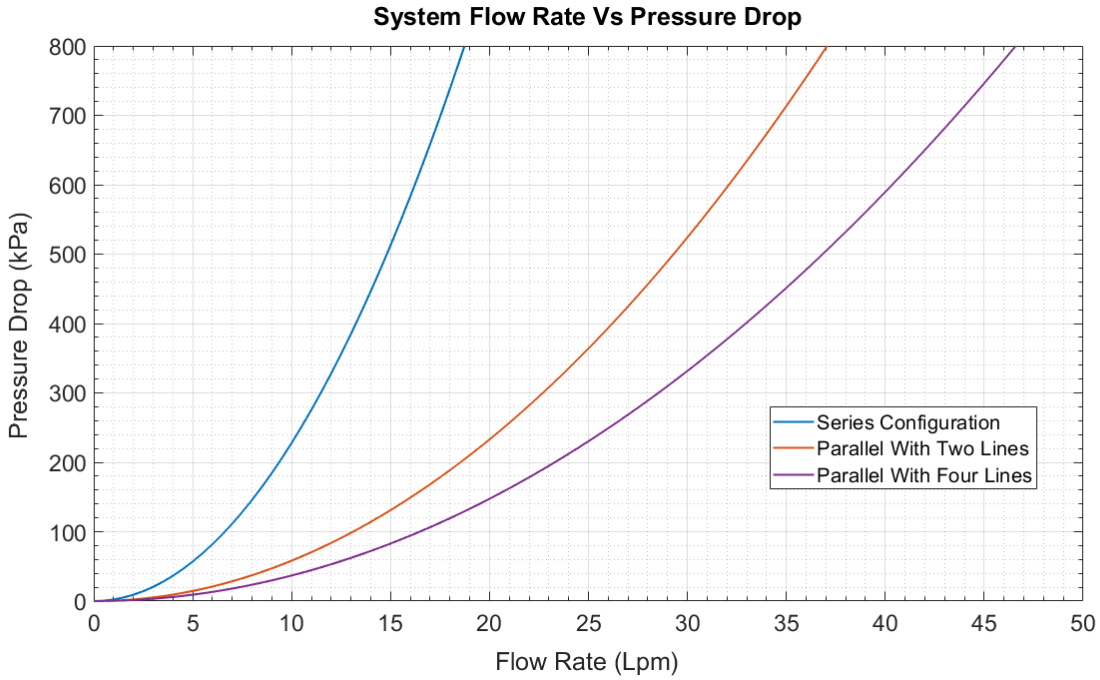

Figure 6.17: System Flow Rate vs. Pressure Drop

At the 8 Lpm recommended flow rate for the electric motor and inverter (Table 6-2), the series configuration will experience a pressure drop of 145.8 kPa. This is a relatively high pressure drop, however the issue comes from having too low of a flow rate through the intercooler and radiator. Based on the radiator and intercooler sizing analysis, a flow rate of 8 Lpm is not sufficient for the required heat transfer. The flow rate can be increased although as shown in Figure 6.17, this will lead to a significantly larger pressure drop making it unfeasible. A parallel system arrangement with each electric motor and inverter pair being on their own line with approximately equal resistance of flow will require a total flow rate of 16 Lpm to distribute 8 Lpm to each line. According to the radiator and intercooler sizing analysis, 16 Lpm is a suitable flow rate for the radiator and intercooler heat exchangers. A 16 Lpm flow rate will result in a pressure drop of 149 kPa, similar to the pressure drop seen for the series configuration. This parallel configuration has been implemented in the vehicle and the schematic is provided in Figure 6.8.

The other option is to have the inverter and motor on their own individual lines resulting in four parallel lines. This would reduce the system pressure drop further and allow for a higher flow rate in the main line increasing heat transfer in the radiator and inverter. However, to achieve a flow rate of 8 Lpm for the inverter, the motors would have a flow rate of 10.8 Lpm due to the difference in flow resistance in the lines. This will result in a total of 37.6 Lpm. Referring to Figure 6.17, the

pressure drop of the parallel system with four lines at a flow rate of 37.6 Lpm is around 518 kPa. This is considered to be too high of a pressure drop to be feasible for a pump to overcome while also achieving such a flow rate requirement.

Figure 6.18 plots the performance curve of a few readily available pumps along with the determined pressure drop of the different configurations. The pump data points are gathered from Lingenfelter [96] and the data for the Shurflo pump has been provided by the supplier [97]. The Shurflo and Stewart-EMP are displacement pumps while the rest are centrifugal pumps. The intersection point between the pump pressure curve and the configuration pressure drop is the flow rate the pump will be able to provide for the system. The Shurflo and Stewart-EMP were the only two pumps that could provide around 16 Lpm flow rate for the system. The Shurflo pump has been selected due to it being cheaper and requiring less power. Note that the Shurflo pump could also be used for the series configuration for a flow rate of 13 Lpm at a pressure of 390 kPa however this is a lower flow rate and the higher pressure can increase the risk of a pipe burst as well as draw more power from the pump.

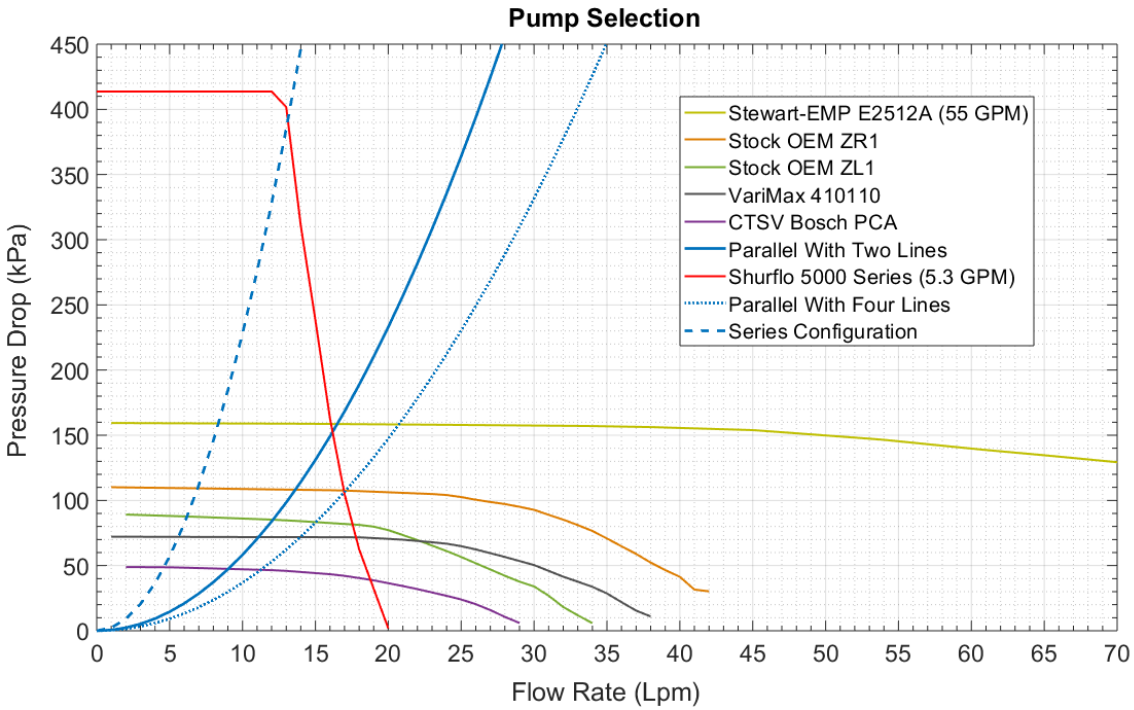

Figure 6.18: Pump Selection

Table 6-3 displays the pressure drop of the components and of the hose of the two line configuration operating at 16 Lpm. Table 6-4 further breaks down the pressure drop of the hoses and fittings in the system. The plumbing consists of three different sized hoses due to the different fitting size of the components, the radiator fitting is 1 inch, the pump, intercooler, and chiller are ¾ inch, and the motor and inverter are ½ inch. A bigger diameter for the hose will result in a lower average flow velocity if the flow rate is kept constant, referring to equation (6-36), this will reduce the head loss which will reduce pressure drop. In addition to the required expansion and reduction fittings for the components, intermediate expansion and reduction fittings can be used to implement larger diameter hoses in between the components. However, the additional fittings will introduce pressure drops which can offset the benefit of using larger hoses, it will also introduce additional joints which have the risk of leaking. This approach is usually more beneficial when the hoses are longer in length. Additionally, larger hoses are less flexible, leading to the use of more elbow fittings which can also increase the pressure drop, Table 6-4 shows that the 90° elbows are a major contributor to the total pressure drop. In order to minimize the pressure drop in the system by maximizing the use of larger diameter hoses, the required reduction fittings are placed just before the components that require a smaller diameter and the expansion fittings are placed right after the components.

Table 6-3: Pressure Drop Breakdown of Two Parallel Line Configuration

	Pressure drop (kPa)
2x Motor and Inverter Pair	42
Intercooler	30
Hoses and Fittings	38
Radiator	40
Total	150

Table 6-4: Hose and Fittings Pressure Drop Breakdown

		units	@ 16 Lpm Flow		@ 8 Lpm Flow
			1" Inner Ø	3/4" Inner Ø	1/2" inner Ø
	Cross Sectional Area	m^2	5.07E-04	2.85E-04	1.27E-04
	Fluid Average Velocity	m/s	0.53	0.94	1.05
	Reynolds Number	-	2.03E+04	2.71E+04	2.03E+04
	Hose roughness e	m	7E-05	7E-05	7E-05
	Relative Roughness	-	2.76E-03	3.67E-03	5.51E-03
	Friction Factor f	-	3.10E-02	3.14E-02	3.51E-02
Hose	**Length**	m	0.350	4.500	4.200
	Total Head Loss	m	0.006	0.331	0.328
	Total Pressure Drop	**Pa**	***58***	***3213***	***3179***
90° Elbow	**Quantity**	-	2	10	16
	Equivalent Length [98]	m	1.620	1.370	1.100
	Total Head Loss	m	0.056	1.009	1.374
	Total Pressure Drop	**Pa**	***541***	***9781***	***13321***
90° Bends	**Quantity**	-	-	6	8
	Radius	m	-	0.200	0.150
	Resistance Coefficient K	-	-	0.490	0.563
	Total Head Loss	m	-	0.131	0.127
	Total Pressure Drop	**Pa**	**-**	***1272***	***1233***
Male/Female Adapter	**Quantity**	-	2	6	8
	Equivalent Length [98]	m	0.460	0.460	0.300
	Total Head Loss	m	0.016	0.203	0.187
	Total Pressure Drop	**Pa**	***154***	***1970***	***1817***
Tee Flow - Run	**Quantity**	-	-	-	2
	Equivalent Length [98]	m	-	-	0.300
	Total Head Loss	m	-	-	0.047
	Total Pressure Drop	**Pa**	**-**	**-**	**454**
Reduction Fitting	**Quantity**	-	1	1	-
	Small Ø - d	m	0.019	0.013	-
	Large Ø - D	m	0.025	0.019	-
	Resistance Coefficient K	-	0.850	1.729	-
	Total Head Loss	m	0.012	0.077	-
	Total Pressure Drop	**Pa**	***116***	***748***	**-**
Expansion Fitting	**Quantity**	-	-	1	1
	Small Ø - d	m	-	0.019	0.013
	Large Ø - D	m	-	0.025	0.019
	Resistance Coefficient K	-	-	0.196	0.316
	Total Head Loss	m	-	0.009	0.004
	Total Pressure Drop	**Pa**	**-**	***85***	***43***
System Total Head Loss		**m**		**3.919**	
System Total Pressure Drop		**Pa**		**37985**	

6.3.4 Refrigeration System

Note that the radiator and intercooler sizing sections do not consider the additional heat transfer achievable using the refrigerated chiller in the system. This is due to the fact that the refrigeration system is currently in its preliminary stage of development and is currently considered as a secondary means of cooling. The layout of the refrigeration system can be reviewed in Figure 6.8

The implementation of a chiller to the electric powertrain and intercooler thermal system can be advantageous, especially during high ambient temperatures. At high ambient temperatures, when the temperature difference between the coolant and air entering the radiator is low, the radiator heat transfer capability will be limited, as discussed in section 6.3.1 Radiator Sizing. At best, the coolant temperature can only drop to as low as the ambient temperature. This can be problematic given that the electric motors have a relatively low maximum coolant temperature requirement. The refrigeration system on the other hand can still absorb heat at the chiller and reject it through the condenser during high ambient temperature conditions. This is due to the high temperature refrigerant entering the condenser as a result of the compressor which will have a sufficient temperature difference to reject the heat absorbed. Another advantage that the refrigeration system possesses is a more effective heat transfer due to the latent heat available from the phase change as oppose to sensible heat transfer.

By increasing the system heat transfer with the use of the chiller, the components can also operate at a higher efficiency leading to a higher power output or lower energy consumption. For example, it has been estimated that a coolant temperature of 20°C for the electric motors will result in an average five percent increase in efficiency in compared to a coolant temperature of 55°C. The intercooler can also increase the power output of the engine by further reducing the charged air temperature since it can contain more oxygen for the combustion process due to the lower air density. The chiller also provides the capability of cold soaking the coolant during low heat load (i.e. vehicle idling or cruising) to then provide a higher cooling capacity when the components are generating a high amount of heat (i.e. high acceleration, high power demand). Note that the chiller has yet to be fully developed and tested to determine its performance characteristics and power draw to justify its use. An important question raised with using the compressor is, does its advantages outweighs the power consumption required which could instead be used for vehicle

range. The advantages need to be properly quantified to compare to the power consumption required to make an informed judgment.

This section primarily outlines the brief design process of the system, the preliminary experiment performed and the required future work. Once the system is fully developed, the intercooler and radiator sizing can then be re-visited for further optimization.

6.3.4.1 Refrigeration Design

The refrigeration system is designed based on an ideal vapor-compression refrigeration cycle, the pressure-enthalpy diagram of this cycle is shown in Figure 6.19. Point 1 is after the evaporator, 2 is after the compressor, 3 is after the condenser, and 4 is after the thermal expansion valve (TXV). The compression (1-2) is assumed to be isentropic, the heat rejection and absorption in the condenser and evaporator respectively is assumed to occur at a constant pressure. Kinetic and potential energy changes are assumed to be negligible.

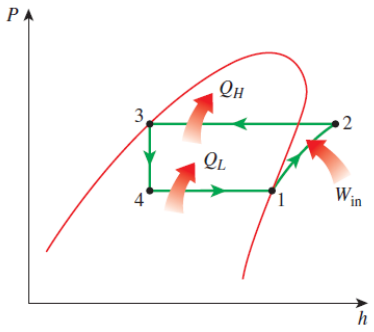

Figure 6.19: Typical Refrigeration P-h Diagram [99]

The rate of heat absorption $\dot{Q}_L$, heat rejection $\dot{Q}_H$ and compressor work $\dot{W}_{in}$ can be calculated using equation (6-46), (6-47), and (6-48) respectively. The heat rejection rate $\dot{Q}_H$ can also be calculated using equation (6-49).

$$\dot{Q}_L = \dot{m}(h_1 - h_4) \tag{6-46}$$

$$\dot{Q}_H = \dot{m}(h_2 - h_3) \tag{6-47}$$

$$\dot{W}_{in} = \dot{m}(h_2 - h_1) \tag{6-48}$$

$$\dot{Q}_H = \dot{Q}_L + \dot{W}_{in} \tag{6-49}$$

The performance of the refrigeration is expressed in terms of coefficient of performance (COP) defined in equation (6-50).

$$COP = \frac{\dot{Q}_L}{\dot{W}_{in}} \qquad (6\text{-}50)$$

Since the radiator and intercooler are sized for the worse case ambient temperature of 45°C, the refrigeration system is not seen as a critical component for the vehicles operation as of now. Therefore, it is currently at a low priority at which there is a very limited budget available. For this reason, the Denso electric compressor has been used for the system. Denso is one of the competition sponsors and have made their electrical compressor available for donation. The 34cc compressor can provide a cooling capacity up to around 8 kW at a maximum rpm of 8,600 at an estimated COP of 2. Table 6-5 displays the estimated mass flow rate achievable by the compressor at the maximum speed of 8,600 rpm and at the most efficient speed of 5,000 rpm (estimated COP of 2.3) at a given saturated pressure.

Table 6-5: Refrigerant Mass Flow Rate Achieved with Compressor

Temperature (°C)	Saturated Pressure (kPa)	Gas Density (kg/m3)	Mass Flow Rate (kg/s)	
			@ 8,600 rpm	@ 5,000 rpm
28	727.31	35.41	0.086	0.050
36	912.35	44.71	0.109	0.063
38	963.68	47.35	0.115	0.067
40	1017.10	50.12	0.122	0.071
42	1072.80	53.04	0.129	0.075
44	1130.70	56.10	0.137	0.079
46	1191.00	59.34	0.145	0.084
48	1253.60	62.74	0.153	0.089
52	1386.20	70.10	0.171	0.099
56	1529.10	78.30	0.191	0.111
60	1682.80	87.46	0.213	0.124
65	1891.00	100.50	0.245	0.142
70	2118.20	115.71	0.282	0.164
75	2365.00	133.69	0.326	0.189
100	3975.10	380.23	0.926	0.539

The values have been collected from the R-134a temperature table provided in the Thermodynamics An Engineering Approach textbook [99]

The vehicle cabin heat balance method simulation performed by Fayazbakhsh et al. suggests that the AC load reaches a peak load of about 3 kW [100]. This leaves about 5 kW cooling capacity for the chiller during such a peak condition. However, there will be times when the cabin fan will not

be in use or a control strategy can be put in place to avoid using cabin fan (reducing load on cabin AC) to increase the cooling capacity of the chiller to approximately 8 kW for short periods of time.

Table 6-6 is generated to determine the mass flow rate required for a heat absorption of 3 kW, 5 kW, and 8 kW at a given saturated pressure in the evaporator/chiller which is located in between the expansion valve and compressor (between point 4 and 1 in Figure 6.19).

Table 6-6: Required Refrigerant Mass Flow for the Required Heat Absorption

Temperature (°C)	Saturated Pressure (kPa)	Saturated Liquid Enthalpy h_f (kJ/kg) [point 4]	Saturated Vapor Enthalpy h_g (kJ/kg) [point 1]	Change in Enthalpy Δh (kJ/kg)	Required Mass Flow Rate $\dot{m}$ (kg/s)		
					@ $\dot{Q}_L = 3\ kW$	@ $\dot{Q}_L = 5\ kW$	@ $\dot{Q}_L = 8\ kW$
18	537.52	76.52	184.01	107.49	0.0279	0.0465	0.0744
6	362.23	59.97	193.94	133.97	0.0224	0.0373	0.0597
4	337.9	57.25	195.51	138.26	0.0217	0.0362	0.0579
2	314.84	54.55	197.07	142.52	0.0210	0.0351	0.0561
0	293.01	51.86	198.6	146.74	0.0204	0.0341	0.0545
-2	272.36	49.17	200.11	150.94	0.0199	0.0331	0.0530
-4	252.85	46.5	201.6	155.1	0.0193	0.0322	0.0516
-6	234.44	43.84	203.07	159.23	0.0188	0.0314	0.0502
-8	217.08	41.19	204.52	163.33	0.0184	0.0306	0.0490
-10	200.74	38.55	205.96	167.41	0.0179	0.0299	0.0478
-12	185.37	35.92	207.38	171.46	0.0175	0.0292	0.0467
-14	170.93	33.3	208.79	175.49	0.0171	0.0285	0.0456
-16	157.38	30.69	210.08	179.39	0.0167	0.0279	0.0446
-20	132.82	25.49	212.91	187.42	0.0160	0.0267	0.0427

The values have been collected from the R-134a temperature table provided in the Thermodynamics An Engineering Approach textbook [99]

The stock thermal expansion valve for the cabin is expected to operate around 2°C, just above 0°C to prevent frost from forming on the evaporator from the moisture in the air as it would block air flow. Referring to Table 6-6, the refrigerant mass flow rate require for a heat transfer rate of 3 kW at 2 °C is 0.0210 kg/s. As for the chiller, since the copper coil is submerged in 50/50 glycol coolant water, the temperature can be below 0, for the first iteration of the design, -14°C has been chosen. This results in a required mass flow rate of 0.0285 kg/s to achieve a heat transfer of 5 kW. Therefore, the sum of the mass flow rate for achieving 3 kW in the cabin and 5 kW in the chiller results to 0.0495 kg/s which is achievable with the compressor as seen in Table 6-5. To achieve an 8 kW heat transfer in the chiller at -14°C, a refrigerant mass flow rate of 0.0456 kg/s is required. Note that the change in enthalpy is determined by finding the difference between the saturated liquid and saturated vapor enthalpy. As shown in Figure 6.19, point 4 is a liquid-vapor mixture

and not at the saturated liquid dome line. Once point 3 is determined, point 4 can be better estimated to get a more accurate enthalpy change to determine the mass flow required.

The operating high pressure (also referred to as head pressure) that the compressor achieves to sufficiently reject the heat absorbed by the system depends on the heat transfer through the condenser. The determining factors for head pressure other than the type of refrigerant are the condenser surface area and cleanliness, the relative humidity and ambient temperature. The high side pressure is determined in principle by the ambient temperature [101]. The heat transfer from the condenser can be determined similarly to equation (6-15). However, since the hot fluid is a condensing vapor that condenses at a constant temperature, the heat capacity rate can be considered to approach infinity ($C_h \rightarrow \infty$). This would result in a heat capacity ratio of zero, which simplifies the heat exchanger effectiveness to equation (6-51). Table 6-7 displays the heat transfer achievable at a given air mass flow rate and the temperature difference between the refrigerant and air. Based on the calculated results in the table, a temperature difference of 8°C shows to be sufficient. This means that for example, at an ambient temperature of 45°C the refrigerant entering the condenser should be 54°C, resulting in a saturated pressure of 1457.65 kPa.

$$\varepsilon = 1 - exp(-NTU) \tag{6-51}$$

Table 6-7: Condenser Heat Transfer (kW) at a Given Temperature Difference and Air Mass Flow Rate

Temperature Difference ΔT	Air Mass Flow Rate (kg/s)									
	0.2	**0.4**	**0.6**	**0.8**	**1**	**1.2**	**1.4**	**1.6**	**1.8**	**2**
2	0.40	0.81	1.21	1.61	2.01	2.42	2.82	3.22	3.63	4.03
4	0.81	1.61	2.42	3.22	4.03	4.83	5.64	6.44	7.25	8.06
6	1.21	2.42	3.63	4.83	6.04	7.25	8.46	9.67	10.88	12.08
8	1.61	3.22	4.83	6.44	8.06	9.67	11.28	12.89	14.50	16.11
10	2.01	4.03	6.04	8.06	10.07	12.08	14.10	16.11	18.13	20.14
12	2.42	4.83	7.25	9.67	12.08	14.50	16.92	19.33	21.75	24.17

Figure 6.20 illustrates the refrigeration system with its points of interest numbered. For the peak steady state operation of the cabin cooling (3 kW) and chiller (5 kW), the expected enthalpy and mass flow rate as well as the heat transfer and inputted work at an ambient temperature of 45°C is shown in Table 6-8. These values are plotted on the R-134a P-h diagram shown in Figure 6.21.

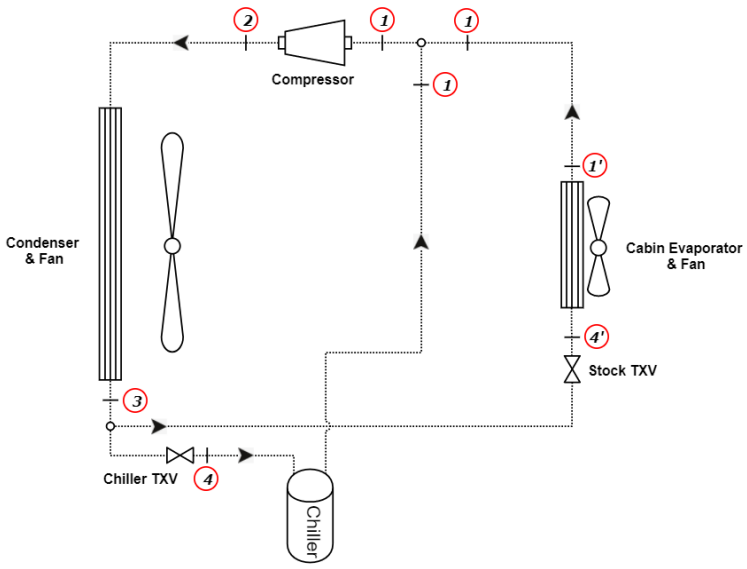

Figure 6.20: Refrigeration schematic with numbered operating points

Table 6-8: Refrigeration parameters at the different operating points

	Enthalpy h (kJ/kg)	Mass Flow Rate (kg/s)	Temperature (°C)	Pressure (kPa)
1	396	0.0411	-14	170.93
1'	404	0.0231	2	314.84
2	454	0.0642	75	1457.65
3	274.3	0.0642	54	1457.65
4	274.3	0.0411	-14	170.93
4'	274.3	0.0231	2	314.84

4'-1' :	$\dot{Q}_{L,1}$ = 3 kW
4-1 :	$\dot{Q}_{L,2}$ = 5 kW
1-2 :	$\dot{W}_{in}$ = 3.73 kW
2-3 :	$\dot{Q}_{H}$ = 11.73 kW
COP :	~ 2.14

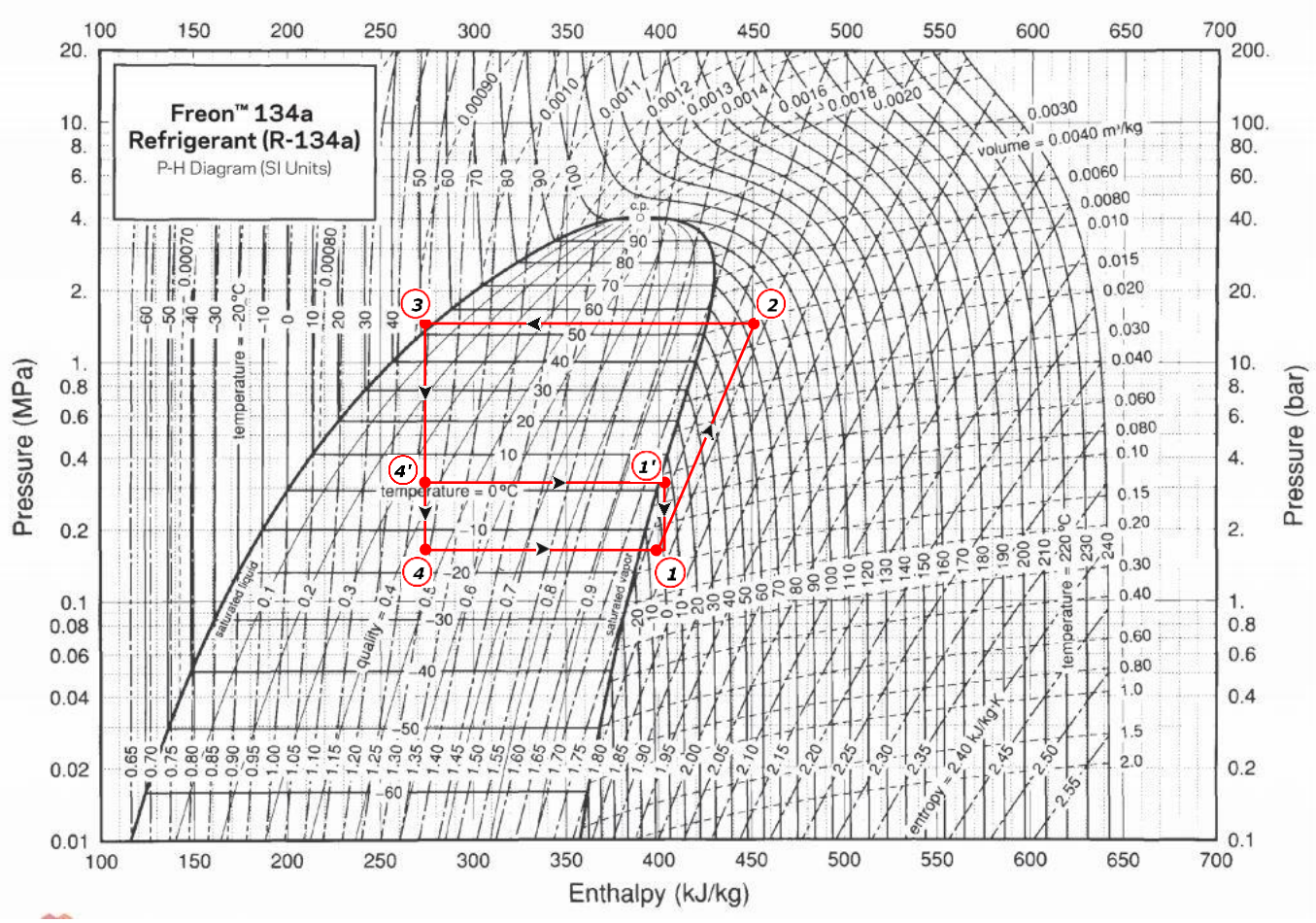

Figure 6.21: P-h Diagram of R-134a [102]

Note that these values plotted in the P-h diagram at the different operating points are expected values for an ideal vapor-compression cycle. The actual vapor-compression cycle will differ mostly due to the irreversibilities that occur in the components. For example, in reality, the compressor operation is not isentropic and therefore the input work would be higher or potentially lower. Another example would be that the heat transfer occurring at the evaporator, chiller or condenser is not at a constant pressure, there will be some pressure drop present. The two common sources of irreversibilities are fluid friction and heat transfer to or from the surroundings. Furthermore, these values are just estimated at one specific operating point, the values are subject to change with the ambient temperature, and a change in the heat transfer load in the evaporator, chiller and condenser.

The refrigerant exiting the chiller and evaporator (points 1 and 1') should be superheated, just outside the saturated pressure dome to avoid any liquid refrigerants from entering the compressor.

If liquid is present in the refrigerant, the compressor can be damaged due to shockwaves when the liquid boils inside the compressor. Similarly, the refrigerant exiting the condenser (point 3) should be subcooled, just outside the pressure dome to avoid any gas from entering the TXV. If gas is present in the refrigerant, there will be a high turbulence inside the TXV, reducing its performance.

6.3.4.2 Chiller Design

The chiller consists of a cylindrical PVC tube that has a coiled copper piping with refrigerant flowing through that is submerged inside the coolant as shown in the top view picture in Figure 6.22. The PVC tube is used for its insulation and the copper pipe for its high heat conductivity. The chiller location in the engine bay can be seen in Figure 5.32: Engine Bay Components. The coolant enters from the top and exits from the bottom of the chiller into the pump. The coil has been designed for the outlet to be at the top so that any un-evaporated refrigerant can pool at the bottom, preventing it form entering the compressor. One main cause of un-evaporated refrigerant existing is if there is a sudden change in load and the thermal expansion valve feedback system lags behind to adjust the orifice.

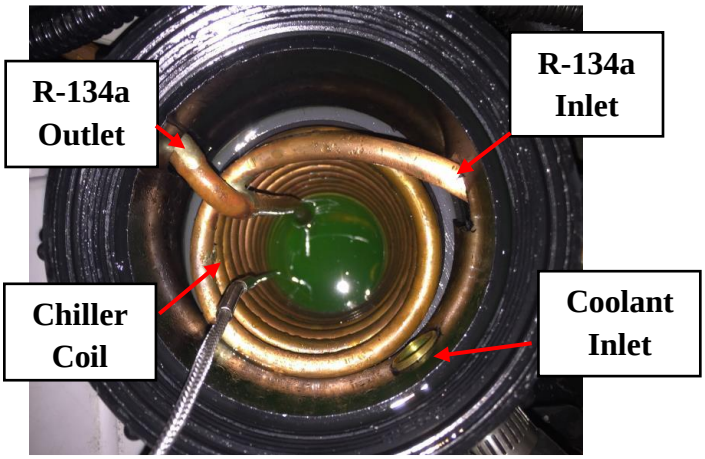

Figure 6.22: Chiller

The following equations from Salimpour [103] are used to determine the UA value for sizing the chiller. The parameters used are provided in Table 6-9.

.

Table 6-9: Chiller Parameters

	Variable	Value
Coolant flow rate	Q	2.67 x 10^{-4} m^3/s (16L/min)
Chiller inner diameter	D	0.089 m^3/s
Coiled Tube outer diameter	d_o	0.0095 m
Coiled Tube inner diameter	d_i	0.008 m
Coil radius	R_c	0.0795 m
Distance between two coils	b	0.02 m
Number of coil turns	n	15
Tube thermal conductivity	k	385 W/m·K
Coolant density	ρ_c	1056.1 kg/m^3
Coolant dynamic viscosity	μ_c	3.9 x 10^{-3} kg/m·s
Coolant Prandtl number	Pr_c	29.87

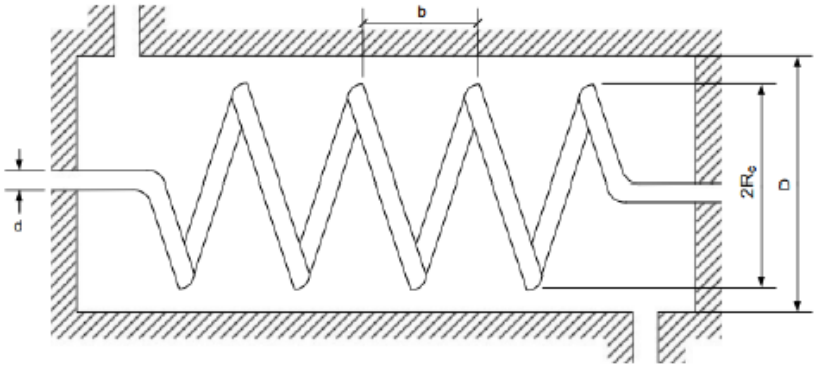

Figure 6.23: Typical Shell and Coiled Tube Heat Exchanger Schematic [103]

Average coolant velocity through the shell (PVC tube) can be calculated using equation (6-52).

$$v_o = \frac{Q}{0.25\pi R_c} = 0.0429\ \frac{m}{s} \tag{6-52}$$

The non-dimensional pitch can be calculated using equation (6-53).

$$\gamma = \frac{b}{2\pi R_c} = 0.04 \tag{6-53}$$

Hydraulic diameter of the shell side is determined using equation (6-54).

$$D_h = \frac{D^2 - 2\pi R_c d_o^2 \gamma^{-1}}{D + 2\pi R_c d_o \gamma^{-1}} = 0.03\ m \tag{6-54}$$

The shell side Reynold's number is determined using equation (6-55).

$$Re_o = \frac{\rho_c v_o D_h}{\mu_c} = 384 \quad (6\text{-}55)$$

The Shell side Nusselt number correlation can then be used to determine the convection heat transfer coefficient h_o, as shown in equation (6-56).

$$Nu_o = 19.64 Re_o^{0.513} Pr_c^{0.129} \gamma^{0.938} = 31.50 = \frac{h_o D}{k} \quad (6\text{-}56)$$

$$h_o = 370 \frac{kW}{m^2 K}$$

The length and outer area of the coil can be determined using equation (6-57) and (6-58) respectively.

$$l = 2R_c \pi n = 7.5\, m \quad (6\text{-}57)$$

$$A_o = l \pi d_o = 0.22\, m^2 \quad (6\text{-}58)$$

The conductive resistance of the tubing can then be calculated using equation (6-59).

$$R = \frac{ln\left(\frac{d_o}{d_i}\right)}{2\pi k l} = 9.48 \times 10^{-6} \frac{K}{W} \quad (6\text{-}59)$$

Due to the refrigerant boiling/evaporating in the chiller, the thermal resistance is considered to be small and thus neglected. The overall heat transfer coefficient can be calculated using equation (6-60).

$$UA_o = \left[\frac{1}{h_o A_o} + R\right]^{-1} = 46.39 \frac{kW}{K} \quad (6\text{-}60)$$

6.3.4.3 Refrigeration Experiment Result & Recommended Future Work

An experiment was performed on the chiller system to determine its heat transfer performance, the results are plotted in Figure 6.24. For this experiment, the radiator was disconnected from the system and the in-cabin evaporator fan was not in operation. The coolant was heated up to 47.8 °C as the starting temperature of the experiment and the ambient temperature was measured to be 24°C. The electric compressor was set to operate at 7000 rpm and the coolant pump was running to provide a flow rate of 16 Lpm, which was then shut off at the 1318 second mark. The pump was shut off during the experiment to compare the behaviour of the refrigeration system under load vs low heat transfer load. Thermocouples were positioned at the chiller coolant inlet (purple line) and the chiller outlet (blue line). The third thermocouple was located on the thermal expansion valve

sensing bulb to measure the outlet refrigeration temperature (orange line). The heat transfer (green line) was then calculated at one second intervals during coolant flow and 10 second intervals after the pump was shut off.

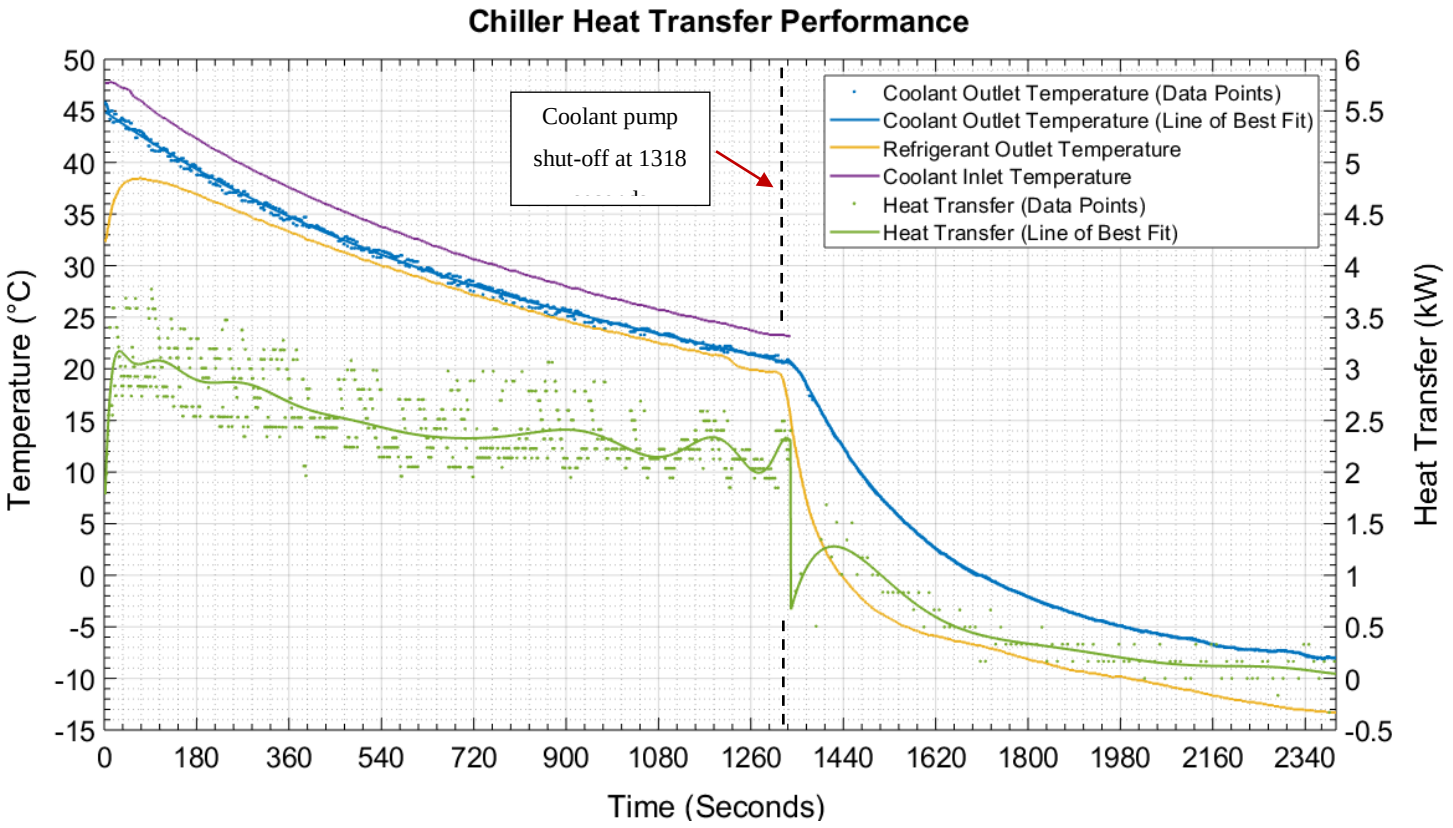

Figure 6.24: Chiller Heat Transfer Performance Result

The measured outlet coolant temperature data points gathered from the experiment during coolant flow is more dispersed in comparison to the other temperature measurements. This is due to the turbulence present in the chiller from the flow. As a result, using the coolant outlet temperature data points and the coolant inlet data points to calculate the heat transfer results in a more scattered data. The heat transfer line of best fit in Figure 6.24 displays an initial heat transfer rate of 3.2 kW, which then decreases in a transient manner. Once the pump is turned off, the heat transfer rate drops which eventually converges to an equilibrium value. During the 3 kW heat transfer operating point, the high pressure was measured to be 823 kPa (temperature of 32°C) and the low pressure at 229 kPa (temperature of -6°C). The current draw was measured to be 8.6 A at 270 V which results to 2.32 kW of work input.

A point of interest in the experiment is the measured refrigerant outlet temperature, during the high load heat transfer (pump running) the refrigerant outlet temperature starts at around 38 °C and drops to 20 °C. This is an unexpected outcome, the refrigerant outlet temperature is expected to have been just slightly above the -15°C (or in the case of this specific experiment, slightly above -6°C) however this was not the case. This indicates that the refrigerant has been fully evaporated within the chiller, as opposed to near the exit of the chiller as expected and displayed in Figure 6.21. It has been concluded that reason for this outcome is that the refrigerant flow rate is too low in the chiller. In addition to the in-cabin TXV pressure drop being lower than the chiller TXV due to the saturated pressure requirements, when the in-cabin evaporator is not experiencing a high heat load, the TXV orifice will expand to adjust for this, which results in an even lower pressure drop in the line. Therefore, since restriction to flow is a lot higher in the chiller line in this situation, the mass flow rate in the in-cabin evaporator line was increased, preventing the chiller from achieving the required refrigerant mass flow rate.

The use of a pressure regulating valve (PRV) in the in-cabin evaporator line should be investigated to mitigate the mass flow rate issue. The PRV can be positioned right after the evaporator to further drop the pressure of the exiting superheated refrigerant. The added restriction will adjust the mass flow rate through the two parallel lines. This will however reduce the efficiency of the system since the pressure in the in-cabin evaporator line is further reduced to then only be increased again by the compressor right after. An electrically controlled solenoid valve can also be positioned before the in-cabin TXV to prevent refrigerant from flowing when cabin cooling is not required. This would increase the efficiency of the system when the evaporator is not in use as it will reduce the work input required for the compressor.

The refrigeration system could be reconfigured to avoid the low mass flow rate by having the components inline as a series system with two TXVs, the T-S diagram for such a system is shown in Figure 6.25. The first TXV will drop the pressure to the required amount for the cabin and the second will drop it to the pressure required for the chiller. This however removes the capability of adding a solenoid valve to prevent the system from absorbing heat from the evaporator when in-cabin cooling is not required.

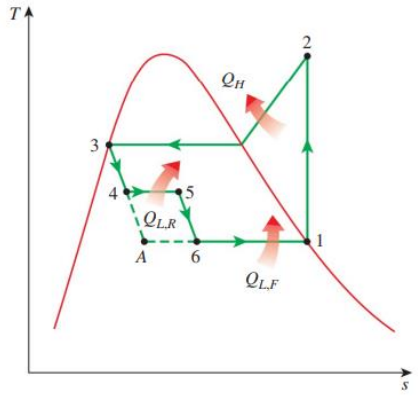

Figure 6.25: Refrigeration System in Series Configuration [99]

Another possible parallel configuration is to place the first expansion valve before the T-junction, as shown in Figure 6.26. It can be seen from the P-h diagram that the advantage this system has over the individual expansion valves set up is that the refrigeration effect of the chiller increases as a more saturated liquid enters the chiller's TXV. This is due to the flash gas being removed at state four.

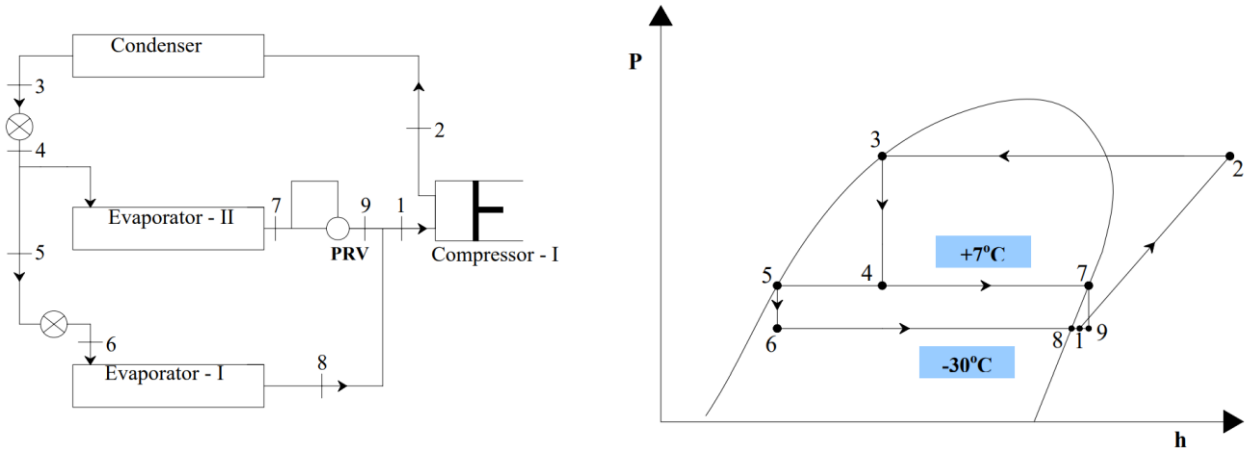

Figure 6.26: Example schematic and P-H diagram of having the TXV before the T Junction [104]

A Schrader valve and/or pressure sensors should positioned before and after every component in the refrigeration system to better develop an actual vapor-compression cycle diagram to better predict the behaviour of the system. The refrigerant saturated temperature in the chiller should be re-evaluated to determine if that is the optimal chiller temperature for the system. Lastly, the amount of refrigerant in the system should also be re-evaluated again to ensure that the system is charged to its optimal amount. Once the refrigeration system is fully operational and the

configuration and operating points are finalized, then the system can be tested to quantify the impacts it can have on vehicle efficiency, performance, and range.

6.4 Battery Thermal Management

6.4.1 Battery Cooling Design Review

There are various methods and arrangements possible for battery cooling which differ in cooling capacity, complexity, weight, and cost. Figure 6.27 provides examples of some battery cooling designs implemented in current production vehicles. The Toyota Prius' battery pack utilizes a forced air convection method by using a fan to blow the air through the system (Figure 6.27(a)). Air cooling methods are typically not used for high performance requirements as it is a weak thermal conductor, for example, water is approximately 20 times more thermally conductive than air. The BMW i3 uses direct refrigeration to remove heat from its battery packs. The batteries are positioned on top of a tray that has refrigeration tubes running through it (Figure 6.27(b)). This is found to be a less commonly implemented cooling method. The hybrid Porsche Panamera's use of coolant to transfer heat from the battery is a more common approach. The coolant flows through the cold plates which are positioned under the battery packs as seen in Figure 6.27(c). The Chevrolet Bolt has thermal fins in between the flat pouch battery cells which also have coolant flowing through them (Figure 6.27(c)). The fins achieve a greater surface area contact for heat transfer and reduces the thermal gradient between the cells. Lastly, the Tesla model S uses coolant which flows through a tube routed in a serpentine arrangement around its cylindrical battery cells. Another unique cooling method is submerging the cells in a dielectric fluid, this is a complicated process and adds weight to the battery pack. XINGMobility has successfully developed such a system [105].

(a) Toyota Prius [106]

(b) BMW i3 [107]

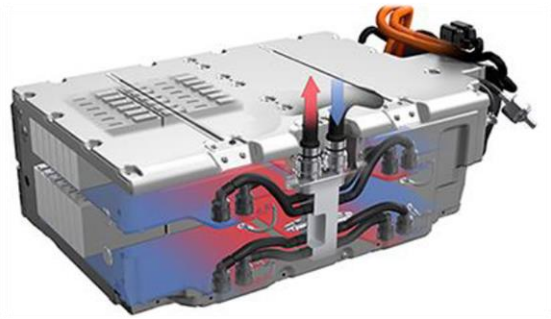

(c) Porsche Panamera S E-Hybrid [108]

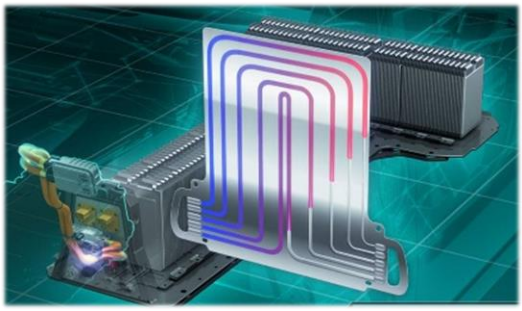

(d) Chevrolet Volt Cooling Fins [109]

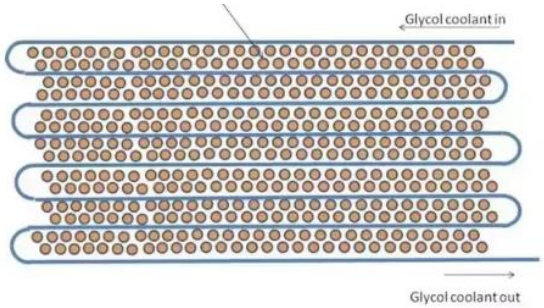

(e) Tesla Model S [110]

Figure 6.27: Battery Pack Cooling Design Examples

Upon designing a thermal management system for the battery pack, it is important to attempt to minimize the temperature gradient among the cells as it can have an impact on battery performance and age [111] [112]. Thermal gradient must be kept in mind when designing the cold plates that go up against the battery pack, the larger the cold plates, the greater the thermal gradient may be from the first cell to the last. The arrangement of the cold plates and coolant flow can help provide a more uniform temperature, i.e. cold plates connected is series vs parallel. Having a heat exchanger directed on the surface of the cells themselves like the Volt can help reduce the thermal gradient of the cells at the cost of added complexity to the system. Not only is the thermal gradient between the cells important but the internal thermal gradient of an individual cell is also of importance. When Hunt et al [113] compared surface cooling vs tab cooling, they discovered that

cell tab cooling could reduce the loss of usable capacity leading to an extension of battery performance and life cycle due to the lower internal thermal gradient within the cell layers.

The use of cold plates positioned under the battery modules were investigated, however there was a high concern with the risk of water leakage which could lead to a battery shortage. This is of a high severity as the team will not be able to afford another battery and it would mean they would be out of the competition. After going over the failure mode analysis it was determined that direct refrigeration cooling would be a safer and more effective approach, in the case of a minor leak, there is a very low chance of shorting the battery as the refrigerant will escape in a gas form at atmospheric pressure. Furthermore if the refrigeration system is designed properly, the flow could be reversed thus heating the cold plates to warm up the battery pack during cold climates. After some design iterations, it was discovered that such a system proved to be complex which required a lot of human resources. Designing a cold plate that can withstand the high refrigerant pressure is challenging and a deep understanding of the refrigerant saturated vapor flow behaviour in the cold plate is required to properly design the system to avoid hot spots. Furthermore, to avoid overcooling the battery packs, an electrically controlled thermal expansion valve would be required which is not readily available for implementation. There is also a risk of condensation occurring on the cold plates which depending on the orientation of the battery pack could lead to a short if the terminals are close to the cold plate.

Upon further analysis and consultation with automotive battery thermal management experts, it was determined that due to the low battery internal resistance; a cooling system is not critical for the purpose of preventing the battery from overheating during the competition vehicle dynamic events. The ideal temperature required for the A123 battery pack is between 10-35°C and its maximum operating point is 60°C. Not using a cooling system will certainly have a negative impact on the cycle life and degradation of the battery. However, for the scope and timeline of this prototype vehicle with the limited available human resources and the risks attributed with system, it has been decided not to pursue the implementation of a cooling system.

An investigation into the possibility of implementing a forced air convection cooling method with the use of fans was also conducted. It was found that the small gaps (~6mm) in between the battery modules and the enclosure walls created a large restriction for the air flow. The high voltage cables located at the top (seen in Figure 5.30) also contributed to the restrictions. The high restriction

limited the effectiveness of using a forced air convection cooling approach. To mitigate this, the use of one way superconducting heat pipe fins were considered to avoid the high restrictive areas of the battery pack. The heat pipes would have been positioned vertically in between the modules were it could draw the heat out and up to its fins extending above the battery pack and cables were there is a low air restriction for the air flow. However, the small gap in between the modules results in the heat pipes to be in a tight fit in between the modules which introduces some new concerns. When the battery modules increase in temperature, they can experience a thermal expansion of up to 2 mm on each side, this does not provide enough clearance for the heat pipes which can result in its rupture as well as module damage. Furthermore, the use of an inlet fan that has access to the cabin for air can be hazardous to the passengers when the fan is not operating. In the off chance that the batteries release a chemical gas, it can seep into the cabin. Therefore the inlet fan must be designed to draw air that is not shared with the cabin or the fan should be designed to be sealed when it is not in use making the design a challenge. Currently the battery pack is sealed from the cabin and has a vent to the outside air in the case of a chemical gas release.

6.4.2 Battery Thermal Analysis and Result

This section provides a basic thermal analysis of the battery pack to provide an understanding of the amount of heat that is generated during operation. This is to confirm that cooling is not a necessity for the prevention of overheating, at least for the intended operation of this prototype vehicle. The A123 battery configuration selected has three parallel strings, each consisting of 15 cells (illustrated in Figure 6.28), totaling to 45 cells per module.

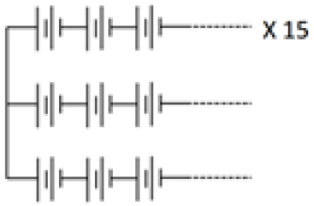

Figure 6.28: Module Configuration

The internal resistance in the battery is what generates the heat [114]. As the cell temperature increases, the internal resistance decreases meaning that the battery will be more efficient up to a certain temperature. The worse case electrical resistance in a cell has been chosen to be 2.8mΩ

based on the internal resistance measurements taken. The total resistance of each modules has been calculated to be 0.014Ω using equation (6-61).

$$R_{module} = \frac{1}{\frac{1}{15R_{int}} + \frac{1}{15R_{int}} + \frac{1}{15R_{int}}} \quad (6\text{-}61)$$

The heat generated by each module can be calculated using equation (6-62)

$$Q_{discharge} = I^2 R \quad (6\text{-}62)$$

The calculation performed to estimate the heat generation of the battery pack at peak 612 amps output for a maximum of 10 seconds is shown below:

$$Q = (612^2)\, 0.014 = 5.2\ kW$$

$$5.2kW \times 10\ seconds = 52\ kJ$$

$$52\ kJ \times 6\ Modules = 315\ kJ$$

The thermal mass has been found to be approximately 26 kJ/K per module, this includes all the different materials that encompasses the module. Using equation (6-63), the pack temperature increase due to that heat generation can be calculated to be 2°C

$$q = mC_p\Delta t \quad (6\text{-}63)$$

$$\Delta t = \frac{315}{26 \times 6} = 2℃$$

For a maximum continuous current draw of 180A (50.4 kW), the battery would be fully depleted in around 19 minutes and its temperature would increase by approximately 20°C. This is assuming that the battery is absorbing all the heat and not rejecting it to ambient from the sides. It is highly unlikely for the vehicle to be demanding such a high continuous power for that short period of time. Referring back to Table 3-1 in section 3.6 Drive Cycle Analysis, the average power supplied by the battery for the US06 drive cycle is 19.16 kW. Figure 6.29 displays the maximum cell temperature measured during a 160 km endurance drive which took almost 2 hours and 30 minutes. During the drive it can be seen that the cell temperature increased by a total of 5°C. Note that the maximum allowable cell temperature is 60°C and that the hotter the cells get, the lower the internal resistance gets leading to a lower heat generation.

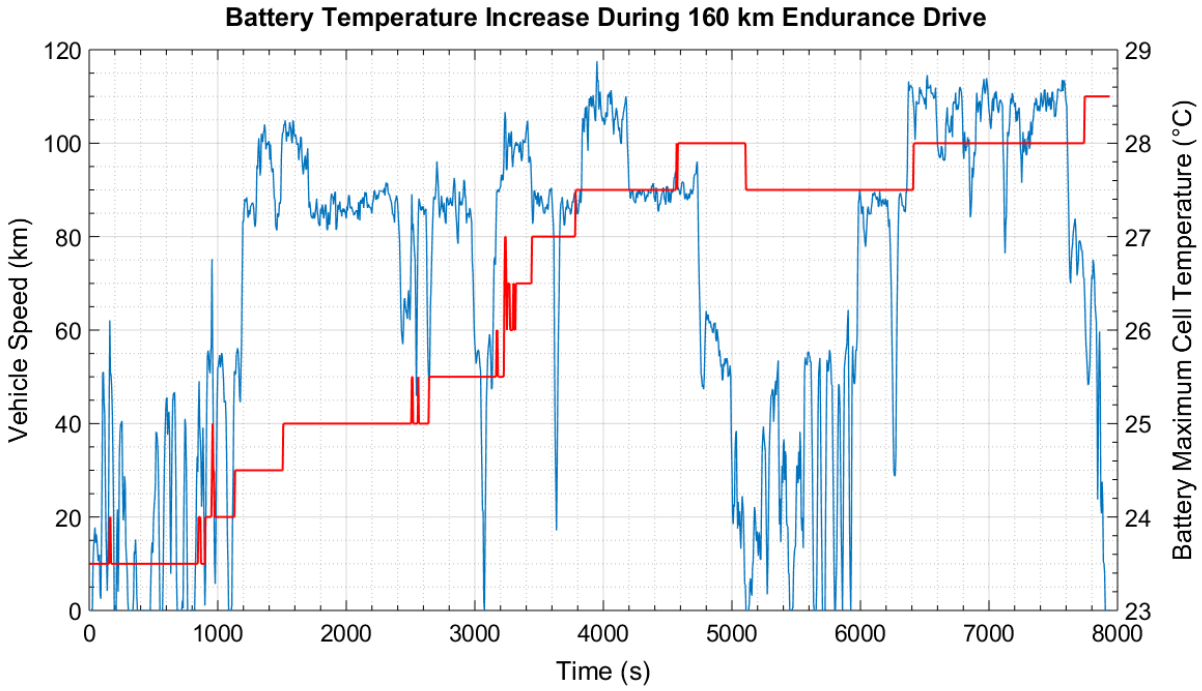

Figure 6.29: Battery Temperature Increase During a 160 km Endurance Drive

CHAPTER 7
Lessons Learnt & Conclusions

7.1 Lessons Learnt

Listed below, are the lessons learnt by this author, either through first hand experiences or indirect experiences, during the hybridization of the Camaro. To elaborate these lessons further, examples of past mistakes, either made or avoided, are provided. Furthermore, in an attempt to provide a convenient means of remembering these lessons, a phrase is developed for each lesson shown in bold and quotation marks. Lastly, the list is in no particular order of importance given that they are highly dependent on the component and/or task itself. For example, the first lesson of anticipating that things do not work the first time is not of high importance to using a developed product/component (i.e. electric motor) purchased from a supplier, as its operation is usually guaranteed. However, lesson 4 "Test it first" is very important for the electric motor, as it should be tested to verify its controls before integrating it into the vehicle. Instead, with the exception of safety, which should always be considered to be of highest importance, these lessons should be treated with equal importance for the development of the vehicle as a whole.

1. **"It never works the first time, or second, or third"** - Although a bit of a pessimistic approach, complicated systems, code, or mounts tend to rarely work or fit the first time round as expected. Unless the person working on the task has in-depth knowledge developed from experience or if it is a repetitive task, it is easy to overlook certain things that prevent the task from executing successfully the first time. Having this mentality helps in allocating a buffer time for troubleshooting when tasks are being scheduled. This can help avoid missing deadlines and make the timeline of the project more realistic. Different parts of the bellhousing for example had to be re-machined and re-designed at least 20 times, costing at least 100 extra

hours than anticipated to complete. This was due to numerous unforeseen problems such as, tolerancing issues, interference with other components, hard access points for assembly, lack of dowels for alignment.

2. **"What's plan D?"** – Do not rely on the first plan to succeed, always have back up plans. If the cost is low or justifiable, purchase spare parts, have extra hardware, develop two different solutions or more at the same time. This can save a lot of vehicle downtime time and possibly cost. The pre-transmission components were seen to have a relatively high risk of failure and high severity; therefore, a spare engine, transmission, clutch, P2 to clutch shaft, and eight spare friction discs were purchased for the mitigation strategy. Additionally, in the event that the clutch had to be removed, a different shaft that could connect P2 directly to the engine was also fabricated. Throughout the hybridization process, every single of the aforementioned spare parts had to be used due to various failures, including five out of the eight spare friction discs. Given the long lead time of the spare parts, if they were not purchased in advanced, it could have led to a prolonged vehicle downtime, delaying vehicle development and testing. Furthermore, using express shipping to reduce lead time would have also increased shipping cost.

3. **"Keep it simple"** – This is applicable to a variety of things. In mechanical designing for example, the number of parts that are required to make the component should be minimized and have a simple shape/profile. This can reduce tolerance issues, cost, weak points, and time taken for fabrication; it can also simplify the assembly procedure, reducing the required time, and reduce the chances of losing a critical part of the component. Electrical and controls/programming tasks are also more likely to fail or consume a significant amount of time if they are overcomplicated. The development of the transmission-shifting controller is a prime example for this case. The transmission required digital input signals to command the gear shifts however, the current it had to draw was more than the specification of the hybrid supervisory controller. As a result, an over complicated analog to digital control board was developed from the ground up that was time consuming; furthermore, given its finesse, this lead to oversights that inhibited its operation, requiring a new design iteration. This occurred during the 3rd year of the EcoCAR 3 competition, which prevented the transmission from operating, preventing the P2 and engine from transferring torque to the wheels. Shortly after

the competition, the problem was solved with a microcontroller prototype board, a couple of resistors to make voltage dividers with, and a breadboard. This was a much simpler solution than the initial one, which took up to two hours to develop, test, and validate. This was then further developed into a reliable circuit board for a long term use. As Confucius once said "life is really simple, but we insist on making it complicated". Similarly, it is easy to overcomplicate the solution when it does not need to be.

4. **"Test it first"** – Always test the idea, solution, component, or code before integrating it into the vehicle, and then test and validate it once it is in the vehicle. This is especially important to do so if an improper integration can have an impact on safety. Depending on the complexity of the component, a bench test can be developed to validate its operation as to avoid having to troubleshoot it in the vehicle; which can be challenging, especially if the component is hard to access in the vehicle. For example, the electric powertrain cooling system was not bench tested initially, it was implemented in the vehicle expecting that it would provide the correct flow rate and heat transfer. When this was not the case, trouble shooting the system was extremely tedious, messy, and time consuming, which also delayed other scheduled vehicle tests. It may be tempting to just implement the solution and see what happens in the vehicle instead of going through the process of developing a test bench, but depending on the task, this can be very counter productive. Essentially, if something is to go wrong, it should be on the bench test instead of the vehicle, were it does not block vehicle development. This should be done especially when components interact with each other to form a complicated system, so that in the event the system fails to operate, the individual component that has already been bench tested can be ruled out as the root cause.

   When a component/code is being integrated into the vehicle, it should be validated to ensure that it operates as intended, especially controls code. For example, the pre-transmission kept seizing sporadically when it was tested in the vehicle after an electrical, mechanical, and controls code change had been made, all within one week without being individually tested. Therefore, it was difficult to determine where the problem stemmed from, complicating and prolonging the troubleshoot. Eventually, it was realized that there was a small weld bead that had gone unnoticed on the modified bellhousing face plate that interfered with the torque converter. Grinding off the weld bead required dropping and disassembling the pre-

transmission assembly, which is a time consuming and relatively complicated process. This could have been avoided if the mechanical system was tested before its integration.

Lastly, bench testing a complicated system can also be very valuable in terms of solidifying the required knowledge and theory instead of conceptualizing it. For example, bench testing the refrigeration system helped in validating the understanding of its performance characteristics and behaviour to change in load. This aided in sizing the system and chiller for the vehicle.

5. **"Just do it"** – Sometimes, it is better to execute a solution or build a prototype to ensure its validity before getting caught up on the "nitty-gritty" details. Test the idea, build a proof of concept to develop a full understanding and confidence before committing the time into fully developing the solution or design. Oftentimes, it may be easier and faster to understand a theory by testing it rather than trying to research it or understand it on paper. This helped a lot when there was a need to understand the result of positioning the water pumps in series to each other vs parallel in the cooling system; it also helped in understanding the difference between using a centrifugal pump vs a displacement pump.

   Depending on the component or code, it is best to avoid fixating on building the perfect final product the first time round; as lesson one suggests, it is likely to fail, which could mean that the work put into finalizing the first iteration could have been for nought. Referring to the transmission controller example made in lesson 3, if the first solution was just tested with a prototype microcontroller and a breadboard, the mistakes would have been avoided before spending the time on fully developing the control board and then finding the mistakes.

6. **"And then do it right"** – once after the solution, concept, or design has been validated and tested, it can then be fully developed with the attention to detail required into a final product. The task should be done right no matter how cumbersome it might be or how limited the available time might be. "Band-Aid" solutions never work as permanent solutions, it will only cost more time; similarly, cutting corners never end well. Take tolerancing seriously, and always "measure twice, and then cut once". For example, the low voltage routing and connection in the vehicle was initially rushed and not treated with the care required, as a result it cost the team an aggregated amount of 200 hours of troubleshooting, rewiring, and re-soldering to address different sporadic issues throughout the development of the vehicle. In

hindsight, this could have been avoided if the time was put into doing it correctly and neatly with the required patience in the first place.

7. **"If it moves, it better be balanced, and run true"** – This is particularly important for shafts and couplers; the shaft should rotate about its centerline (run true) and the mass should be balanced to avoid vibrations and stresses on the joints. This was the main reason that the P2 motor spline sheared, the clutch shattered, and the support bearing of the propeller shaft failed. Dowels are key in ensuring that the components connecting to each other are aligned. Never rely on bolts for the alignment, they do not provide the required tolerancing.

8. **"Give it some slack"** - In a porotype vehicle, small items such as low voltage components and controllers are either added later on, or repositioned to increase space for other components. Always include extra slack in the electrical wires to accommodate for these changes. Have extra dummy wires positioned to avoid routing extra wires in the future as it can be very time consuming. Similarly, always purchase a few extra hardware such as bolts and nuts, and purchase extra raw material for fabrication. This can save time as well as allow for some wiggle room in the design if it is not finalized yet and is anticipated to be modified.

9. **"Serviceability, Serviceability, Serviceability" –** Serviceability and maintenance must be kept in mind when designing components and mounts for a prototype vehicle that undergoes various design iterations, failures, and troubleshooting. It can save a tremendous amount of time on the vehicle. When designing a mount that requires tools to be assembled, always ensure that there is enough space for them, especially when they are surrounded by objects in the vehicle. For example, the pre-transmission powertrain had to be disassembled at least ten times throughout the project. If this complicated assembly had poor serviceability, then the additional accumulated time would have used up valuable vehicle development time. Furthermore, if the assembly process was not seamless, then it could have increased the likelihood of damaging the expensive powertrain components during the process.

10. **"One step at a time"** – A problem, or task should be approached one step at a time, especially when it is complicated and being done for the first time. Attention should be given at the task at hand and not spread thin across many tasks at once. It can be beneficial to think ahead as to avoid obstacles in a design and to plan ahead; however, this should be done with caution. It may be counterproductive if the individual or team is working on a solution while their mind

is engrossed with what is to come 20 steps ahead, preventing them from giving their full attention to the current task. If future planning is required, then it should be done at an allocated time and not during the time the task is being carried forward. For example, the initial vehicle model should be basic and simple, using average values and appropriate assumptions, similar to the approach taken in 4.5 Powertrain Performance Analysis. Once the basic model is developed and the fundamentals are understood, the model can then be further developed to address more complicated issues, becoming more representative of the vehicle. Starting with a basic model can quickly provide the estimated values of the vehicle performance and energy consumption, developing an intuition for the values, with a lower possibility of making an error.

Another example that portrays the importance of this lesson is the vehicle integration process. Given the complexity of the selected architecture, the integration should have been performed in a modular manner. For example, the priority should have been given to ensuring the operation of the energy storage system, followed by the operation of the P3 motor. This would have allowed the vehicle to operate in electric mode charge depletion with the P3 motor. After that, priority should have been given to the operation of the transmission followed by the operation of the P2 motor. This would have then allowed for the vehicle to operate in electric mode charge depletion with both motors. Lastly, the engine could have then been prioritized for operation, followed by powertrain optimization. This "step by step" approach of developing the vehicle can potentially be very affective, as the team would be focusing on one step at a time. Furthermore, this approach can contribute to steadily boosting team moral, if the vehicle is to incrementally develop successfully in a steady pace. Instead, the approach taken was to integrate everything simultaneously, scattering the team resources and facing many challenges and obstacles at once. This exhaustive approach resulted in the fatigue of the team, increasing mistakes that could have been avoided. As a result, the vehicle failed to have basic functionalities during the second year of the competition.

Therefore, depending on the complexity of a task, the resources and expertise available, including the scope and timeline, the project should be separated into multiple steps or milestones to strive for in a given timeline. At times, it may be tempting to skip steps to

accomplish a task sooner however, this can jeopardize the completion of the project, "slow and steady wins the race".

11. **"Don't bite off more than you can chew"** – It is vital to plan accordingly to the team's available expertise and resources, failure to do so can result in missing critical deadlines. Improper planning as a result of this can occur when an individual or team is overly ambitious, having unrealistic expectations of their capabilities. It can also occur if the complexity of the task is significantly underestimated. For example, given the scope, aggressive timeline, and limited resources available, the redesign of the ESS aluminum enclosure to carbon fiber for reduction of weight was not pursued. Instead, the priority was focused on the development of the powertrain system, enabling the team in meeting their deadline.

12. **"Little things can sometimes lead to big problems"** – It is easy to overlook a task that might be considered insignificant at the time, only to then cause significant problems in the future. For example, when finalizing the component selection and its space claim, the routing of the auxiliary components must not be forgotten during the process. If the components are positioned such that the exhaust routing, or high voltage routing is made unfeasible, then there might be a need for a complete design overhaul, which costs valuable time. Worse yet, upon integration, it might be only realized then that the powertrain design is not feasible.

    For example, it was noticed that the exhaust had minor leaks present a few weeks prior to the competition date, the competition rules state that the exhaust needs to be leak proof before the vehicle can participate in the competition events. The decision was made to not prioritize this leak and instead continue developing the powertrain given the limited amount of time available before competition. It was decided that the exhaust can be fixed rather quickly during the competition with the aid of the expertise of the technicians available at the provided facilities. However, this was not the case, it was a surprise to discover the additional effort and time required to leak proof the exhaust. What was assumed to take only two hours ended up taking two full valuable days of the competition.

    Another important factor to keep in mind when selecting and integrating the powertrain is the noise vibration harshness (NVH). Upon component selection, the focus was on the feasibility of operating the components, in contrast, attention to consumer acceptability was limited. This resulted in an oversight of the NVH of the internal combustion engine. After integrating the

engine, it was then noticed that the vibrations transferred to the cabin of the vehicle, making it an uncomfortable experience.

13. **"Read the instructions and specifications, and then read them again"** – For some, it may be tempting to jump directly into the integration or execution of a task without feeling the need to read the instructions. This can sometimes occur when the individual is feeling very confident and lacks the patience in reading the instructions first. Regardless of the simplicity of the task, if there are instructions, it must be read carefully. It can be very easy to make one simple mistake that may cost the project valuable time and money by missing a critical information. For example, the specifications of the water pump suggested that the fitting should be threaded unto the plastic outlet port until it is finger tight. This was not read and the fitting was tightened with a tool resulting in the port cracking open. It took an additional six hours to solve the issue, which could have been easily avoided if the instructions were read.

14. **"Sometimes it's best to let it go"** – It is easy to be consumed by a non-critical task of interest that is deemed to possess a low priority. This will inhibit appropriate allocation of the available resources, jeopardizing the successful completion of the project. Additionally, when a design or code does not work as intended, it can be more productive to start over as oppose to investing additional resources to salvage it. There is no point beating a dead horse.

15. **"Don't fix what's not broken"** – Resources are not being used optimally if some of it is going to improving an already working solution that will have minimal affect on vehicle development. Especially when more pressing matters require attention.

16. **"Documentation is your best friend" –** Documenting the work done and keeping it up to date may be a very tedious process but it can be extremely powerful in the future for reference. The documentations can be installation manuals, list of controls changes, test results, failure analysis, lessons learnt, execution procedures, schematics, and so forth. It reduces troubleshooting time, reduces installation/assembly time and mistakes, it also enables the required knowledge transfer for new members, which is of high importance since there is a high turnover rate from students graduating in this team. Pictures should be taken of everything that is being integrated to better illustrate the design and integration. If only one member is capable of installing a component or executing a code, then a problem exists with the documentation.

17. **"Don't let chaos prevail"** – An overwhelming amount of pressure due to tight deadlines and unanticipated challenges can be detrimental to making the best judgements in the "heat of the moment". No matter how simple or complicated the problem, how critical or non-critical it is, it should be approached in a systematic and organized manner. Take a step back to understand the problem, prioritize it, analyse it, seek support if possible, brainstorm and develop a plan and/or solutions, test is, evaluate it, and integrate it. Most important of all, document the progress and do not lose motivation. It is not ideal to go running around like a mad scientist trying to juggle between different problems without any organization.

18. **"When in doubt, don't shrug it off"** – When the conclusion to a solution is "it's good enough", it usually means it is not, and will eventually fail. When there is doubt in a solution, or integration, it should be followed up by a thorough investigation as to remove the doubt. Most of the time, there is a good reason for the doubt existing in the first place. Any doubt in regards to safety should be certainly investigated thoroughly.

19. **"Don't be insane"** – Einstein's definition of insanity is "doing the same thing over and over and expecting different results". Similarly, when a problem persists, or a failure has occurred, do not integrate it again or perform the same tasks expecting a different result. The failure will only occur again costing time and money. The problem must be understood, documenting the different attempts made and the corresponding problems/failures will help in preventing others from repeating it too. If the root of the problem cannot be determined, a fresh set of eyes can be of great help.

20. **"Make no assumptions"** – It is good practice to avoid assumptions and speculations as much as possible, depending on their significance, they can come at a high price of cost and time. Assumptions should be translated into knowledge through experiments/tests, research and analyse, or seeking validation from a reliable expert. Suggestions from experts should also be taken with caution as they may have knowledge in the component itself but not the whole system. For example, a transmission expert suggested that if the spacer was to be reduced by 0.2 inches then the failure with the transmission and torque converter will be avoided. Although it did solve the interference problem between them, it did result in shearing the spline of the motor.

21. **"Communication is key"** – Not everybody thinks and sees things the same way, and they certainly do not share the same level of passion, work ethic, or expectations. It is imperative to communicate the constraints, specifications and criteria of a well defined problem when the task is being delegated to someone else. The correct terminologies should be understood and used to ensure that everyone is on the same page. Furthermore, when seeking advice from experts, it is critical to communicate the problem well so that they can give the most accurate feedback. Lack of communication can be one of the biggest contributors to using resources ineffectively.

22. **"Who's steering?**" – For a team to work successfully together on a complicated project, their responsibilities and accountabilities must be clear, concise, and agreed upon. Without this, the team can lack organization; team members might not follow through their tasks or complete it within the scheduled timeline. If a member is responsible for a particular task, they may feel more obligated to put in the extra effort to maintain or build their reputation, it might also allow them to feel more appreciated and responsible for the team. Without clear roles and responsibilities, a limited few might take an unhealthy or unfeasible amount of responsibilities upon themselves.

23. **"keep it fun"** – This is especially important when the majority of the team consists of volunteers who have no obligations in committing to the team. Although putting in the effort to make the endeavour fun might seem time consuming, it tends to pay off in the long run. It can attract more talent, encourage students to put in more effort, and reduce fatigue.

24. **"keep it safe"** – It goes without saying that safety is the number one concern regardless of what the task might be. A project like hybridizing a vehicle can have numerous safety hazards associated with it. Always ensure that the correct personal protective equipment (PPE) is being utilized, lockout/tagout exposed high voltage cables and lugs, and remove the manual service disconnect when working on the vehicle. Always test a new controls code with caution if it can have an impact on the safety of the vehicle and others surrounding it. It can be tempting to put safety on the sidelines when under high pressure or when something needs to be done as quickly as possible, this should be avoided at all costs. Always be prepared for the worse case scenario, invest the time in researching the safest approach to a task, never learn what it is the hard way.

7.2 Conclusions

Hybrid electric vehicles are a great segue from fossil-fueled vehicles to all-electric vehicles. They avoid most of the barriers electric vehicles face and have the capability of producing lower emissions in comparison to fossil-fueled vehicles. Hybrid electric vehicles are available in many forms, configuration, and architecture design, which range in different levels of complexity and benefits. This thesis outlined the processes undertaken to hybridize the 2016 V6 Camaro for the EcoCAR 3 competition to provide insight into the complexities that are present in hybrid electric vehicles.

Prior to investigating the different vehicle architectures and powertrain components, the vehicle technical requirement must be first determined based on the targeted market. This is crucial as the VTR paves the way for the powertrain and architecture selection. Afterwards, the VTR should be translated into power and energy requirements to help narrow down to the feasible powertrain components and possible combinations. Basic analysis, vehicle modelling, and space claiming can then be performed to further narrow down the selection pool. Space claiming the components with a 3D solid modelling software ensures that the selected components and their auxiliary components can fit within the vehicle. It can also provide insight into the difficulty of the structural and mount design required for integration. Basic analysis and vehicle modelling can determine if the selected components can enable the vehicle to achieve the VTR, it can also ensure that they compliment each other to optimize vehicle efficiency. For example, when looking at a gen-set, the efficiency map of the engine and electric motor should align during the required operating conditions. Another example would be ensuring that the selected energy storage system provides sufficient power and voltage for the electrical motor to output the propulsion power required to meet the VTR. The remaining architecture designs and powertrain components that meet the VTR can then be compared in a decision matrix to make the final decision. If there is a close tie between certain selections, then a more refined vehicle model for them may be required to generate a more accurate vehicle specification to help with the decision making process. Note that a project or task will consume a certain amount of human resources, cost, and time. The availability of these three factors within the team must be considered as additional constraints when making a decision to ensure its successful completion.

The selected single shaft, pre and post-transmission, series-parallel, plug in hybrid electric vehicle architecture is certainly one of the most complicated to integrate and control. The capability of switching between series or parallel depending on the vehicle condition allows the vehicle to benefit from both worlds with less limitations, while paying the expense for both a series and parallel architecture. This architecture provided the vehicle with six distinct vehicle operating modes termed as:

1. **CD P3 Only:** P3 provides propulsion when vehicle power demand is low.
2. **CD Full Electric:** P2 and P3 provide propulsion for a higher vehicle power demand.
3. **CD Performance:** The engine, P2, and P3 provide propulsion for maximum vehicle performance.
4. **CS Series:** The engine and P2 gen-set provide electrical power while P3 provides the propulsion at a low vehicle power demand.
5. **CS Parallel:** The engine and P3 provide propulsion for a higher vehicle power demand while P2 converts some of the output mechanical power from the engine into electrical power.
6. **CS Engine Only:** When it is more efficient to operate the engine for propulsion under low vehicle power demand while the ESS state of charge is low, as oppose to CS series or CS parallel.

The vehicle required two relatively large and expensive electrical motors so that P2 can be used as a gen-set with the engine for CD series mode, and P3 to provide propulsion to meet the drive cycle performance demand. A small engine was selected to reduce fuel consumption while a large energy storage system had to be selected to provide sufficient power in addition to the engine to meet the 0-100 km/h acceleration time in CD performance mode; including the 50 km electric range requirement in CD full electric or CD P3 only mode. A transmission was still required to allow for the engine to provide sufficient torque to the wheels at different vehicle speeds during parallel mode, adding mass and complexity to the vehicle controls. The transmission was also used to disconnect the gen-set from the wheels for CS series mode. Lastly, a clutch was required to allow the engine to disconnect from the driveline during the CD full electric mode. A rule based control

strategy was implemented that took into consideration the vehicle speed, torque demand, state of charge, and overall efficiency to pick the most optimal vehicle mode during operation.

The integration of the non-GM Weber multi purpose engine also complicated the hybridization process further. The small displacement turbo charged Weber engine was seen as the ideal internal combustion engine to use due to its low fuel consumption, and sufficient power output for charge sustaining and for performance mode. It did however require a custom made automotive grade fuel system as there was none readily available to be installed in the vehicle. Furthermore, converting the engine to run on E85 fuel also added to the complexity. The engine had to be retuned on an engine dynamometer and an expensive after market engine controller was required to run the developed tune and control the engine in the vehicle. An engine harness had to also be developed as there was none readily available to purchase. Additionally, there was limited GM technical support available since this was a non-GM component.

The GM stock transmission was kept as part of the architecture to simplify the hybridization and minimize cost by avoiding the purchase of a new transmission. Although it did simplify the mechanical integration of the powertrain since the stock transmission mounts were reused, the complications it introduced to the vehicle controls was underestimated. The transmission required specific signal inputs that are provided by the stock V6 engine to operate accordingly, since a non-GM engine was being used, this produced additional challenges in compatibility between the engine and the transmission. The transmission controller also introduced restrictions to the new integrated powertrain since it was specifically designed to operate the transmission based on the characteristics of the V6 engine. For example, the transmission controller would force a gear shift based on torque input and speed which would have ideally prevented the V6 engine from stalling, this restriction limited the operating conditions of the P2 motor and Weber engine. Lastly, due to confidentiality, information regarding the transmission controller was limited essentially making it a black box that takes in certain input signals and outputs them for the operation of the transmission. This significantly increased the challenge of determining the correct signals required. Reverse engineering the transmission controller to determine the required signals was very time consuming given the complicated nature of the intricate design of an automatic transmission.

The most mechanically challenging design and integration part of the powertrain was the pre-transmission assembly and energy storage system. The relatively small opening and space in

the trunk were the two main contributors to the challenge of integrating the ESS. A significant amount of effort was invested in developing a design that would simplify the assembly procedure of the high voltage battery pack while minimizing its footprint in the trunk and ensuring enough space for a safe assembly. This resulted in removing a portion of the trunk floor for the four assembled modules to enter through, while the two other modules were assembled in the trunk from the rear passenger access point prior to that. Similarly, the design of the pre-transmission assembly posed some challenges due to its required compactness and limited access points due to the surrounding components. The custom made bellhousing had to contain, align, and support the weight of the P2 motor and clutch as one rigid piece with the transmission and engine to remove stress from the shaft and torque converter coupler. Given the high risk of failure attributed to the pre-transmission powertrain, it was designed to have a high serviceability. This was to simplify and minimize the procedure time of removing the powertrain from the vehicle for troubleshooting and testing.

One of the most common root cause of the mechanical critical failures experienced was attributed to the misalignment and imbalance of the driveline. It resulted in the shatter of the friction disk, the P2 motor spline shear, and the failure of the support bearing of the propeller shaft. These failures caused an un-anticipated delay in the vehicle development. Another occurrence that had a significant delay on the vehicle development was the unreliability of the integrated low voltage system. The added components in the vehicle each required numerous low voltage wirings to connect to sensors, relay boxes, controllers, fuse boxes, and the hybrid supervisory controller. Depending on the wire, one lose connection, one unreliable solder job can impede the vehicle from operating all together. These wires were routed throughout the vehicle, bundled in harnesses and throughout areas that were hard to access. Problems with the electrical wiring sometimes lead to misdiagnosing the problem as being a controls code bug, which consumed more time for troubleshooting.

Historically at UWAFT, the thermal management of the powertrain was oftentimes considered as an afterthought, the correct configuration and components were determined through trial and error. This approach usually consumed a lot of time and resources, and delayed other scheduled vehicle tests. Instead, performing the required thermal management analysis and system pressure drop analysis can aid in selecting the correct components such as, heat exchangers and pump, including

the configuration and routing initially, reducing time spent on the integration process. Given that the recommended coolant temperature of the electric powertrain is significantly lower than an internal combustion engine, the radiator may be ineffective at times during high ambient temperatures. Therefore, incorporating a refrigeration system chiller can be more effective at high ambient temperatures.

At the present time of writing this thesis, the vehicle has accumulated up to a total mileage of 3,000 km from controls tests and endurance tests. Currently the vehicle is fully operational with the exception of the combustion engine that failed during the fourth year competition of EcoCAR 3. The gasket preventing the oil and coolant from seeping into the combustion chamber was damaged inhibiting the operation of the engine. Therefore at this time, the vehicle cannot be fully tested to compare some of its specifications to the VTR. Table 7-1 lists the VTR and the current specification of the vehicle, either tested or simulated. The simulations show that the vehicle meets the VTR for the energy consumptions, GHG emissions, vehicle range, gradeability requirement, and double lane change speed. It meets the 80-110 km/h acceleration time but is 0.15 seconds shy of the 0-100 km/h acceleration time requirement. The vehicle tests that were performed resulted in the vehicle meeting the brake distance requirement, cargo capacity, passenger capacity, and starting time. The curb mass was 72kg more than the requirement and 0.03G less than the lateral acceleration requirement.

Table 7-1: Vehicle Technical Requirement and Specification

	unit	UWAFT Target	Vehicle Specifications*
Acceleration, 0-100 km/h	Seconds	5.8	S: 5.95
Acceleration, 80 - 110 km/h	Seconds	3.5	S: 2.65
Top Speed	Km/h	240	S: >240
Braking, 100-0 km/h	Metre	35	T: <35
Acceleration Torque Split (Front/Rear)	-	0/100	T: 0/100
Lateral Acceleration, 90m Skid Pad	-	0.85 G	T: 0.82 G
Double Lane Change	km/h	86	S: >86
Max Grade ability	Degrees	20	S: 26
Highway Grade ability, @ 20 min	-	6% @ 100 km/h	S: > 6% @ 100 km/h
Cargo Capacity	m^3	0.08	T: >0.08
Passenger Capacity	-	4	T: 4
Curb Mass	kg	1800	T: 1872
Starting Time	Seconds	3	T: 1.6
Total Vehicle Range	km	300	S: 305
CD Mode Range	km	50	S: 55
CD Mode Total Energy Consumption	Wh/km	268	S: 223
CS Mode Fuel Consumption (gasoline equivalent)	Lge/100km	7.8	S: 5.2
UF-Weighted Fuel Energy Consumption	Wh/km	736	S: 227
UF-Weighted Total Energy Consumption	Wh/km	758	S: 344
UF-Weighted WTW Petroleum Energy Use	Wh PE/km	621	S: 66
UF-Weighted WTW Greenhouse Gas Emissions	g GHG/km	223	S: 113

*T: Tested, S: Simulated

Hopefully this thesis can prove itself to be resourceful for future projects involving the design of a hybrid electric vehicle and help reduce the time taken for its development. The analysis and results provided can help provide some intuition for the vehicle performance and thermal management values. The integration section provides some insight into the complexity of this architecture to help better estimate the time required for the architecture integration, which helps to plan more accordingly. The lessons learnt is provided to help avoid mistakes that could cost the project valuable time and to develop the vehicle more effectively.

CHAPTER 8
Recommendations

8.1 Internal Combustion Engine

As mentioned in the conclusion, at the time of writing this thesis, the vehicle is fully operational with the exception of the combustion engine. The head gasket that is meant to seal the combustion chamber has failed, rendering the engine non-operational. The cause of this is unknown and must be investigated before replacing the head gasket. The current suspicion is that the ethanol fuel has damaged the gasket, if that is the case then it must be replaced with an ethanol-compatible gasket. Another suspicion is that the radiator being currently used is too big, which develops too high of a coolant back pressure, this could potentially be the cause of the damage, which is worth investigating. Furthermore, reducing the size of the radiator will also reduce the parasitic power loss of the engine from the internal water pump as the pressure drop decreases. It is also worth reassessing the in-house developed engine tune to ensure that it is not harming the engine or that it is not the cause to the gasket damage.

Other recommendations that can be made in regards to the engine relates to the noise vibration harshness, which applies to the consumer acceptability. The dampers on the engine mount are too stiff, which are transferring the engines vibration to the cabin making it an uncomfortable experience. Therefore, the dampers should be replaced to avoid this. Additionally, the engine is also uncomfortably loud, sound dampers should be used in the engine bay to reduce the noise. The NVH of the engine was an oversight and as a result, the vehicle technical requirement should be adjusted to include vehicle NVH in the future. An acceptable decibel value as well as vibration frequency and pitch level can be determined to work towards to for the Camaro and future vehicles at UWAFT.

8.2 Driveline

At this time, the transmission is restricting the pre-transmission powertrain by forcing a gear shift when it is not required by the vehicle, limiting the torque output; this is due to the transmission using a shift map designed for the stock V6 engine. Bypassing the shift map and having complete shift control of the transmission is required to maximize the torque to the wheels. Perhaps the input shaft speed and/or torque signals can be manipulated to better control the shift timing. Caution must be taken with this approach as a mistake may damage the transmission.

The stock torque converter should be replaced with one that has a stall speed more tailored to the torque curve of the Weber engine and P2 motor, as it can improve the efficiency and performance of the vehicle.

It is also worth considering the possibility of using a one way clutch instead of the friction clutch, since it can be more responsive and passively controlled, removing the need for a release bearing, actuator, and master cylinder hydraulic system. A wet friction clutch can also be another possible replacement option that can be investigated, as it has a smoother performance and longer life than the friction clutch; although, some of the energy can be lost to the fluid it is immersed in.

8.3 Thermal Management

As a result of designing the thermal management system based on the worse case heat generation scenario, which does not occur often, the system is overdesigned and oversized. Therefore, there is room for refinement to reduce the size of the heat exchanger, which will reduce the pressure drop, leading to the pump consuming less power. A lower power consumption can lead to more available propulsion power for the vehicle performance as well as less energy consumption, which can extend the vehicle range. A more accurate thermal management model that is validated through test data needs to be developed to pursue this.

Further analysis is required in determining the optimal location of the intercooler in the thermal loop. For example, if the intercooler is to be positioned right after the chiller, before the electric motors and inverters, then it will receive coolant at a lower temperature. This can increase the engine power output since the charged air can be further reduced in temperature, increasing the air density. However, the hotter coolant entering the electric motors and inverters can reduce their

efficiency, assuming the intercooler does not cause them to overheat. Therefore, an analysis is required in determining the affect on the overall vehicle efficiency and performance by positioning the intercooler first.

The use of a pressure regulating valve and/or electrically controlled solenoid valve should be investigated to increase the refrigerant flow rate through the chiller to increase its cooling capacity. Additionally, the reconfiguration of the refrigeration system to an inline series system or repositioning the TXV in the parallel configuration to before the T-junction should be also investigated. Lastly, the selected saturation temperature of the refrigeration system for the chiller should be re-evaluated to determine if it is the optimal temperature for the system. Once the refrigeration system is finalized, the actual vapor-compression cycle can be determined and a representative model can be developed based on experimental results. With the model, the impact of the refrigeration system on vehicle efficiency, performance, and range can be determined. Afterwards, based on the model, when the vehicle is in performance mode, a control strategy can be developed for the compressor to cold soak the coolant when there is available power and then shut-off when maximum propulsion power is required. This will provide a low temperature coolant during the required vehicle maximum performance to further increase the power output of the engine and electric motors.

Note that in a situation where the ambient air temperature is higher than the coolant temperature, then the heat will transfer into the radiator, the opposite to what it is intended to do. Therefore, an electronic solenoid valve is required to bypass the radiator under conditions when the coolant temperature is lower than the ambient temperature.

8.4 Vehicle Testing and Refinements

The vehicle control strategy and energy management strategy still has a lot of room for refinement. Once the engine is operational again, and the gasket issue is resolved, the vehicle chassis dynamometer at the University of Waterloo can be utilized for further vehicle testing. This will allow for the refinement of the engine tune as it can be tuned directly in the vehicle on the chassis dynamometer. Furthermore, an efficiency map of the different vehicle modes can be established to validate and refine the vehicle model. The model can then be used to refine the energy

management strategy for an increase in the vehicle efficiency, reduction of energy/fuel consumption, and reduction of emissions. At this point, the vehicle can also be tested for its specifications to see if it meets the VTR.

Currently, the new implemented powertrain does not a have a stability control system. This should be developed to improve vehicle handling and potentially increase vehicle performance.

8.5 Vehicle Mass

The mounts in the vehicle for the auxiliary and powertrain components have all been overdesigned with a high safety factor. Therefore, these mounts have a lot of room for refinement to reduce their weight, bringing the vehicle weight closer to the VTR. Furthermore, the ESS enclosure, trunk decklid, and front hood can be replaced with carbon fiber to also reduce the vehicle weight.

8.6 Supplemental Theses

This thesis has just scratched the surface of capturing the work that went into hybridizing the Camaro. To provide even more information for future readers, supplemental theses that would complement this thesis are suggested for the following topics:

- A deep dive into the vehicle mounting design for all the new components in the vehicle, both auxiliary and powertrain. It would outline the finite element analysis performed on them and illustrate all the various design iterations and how they were improved including the decision matrix used for each selected design. It will also cover the vehicle dynamic analysis performed to replace the springs, dampers, and anti sway bar to adjust the handling of the vehicle due to the added mass and the change in the mass distribution. Finally, it would also describe the root cause of the gasket failure including its solution. Followed by an outline of the process undergone to tune the engine both on the engine dynamometer and chassis dynamometer with results provided for the optimized tune.
- A deep dive into the vehicle controls integration and the hybrid supervisory controller. This will review the developed vehicle controls architecture and discuss the methodology used. It will outline all the various controllers in the vehicle and controls logic implemented so

that the hybrid supervisory controller can provide them with the required signals to operate the vehicle in harmony. Lastly, it will elaborate on how the vehicle control strategy and energy management strategy has been optimized to maximize the vehicle propulsion power and vehicle range, and minimize fuel/energy consumption including emissions.

- A deep dive into the vehicle electrical integration, this includes the process underwent to implement the low voltage and high voltage systems. It will review the routing, schematics, fusing, and the design of the high voltage junction box. It will utilize a model to display a breakdown of the non-powertrain power usage throughout the vehicle using vehicle test data. It will also discuss how the power consumption was reduced via removing parasitic losses. There will be an in-depth information regarding the operation of the electrical motors and inverters including the required tune to further optimize them. Additionally, it will provide an overview of the implementation of the advanced driver-assistance system (ADAS) in the vehicle and its operation including the required algorithms developed.
- A deep dive into the vehicle modelling process, including thermal modelling. It will elaborate on how the software in the loop (SIL), hardware in the loop (HIL), vehicle in the loop (VIL) was used to develop, refine, and validate the model. There will be an in-depth discussion on the development of the plant model and controller model, including the theory used.

References

[1] Ecotricity, "The end of fossil fuels," [Online]. Available: Forecast of Fossil Fuel Reserves. [Accessed 25 August 2018].

[2] Statistics Canada, "Greenhouse Gas Emissions from Private Vehicles in Canada," Government of Canada, 19 12 2012. [Online]. Available: https://www150.statcan.gc.ca/n1/pub/16-001-m/2010012/part-partie1-eng.htm. [Accessed 26 August 2018].

[3] Oak Ridge National Laboratory, "Transportation Energy Data Book," U.S. Department of Energy, 2018.

[4] Matthew Nitch Smith, "The number of cars worldwide is set to double by 2040," Business Insider, 22 April 2016. [Online]. Available: https://www.weforum.org/agenda/2016/04/the-number-of-cars-worldwide-is-set-to-double-by-2040. [Accessed 26 August 2018].

[5] MAREX, "Transport Uses 25 Percent of World Energy," The Maritime Executive, 19 November 2015. [Online]. Available: https://www.maritime-executive.com/article/transport-uses-25-percent-of-world-energy#gs.pNEUWx0. [Accessed 06 September 2018].

[6] C. M. a. M. A. Masrur, Hybrid Electric Vehicles, Wiley, 2018.

[7] "The Paris Agreement," United Nations Climate Change, [Online]. Available: https://unfccc.int/process-and-meetings/the-paris-agreement/the-paris-agreement. [Accessed 08 December 2018].

[8] D. Muoio, "These Countries are Banning Gas-Powered Vehicles by 2040," Business Insider, 23 Ocotber 2017. [Online]. Available: France and the United kingdom have stated that both petrol and diesel engine cars are to be banned by 2040 with Beijing and India looking to follow.. . [Accessed 07 September 2018].

[9] A. Gray, "Countries are announcing plans to phase out petrol and diesel cars. Is yours on the list?," World Economic Forum, 26 September 2017. [Online]. Available: https://www.weforum.org/agenda/2017/09/countries-are-announcing-plans-to-phase-out-petrol-and-diesel-cars-is-yours-on-the-list/. [Accessed 07 September 2018].

[10] M. Pressman, "Four Charts Show Why Electric Vehicles are the Future," EVANNEX, 27 April 2018. [Online]. Available: https://evannex.com/blogs/news/four-charts-showcase-why-electric-cars-will-take-over. [Accessed 07 September 2018].

[11] K. Naughton, "The Near Future of Electric Cars: Many Models, Few Buyers," Bloomberg, 19 December 2019. [Online]. Available: https://www.bloomberg.com/news/features/2017-12-19/the-near-future-of-electric-cars-many-models-few-buyers. [Accessed 07 September 2018].

[12] S. Qadiri, "Are Electric Vehicles Really the Future of the Car Industry," Atelier, 13 March 2018. [Online]. Available: https://atelier.bnpparibas/en/smart-city/article/electric-vehicles-future-car-industry. [Accessed 07 September 2018].

[13] B. Kahn, "The Electric Car Revolution May Come Sooner Than We Thought," NBC news, 07 July 2017. [Online]. Available: https://www.nbcnews.com/mach/tech/electric-car-revolution-may-come-sooner-we-thought-ncna780516. [Accessed 7 September 2018].

[14] U. o. Waterloo, "University of Waterloo Alternative Fuels Team (UWAFT)," University of Waterloo, [Online]. Available: https://uwaterloo.ca/sedra-student-design-centre/directory-teams/university-waterloo-alternative-fuels-team-uwaft. [Accessed 5 December 2018].

[15] A. V. T. Competition, "Home," Advanced Vehicle Technology Competition, [Online]. Available: http://avtcseries.org/. [Accessed 05 December 2018].

[16] E. 3, "EcoCAR 3: An Advanced Vehicle Technology Competition," EcoCAR 3, [Online]. Available: http://ecocar3.org/about/. [Accessed 05 December 2018].

[17] A. N. Laboratory, "Non-Year-Specific Rules," U.S. Department of Energy, Lemont, 2018.

[18] W. Liu, Introduction to Hybrid Vehicle System Modelling and Control, Hoboken: Wiley, 2013.

[19] S. F. A. G. Amir Khajepour, in *Electric and Hybrid Vehicles Technologies, Modeling and Control: A Mechatronic Approach*, John Wiley & Sons Ltd, 2014, p. 55.

[20] C. M. a. M. Masrur, Hybrid Electric Vehicles, Principles and Applications with Practical Perspectives, Wiley, 2018.

[21] B. Chabot, "Shifting Gears, Electrification Energizes the Transmission Market," Motor Magazine, 16 May 2017. [Online]. Available: http://newsletter.motor.com/2017/20170516/!ID_ShiftingGears_EVTs.html. [Accessed 14 September 2018].

[22] P. Murtha, "2015 Initial Quality Study: 10 Most Important Factors in Vehicle Purchase," J.D. Power, 13 July 2015. [Online]. Available: http://www.jdpower.com/cars/articles/jd-power-studies/2015-initial-quality-study-10-most-important-factors-vehicle-purchase. [Accessed 1 August 2018].

[23] "Wealthiest 1% earn 10 times more than average Canadian," CBC, 11 September 2013. [Online]. Available: https://www.cbc.ca/news/business/wealthiest-1-earn-10-times-more-than-average-canadian-1.1703017. [Accessed 31 July 2018].

[24] S. Mertl, "Average price of a new car rose again last year, but at a slower pace," Automotive News Canada, 8 february 2018. [Online]. Available: http://canada.autonews.com/article/20180208/CANADA/180209785/average-price-of-new-car-rose-again-last-year-but-at-slower-pace. [Accessed 31 July 2018].

[25] A. Koehl, "Let's talk about the car population problem," The star, 19 February 2014. [Online]. Available: https://www.thestar.com/opinion/commentary/2014/02/19/lets_talk_about_the_car_population_problem.html. [Accessed 31 July 2018].

[26] "Julia LaPalme," Motor Trend, 16 October 2015. [Online]. Available: https://www.motortrend.com/cars/chevrolet/camaro/2016/2016-chevrolet-camaro-rs-v-6-first-test-review/. [Accessed 31 July 2018].

[27] "Tax filers and dependants with income by total income, sex and age," Statistics Canada, 31 July 2018. [Online]. Available: https://www150.statcan.gc.ca/t1/tbl1/en/tv.action?pid=1110000801. [Accessed 31 July 2018].

[28] "Statista," Canada: Degree of urbanization from 2007 to 2017, 2017. [Online]. Available: https://www.statista.com/statistics/271208/urbanization-in-canada/. [Accessed 1 August 2018].

[29] University of Waterloo Alternative Fuels Team, "Consumer Market Research Report," University of Waterloo Alternatives Fuel Team, Waterloo, 2014.

[30] S. W. D. a. R. G. B. S.C. Davis, Transportation Energy Data Book- Edition 33, Oak Ridge: Oak Ridge National Laboratory, 2014.

[31] "Vehicle and Fuel Emissions Testing," United States Environmental Protection Agency, [Online]. Available: https://www.epa.gov/vehicle-and-fuel-emissions-testing/dynamometer-drive-schedules. [Accessed 27 August 2018].

[32] University of Waterloo, "Feasibility Study Report," Waterloo, 2014.

[33] University of Waterloo Alternatives fuel Team, "Vehicle Design Report," Waterloo, 2015.

[34] "Engineering Toolbox," 2004. [Online]. Available: https://www.engineeringtoolbox.com/friction-coefficients-d_778.html. [Accessed 27 May 2018].

[35] I. Husain, Electric and Hybrid Vehicles Design Fundamentals, Boca Raton: CRC Press, 2011.

[36] A. N. Laboratory, "GREET Model," [Online]. Available: https://greet.es.anl.gov/. [Accessed 26 November 2018].

[37] S. Toma, "LG Chem Might Build an Automotive Battery Factory in Poland," Autoevolution, 18 April 2016. [Online]. Available: https://www.autoevolution.com/news/lg-chem-might-build-an-automotive-battery-factory-in-poland-106629.html. [Accessed 10 September 2018].

[38] J. Voelcker, "Electric car battery warranties compared," Green Car Reports, 20 December 2016. [Online]. Available: https://www.greencarreports.com/news/1107864_electric-car-battery-warranties-compared. [Accessed 10 September 2018].

[39] A. Ingram, "Electric-Car Battery Breakthroughs: Ultimate Guide," Green Car Reports, 10 June 2013. [Online]. Available: https://www.greencarreports.com/news/1084687_electric-car-battery-breakthroughs-ultimate-guide. [Accessed 10 September 2018].

[40] "A Peek Inside The Battery of a Tesla Model S," Qnovo, 11 November 2014. [Online]. Available: https://qnovo.com/peek-inside-the-battery-of-a-tesla-model-s/. [Accessed 10 September 2018].

[41] "New Metal-Air Battery Drives Car 1800Km Without Recharge," IFLScience, [Online]. Available: https://www.iflscience.com/technology/new-metal-air-battery-drives-car-1800km-without-recharge/. [Accessed 10 September 2018].

[42] Fuji Pigment Co., Ltd, "Jufi Pigment Unveils Aluminium-Air Battery Rechargeable by Refilling Salty or Normal Water," CISION PR Newswire, 08 January 2015. [Online]. Available: https://www.prnewswire.com/news-releases/fuji-pigment-unveils-aluminium-air-battery-rechargeable-by-refilling-salty-or-normal-water-300017712.html. [Accessed 10 September 2018].

[43] "Drivetrain Losses (effeciency)," x-engineer, 2018. [Online]. Available: https://x-engineer.org/automotive-engineering/drivetrain/transmissions/drivetrain-losses-efficiency/. [Accessed 30 August 2018].

[44] insideEVs, "A123 Files Suit for Apple Pouching Battery Talent," InsideEVs, 21 February 2015. [Online]. Available: https://insideevs.com/a123-files-suit-apple-poaching-battery-talent/. [Accessed 19 August 2018].

[45] A. Hughes, in *Electric Motors and Drives Fundamentals, Types and Application*, Elsevier, 2006, pp. 22-150.

[46] TM4, "Motive medium voltage," TM4, 2018. [Online]. Available: https://www.tm4.com/products/motive-high-speed-electric-powertrain/motive-medium-voltage/. [Accessed 27 September 2018].

[47] Phi-Power, "Products," Phi-Power, 2018. [Online]. Available: http://www.phi-power.com/en/products/. [Accessed 27 September 2018].

[48] Protean Electric, "Wheel torque and speed in vehicles with in-wheel motors," Protean Electric, 20 September 2017. [Online]. Available: https://www.proteanelectric.com/wheel-torque-and-speed-in-vehicles-with-in-wheel-motors/. [Accessed 27 September 2018].

[49] GKN, "Electric Driveline Solutions," GKN, [Online]. Available: https://www.gkn.com/en/our-divisions/gkn-driveline/our-solutions/electric-drivelines/edrive-solutions/. [Accessed 27 September 2018].

[50] BOSCH, "eAxle," BOSCH, [Online]. Available: https://www.bosch-mobility-solutions.com/en/products-and-services/passenger-cars-and-light-commercial-vehicles/powertrain-systems/electric-drive/eaxle/. [Accessed 27 September 2018].

[51] "IDTechEx," February 2018. [Online]. Available: https://www.idtechex.com/research/reports/electric-motors-for-electric-vehicles-2018-2028-000581.asp?viewopt=showall. [Accessed 5 May 2018].

[52] N. Hashemnia and B. Azsaei, "Comparitive study of using different electric motors in the electric vehicles," in *IEEE*, Vilamoura, 2008.

[53] B. C. Groen, *Investigation of DC Motors for Electroc and Hybrid Electric Motor Vehicle Applications Using an Infinitely Variable Transmission*, Brigham Young University, 2011.

[54] K. C. a. W. Li, *Overview of electric machines for electric and hybrid vehicles*, University of Hong Kong.

[55] S. S. a. V. Kumar, "Optimized Motor Selection for Various Hybrids and Electric Vehicles," in *SAE International*, 2013.

[56] S. Rogers, "U.S. Department of Energy," 10 May 2011. [Online]. Available: https://www.energy.gov/sites/prod/files/2014/03/f10/ape00a_rogers_2011_o.pdf. [Accessed 5 May 2018].

[57] "GKN Brings 2012 Electric Pikes Peak Winner To Festival Of Speed," Inside EVs, 2012. [Online]. Available: https://insideevs.com/gkn-brings-2012-electric-pikes-peak-winner-festival-speed/. [Accessed 24 September 2018].

[58] P. R. D. Reitz, "Reciprocating Internal Combustion Engines," 27 June 2012. [Online]. Available: https://cefrc.princeton.edu/sites/cefrc/files/Files/2012%20Lecture%20Notes/Reitz/Princeton-CEFRC1.pdf. [Accessed 22 September 2018].

[59] "Brake Specific Fuel Consumption (BSFC)," x-engineer, [Online]. Available: https://x-engineer.org/automotive-engineering/internal-combustion-engines/performance/brake-specific-fuel-consumption-bsfc/. [Accessed 22 September 2018].

[60] W. W.Pulkrabek, Engineering Fundamentals of The Internal Combustion Engine, Prentice Hall, 1997.

[61] T. A. Ronald Timpe, "Comparison of Carbon Dioxide Emissions from Gasoline and E85," University of North Dakota Energy & Environmental Research Center, 2005.

[62] "Ethanol Vehicle Emissions," U.S. Department of Energy , 03 March 2018. [Online]. Available: https://www.afdc.energy.gov/vehicles/flexible_fuel_emissions.html. [Accessed 14 June 2018].

[63] Minnesota Bio-fuels Association, "Ethanol and Octane for Beginners," 17 May 2016. [Online]. Available: https://mnbiofuels.org/media-mba/blog/item/1511-octane-and-ethanol-for-beginners. [Accessed 07 October 2018].

[64] C. A. R. G. C. Enrico Mattarelli, "Comparison between 2 and 4-Stroke Engines for a 30kW Range Extender," *SAE International*, 2014.

[65] L. Ward, "The Lighter, Better, More Efficient Two-Stroke Engine," Popular Mechanics, 3 october 2011. [Online]. Available: https://www.popularmechanics.com/cars/a7167/the-lighter-better-more-efficient-two-stroke-engine/. [Accessed 13 June 2018].

[66] M. Petrany, "Renault Is Working On A 2-Stroke 2-Cylinder Twin-Charged Diesel Engine," Jalopnik, 16 December 2014. [Online]. Available: https://jalopnik.com/renaults-new-tech-includes-a-compact-ev-motor-and-a-gas-1670217593. [Accessed 13 June 2018].

[67] "Learn the facts: Turbocharging and its impact on fuel consumption," Natural Resources Canada, 12 January 2016. [Online]. Available: http://www.nrcan.gc.ca/energy/efficiency/transportation/cars-light-trucks/buying/16747. [Accessed 12 July 2018].

[68] "The 2-Liter Turbo Engine: The Benchmark for Power, Efficiency, and Versatility," Enthusiastview, 16 March 2016. [Online]. Available: https://enthusiastview.wordpress.com/2016/03/16/the-2-liter-turbo-engine-the-benchmark-for-power-efficency-and-versatility/. [Accessed 12 July 2016].

[69] P. Cheney, "The trouble with turbos: why fuel economy can be worse, not better," The Globe and Mail, 16 May 2018. [Online]. Available: https://www.theglobeandmail.com/globe-drive/adventure/red-line/the-

trouble-with-turbos-why-fuel-economy-can-be-worse-not-better/article29705614/. [Accessed 13 July 2018].

[70] A. R. B. Walton, "Fuel Efficiency Benefit for Electrified Vehicles from Advanced Spark-ignition Engine Technologies," Argonne National Laboratory, Barcelona, Spain, 2013.

[71] P. Ellsworth, "Increasing Efficiency of Hybrid Electric Vehicles Using Advanced Controls," University of Waterloo, Waterloo, 2016.

[72] Textron Motors, "MPE 850 Four Stroke Engine," 2016. [Online]. Available: https://textronmotors.txtsv.com/Portals/0/TextronMotors/PDFs/160222_MPE850_Offroad_spec.pdf?ver=2016-03-30-132601-707. [Accessed 24 September 2018].

[73] B. Halvorson, "Your Next Vehicle Is More Liekely To Have A CVT: Here's Why," The Washington Post, 27 May 2014. [Online]. Available: https://www.washingtonpost.com/cars/your-next-vehicle-is-more-likely-to-have-a-cvt-heres-why/2014/05/27/76abd984-e5b4-11e3-a70e-ea1863229397_story.html?noredirect=on&utm_term=.9740d1c466c5. [Accessed 29 August 2018].

[74] vini_i, "Motor Vehicle Maintenance & Repair," Stack Exchange, 20 January 2016. [Online]. Available: https://mechanics.stackexchange.com/questions/25034/what-is-a-sprag-unit-and-what-does-it-do. [Accessed 20 September 2018].

[75] J. Nisewanger, "Toyota's Prius Prime Shows One Way for a Better Plug-in Hybrid," hybrid cars, 07 April 2016. [Online]. Available: https://www.hybridcars.com/toyotas-prius-prime-shows-one-way-for-a-better-plug-in-hybrid/. [Accessed 21 September 2018].

[76] R. Kartha, "The Evolution of a Supervisory Controller for a Split Parallel Plug-in Hybrid Electric Vehicle," University of Waterloo, Waterloo, 2017.

[77] P. DiGioacchino, "Predictive Powertrain Management through Driver Behaviour Recognition," University of Waterloo, Waterloo, 2018.

[78] dSpace, "MircoAutoBox II," dSpace, [Online]. Available: https://www.dspace.com/en/inc/home/medien/product_info/prodinf_mabx.cfm. [Accessed 06 December 2018].

[79] Textron Motors, "Installation Manual," 2015.

[80] K. Nakata, S. Nogawa, D. Takahashi, Y. Yoshihara, A. Kumagai and T. Suzuki, "Engine Technologies for Achieving 45% Thermal Efficiency of S.I. Engine," *SAE International Journal of Engines*, vol. 9, no. 1, pp. 179-192, 2015.

[81] "A New Look at Cooling System Technology," 24th September 2012. [Online]. Available: http://vr-12.com/a-new-look-at-cooling-system-technology/. [Accessed 03 June 2018].

[82] MIT, "Lecture 2018 Heat Transfer," 2018. [Online]. Available: http://web.mit.edu/2.61/www/Lecture%20notes/Lec.%2018%20Heat%20transf.pdf. [Accessed 1 October 2018].

[83] F. S. Richard van Basshuysen, Combustion Engine Handbook, SAE International, 2002.

[84] P. Ellsworth, *Increasing Efficiency of Hybrid Electric Vehicles Using Advanced Controls*, University of Waterloo, 2016.

[85] J. LaPalme, "2016 Chevrolet Camaro RS V-6 First Test Review," Motor Trend, 16 October 2015. [Online]. Available: https://www.motortrend.com/cars/chevrolet/camaro/2016/2016-chevrolet-camaro-rs-v-6-first-test-review/. [Accessed 28 September 2018].

[86] F. P. Incropera, D. P. Dewitt, T. L. Bergman and A. S. Lavine, Principles of Heat and Mass Transfer, Wiley, 2014.

[87] "Digital Display Meter: Inline Digital Meter," Sotera, [Online]. Available: https://www.sotera.com/index.cfm/products/productdetail/?p=507&ps=132. [Accessed 03 October 2018].

[88] T. (. Wang, "Investigation of Advanced Engine Cooling Systems-Optimization and Nonlinear Control," TigerPrints, Clemson, 2016.

[89] MapleSoft, "Designing a More Effective Car Radiator," 2008. [Online]. Available: https://www.maplesoft.com/support/help/maple/view.aspx?path=applications%2FRadiatorDesign. [Accessed 2 October 2018].

[90] C. W. B. Man-Hoe Kim, "Air-side thermal hydraulic performance of multi-louvered fin aluminum heat exchangers," *International Journal of Refrigeration*, pp. 390-400, 2002.

[91] Amazon, "Barrel Style Liquid to Air Intercooler, 4"x10" (type 25)," Amazon, [Online]. Available: https://www.amazon.com/Barrel-Style-Liquid-Intercooler-Type/dp/B00MDKMKWQ. [Accessed 07 October 2018].

[92] F. M. White, Fluid Mechanics, New Delhi: McGraw Hill, 2013.

[93] "Moody Diagram," The Engineering Toolbox, [Online]. Available: https://www.engineeringtoolbox.com/moody-diagram-d_618.html. [Accessed 24 October 2018].

[94] "Pressure Loss From Fittings - Expansion and Reduction In Pipe Size," Netrium, 2 November 2012. [Online]. Available: https://neutrium.net/fluid_flow/pressure-loss-from-fittings-expansion-and-reduction-in-pipe-size/. [Accessed 27 October 2018].

[95] H. Kudela, "Pipline Systems," [Online]. Available: http://www.itcmp.pwr.wroc.pl/~znmp/dydaktyka/fundam_FM/Lecture_no7_Pipeline_Systems.pdf. [Accessed 27 October 2018].

[96] "Intercooler pump flow testing results," Lingenfelter Performance Engineering, 11 April 2013. [Online]. Available: https://www.lingenfelter.com/forum_lingenfelter/forum/lingenfelter-forum/camaro-gen-5-2010-2013/1191-intercooler-pump-flow-testing-results. [Accessed 31 October 2018].

[97] "Shurflo 5000 Series," Pentair, [Online]. Available: https://www.pentair.com/en/applications/moving-water/agricultural-spraying/pumps/automatic-demand-pumps.html. [Accessed 31 October 2018].

[98] "PVC - Friction Loss in Fittings and Equivalent Length," The Engineering Toolbox, [Online]. Available: https://www.engineeringtoolbox.com/pvc-pipes-equivalent-length-fittings-d_801.html. [Accessed 26 October 2018].

[99] Y. A. Cengel and M. A. Boles, Thermodynamics An Engineering Approach, New York: Mc Graw Hill Education, 2015.

[100] M. A. F. a. M. Bahrami, *Comprehensive Modeling of Vehicle Air Conditioning Loads Using Heat Balance Method,* SAE International, 2013.

[101] Unicla, "Compressor Selection Criteria," 2007. [Online]. Available: https://www.supercool.com.au/files/pdfs/unicla/CompressorSelectionCriteria.pdf. [Accessed 13 November 2018].

[102] Chemours, "freon-134a-pressure-enthalpy-si-units," [Online]. Available: https://www.chemours.com/Refrigerants/en_US/assets/downloads/freon-134a-pressure-enthalpy-si-units.pdf. [Accessed 12 November 2018].

[103] M. Salimpour, "Heat Transfer Coefficients of Shell and Coiled Tube Heat Exchangers," *Experimental Thermal and Fluid Science,* vol. 33, pp. 203-207, 2009.

[104] I. Kharagpur, "Multi-Evaporator And Cascade Systems," [Online]. Available: https://nptel.ac.in/courses/112105129/pdf/RAC%20Lecture%2013.pdf. [Accessed 13 November 2018].

[105] "XING Modular Battery System," XINGMobility, [Online]. Available: https://www.xingmobility.com/xing-battery-system. [Accessed 06 June 2108].

[106] D. Patrascu, "Toyota Prius' Battery Recycling Plan," Autoevolution, 2 July 2009. [Online]. Available: https://www.autoevolution.com/news/toyota-prius-battery-recycling-plan-8360.html. [Accessed 06 July 2018].

[107] G. S. Bower and K. Ritter, "BMW and LG Chem Trump Tesla in Battery Thermal Management," HybridCARS, 07 Decemeber 2015. [Online]. Available: https://www.hybridcars.com/bmw-and-lg-chem-trump-tesla-in-battery-thermal-management/. [Accessed 13 November 2018].

[108] L. J. Masson, "Panamera S E-Hybrid: A True Plug-in and a True Porsche," 16 May 2013. [Online]. Available: http://www.plugincars.com/panamera-s-e-hybrid-true-plug-and-also-true-porsche-127237.html. [Accessed 4th June 2018].

[109] G. S. B. a. K. Ritter, "2017 Chevy Bolt Battery Cooling and Gearbox Details," 19th Jan 2016. [Online]. Available: http://gm-volt.com/2016/01/19/129946/. [Accessed 04 June 2018].

[110] G. Bower, "Tesla or GM: Who Has The Best Battery Thermal Management," INSIDEEVs, 04 December 2015. [Online]. Available: https://insideevs.com/tesla-or-gm-who-has-the-best-battery-thermal-management-bower/. [Accessed 13 July 2018].

[111] O. B. B. B. Matthia Fleckenstein, "Aging Effect of Temperature Gradients in Li-ion Cells Experimental and Simulative Investigations and the Consequences on Thermal Battery Management," *World Electric Vehicle,* vol. 5, pp. 0322-0333, 2012.

[112] B. W. M. V. S. V. Y. a. G. J. O. M Marinescu, "The Effect of Thermal Gradients on the Performance of Battery Packs in Automotive Applications," in *IET*, London, UK, 2013.

[113] Y. Z. Y. P. a. J. O. Ian A.Hunt, "Surface Cooling Causes Accelerated Degradation Compared to Tab Cooling for Lithium-Ion Pouch Cells," *The Electrochemical Society,* pp. A1846-A1852, 2016.

[114] R. Fitzpatrick, "Power and Internal Resistance," 14 July 2007. [Online]. Available: http://farside.ph.utexas.edu/teaching/302l/lectures/node62.html. [Accessed 06 June 2018].

[115] S. .. K. A. A. K. T.Porselvi, "Selection of Power Rating of an Electric Motor for Electric Vehicles," *IJESC,* vol. 7, no. 4, 2017.

[116] "The Engineering Toolbox," 2008. [Online]. Available: https://www.engineeringtoolbox.com/rolling-friction-resistance-d_1303.html. [Accessed 27 May 2018].

[117] D. Moreels, "Axial Flux vs Radial Flux: 4 Reasons Why Axial Flux Machines have a Higher Power Density," Magnax, 31 January 2018. [Online]. Available: https://www.magnax.com/magnax-blog/axial-flux-vs-radial-flux.-4-reasons-why-does-axial-flux-machines-deliver-a-higher-power-density. [Accessed 31 May 2018].

[118] Billyk, "2006 Ford Escape Hybrid AC," 25th July 2011. [Online]. Available: http://www.escape-city.com/viewtopic.php?f=38&t=10024. [Accessed 04 June 2018].

[119] P. M. J. K. Arunachalam, "Conversion of Mechanical Water Pump to Electric," *International Journal of Mechanical and Mechatronics Engineering*, vol. 8, no. 12, 2014.

[120] "Energy Flows in Engine," [Online]. Available: http://www.engr.colostate.edu/~allan/heat_trans/page3/page3.html. [Accessed 05 June 2018].

[122] R. C. Lucas D Pugnali, "Feasibility Study of Operating 2-Stroke Miller Cycles on a 4-Stroke Platform through Variable Valve Train," *SAE International*, 2015.

[123] "Absolute Roughness of Pipe Material," Neutrium, 19 May 2012. [Online]. Available: https://neutrium.net/fluid_flow/absolute-roughness/. [Accessed 24 October 2018].

Appendix A: Drive Cycle Velocity Profiles

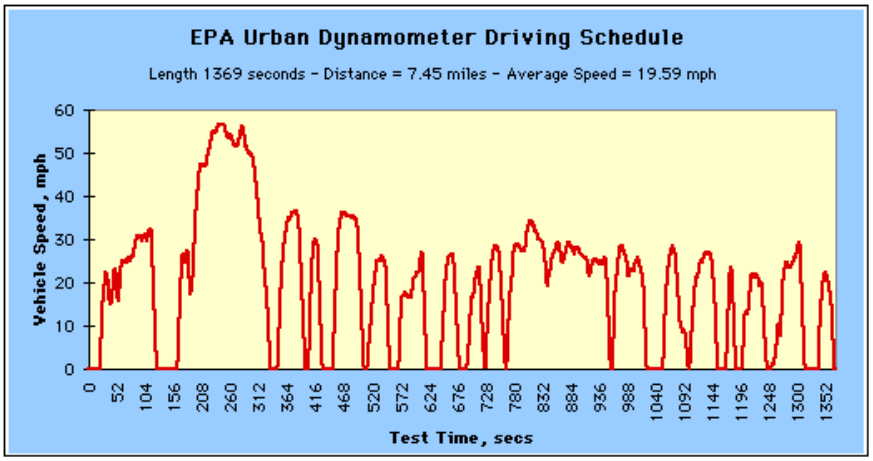

Figure 9.1: UDDS Drive Cycle [31]

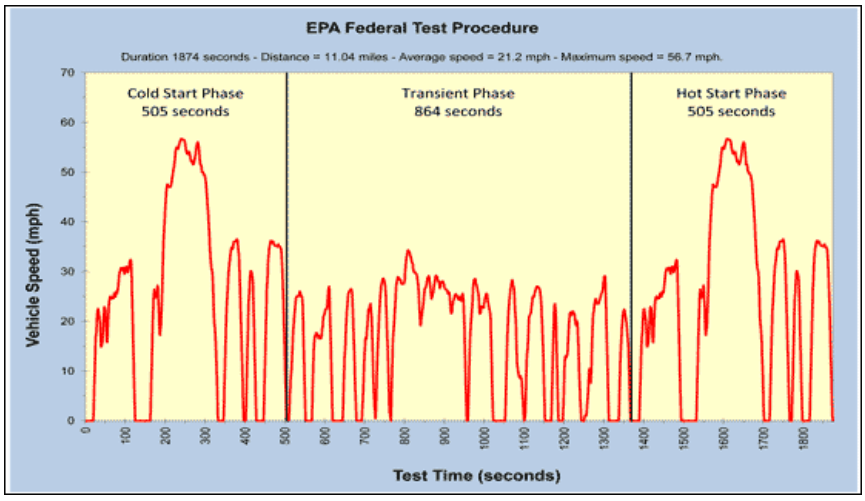

Figure 9.2: FTP -75 Drive Cycle [31]

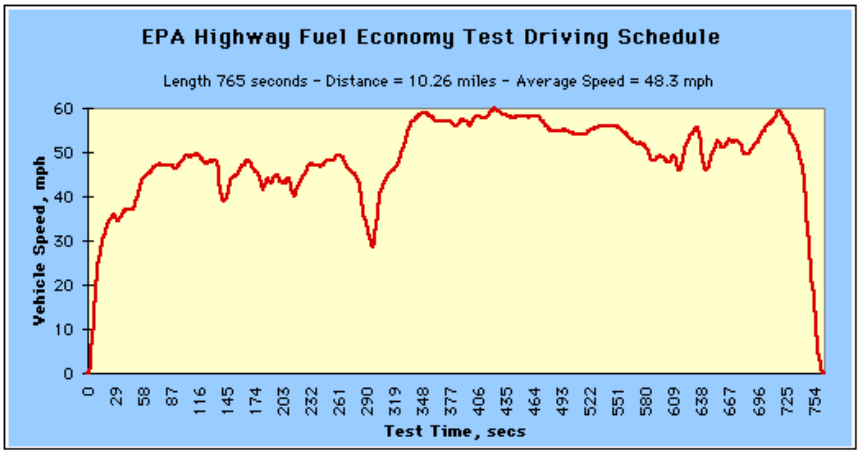

Figure 9.3: HWFET Drive Cycle [31]

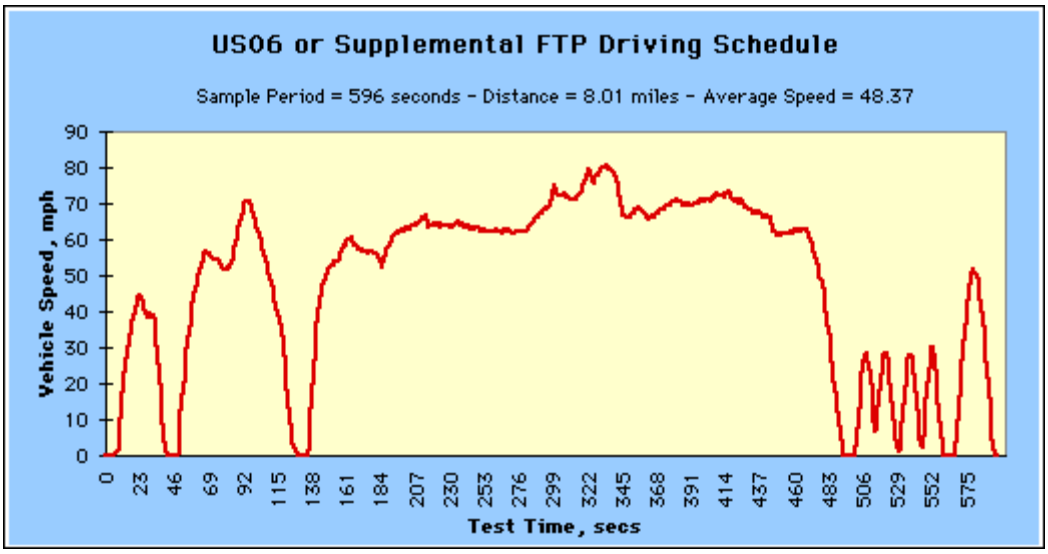

Figure 9.4: US06 Drive Cycle [31]

Appendix B: Architecture Selection Space Claim

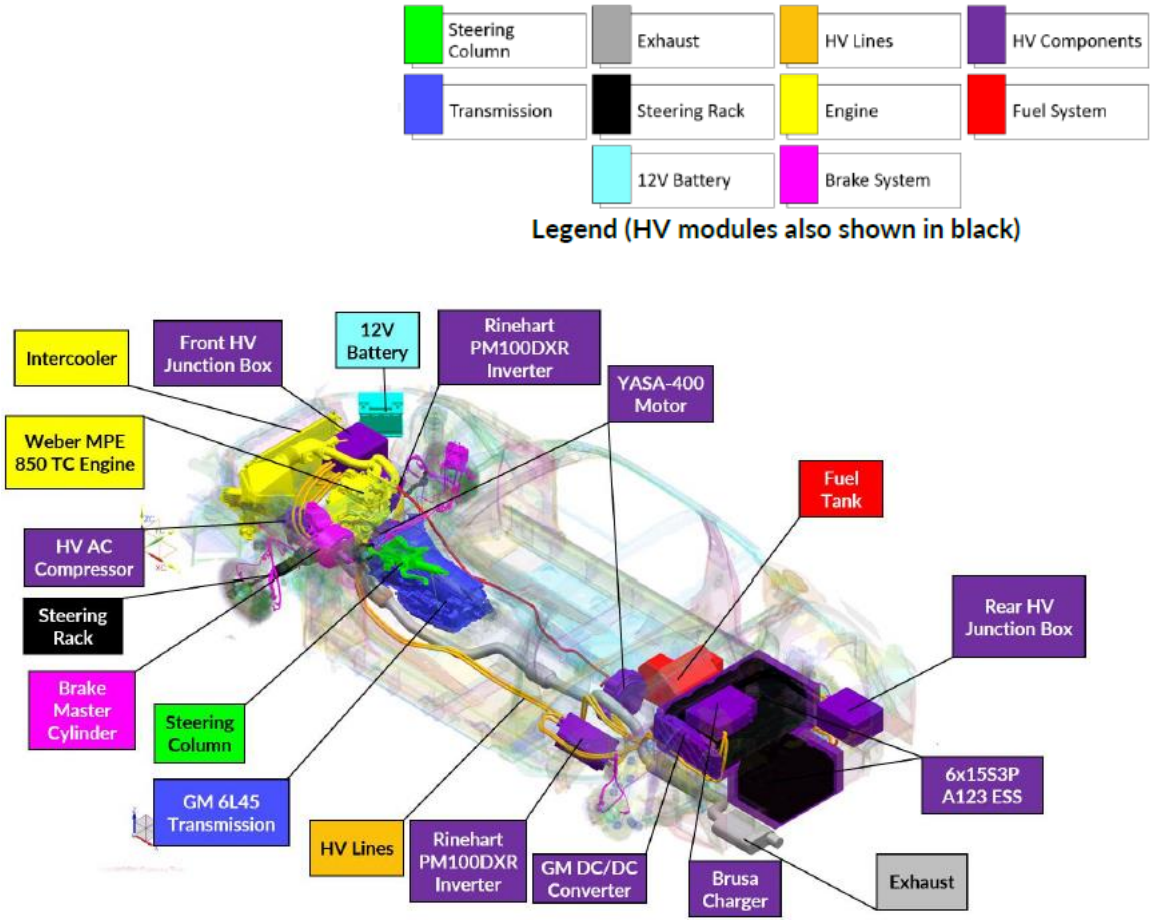

Figure 9.5: Vehicle One - Isometric View [32]

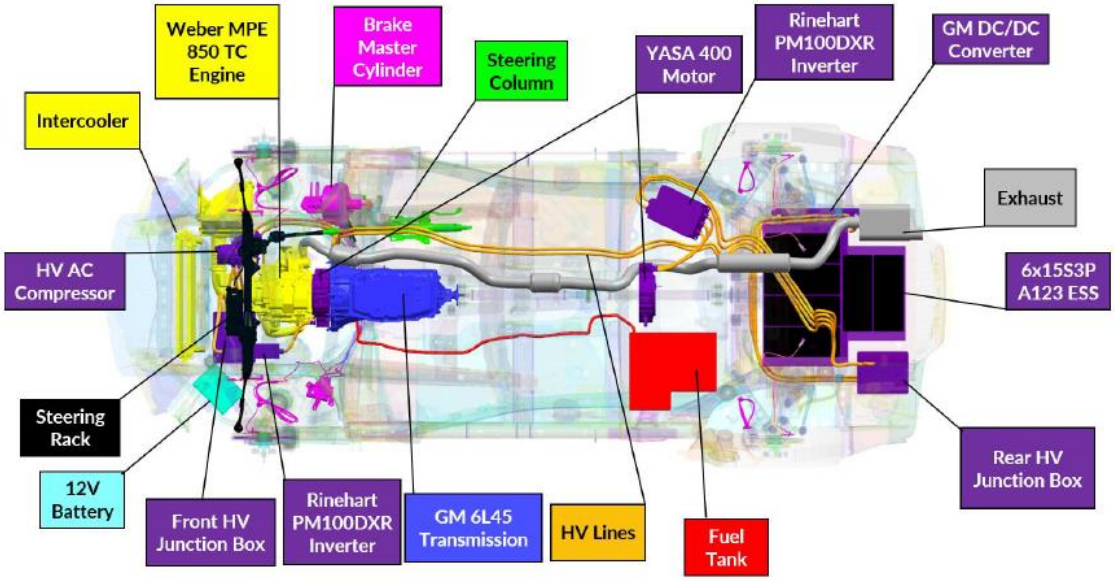

Figure 9.6: Vehicle One - Bottom View [32]

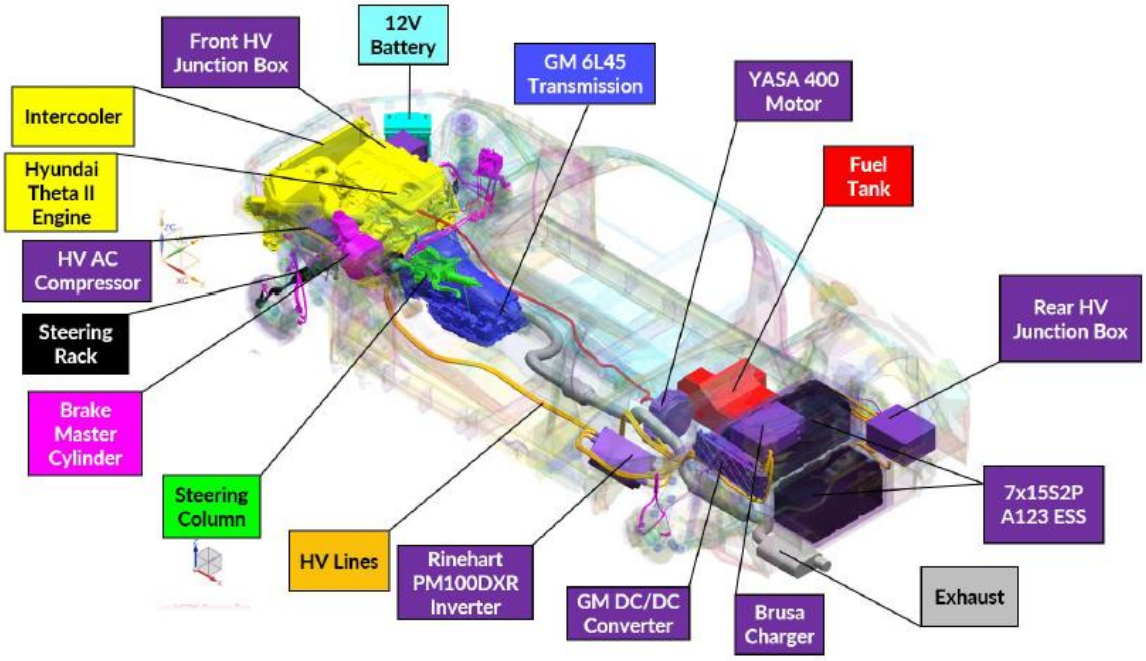

Figure 9.7: Vehicle Two - Isometric View [32]

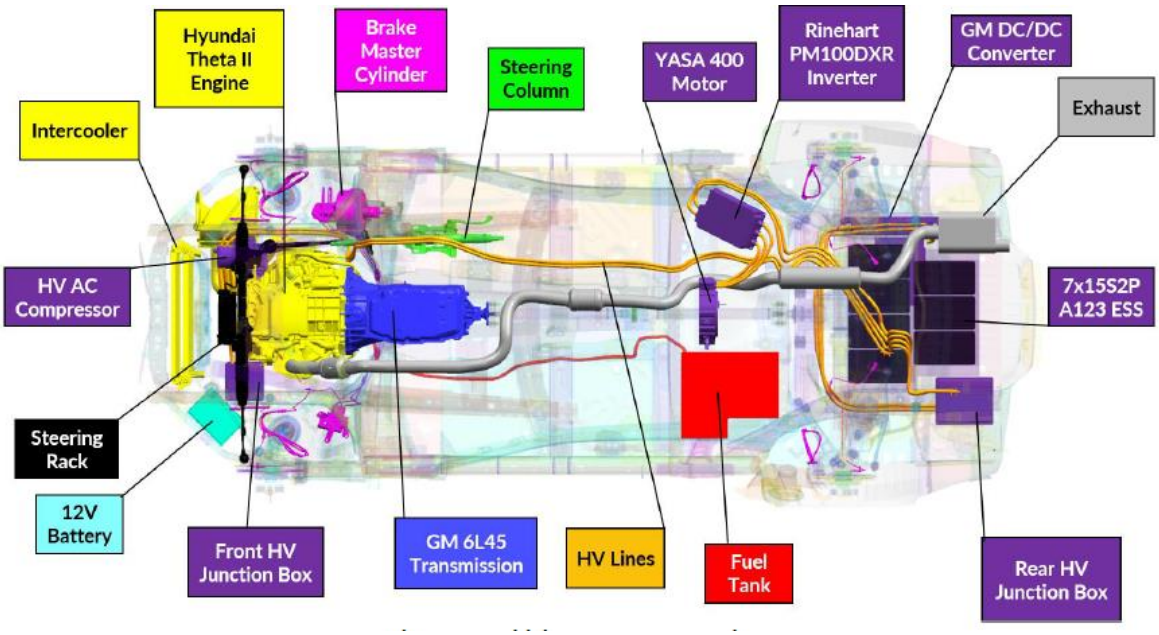

Figure 9.8: Vehicle Two - Bottom View [32]

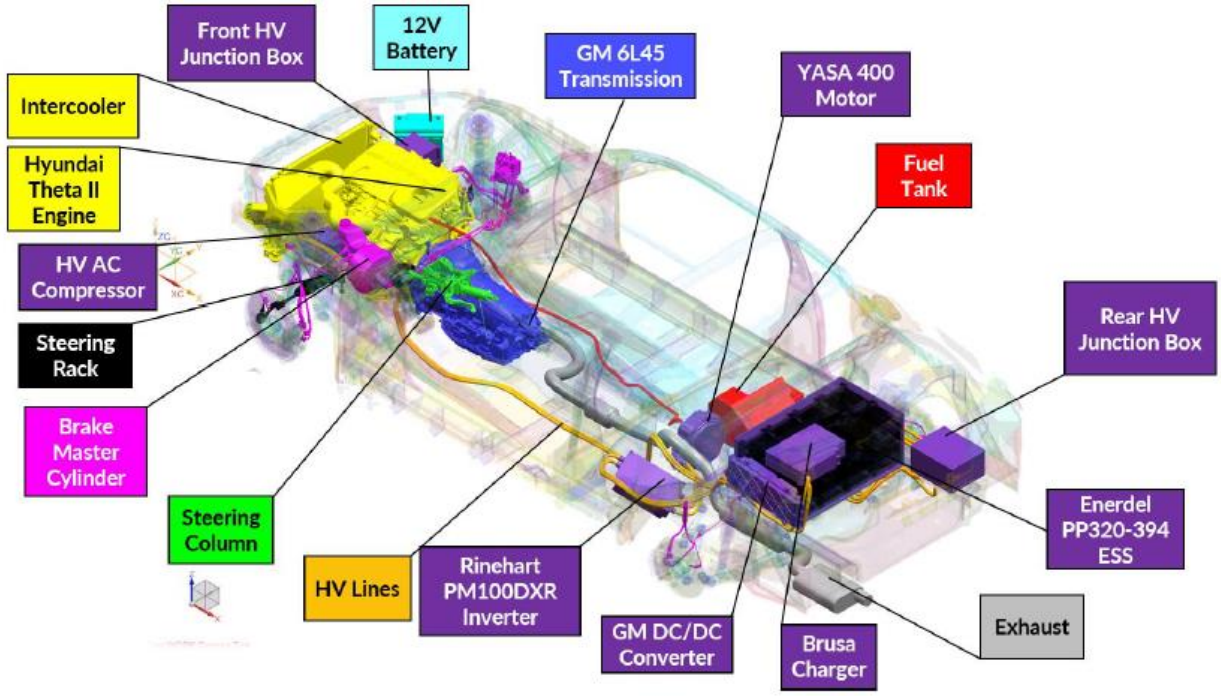

Figure 9.10: Vehicle Three - Isometric View [32]

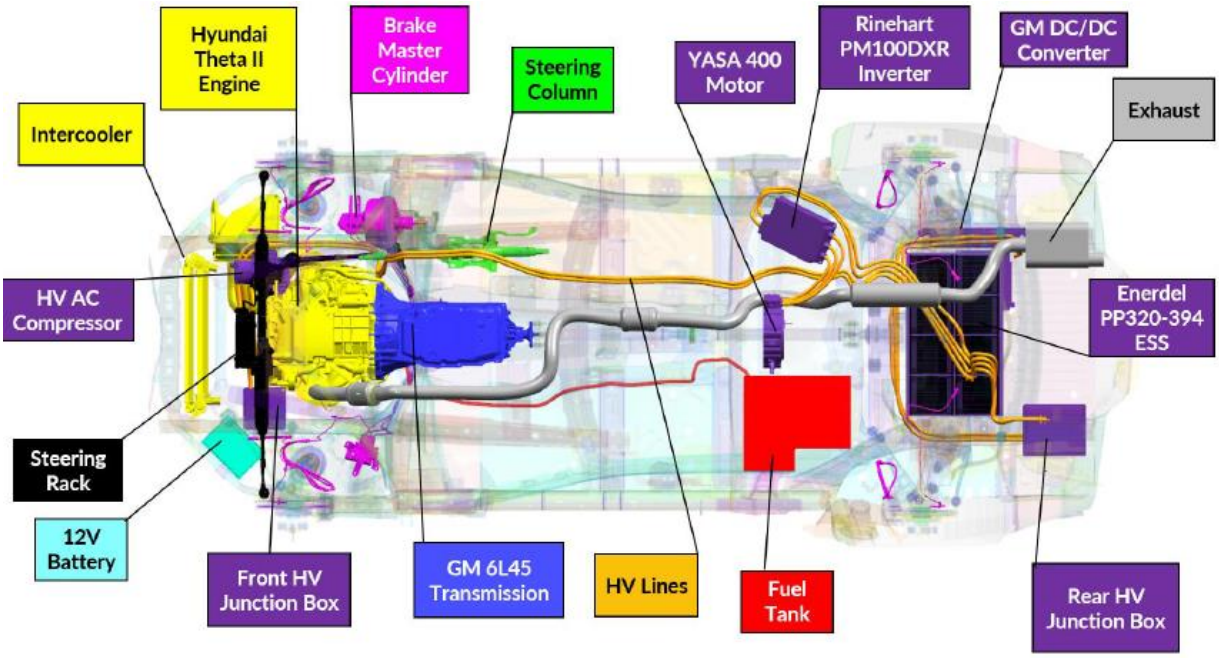

Figure 9.11: Vehicle Three - Bottom View [32]

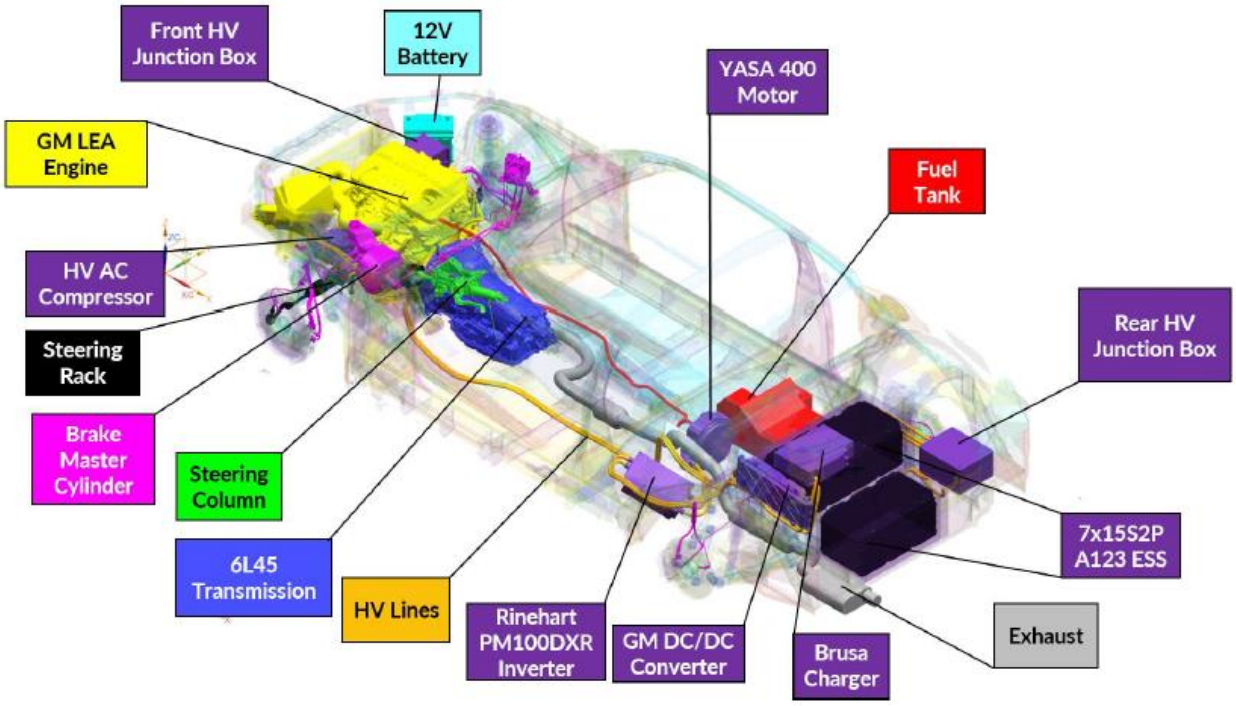

Figure 9.12: Vehicle Four - Isometric View [32]

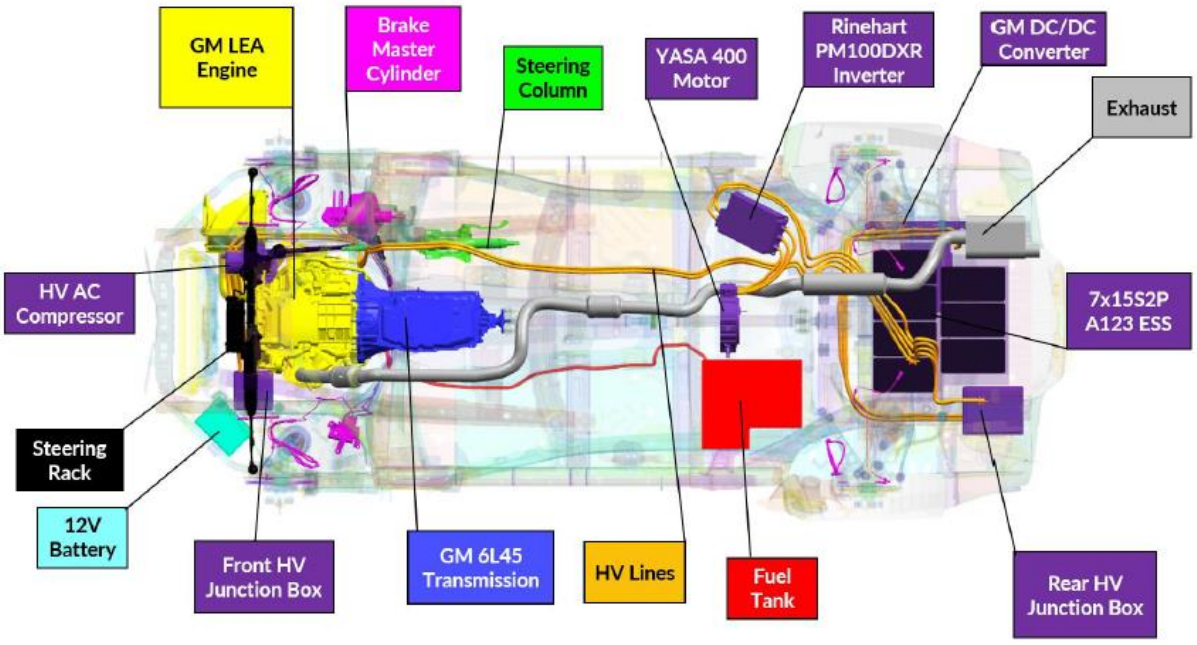

Figure 9.13: Vehicle Four - Bottom View [32]

Table 9-1: Vehicle Weight Analysis [32]

	Description	Veh. 1 (kg)	Veh. 2 (kg)	Veh. 3 (kg)	Veh. 4 (kg)
Stock	Stock Camaro	1679*			
Added	Weber MPE 850 TC	59			
	Hyundai Theta II		137	137	
	GM LEA				150
	YASA-400	48 (24 x 2)	24	24	24
	Rinehart PM100DXR Inverter	15 (7.5 x 2)	7.5	7.5	7.5
	GM DC-DC Converter	5.5	5.5	5.5	5.5
	Brusa HV Charger	6	6	6	6
	A123 16.2 kWh	130			
	A123 12.6 kWh		101		101
	Enerdel PP320-394			158	
	Battery Enclosure	30.4	30.4	30.4	30.4
	TOTAL	**293.9**	**311.4**	**368.4**	**324.4**
Subtracted	Stock Engine	157	157	157	157
	Fuel Savings	39	38	38	39
	TOTAL	**196**	**195**	**195**	**196**
	DIFFERENCE	97.9	116.4	173.4	128.4
	Weight Distribution	F: 45.6% R: 54.4%	F: 47.7% R: 52.3%	F: 46.2% R: 53.8%	F: 48.1% R: 51.9%
	Rear Reduction to get 50/50 distribution	157	82.5	139.5	68.5